Study of chikungunya virus entry and host response to infection

Marie Cresson

N°d'ordre NNT : 2019LYSE1050

THESE de DOCTORAT DE L'UNIVERSITE DE LYON
opérée au sein de
l'Université Claude Bernard Lyon 1

Ecole Doctorale N° 341 – E2M2
Evolution, Ecosystèmes, Microbiologie, Modélisation
Spécialité de doctorat : Biologie
Discipline : Virologie

Soutenue publiquement le 15/04/2019, par :

Marie Cresson

Study of chikungunya virus entry and host response to infection

---

Devant le jury composé de :

Choumet Valérie - Chargée de recherche - Institut Pasteur Paris	**Rapporteure**
Meng Guangxun - Professeur - Institut Pasteur Shanghai	**Rapporteur**
Lozach Pierre-Yves - Chargé de recherche - CHU d'Heidelberg	**Rapporteur**
Kretz Carole - Professeure - Université Claude Bernard Lyon 1	**Examinatrice**
Roques Pierre - Directeur de recherche - CEA Fontenay-aux-Roses	**Examinateur**

Maisse-Paradisi Carine - Chargée de recherche - INRA	**Directrice de thèse**
Lavillette Dimitri - Professeur - Institut Pasteur Shanghai	**Co-directeur de thèse**

UNIVERSITE CLAUDE BERNARD - LYON 1

Président de l'Université	**M. le Professeur Frédéric FLEURY**
Président du Conseil Académique	M. le Professeur Hamda BEN HADID
Vice-président du Conseil d'Administration	M. le Professeur Didier REVEL
Vice-président du Conseil Formation et Vie Universitaire	M. le Professeur Philippe CHEVALIER
Vice-président de la Commission Recherche	M. Fabrice VALLÉE
Directeur Général des Services	M. Alain HELLEU

COMPOSANTES SANTE

Faculté de Médecine Lyon Est – Claude Bernard	Directeur : M. le Professeur J. ETIENNE
Faculté de Médecine et de Maïeutique Lyon Sud – Charles Mérieux	Directeur : Mme la Professeure C. BURILLON
Faculté d'Odontologie	Directeur : M. le Professeur D. BOURGEOIS
Institut des Sciences Pharmaceutiques et Biologiques	Directeur : Mme la Professeure C. VINCIGUERRA
Institut des Sciences et Techniques de la Réadaptation	Directeur : M. le Professeur Y. MATILLON
Département de formation et Centre de Recherche en Biologie Humaine	Directeur : Mme la Professeure A-M. SCHOTT

COMPOSANTES ET DEPARTEMENTS DE SCIENCES ET TECHNOLOGIE

Faculté des Sciences et Technologies	Directeur : M. F. DE MARCHI
Département Biologie	Directeur : M. le Professeur F. THEVENARD
Département Chimie Biochimie	Directeur : Mme C. FELIX
Département GEP	Directeur : M. Hassan HAMMOURI
Département Informatique	Directeur : M. le Professeur S. AKKOUCHE
Département Mathématiques	Directeur : M. le Professeur G. TOMANOV
Département Mécanique	Directeur : M. le Professeur H. BEN HADID
Département Physique	Directeur : M. le Professeur J-C PLENET
UFR Sciences et Techniques des Activités Physiques et Sportives	Directeur : M. Y.VANPOULLE
Observatoire des Sciences de l'Univers de Lyon	Directeur : M. B. GUIDERDONI
Polytech Lyon	Directeur : M. le Professeur E.PERRIN
Ecole Supérieure de Chimie Physique Electronique	Directeur : M. G. PIGNAULT
Institut Universitaire de Technologie de Lyon 1	Directeur : M. le Professeur C. VITON
Ecole Supérieure du Professorat et de l'Education	Directeur : M. le Professeur A. MOUGNIOTTE
Institut de Science Financière et d'Assurances	Directeur : M. N. LEBOISNE

This work has been realized in the **Viral Infections and Comparative Pathology (IVPC)** joined research unit from **INRA**, **Lyon 1 university** and **EPHE** in Lyon (France) and the **Pasteur Institute of Shanghai - Chinese Academy of Sciences** in Shanghai (China).

Remerciements

Aux membres du jury pour avoir évalué et jugé mon travail ainsi que pour leurs questions pertinentes et la discussion durant ma soutenance de thèse.
À la Pr Carole Kretz d'avoir accepté de présider le jury. Aux Dr Valérie Choumet, Dr Pierre-Yves Lozach et Pr Guangxun Meng pour avoir lu en profondeur et fait une analyse critique et constructive de ce manuscrit. À la Pr Carole Kretz et au Dr Pierre Roques pour leurs questions et nos échanges lors de la soutenance.

Aux Dr Branka Horvat, Dr Fabrice Vavre, Dr Nathalie Davoust, Pr Jin Zhong pour leurs conseils et leurs encouragements lors des comités de suivi de thèse.

Cette thèse et mes voyages à Shanghai ont été possibles, entre autres, grâce à la bourse doctorale Calmette et Yersin du réseau international des instituts Pasteur, aux bourses doctorales du gouvernement chinois et à la bourse de mobilité Cai Yuanpei de Campus France.

À Dimitri et à Carine pour m'avoir permis de réaliser cette thèse entre Lyon et Shanghai qui a été très riche d'enseignements aussi bien d'un point de vue scientifique qu'humain.
Ces 4 années ont été remplies d'apprentissages, de belles rencontres et de découvertes.
Merci à toi, Carine, pour ta présence, ton accompagnement et tout ce que tu as partagé et m'as appris durant ces 4 années.
Merci Dimitri de m'avoir permis de partager cette expérience chinoise à Shanghai en m'embarquant dans ce projet. J'ai eu la chance de vivre une expérience incroyable, en parallèle de mon apprentissage scientifique, en découvrant un pays, une culture et une autre manière de travailler. Merci de m'avoir soutenu dans mes démarches et d'avoir partagé tes connaissances avec moi.

Aux Alphagirls, Carine, Lucie, Céline, Catherine et Aurélie pour leur bonne humeur, nos discussions scientifiques ou non et les heures passées dans les labos.

À Lucie, je ne vais pas pouvoir écrire en détails tout ce pour quoi je te remercie, cela prendrait des pages… Merci pour avoir partagé ta bonne humeur, ta science et ta folie avec moi tous les jours durant ces années. Merci d'avoir été présente pour discuter de nos questions et doutes sur nos expériences et nos projets. Merci d'avoir été présente pour partager les craquages de fin de journée, les milliers conneries et les apéros. Merci d'avoir partagé des discussions sur nos futurs, sur la vie et surtout sur la nourriture (avec une préférence pour la nourriture chinoise quand même). Ta gentillesse et ton altruisme ont déteint sur moi, du moins je l'espère car je pense être devenue une meilleure personne en partageant ces moments avec toi.

À Céline pour m'avoir aidé dans mes expériences, d'avoir compris ce que je voulais faire à chaque fois et d'avoir partagé ta bonne humeur.

À Catherine, pour ta joie et ta bonne humeur au quotidien, ne change rien !

À Aurélie, pour avoir su si vite t'intégrer dans notre équipe, pour ta soif d'apprendre et de comprendre la biologie et la virologie et ta bonne humeur.

Merci à vous 4, Carine, Céline, Catherine et Aurélie, pour nous avoir suivi Lucie et moi en Chine pour rencontrer l'équipe à Shanghai et découvrir notre environnement de vie et de travail.

Évidemment, Céline ne va pas sans, Maitre Daouda, dit Kathy, merci à toi pour les belles rigolades, chansonnettes et bonne humeur dans le bureau. Merci pour nos discussions et tes conseils précieux pour les manips.

À Maryline pour ta gentillesse, ton écoute, nos discussions et ta culture générale people inégalable. Tu es la grande sœur au laboratoire toujours prête à donner des conseils.

À Wil pour ces heures passées à discuter en culture cellulaire, pour ton soutien et pour ton aide. Je n'arriverai pas à écrire des remerciements aussi longs que les tiens ni à faire des jeux de mots aussi ~~nuls~~ drôles, mais je tenais à te remercier pour m'avoir remotivé les jours de doutes, pour avoir partagé ta passion pour la recherche, ton savoir scientifique et ta paraformaldéhyde.

À Marie-Pierre, Maxime, Barbara V, Fabienne, Barbara G, qui se sont occupés du laboratoire P3 durant mes années au laboratoire et qui m'ont permis de me former à la manipulation des pathogènes, d'y passer quelques centaines d'heures ~~à chanter à tue-tête~~ et d'apprendre à dompter un autoclave.

Et un ENORME merci à tous les gens du l'IVPC que je n'ai pas cité pour leur bonne humeur, leur aide, leur écoute. Dans le désordre, Fabienne, Marie-Pierre, Alexandra, Saw-See, Barbara G, Angélique, Sylvie, Sophie, Christine, Fred, Maxime, Barbara V, Caroline, Jean-Michel, Marlène, François, Margot, Justine, Margaux, Claire, Etienne, Clémentine, Julien, Nader…

À toute la bande de chercheurs/ingénieurs -en biérologie- de Lyon, dans le désordre, Maryline, Nicolas B, Lucie, Wilhelm, Marie, Stéphane, Lucile, Claire, Nicolas D, Marlène… Merci pour tous ces bons moments passés ensemble.

À toute l'équipe de Shanghai pour leur accueil et leur aide. À Émilie, Luyan, Li, Wuning et tous les autres pour m'avoir accompagné durant mes premiers pas à Shanghai, expliqué des centaines de choses et assisté dans mes démarches administratives.

À Lucie, Antoine, Clara, Blanche, Simon et toutes les personnes que j'ai eu l'occasion de rencontrer et de partager des moments à Shanghai. Merci aux gens rencontrés dans le cadre de l'institut Pasteur avec qui j'ai l'occasion de partager de très bons moments et des discussions intéressantes.
Merci à Antoine et Lucie de m'avoir fait découvrir tellement de terrasses, restaurants, bars, brunch... Merci à Lucie pour nos discussions scientifiques à toute heure, dans un canapé, en terrasse, au labo ou en scooter. Merci à Lucie et Clara pour leur immense talent de Zapateuse.

Aux différentes personnes de l'IGFL que j'ai eu le plaisir de côtoyer pendant ma thèse. En particulier, merci à Frédéric Flamant pour son aide pour l'analyse de mon screening, pour les mille et unes questions que j'avais sur le criblage et CRISPR. Merci également à Benjamin Gillet et Sandrine Hughes pour leur accompagnement lors des séquençages, pour leur écoute et leur gentillesse.

À l'équipe de Patrick Mehlen du Centre Léon Bérard avec qui nous avons eu le plaisir de collaborer. Merci particulièrement à Andrea pour avoir partagé ses astuces de bio mol, ses protocoles qui fonctionnent et ses kits. Merci à Ambroise et Hong pour le travail que nous avons pu faire ensemble.

À ma famille, mon père et Valérie, mes frères et sœurs, Matthieu, Virginie, David et Hélène pour m'avoir permis d'arriver jusqu'à là et m'avoir soutenu sans jamais vraiment être sûrs de comprendre exactement ce que je faisais tous les jours au labo.

À tous mes amis, pour particulièrement l'équipe *albertviande*, pour leur présence durant toutes ces années depuis la primaire et le collège et pour m'avoir encouragé pour certains à tenter cette aventure entre Lyon et Shanghai. Merci à Margaux, Sarah et Anaïs d'être venues découvrir des petits bouts de cette immense Chine avec moi. Ces voyages resteront inoubliables.

À Clément, pour ton amour, ta présence à mes côtés et ton soutien. Merci pour ces moments passés et surtout pour tous ceux à venir…

Abstract

Alphaviruses are a group of enveloped, positive-sense RNA viruses which are distributed almost worldwide and are responsible for a considerable number of human and animal diseases. The viruses are transmitted by bloodsucking arthropods and replicate in both arthropod and vertebrate hosts. Of these viruses, chikungunya virus has recently re-emerged and caused several outbreaks on all continents in the past decade. Chikungunya virus (CHIKV) induces a disease characterized by fever, muscle pain, acute and chronic arthralgia.
Even if CHIKV shares many aspects with alphaviruses studied for many years such as Sindbis virus and Semliki forest virus, molecular mechanisms of chikungunya virus replication and virus-host interactions remain poorly understood. At the beginning of our study, regarding alphavirus entry, some attachment factors and receptors have been proposed with more or less evidence. However, very recently, the cell adhesion molecule Mxra8 has been identified as a receptor for multiple arthritogenic alphaviruses including CHIKV with similar strategies we used.
The aim of my project was to better understand and characterize the chikungunya virus entry and the host factors involved during replication steps in mammals. Several different approaches have been used in this work.

As a first step, we have demonstrated a decrease of chikungunya and Sindbis viruses' infection after iron treatment in form of ferric ammonium citrate. Interestingly, the metal ion transporter NRAMP2, regulated by iron was known to be involved in Sindbis virus (SINV) entry in mammals. However, our data have shown that NRAMP2 is not required for CHIKV entry. In parallel, we have demonstrated that knockout of transferrin receptor, a protein involved in iron transport and a receptor for several viruses, does not affect chikungunya virus entry. We have suggested a direct antiviral effect of iron as ferric ammonium citrate as it has been recently published for Zika virus, influenza A virus and human immunodeficiency virus.

On the other hand, other preliminary studies in collaboration allowed to identify cell membrane proteins of tetraspanin-enriched microdomains (TEM) as broad cell entry factors for pathogens of eight virus families. These include, among others, highly pathogenic Ebola virus, chikungunya virus, Lassa virus and influenza A virus. We focused on two proteins emphasized as potential candidate involved in CHIKV entry, namely CD46 and TM9SF2. Our validation experiments suggest that CD46 is not required for viral entry in human cells while TM9SF2 protein appeared to be involved in chikungunya efficient infection. This protein has been published by another laboratory in the meantime as required for CHIKV infection of human haploid cells.

In the last axis, we have set up and carried out a genome-wide loss of function screen with the CRISPR/Cas9 technology in order to identify host factors important for chikungunya virus entry, replication or virus-induced cell death. The screen analysis has revealed the weaknesses of our approach which would allow optimizing future screens. Nonetheless, this screen enabled us to identify potential candidates required for CHIKV. Some of these candidates have been tested individually for their potential involvement in CHIKV biology. Promising results have been obtained with the protein candidate DYNLT3, a dynein light chain. The involvement of this candidate in CHIKV infection should be studied in more depth in further experiments.

Key words: arbovirus, alphavirus, chikungunya, viral entry, iron, CRISPR/Cas9, screening

摘要

甲病毒是分布在全世界并可引起大量人类和动物疾病的一组包膜型、正链 RNA 病毒，它们由吸血节肢动物传播并在宿主（节肢动物和脊椎动物）中复制。在这些病毒中，基孔肯雅病毒(chikungunya virus，CHIKV）最近重新出现，并在过去十年中在各大洲引起了几次爆发。基孔肯雅病毒(chikungunya virus，CHIKV)是一种以发热、肌肉疼痛、急慢性关节痛为特征的疾病。即使在多年研究中发现 CHIKV 与 Sindbis 病毒和 Semliki 森林病毒等甲型病毒有许多共同之处，但其复制及其与宿主相互作用的分子机制仍知之甚少。在我们的研究之初，关于 AlphaVirus 入侵宿主的附着因子和受体，已经伴随着或多或少的证据提出了。然而最近，细胞粘附分子 MXRA8 被鉴定为多种关节源性甲病毒的受体，包括我们使用类似研究策略的 CHIKV。本研究项目的目的是更好地理解和描述在基孔肯雅病毒入侵哺乳动物并涉及复制步骤过程中的宿主因素。在这项工作中使用了几种不同的方法。

作为第一步，我们已经证明了 Chikungunya 和 Sindbis 病毒经柠檬酸铁铵处理后的感染减少。有趣的是，铁调控的金属离子转运体 NRAMP2 参与哺乳动物 Sindbis 病毒(SINV)的进入是已知的。然而，我们的数据表明，NRAMP2 对于 CHIKV 的入侵不是必需的。同时，我们已经证明，敲除这种参与铁转运并作为几种病毒的受体的转铁蛋白受体并不影响基孔肯雅病毒的进入。我们推测，正如最近发表的柠檬酸铁铵对寨卡病毒、甲型流感病毒和人体免疫缺陷病毒的抗病毒作用一样，铁也具有直接抗病毒作用。

另一方面，在协作中进行的其他初步研究允许鉴定将富含四硫鸟苷微区(TEM)的细胞膜蛋白作为八个病毒家族病原体的广泛细胞进入因子，其中包括高致病性埃博拉病毒、Chikungunya 病毒、Lassa 病毒和甲型流感病毒。我们重点研究了两种可能参与 CHIKV 进入的蛋白作为潜在候选物，即 CD46 和 TM9SF2。我们的验证实验表明，病毒进入人体细胞并不需要 CD46，而 TM9SF2 蛋白似乎参与了基孔肯雅的有效感染。该蛋白已在另一个实验室发表，同时也是 CHIKV 感染人单倍体细胞所必需的。

在最后一个轴中，我们利用 CRISPR / Cas9 技术建立并进行了全基因组功能丧失筛选，以鉴定对基孔肯雅病毒进入，复制或病毒诱导的细胞死亡中具有重要意义的宿主因子。筛选分析揭示了我们的方法的弱点，这将允许优化未来的筛选。尽管如此，这种筛选使我们能够识别 CHIKV 所需的潜在候选因子。这些候选因子中的一些已经被单独测试他们对 CHIKV 生物学过程的潜在参与。用蛋白质候选物 DYNLT3（一种动力蛋白轻链）已经获得了有希望的结果，应该在进一步的实验中更深入地研究该候选物在 CHIKV 感染中的参与。

Résumé

Les alphavirus sont un groupe de virus enveloppés à ARN simple brin positif retrouvés sur la totalité du globe et responsables de nombreuses maladies humaines et animales. Ces virus sont transmis par des arthropodes hématophages au cours d'un repas sanguin et se répliquent chez les hôtes vertébrés et arthropodes. Durant la dernière décennie, une réémergence du virus du chikungunya a été observée causant de nombreuses épidémies sur tous les continents. Le virus du chikungunya (CHIKV) induit une maladie caractérisée par de la fièvre, des douleurs musculaires et une arthralgie. Bien que le CHIKV partage de nombreuses similitudes avec le virus Sindbis (SINV) et le virus de la forêt de Semliki (SFV) étudiés depuis de nombreuses années, les mécanismes moléculaires de réplication du CHIKV et les interactions hôte-virus restent peu caractérisées. Concernant l'entrée des alphavirus, différents facteurs d'attachement et récepteurs ont été décrits. La molécule d'adhésion, Mxra8, a récemment été identifiée comme récepteur du CHIKV et d'autres virus arthritogéniques à l'aide de stratégies similaires à celles que nous avons utilisées.

L'objectif de mon travail était de mieux comprendre et caractériser l'entrée du virus du chikungunya et les facteurs de l'hôte impliqués dans la réplication chez les mammifères. Plusieurs approches distinctes ont été utilisés dans ce projet.

Dans un premier temps, nous avons mis en avant une diminution de l'infection du CHIKV et du SINV après un traitement avec du fer sous forme de citrate d'ammonium ferrique. De manière intéressante, le transporteur d'ion métallique, NRAMP2, régulé par le fer a été identifié comme un facteur d'entrée du SINV chez les mammifères. Néanmoins, nos résultats ont permis de montrer que NRAMP2 n'est pas impliqué dans l'entrée du CHIKV. En parallèle, nous nous sommes intéressés au récepteur à la transferrine (TFRC), impliqué dans le transport cellulaire du fer et connu comme le récepteur d'entrée de plusieurs virus. Nous avons démontré que la déplétion de TFRC n'avait pas d'impact sur l'entrée du CHIKV. Nous avons suggéré un effet antiviral direct du citrate d'ammonium ferrique comme il a été récemment publié pour le virus Zika, le virus de la grippe A et le virus de l'immunodéficience humaine.

D'autre part, des études préliminaires en collaboration ont permis d'identifier des protéines membranaires des microdomaines enrichis en tetraspanine comme facteurs d'entrée pour huit familles de virus différentes. Parmi ces virus on retrouve notamment le virus Ebola, le virus du chikungunya, le virus Lassa et le virus de la grippe A. Nous nous sommes intéressés à deux protéines, CD46 et TM9SF2, qui avaient été mis en avant comme potentiels candidats pour l'entrée du CHIKV. Nos expériences de validation suggèrent que la protéine CD46 n'est pas impliquée dans l'entrée du CHIKV tandis que le protéine TM9SF2 semble être impliquée dans l'infection des cellules par le CHIKV. Un autre laboratoire a mis en avant entre temps le rôle de la protéine TM9SF2 dans l'infection de cellules haploïdes humaines par le CHIKV.

Dans le dernier axe, nous avons mis en place et réalisé un criblage « perte de fonction » sur le génome entier en utilisant la technologie CRISPR/Cas9 afin d'identifier des facteurs de l'hôte importants pour l'entrée du CHIKV, sa réplication ou la mort viro-induite. L'analyse de ce criblage a révélé certains points faibles de notre approche qui permettront d'optimiser les futurs criblages. Néanmoins, le criblage a permis d'identifier des candidats potentiels nécessaires au CHIKV qui ont été testés individuellement afin de confirmer leur implication dans la biologie du CHIKV. Des résultats intéressants ont notamment été obtenus avec la protéine DYNLT3, une chaine légère du complexe de la dynéine. L'implication de ce candidat dans l'infection par le CHIKV va être étudiée plus en détails dans des expériences futures.

Mots clés : arbovirus, alphavirus, chikungunya, entrée virale, fer, CRISPR/Cas9, criblage

ABBREVIATION

A

Ae	*Aedes*
AURAV	Aura Virus
Atg	Autophagy-related gene

B

BCV	Buggy Creek virus
BF	Barmah Forest
bp	base pair
BSL	Biosafety level

C

C	Capsid
Cas	CRISPR-associated
CDS	Cytosolic DNA Sensor
CHIKV	Chikungunya virus
CHIKV LRic	Chikungunya virus La Réunion infectious clone
Co-IP	Co-immunoprecipitation
CPS	Count per second
CPV	Cytopathic vacuoles
CRISPR	Clustered Regularly Interspaced Short Palindromic Repeats
crRNA	CRISPR RNA

D

dCas9	deactivated Cas9
DENV	Dengue virus
DMT	Divalent metal transporter
DNA	Deoxyribonucleic acid
DSB	Double-strand break
dsRNA	double-stranded RNA
DYNLT3	Dynein Light Chain Tctex-Type 3

E

EBV	Epstein-Barr virus
ECSA	East Central South African
EEEV	Eastern equine encephalitis virus
EMCV	Encephalomyocarditis virus
ER	Endoplasmic reticulum
EV	Enterovirus

F

FAC	Ferric ammonium citrate
FBS	Fetal bovine serum
FISH	Fluorescent in-situ hybridization
FITC	Fluorescein isothiocyanate
FUZ	Fuzzy homologue

G

GAG	Glycosaminoglycan
gDNA	genomic DNA
GeCKO	Genome-scale CRISPR Knock-Out
GETV	Getah virus
GFP	Green Fluorescent Protein

H

HC	Heavy chain
HCV	Hepatitis C virus
HDR	Homology-Directed Repair
HF	High fidelity
HI	Hemoagglutination Inhibition
HIV	Human immunodeficiency virus
HPV	Human Papillomavirus
HR	Homologous recombination
HS	Heparan sulfate
HSV	Herpes Simplex virus

I

IAV	Influenza A virus
IC	Intermediate chain
IFA	Immunofluorescence assay
IFN-I	type I interferon
IgG	Immunoglobulin G
IL	Interleukin
IRE	Iron Responsive Element
IRES	Internal Ribosome Entry Sequence
IRF	IFN regulatory factor
IRP	Iron Responsive Protein
ISG	Interferon stimulated gene

K

kDa	kilodalton
KO	Knockout

L

LC	Light chain
LC3B	Light chain protein 3B
LC3C	Light chain protein 3C
LIC	Light intermediate chain
LIP	Labile Iron Pool
LDL	Low-Density Lipoprotein
luc	luciferase

M

MAYV	Mayaro virus
MCP	Membrane cofactor protein
MEF	Mouse embryonic fibroblasts
MIDV	Middelburg virus
miRNA	microRNA
MLV	Murine Leukemia virus
MnoV	Murine norovirus
MOI	Multiplicity Of Infection
mRNA	messenger RNA
MT	Microtubules
MTOC	Microtubule organizing center
MyD88	Myeloid differentiation primary response protein 88

N

NC	Nucleocapsid core
NDP52	Nuclear dot protein 52
NDUV	Nmudu virus
NES	Nuclear export signal
NFκB	Nuclear factor κB
NHEJ	Non-Homologous End-Joining
NK	Natural Killer
NLS	Nuclear Localization Signal
NRAMP	natural resistance-associated macrophage
ns	non significative
nsp	non structural protein
NT	untreated

O

ONNV	O'nyong nyong virus
ORF	Open Reading Frame

P

PAM	Protospacer Adjacent Motif
PBS	Phosphate buffered saline
PFA	Paraformaldehyde
pre-crRNA	precursor crRNA
PS	Phosphatidylserine
PV	Poliovirus
PVR	Poliovirus Receptor

R

RdRp	RNA-dependent RNA polymerase
RC	Replication Complex
RIG-I	Retinoic acid-Inducible gene I
RISC	RNA-induced silencing complex
RLR	(RIG-I)-like receptor
RNA	Ribonucleic acid
RNAi	RNA interference
ROS	Reactive Oxygen Species
RRV	Ross River virus
RT-qPCR	quantitative reverse transcription-polymerase chain reaction
RV	Rabies virus

S

SDC	Syndecan
SDS-PAGE	Sodium dodecyl sulfate Polyacrylamide gel electrophoresis
SDV	Sleeping Disease virus
SESV	Southern Elephant Seal virus
SFV	Semliki Forest virus
sgRNA	single guide RNA
shRNA	short-hairpin RNA
siRNA	short-interfering RNA
SLC	Solute light carrier
Sp	*Streptococcus pyogenes*
SPDV	Salmon Pancreatic Disease virus
ssRNA	single stranded RNA

T

TALE	Transcription-activator-like effector
TALEN	Transcription-activator-like effector nuclease

TCID50	Tissue culture infective dose 50%
TEM	Tetraspanin-enriched microdomains
TFRC	Transferrin receptor
TGN	Trans Golgi network
TLR	Toll-like receptor
TNF	Tumor Necrosis Factor
tracrRNA	trans-activating crRNA
TRIF	TIR domain-containing adaptater-inducing IFN-β

U

UTR	Untranslated region

V

VACV	Vaccinia virus
VEEV	Venezuelan equine encephalitis virus
VLP	Virus-Like Particles
VSV	Vesicular Stomatitis virus

W

WEEV	Western equine encephalitis virus
WNV	West Nile virus
WT	Wild Type

Y

YFV	Yellow fever virus

Z

ZFN	Zinc Finger Nucleases
ZIKAV	Zika virus

TABLE OF CONTENTS

BIBLIOGRAPHIC SYNTHESIS

I - ALPHAVIRUS

1 - Taxonomy and phylogeny

Regarding the Baltimore classification based on viral genome, the genus alphavirus belongs to group IV with a single strand RNA genome of positive polarity. Alphaviruses are members of the *Togaviridae* family which also includes the rubivirus genus into which Rubella virus is the sole member. On the other hand, alphaviruses also belong to the arbovirus group, for arthropod-borne virus, which refers to any viruses transmitted by arthropod vectors such as mosquitoes or ticks. However, this arbovirus classification based on the transmission mode is only an ecological based assembly and it gathers morphologically heterogeneous viruses belonging to several distinct families.

Alphavirus genus includes approximately 30 different species classified into 7 serocomplexes of mosquito borne alphaviruses according to antigenic relationships determined in serum neutralization assays (Calisher et al., 1988).

The seven antigenic complexes include Barmah Forest (BF), Eastern equine encephalitis (EEE), Middelburg (MID), Nmudu (NDU), Semliki Forest (SF), Venezuelan equine encephalitis (VEE) and Western equine encephalitis (WEE) (Fig. 1 and fig. 2).

Alphavirus exceptions of mosquito-borne transmission include salmon pancreatic disease virus (McLoughlin and Graham, 2007), sleeping disease virus (Villoing et al., 2000) and southern elephant seal virus (La Linn et al., 2001).

COMPLEX and VIRUSES	
Barmah Forest complex	Barmah Forest Virus (BFV)
Eastern Equine Encephalitis complex	Eastern Equine Encephalitis Virus (EEEV)
Middelburg Virus complex	Middelburg Virus (MIDV)
Ndumu complex	Ndumu Virus (NDUV)
Semliki Forest Complex	Chikungunya Virus (CHIKV)
	Mayaro Virus (MAYV)
	Getah Virus (GETV)
	O'Nyong Nyong Virus (ONN)
	Ross River Virus (RRV)
	Semliki Forest Virus (SFV)
Venezuelan Equine Encephalitis complex	Venezuelan Equine Encephalitis Virus (VEEV)
Western Equine Encephalitis complex	Aura Virus (AURA)
	Sindbis Virus (SINV)
	Sindbis (Ockelbo Virus) (OCKV)
	Buggy Creek Virus (BCV)
	Fort Morgan Virus (FMV)
	Highlands J Virus (HJV)
	Western Equine Encephalitis Virus (WEEV)
Unclassified alphaviruses	Salmon Pancreatic Disease Virus (SPDV)
	Sleeping Disease Virus (SDV)
	Southern Elephant Seal Virus (SESV)

Figure 1: The seven antigenic complexes and viral species
Italic = recombinant viruses

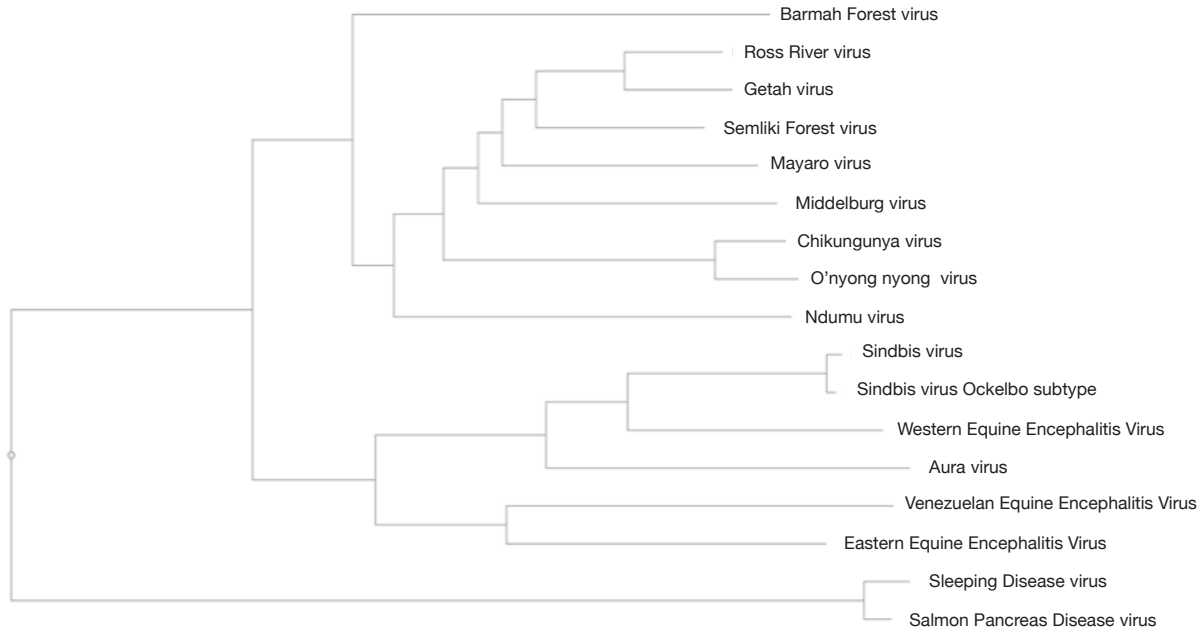

Figure 2: Phylogenetic tree of alphaviruses generated from structural polyprotein sequences
Phylogenetic tree generated with Archaeopteryx tool based on FASTA sequences.

2 - Geographical distribution

Alphaviruses are distributed worldwide and have been historically grouped into Old World and New World alphaviruses depending on their geographic localization (Fig.3) (Strauss and Strauss, 1994). Old world alphaviruses such as Sindbis, o'nyong-nyong, Ross River and chikungunya viruses were mainly found in Asia, Australia, Europe and Africa. On the contrary, New world alphaviruses, including equine encephalitis viruses like Venezuelan Equine encephalitis were mainly found in North America and South America.

Old world alphaviruses are arthritogenic and typically cause rash, fever and arthritis and occasionally encephalitis for some viruses like Ross river and chikungunya viruses. In contrast, New World alphaviruses have encephalitogenic properties and cause encephalitis in equines and humans.

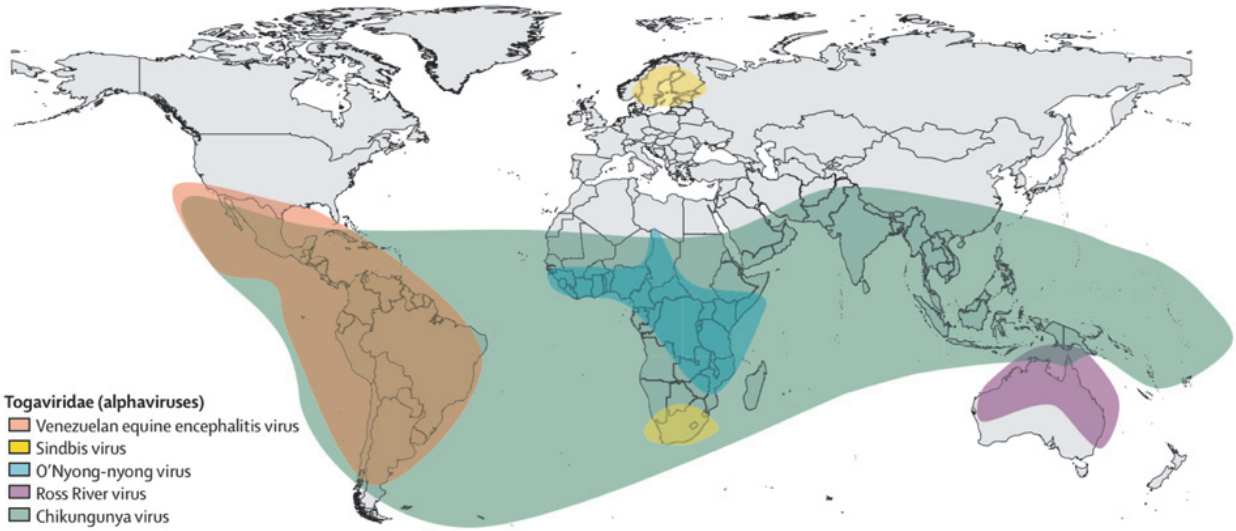

Figure 3: World distribution of major alphavirus infections (Charlier et al., 2017)

3 - Alphavirus structure and genome

a. Virion structure

Alphaviruses are small (60-70 nm diameter), icosahedral-shaped, enveloped viruses (Powers et al., 2001; Strauss and Strauss, 1994). The nucleocapsid is composed of 240 capsid protein monomers holding the RNA genome (Fig.4). This nucleocapsid is surrounded by a viral envelope composed of host-cell derived bilayer lipid membrane including cholesterol and sphingolipid molecules. The two envelope glycoproteins E1

and E2 are transmembrane proteins with a C-terminal cytoplasmic region. E1 and E2 associate as heterodimer subunits, which are in turn assembled into trimers to form the spikes with a total of 80 spikes at the surface of the virus.

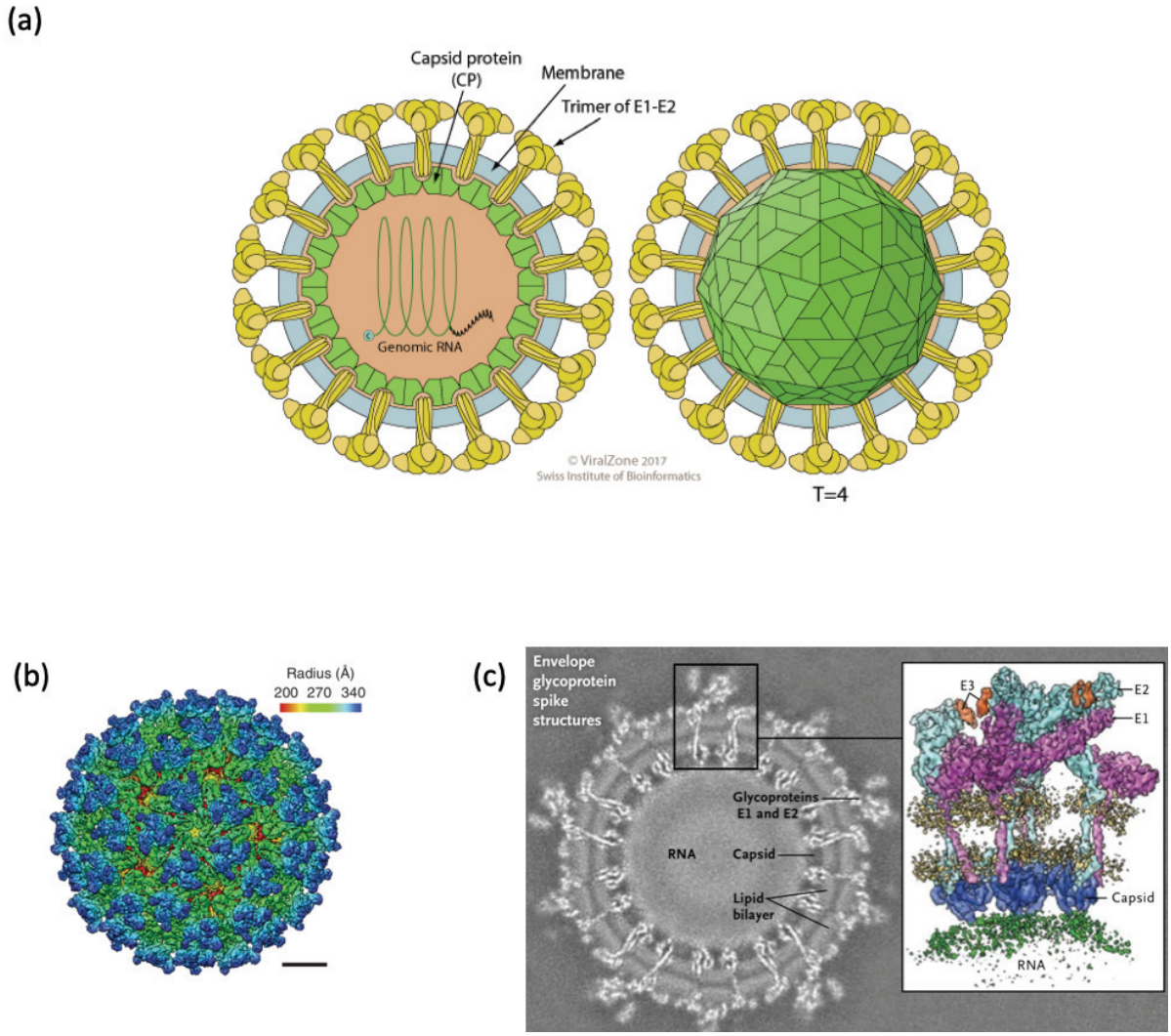

Figure 4: Structure of chikungunya virus particle

(a) Schematic representation of the alphavirus virion

(b) 3D reconstruction of alphavirus particles (VEEV on this figure), showing the E1 basal triangle (green) and E2 central protrusion (blue) for each spike. Scale bar: 10 nm. (Zhang et al., 2011)

(c) High-resolution cryo-electron microscopic reconstructions of alphavirus particle and spike-protein predicted structures based on atomic resolution structures of the envelope glycoproteins (Weaver and Lecuit, 2015).

b. Genome

Alphaviruses have a single stranded positive-sense RNA genome ((+)ssRNA) with a 12 kb approximate length (Fig.5(a)). The alphavirus genome encodes two open reading frames (ORFs): one flanked by a 5' cap and an untranslated region for the non

structural proteins and one controlled by a subgenomic promoter for structural proteins. The second ORF has a 3' untranslated region and a poly(A) tail. A junction region between the non structural and structural ORF contains the nucleotide encoding the C-terminus of non structural polyprotein, a promoter for transcription of the 26S subgenomic mRNA, and the start site and 54 nucleotides untranslated leader sequence of the 26S mRNA. The short 5′ untranslated region and the longer 3′ untranslated region comprising stem-loop structures and direct repeats regulate viral gene expression, replication, translation and virus-host interactions (Hyde et al., 2015). For chikungunya virus, these regions are thought to be associated with adaptation to mosquito hosts (Chen et al., 2013b). Similarly, for insect only alphaviruses, these regions restrict replication in mammals.

The non structural ORF encodes non structural proteins (nsp1-nsp4) for transcription and replication of viral RNA genome, polyprotein cleavage and RNA capping and is translated in the early times of infection (Fig.5(a)).
The non structural protein 1 (nsp1, ~60 kDa) exhibits both guanine-7-methyltransferase and guanylyl transferase enzymatic activities required for capping and methylation of newly synthesized genomic RNA and subgenomic RNA.
The nsp2 (~90 kDa) is a multifunctional protein. The nsp2 contains a triphosphatase activity involved in the capping process (Vasiljeva et al., 2000), a helicase activity required for unwinding dsRNA replicative intermediates (Gomez de Cedrón et al., 1999) and also a cysteine protease activity required for the cleavage of the non structural polyprotein (Hardy et al., 1989).
The nsp3 (~60 kDa) possesses an ADP-ribose 1-phosphate phosphatase activity and an RNA-binding activity. The nsp3 is involved in minus-strand and subgenomic RNA synthesis.
Finally, nsp4 (~70 kDa) exhibits an RNA-dependent RNA polymerase (RdRp) activity required for viral RNA replication.

The non structural proteins permit the synthesis of five structural proteins, respectively, Capsid, E3, E2, 6K, E1 encoded by the structural ORF (Fig.5(a)).
The capsid protein has a molecular weight of about 30 kDa. Monomeric capsid (C) proteins assemble to form the nucleocapsid. The C-terminal domain of the capsid protein has a serine protease activity which co-translationally cleaves itself out of the nascent structural polyprotein (Fig.5(b)).
The E1 protein and pE2 precursor are assembled in heterodimers in the endoplasmic reticulum (Fig.5(c)). Furin cleavage of the pE2 precursor during virus maturation in the

Golgi release E3 and E2 proteins and leads to the transport of E1-E2 heterodimers to the plasma membrane. E1-E2 heterodimers form trimeric spikes on the virus surface. E2 glycoprotein (~40 kDa) is responsible for attachment to host cell receptor while E1 protein (~44 kDa) mediates entry of the nucleocapsid from endosomes to cytoplasm thanks to a fusion peptide. The role of E3 is poorly characterized and appears to vary between alphaviruses. E3 protein might mediate spike assembly and spike activation for viral entry (Jose et al., 2009; Snyder and Mukhopadhyay, 2012). It can stay tightly connected to the E1-E2 heterodimer for some alphaviruses but not for others.
6K is a small polypeptide present in viral particles in small amounts (7-30 copies). 6K protein is considered as necessary for the structure of alphavirus particle (McInerney et al., 2004) although viral particles lacking 6K were structurally undistinguishable of wild type particles. In addition, the 6K protein is able to form a cation-selective channel and alter the permeability of the cell membrane.

(a)

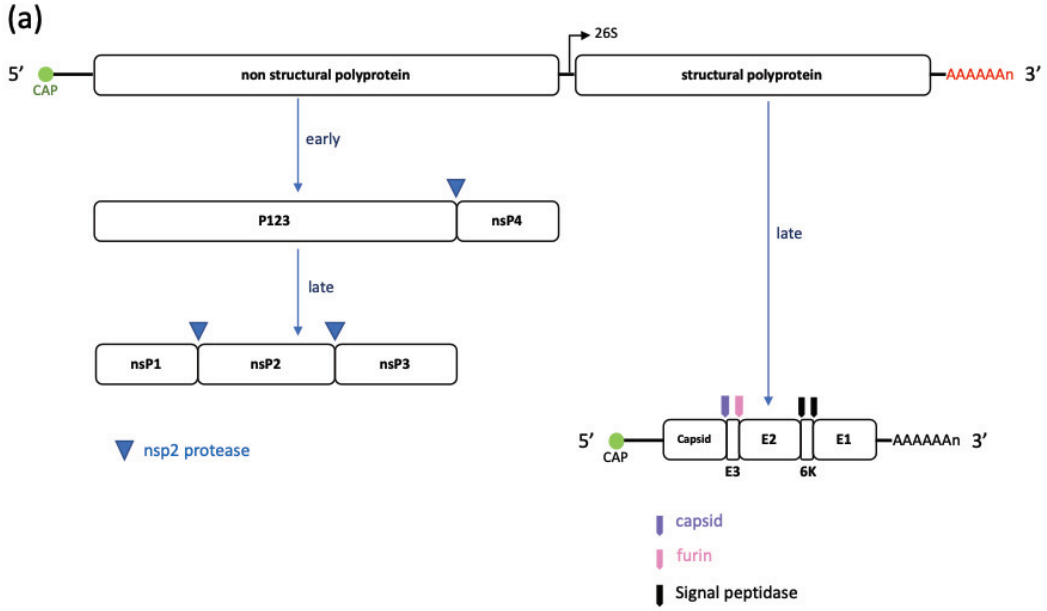
26S
5′
CAP
non structural polyprotein
structural polyprotein
AAAAAAn 3′
early
P123
nsP4
late
nsP1
nsP2
nsP3
nsp2 protease
late
5′
CAP
Capsid
E2
E1
AAAAAAn 3′
E3
6K
capsid
furin
Signal peptidase

(b)

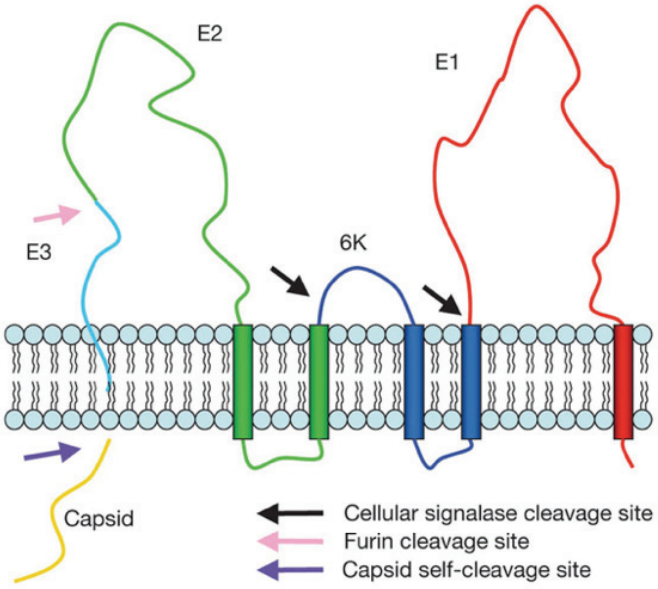
E2
E1
E3
6K
Capsid
Cellular signalase cleavage site
Furin cleavage site
Capsid self-cleavage site

(c)

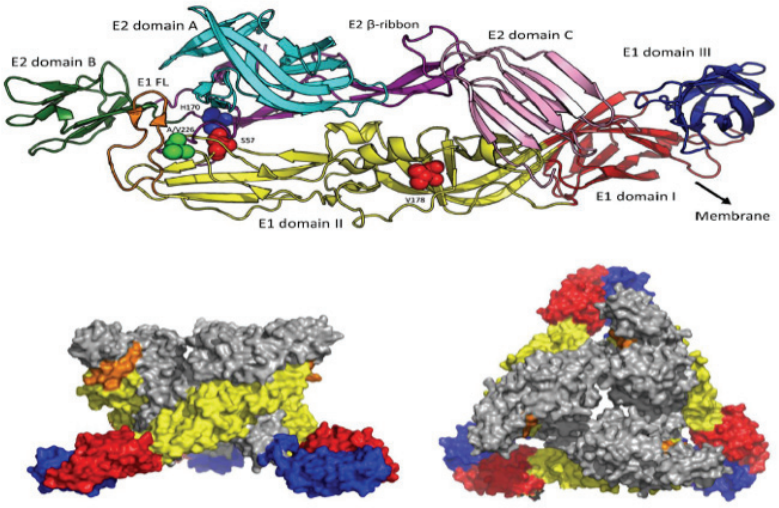
E2 domain A
E2 β-ribbon
E2 domain C
E1 domain III
E2 domain B
E1 FL
E1 domain I
E1 domain II
Membrane

Figure 5: Alphavirus genome and structural proteins

(a) *Alphavirus genome is a (+)ssRNA genome, encoding two open reading frames. It possesses 5' cap and 3' poly(A) tail. 5' and 3' sequences carry untranslated regions (UTR) and the junction region between nonstructural and structural proteins is also non-coding. The nonstructural proteins (nsp1-nsp4) are translated from the genomic RNA while structural proteins (Capsid-E3-E2-6K-E1) are translated from subgenomic 26S RNA. The two polyproteins are cleaved by host proteases (furin/signal peptidase) and viral proteins with a protease activity (nsp2/capsid).*

(b) *Alphavirus structural proteins arrangement on the endoplasmic reticulum membrane. (Li et al., 2010)*

(c) *Structure of the E2/E1 dimer.*
Top: Ribbon diagram depicting the ectodomains of the CHIKV E1 and E2 glycoproteins. At neutral pH, the E2/E1 dimer interaction is stabilized by the hydrogen bond between E2-H170 and E1-S57. Both E1-A/V226 and E1-V178 are important for lipid sensing prior to fusion. Bottom: Surface view of a virus spike (from the side and the top). E1 is colored as in the ribbon diagram, E2 is depicted in gray. (van Duijl-Richter et al., 2015)

4 - Alphavirus replication cycle in mammalian cells

The complete alphavirus replication cycle is represented and described in figure 7. Each replication step will be discussed in detail below.

a. Receptor binding and entry

The receptor mediated endocytosis is the main mode of entry for alphaviruses. The entry process begins with the non-specific interaction of the virus to attachment factors, followed by more specific binding to receptors/co-receptors at the cell surface (Fig.7). Attachment factors concentrate viruses at the host cell surface allowing them to scan the cell surface and promote receptor binding which is usually more specific.

Glycosaminoglycans (GAGs) are large complex carbohydrate molecules expressed on the surface of most mammalian cell types. Since GAGs are ubiquitously present on the cell surface, many pathogens use them for initial cell attachment or possibly as sole entry receptors. GAGs include among others heparan sulfate (HS), chondroitin sulfate and dermatan sulfate. Several alphaviruses have been shown to use GAGs for entry into mammalian cells *in vitro* (Bernard et al., 2000; Gardner et al., 2013; Klimstra et al., 1998; Smit et al., 2002). The infection with natural isolates of EEEV and low passage strains of VEEV has been shown to be dependent on GAGs (Gardner et al.,

2013; Wang et al., 2003). However, for the other alphaviruses, the affinity of binding to HS appears to be acquired after a series of passages in cell culture (Klimstra et al., 1998).

DC-sign and L-sign have been identified as attachment factors for alphaviruses (Klimstra et al., 2003). DC-sign and L-sign are C-type lectins that bind to mannose-rich carbohydrate structures. It has been shown that high-mannose N-glycans on the viral glycoproteins of phleboviruses (arbovirus group), bind to DC-sign permitting virus internalization and infection (Lozach et al., 2011). However, so far, a direct role of DC-sign in alphavirus internalization beyond attachment has not been demonstrated. We can hypothesize that, in particular cell lines, DC-sign might be sufficient for attachment and internalization of alphaviruses. It should be noticed that viruses produced by insect cells have high mannose residues which interact better to DC- and L-SIGN. Therefore, the dependence on these molecules may not be equivalent if the virus enters after a mosquito bite (high mannose) or after production *in vivo* from infected mammal cells (complex sugars).

Other cell surface molecules have been reported to be involved in viral attachment at cell surface such as major histocompatibility antigen class I, integrin a1b1, heat shock protein 70 and the high-affinity laminin receptor (van Duijl-Richter et al., 2015).

In parallel, the natural-resistance associated macrophage protein (NRAMP2) has been proposed as the receptor for SINV in *Drosophila*, mosquito and mammalian cells (Rose et al., 2011). This molecule has been identified using a whole genome screen in *Drosophila* cells using siRNA technology. More recently, the cell adhesion molecule Mxra8 has been identified as an entry mediator for chikungunya, Ross River, Mayaro and O'nyong nyong viruses through a CRISPR/Cas9 screen in mice cells (Zhang et al., 2018).

For some viruses, the domains involved in binding to attachment factors or receptors are well characterized, however, regarding alphaviruses, only a few studies demonstrated E2 binding to attachment factors or receptors and little is known about envelope protein domains involved in binding. It has been shown that domains A and B of the extracellular part of the E2 protein facilitate cell binding. Domain B binds cell-surface glycosaminoglycans (GAG) while domain A might bind to another cell-surface molecule, suggesting at least two different cell entry mechanisms, one GAG-dependent and another GAG-independent (Weber et al., 2017). With the recent

identification of Mxra8, more studies will be possible to characterize the molecular mechanism of envelope binding to receptor for arthritogenic alphaviruses.

Following the binding to the receptors, alphaviruses are rapidly internalized *via* the formation of clathrin-coated vesicles involving adaptor protein-2, dynamin, epsin and Eps15 (Bernard et al., 2010; van Duijl-Richter et al., 2015). The GTPase activity of dynamin protein facilitates indeed the formation and the budding of the clathrin-coated pits (Sourisseau et al., 2007). Clathrin-coated vesicles are subsequently uncoated and form endosomes.
Some entry mechanisms will be described in chapters 1 and 2 of part I of the experimental report.

Alternative mechanisms for alphavirus entry have also been reported illustrated by the ability of Sindbis virus to enter into cells in absence of low-pH endocytosis, the efficient chikungunya infection in cells depleted for clathrin and the direct fusion of Semliki Forest virus at the cell surface (Leung et al., 2011). The possible relevance of these mechanisms *in vivo* still needs to be investigated.

b. Fusion and nucleocapsid disassembly

In the endosomal membrane, the vacuolar ATPase acts as a proton pump to acidify the lumen of endosomes (Mellman et al., 1986). Thus, viruses are exposed to increasingly low pH as they transit through the endocytic pathway. For alphaviruses, fusion generally occurs within the early endosome compartment, with a pH around 5 to 6. This low-pH environment induces conformational changes in the E1-E2 heterodimer leading the exposition of the previously buried E1 fusion loop. The hydrophobic fusion loop located in domain II of E1 protein inserts in the target membrane and E1 homotrimers are formed by domains I and II of the protein. Cooperative action of several homotrimers mediates the membrane fusion through a hemifusion step. Thereafter a fusion pore is formed through which nucleocapsid reaches the cytoplasm (Fig. 6).
E1 protein might form two distinct populations with only a small fraction of E1 protein reacting with the membrane and generating the fusion pore. The second population of E1 might create ion-permeable pores in the viral membrane (Wengler, 2004).
Both together, these processes allow the release of nucleocapsid into the cytoplasm. Uncoating of nucleocapsids occurs rapidly after their penetration into the cytoplasm. This uncoating is facilitated by the interaction of capsid protein with 60S ribosomal RNA (SINGH' and HELENIUS, 1992; Wengler et al., 1992).

Alphavirus fusion is also dependent on membrane lipid composition. Presence of cholesterol is required for chikungunya virus (CHIKV), Sindbis virus (SINV) and Semliki forest virus (SFV) entry (Bernard et al., 2010; Kielian and Helenius, 1984) while VEEV is still able to enter in cells depleted of cholesterol (Kolokoltsov et al., 2006). Cholesterol is essential for the fusion of many enveloped viruses with cell membranes. Cholesterol changes the penetration of fusion peptides in membranes, it alters the intrinsic membrane curvature and bending in membrane fusion and it alters the lifetime of hemifusion intermediates. For alphaviruses, the cholesterol dependence might be attributed to a specific residue at position 226 in E1 protein sequence even if the mechanism is not completely understood. VEEV has a different residue at position 226 compared to SFV, SINV and CHIKV and traffics to late endosomes depleted of cholesterol, while SFV, SINV and CHIKV fuse with early endosomes, enriched in cholesterol (Leung et al., 2011). Moreover, small amounts of sphingolipids in the target membrane are also required for fusion and might play a role in accessibility of cholesterol (Kielian et al., 2010). During a recent CHIKV outbreak, the mutation of the amino acid 226 (alanine to valine) was selected in the Indian Ocean lineage (IOL) emerging strain. It has proposed that this mutation allows the virus to adapt to *Aedes albopictus* and improve the use of cholesterol (Tsetsarkin et al., 2007). This will be discussed in further details in paragraph II-1.

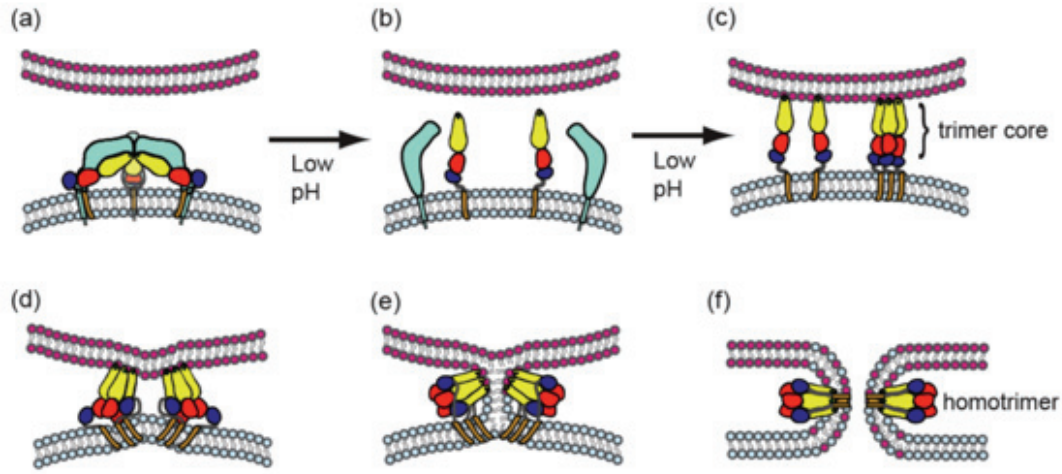

Figure 6: Steps of the alphavirus membrane fusion process (Kielian et al., 2010)

(a) Pre-fusion state with dimer of E2 (in light blue) and E1 (in colors) in the viral membrane. Target membrane is in pink color.
(b) Low pH dissociation of E2-E1 heterodimer. Exposition of E1 fusion loop.
(c) Insertion of E1 in the target membrane and E1 trimer formation.
(d) Conformational transition to the E1 trimeric hairpin brings viral and target membranes together.
(e) Hemifusion step with the merge of the two outer leaflets.
(f) E1 stable post-fusion homotrimer.

c. Replication

Replication is initiated by the expression of the nsp1234 precursor from the RNA genome and the subsequent cleavage in *cis* by nsp2 protease activity between nsp3 and nsp4 to yield P123 and nsp4 (Fig.5). P123 and nsp4 associate to perform the early replication complex (RC) which performs full-length minus-strand RNA intermediate synthesis. The proteolytic maturation of P123 allows the release of nsp1, nsp2 and nsp3, which associate to form mature RC to ensure positive-sense 49S RNA and 26S subgenomic RNA synthesis (Fig.7) (Shirako and Strauss, 1994). Viral RNA synthesis takes place within membrane spherules on the plasma membrane, also known as type I cytopathic vacuoles (CPVs).

The subgenomic RNA drives the expression of the C-pE2-6K-E1 precursor, which is processed by an autoproteolytic serine protease activity of the capsid protein (Strauss and Strauss, 1994). Capsid protein is released from the nascent polypeptide chain while the remainder of the polyprotein enters the endoplasmic reticulum for processing by signal peptidase and maturation (Fig.5). pE2 and E1 associate in heterodimer in the Golgi followed by the oligomerization of three heterodimers to form the immature spike complex. Immature spikes are exported to the plasma membrane through the host secretory system and pE2 is cleaved by cellular furin into E3 and E2 which renders the spike fusogenic (Fig.7).

d. Assembly and release

Alphavirus assembly begins with the association between nucleocapsid and RNA genome (Fig.7) (Rebecca Brown et al., 2018). A specific sequence in the N-terminal region of the capsid is required for RNA-binding and packaging (Mendes and Kuhn, 2018). This association leads to the assembly of 240 copies of capsid protein to form the nucleocapsid with icosahedral symmetry (with T=4 symmetry). This nucleocapsid assembly occurs in the cytoplasm and E2 protein interacts with nucleocapsid for budding through the cell membrane (Fig.7) (Owen and Kuhn, 1997; Zhao and Lindqvist, 1994).

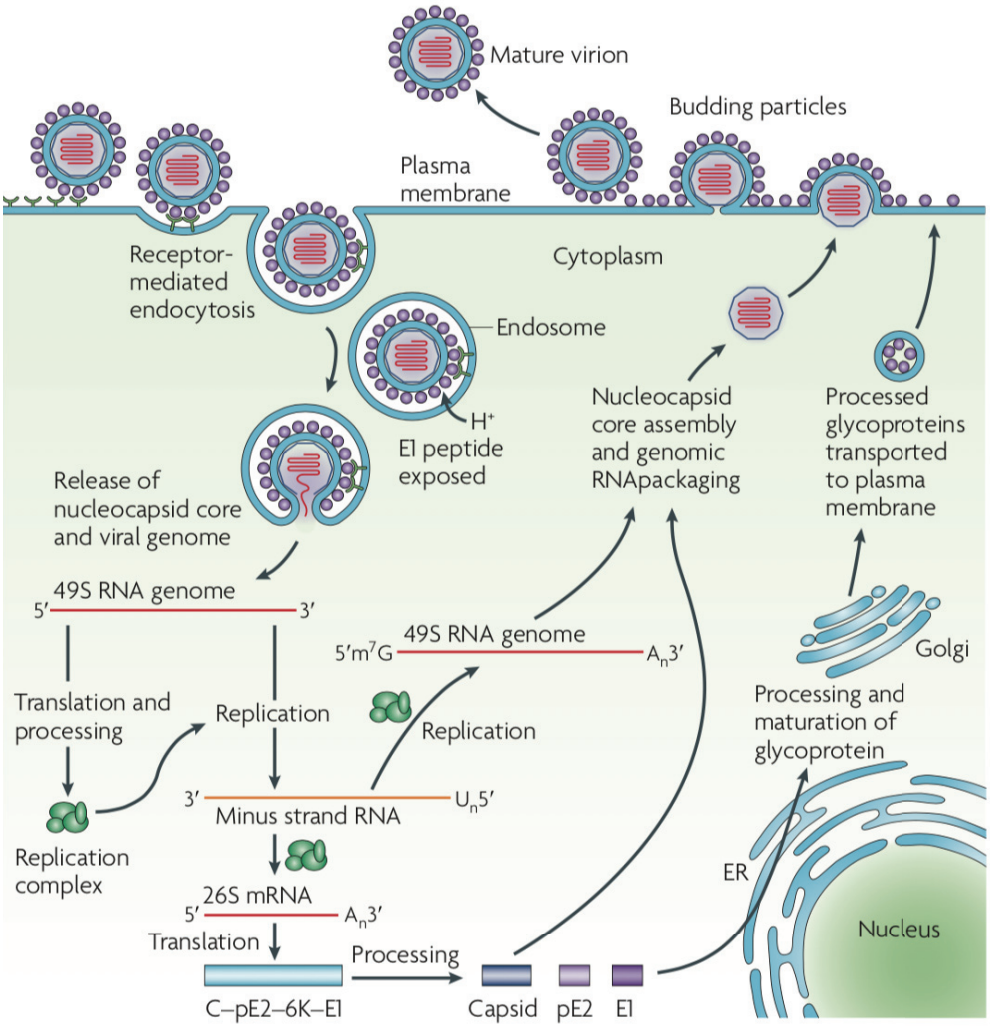

Figure 7: Alphavirus life cycle

Alphaviruses bind to receptors on the plasma membrane and are internalized by clathrin-mediated endocytosis. The low-pH dependent fusion of the viral and the endosomal membranes leads to the release of the nucleocapsid into the cytoplasm. Virus replication occurs in the cytoplasm and the envelope glycoproteins are transported to the cell surface where new virions bud. (Schwartz and Albert, 2010)

II - CHIKUNGUNYA VIRUS

1 - History of chikungunya virus epidemics

CHIKV was originally isolated in 1952 from the serum of a febrile patient from the Makonde Plateau in Tanzania (Robinson, 1955 and Ross, 1956). The epidemic disease was characterized by fever, joint pain and rash. The disease was initially diagnosed as a “dengue-like” illness until chikungunya virus was identified. The virus takes its name from the local word chikungunya, meaning “that which bends up”, coming from the stooped posture of infected individuals that resulted from the pain. After the identification of the virus, outbreaks of chikungunya virus occurred sporadically with reports of human infection across central Africa from Senegal to Uganda to South Africa. African outbreaks were numerous but tend to be limited. Subsequent spread to southern Asian countries probably occurred via shipping, where large urban outbreaks were reported.
Three distinct lineages of chikungunya virus have been identified by genetic analyses: the west African lineage, the East Central South African (ECSA) lineage and the Asian lineage.
A re-emergence of chikungunya virus epidemics occurred in coastal Kenya in 2004 and spread to several Indian Ocean islands including the Comoros, Mauritius, the Seychelles, Madagascar, Mayotte and La Reunion. The magnitude of the CHIKV outbreak in La Reunion island was unexpected, with approximately 266 000 cases (34% of the total island population).

The strain which initiated the outbreak in the Indian Ocean islands, named Indian Ocean lineage (IOL), expressed an E1 envelope glycoprotein with the amino acid alanine (A) at position 226 (A226). However, strains isolated from the same geographic region later in the outbreak expressed either the alanine (A226) or valine residues at position 226 (V226) in the same E1 glycoprotein. The new V226 genotype largely dominated in infected humans. It was proposed that E1 A226V mutation is directly responsible for a significant increase in CHIKV infectivity for *Aedes albopictus,* the predominant mosquito vector in this area (Tsetsarkin et al., 2007). It provides a plausible explanation of how this mutant virus caused an epidemic in a region lacking the typical vector *Aedes aegypti*. If initially, the mutation in the E1 glycoprotein was shown to modify cholesterol dependence of the virus (Tsetsarkin et al., 2007), the same group finally argue that chikungunya virus adaptation to *Aedes albopictus*

mosquitoes does not correlate with acquisition of cholesterol dependence or decreased pH threshold for fusion reaction (Tsetsarkin et al., 2011).

In 2006, the re-emergence of chikungunya virus was reported in India with more than one million cases with *Aedes aegypti* implicated as the mosquito vector. In 2007, an exportation event of CHIKV from India to Italy resulted in the first autochthonous transmission in a subtropical area. The spread in Italy was limited in both space and time, however, it demonstrated the risk of transmission in areas where only vector *Aedes albopictus* was present.
More recently a global expansion of chikungunya virus distribution occurred from 2011 to 2014 with outbreaks in the western Pacific, the South Pacific, the Caribbean and the spread of Asian lineage strains in Americas and of ECSA lineage to Brazil. The map in figure 8 shows the different countries where chikungunya cases have been reported.

2 - Mosquito vectors

a. Vectors and distribution

In Africa, chikungunya virus is a zoonotic virus principally transmitted to primates by female *Aedes* mosquitoes. Enzootic strains of CHIKV have been detected in diverse mosquito species such as *Aedes (Ae) aegypti, Ae. furcifer, Ae. taylori, Ae. luteocephalus, Ae. africanus* and *Ae. neoafricanus* (Coffey et al., 2014). In Asia, the virus is mainly maintained in cycles between *Ae. aegypti*, *Ae. albopictus* and humans. *Ae. aegypti* is well adapted to the urban environment and prefers to feed on humans while *Ae. albopictus* is primarily a forest specie that has become adapted to rural, suburban and urban human environments. These two anthropophilic mosquitoes are widely distributed and can coexist in the same areas and often share larval habitats. Indeed, since several decades *Ae. albopictus* mosquitoes are established in many parts of the world, including Europe, north and south America (Fig.9).

The expansion of *Ae. albopictus* distribution is linked to climate changes, human activities and global commerce exchanges. *Ae. albopictus* presents many features of a good viral vector. It is aggressive and diurnal, it survives in both rural and urban habitats, it has a long lifespan and it is zoophilic and anthropophilic. Moreover, eggs are resistant to desiccation and remain viable for many months without water. The propagation of this competent anthropophilic vector enables the spread of chikungunya virus (Higgs and Vanlandingham, 2015).

The global distribution of *Aedes aegypti* and *Aedes albopictus* mosquitoes is shown on the map of figure 9.

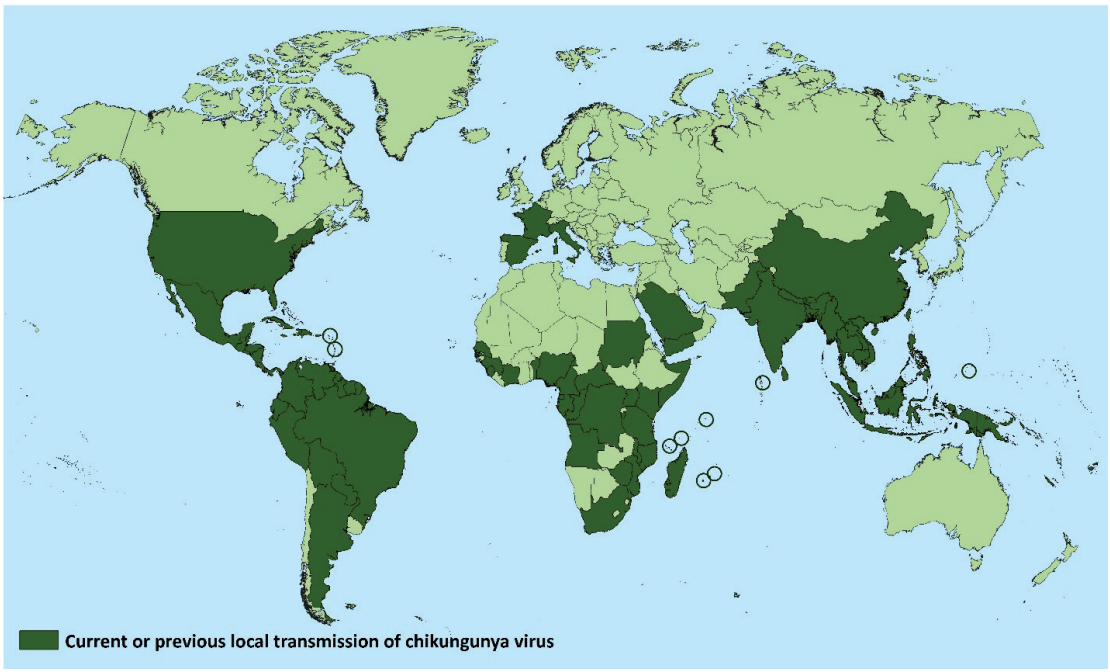

*Does not include countries or territories where only imported cases have been documented.

Figure 8: Countries and territories where chikungunya case have been reported - May 2018 *(Centers for Disease Control and Prevention)*

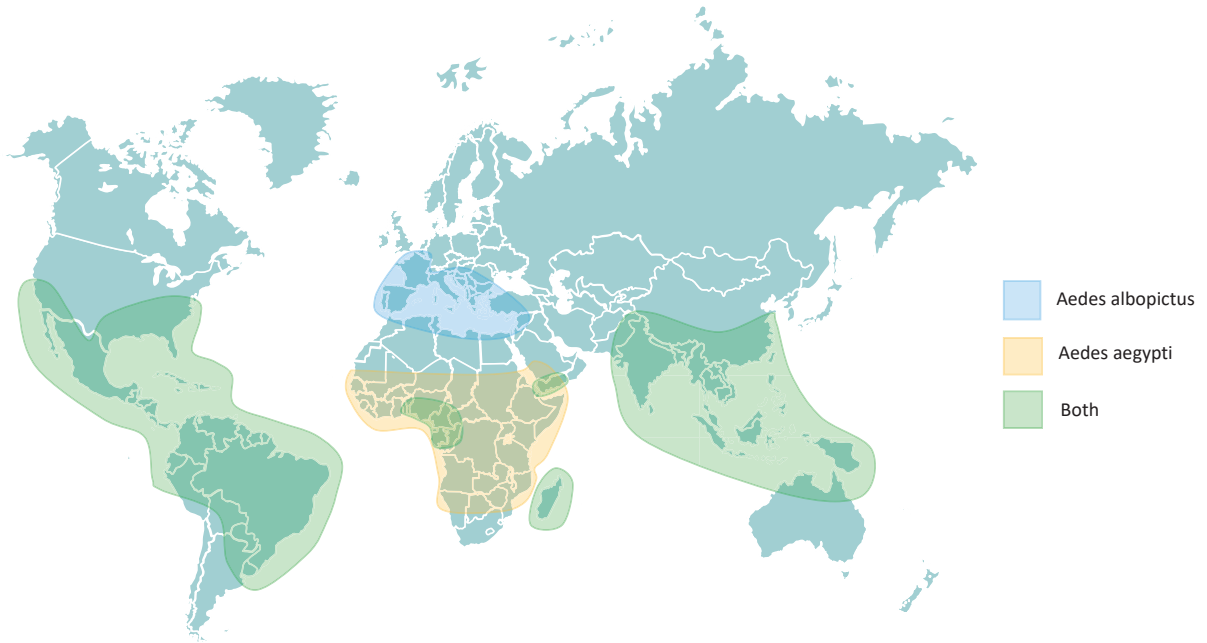

Figure 9: World distribution of *Aedes aegypti* and *Aedes albopictus* vectors

b. Viral infection in mosquitoes

Aedes mosquitoes are competent vectors for chikungunya virus. This means that *Aedes* mosquitoes are able to acquire the virus, replicate it and successfully transmit it to another susceptible host. Chikungunya virus causes a chronic non-cytopathic infection in mosquito cells (Li et al., 2012). Female mosquitoes mainly become infected after a blood meal on viremic individuals (Fig.10), although vertical transmission *via* infected eggs may also occur at a low rate (Agarwal et al., 2014). During the extrinsic incubation period in the vector, CHIKV replicates in the epithelial cells of the midgut and disseminates through the body cavity to infect the salivary glands. Infection of salivary glands allows the release of the virus into the salivary ducts for oral transmission to vertebrates (Lim et al., 2018).

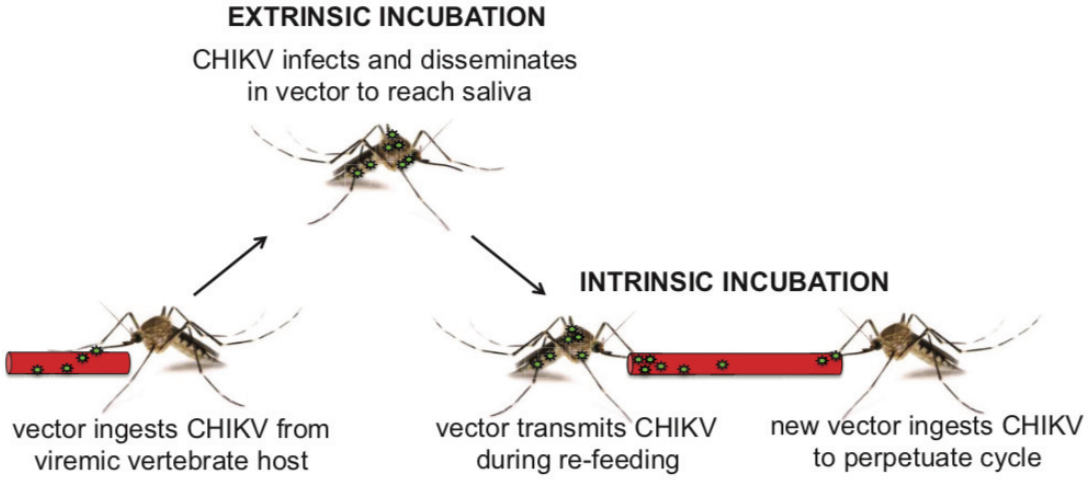

Figure 10: Process of infection and transmission of chikungunya virus by vectors (Coffey et al., 2014)

c. Transmission cycle

Chikungunya virus circulates through two transmission cycles: an enzootic sylvatic cycle and an epidemic/endemic urban cycle, described in figure 11. The enzootic sylvatic cycle involves nonhuman primates and other vertebrates as reservoir hosts and arboreal *Aedes* mosquitoes.

The urban cycle involves anthropophilic vectors *Ae. aegypti* and *Ae. albopictus* and human amplification hosts.

Interestingly, all of the four arboviruses emerging recently (YFV, DENV, CHIKV and ZIKV) share this transmission cycle. The viruses were able to switch to an urban cycle, causing large epidemics, typically based in cities, as they were able to sustain interhuman transmission. They generate viremia titers sufficient to infect at least some

mosquito species including urban *Ae. aegypti* and when the density of mosquitoes and humans are sufficient, an urban cycle can be established.

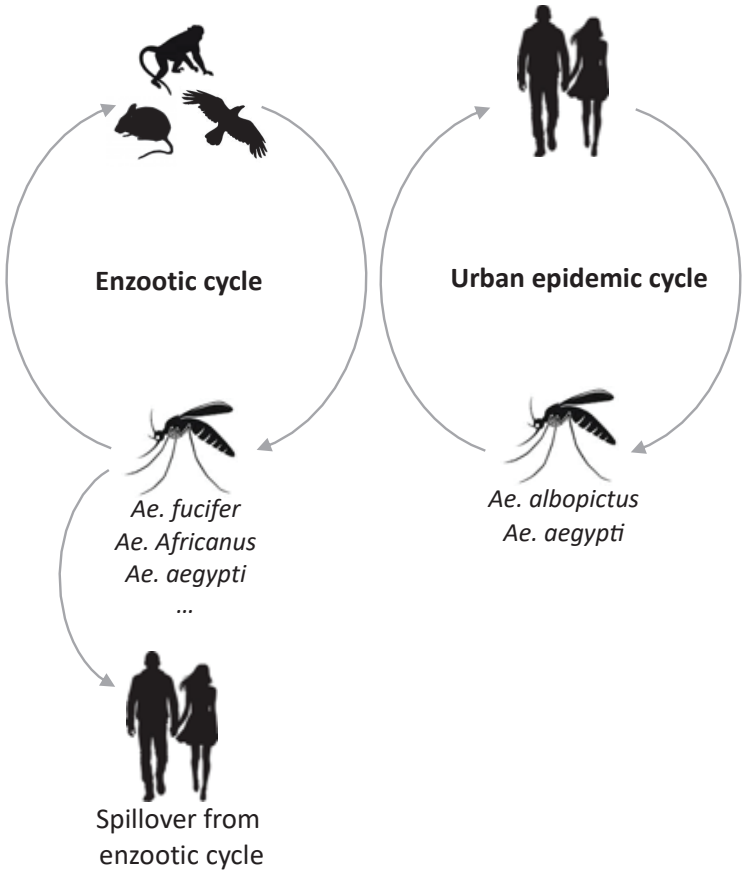

Figure 11: Sylvatic and urban cycle of alphavirus transmission

3 - Chikungunya infection in humans

a. Pathogenesis

Transmission of chikungunya virus to humans generally occurs through a bite by infected *Ae. aegypti* or *Ae. albopictus* mosquito. Some cases of mother-to-child transmission during childbirth have been observed (Gerardin et al., 2008).
Following transmission, CHIKV replicates in the skin mainly in fibroblasts and then disseminates to the liver, joints, muscles and lymphoid tissues, probably through the blood. During the acute phase, the viral load can reach 10^8 particles per milliliter of blood.

CHIKV infection is symptomatic in more than 75% of cases. CHIKV is responsible for a febrile illness called chikungunya fever. The incubation period is usually comprised

between 2 to 7 days and is followed by a rapid-onset clinical disease. Symptoms of chikungunya include sudden high-grade fever, headache, maculopapular rash, severe joint pains (arthralgia), muscle pains (myalgia) and digestive troubles. The acute phase of infection usually lasts from a few days to a couple of weeks.
For 30 to 40% of infected individuals, recurrent joint pains are observed during chronic phase. This chronic phase can last from a few months to several years (Brighton et al., 1984, Toivanen, 2008, Sissoko et al., 2009). Mechanisms underlying chronic persistence of joint pains are not well understood and notably the fact that infectious virus cannot be isolated from these patients, even if some CHIKV antigens have been observed in some joints.

CHIKV-associated neuropathology was described early in the 1960s but neurological diseases were rarely observed and CHIKV was usually considered as a non-fatal disease. However multiple cases of neuro-invasive CHIKV infection with encephalitis and meningoencephalitis were reported during the outbreak in La Reunion island with a high mortality rate of 1:1000 principally among newborns, infants and elderly individuals (Renault et al., 2007, Staikowsky et al., 2009, Economopoulou et al., 2009).

b. Cellular tropism

Chikungunya virus is able to infect a variety of humans and non-humans cell lines. Sourisseau et al. published in 2007 a list of human cell types that support the replication of CHIKV including among others epithelial carcinoma cell line HeLa, primary skin fibroblasts and kidney epithelial cell line HEK 293T. They show that fibroblasts, epithelial and endothelial cells are the best cellular hosts for efficient viral infection in humans. CHIKV can also replicate in macrophages. However, CHIKV fails to replicate in primary lymphocytes, monocytes and monocyte-derived dendritic cells as well as in monocytoid and lymphoid cell lines (Sourisseau et al., 2007). Sensitivity to CHIKV of neuroblastoma cell line SH-SY5Y has been also reported (Solignat et al., 2009). In addition, it was shown that CHIKV infects skeletal muscle progenitor cells and not muscle fibers. *In vitro*, CHIKV replicates in human muscle progenitors and satellite cells but not in myotubes (Ozden et al., 2007).

c. Cellular response

i. Autophagy

Autophagy is an intracellular catabolic process important for the removal of protein aggregates and damaged organelles (Kuma et al., 2010). This process also serves as innate immune response to remove intracellular pathogens such as viruses (Deretic et al., 2013).

Briefly, the autophagy process is initiated by the formation of double-membrane vesicles surrounding substrates to be degraded which is called an autophagosome. The fusion of autophagosomes with late endosomes and lysosomes results in the formation of a degradative compartment called autophagolysosomes. This complete process required a dedicated protein machinery including autophagy-related genes (Atgs) and cellular organelles (Fig.12).
Chikungunya virus activates autophagy process during infection (Krejbich-Trotot et al., 2011, Joubert et al., 2012). Indeed, an increase of autophagosome number was measured in HEK 293 cells after CHIKV infection (Krejbich-Trotot et al., 2011). CHIKV also provokes the conversion from LC3-I to LC3-II, a marker of autophagosomes, in mouse cells and primary and immortalized human cells (Joubert et al., 2012, Judith et al., 2013). Joubert et al. also show that CHIKV infection induces *de novo* autophagosome formation and fusion with lysosomes by monitoring the formation of both autophagosomes and autophagolysosomes and using lysosomal inhibitor. CHIKV promotes autophagic process by the independent induction of endoplasmic reticulum (ER) pathway and oxidative stress pathway (Joubert et al., 2012). Indeed, ER stress induced by CHIKV infection activates the unfolded protein response (UPR) which in turn triggers autophagy. CHIKV also induces Reactive Oxygen Species (ROS) production leading to autophagic process activation.

Depending on cell type and virus, the autophagy pathway can play both an antiviral or a proviral role (Dong and Levine, 2013).

On one hand, the autophagy machinery has an antiviral effect on CHIKV infection. Depletion of a particular autophagy receptor, p62, increases CHIKV replication (Judith et al., 2013). Indeed, p62 recruits the capsid of CHIKV to the autophagosome via LC3B in a SMURF1-independent manner and a ubiquitin-dependent manner for degradation, and thus prevents the cytotoxic effect induced by CHIKV capsid (Fig.13). Same observation of capsid clearance by autophagy was made for SINV but with a process SMURF1-dependent and ubiquitin-independent (Orvedahl et al., 2010).
On the other hand, CHIKV also subverts the autophagy process to aid its replication. Several pieces of evidence show that blockage of autophagy reduces CHIKV infection whereas its induction enhances infection. Using inhibitor of autophagy and small interfering RNA (siRNA) targeting the autophagy protein Beclin-1 in human embryonic kidney cells, Krejbich-Trotot et al. demonstrated that autophagy is required for effective CHIKV replication and enhances viral replication (Krejbich-Trotot et al., 2011). Depletion of two autophagy actors, Beclin-1 and Atg7, also decreases CHIKV

replication in HeLa cells (Judith et al., 2013). Moreover, the autophagy receptor NDP52 interacts with CHIKV nsp2 in human cells and recruits it to the trans-Golgi network by binding to membrane-anchored LC3C (Fig.13). It induces autophagic process and seems to support viral replication by facilitating the assembly of the replication complex (Bouraï et al., 2012, Judith et al., 2013). This dual role of autophagy is illustrated and resumed in figure 13.

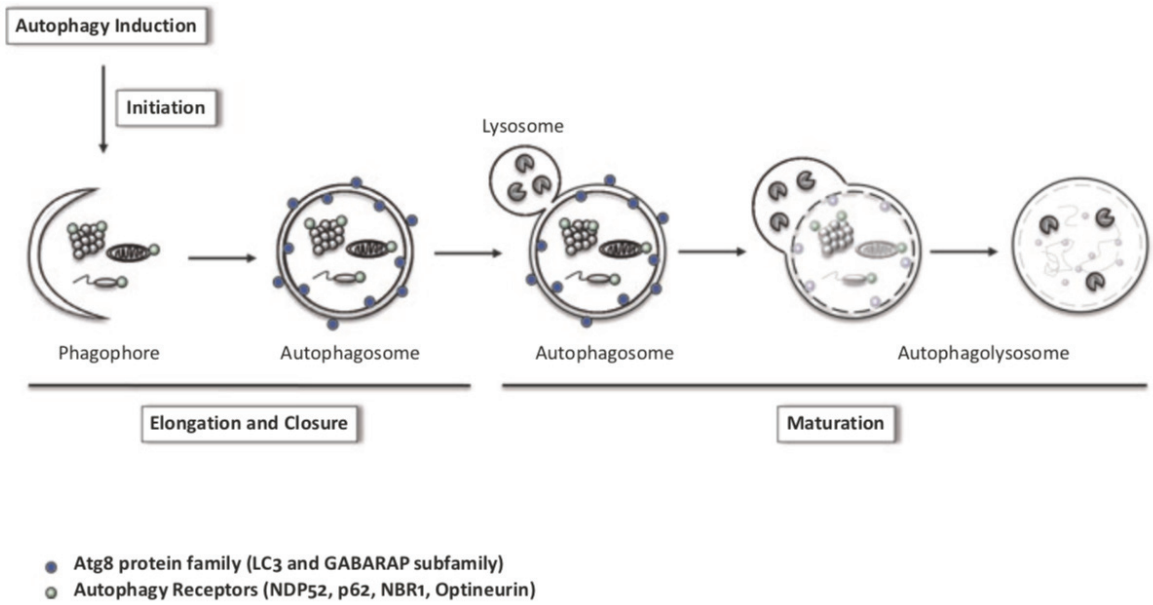

Figure 12: Overview of the autophagy pathway
Autophagy is induced by stress signals and initiated by the formation of isolation membranes or phagophore from the ER which involves Beclin-1 and VPS34 protein complex. Several proteins and complexes are required for the elongation and the closure of the autophagosome. Maturation steps begin by the fusion with endocytic compartment including early endosome, multi-vesicular body, late endosome and lysosome. The fusion with the lysosome leads to the acidification of the lumen of the autophagolysosome and the acquisition of hydrolytic enzymes, followed by the degradation and the recycling of sequestered materials.

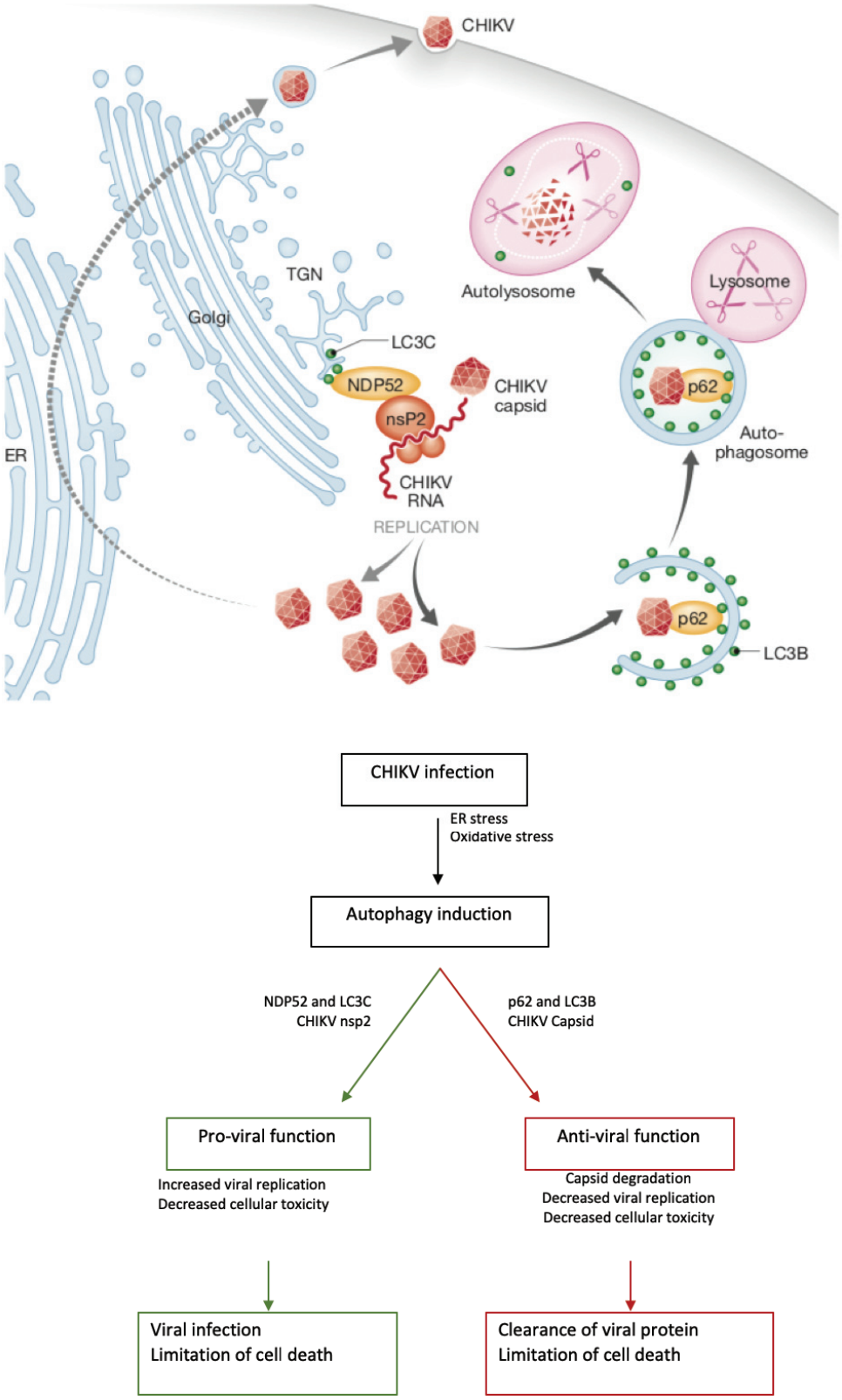

Figure 13: Dual effect of the autophagic machinery on CHIKV replication
ER: endoplasmic reticulum, LC3B: light chain protein 3B, LC3C: light chain protein 3C, NDP52: nuclear dot protein 52, TGN: trans Golgi network.
(adapted from Münz, 2013)

i. Apoptosis

Many different signals can trigger apoptosis such as viral entry, cellular injury and death receptor signaling, leading to a cascade of activation of cysteine aspartyl proteases known as caspases. Caspases are essential for the initiation and the execution of the apoptotic process. This activation induces membrane modification, cleavage of cellular constituents and DNA fragmentation. Apoptosis is characterized by the release of membrane-delimited apoptotic bodies and blebs which are taken up by neighboring cells and professional phagocytes in a non-inflammatory manner. Apoptosis occurs by both intrinsic and extrinsic pathways.
In the intrinsic pathway, also called mitochondrial-dependent apoptosis, mitochondrial events trigger the activation of initiating caspase-9. The extrinsic pathway is mainly mediated by signal transduction through death receptors which activates caspase 8 or 10. Nevertheless, both pathways lead to the activation of effector caspases and may be interconnected.

In many viral infections, apoptosis is used as a first-line defense mechanism (Fig.14) (Upton and Chan, 2014). In the case of CHIKV, infection induces cytopathic effects and rapidly triggers apoptosis to limit virus production and spreading (Sourisseau et al., 2007). Indeed, infection with CHIKV leads to the relocalization of Bax protein to the mitochondria and the cleavage of PARP, a target of effector caspases. It has also been shown that CHIKV infection triggers both caspase-9-dependent and caspase-8-dependent pathways (Krejbich-Trotot et al., 2011).

Furthermore, apoptosis could also have a proviral role (Fig.14). It has been demonstrated that CHIKV hijacks the apoptotic machinery through the formation of apoptotic blebs enclosing viral components subsequently engulfed by neighboring cells (Krejbich-Trotot et al., 2011). This mechanism limits the inflammatory response and promotes viral spreading.

Interestingly, Joubert et al. have shown a relationship between autophagy process and apoptosis in the context of viral infection. Based on kinetic studies, they demonstrated that autophagy is a pro-survival mechanism that delays apoptotic cell death induced by CHIKV but is ultimately overwhelmed by viral replication (Joubert et al., 2012)

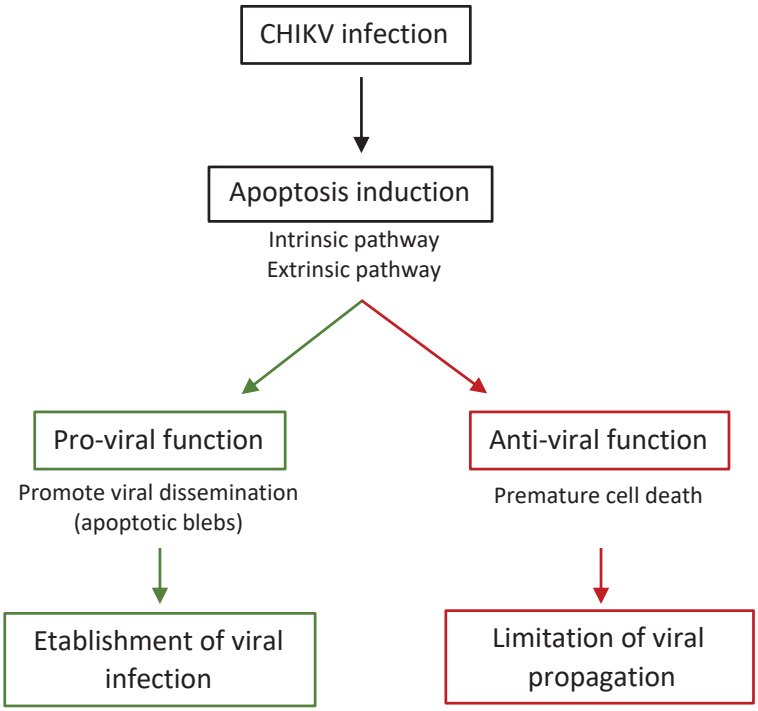

Figure 14: Proviral and antiviral roles of apoptosis on CHIKV infection

d. Immune response

The innate immune response against CHIKV induces activation of components of the cell-mediated immunity. In fibroblasts and other infected cells, single-stranded RNA (ssRNA) and intermediate double-stranded RNA (dsRNA) can be recognized by pathogen recognition receptors called Toll-like receptors (TLRs) and retinoic acid-inducible gene I (RIG-I)-like receptors (RLRs) (Fig.15). TLR7 and TLR8 are engaged by ssRNA while TLR3 is triggered by dsRNA. The two RLRs, RIG-I and MDA5, detect viral RNA in the cytoplasm. These receptors activate a cascade of signalization *via* their common adaptor called mitochondrial antiviral signaling (MAVS). This triggers the induction of type I interferon (IFN-I) and production of pro-inflammatory cytokines (Her et al., 2015; Schwartz and Albert, 2010). In addition, MAVS also recruits caspase-8 to mitochondria to mediate caspase-3 activation and apoptosis in a Bax/Bak-independent manner (El Maadidi et al., 2014). Interestingly, this response links innate antiviral signaling to apoptosis.

Induction of cytokines and chemokine recruits Natural Killer (NK) cells, macrophages, inflammatory monocytes, and $CD4^+$ and $CD8^+$ T cells. Hence, CHIKV infection leads to a protective cellular and humoral adaptive immunity. T cells are important effector cells during viral infection. Both $CD4^+$ and $CD8^+$ T cells can eliminate virus-infected cells. $CD8^+$T cells seem to be preferentially activated in the early stages of infection

while a switch from $CD8^+$ T cells to $CD4^+$ T cell lymphocyte-mediated immune response occurs in the later stages of acute infection. The activation of the humoral response induces the development of neutralizing antibodies (Tanabe et al., 2018).

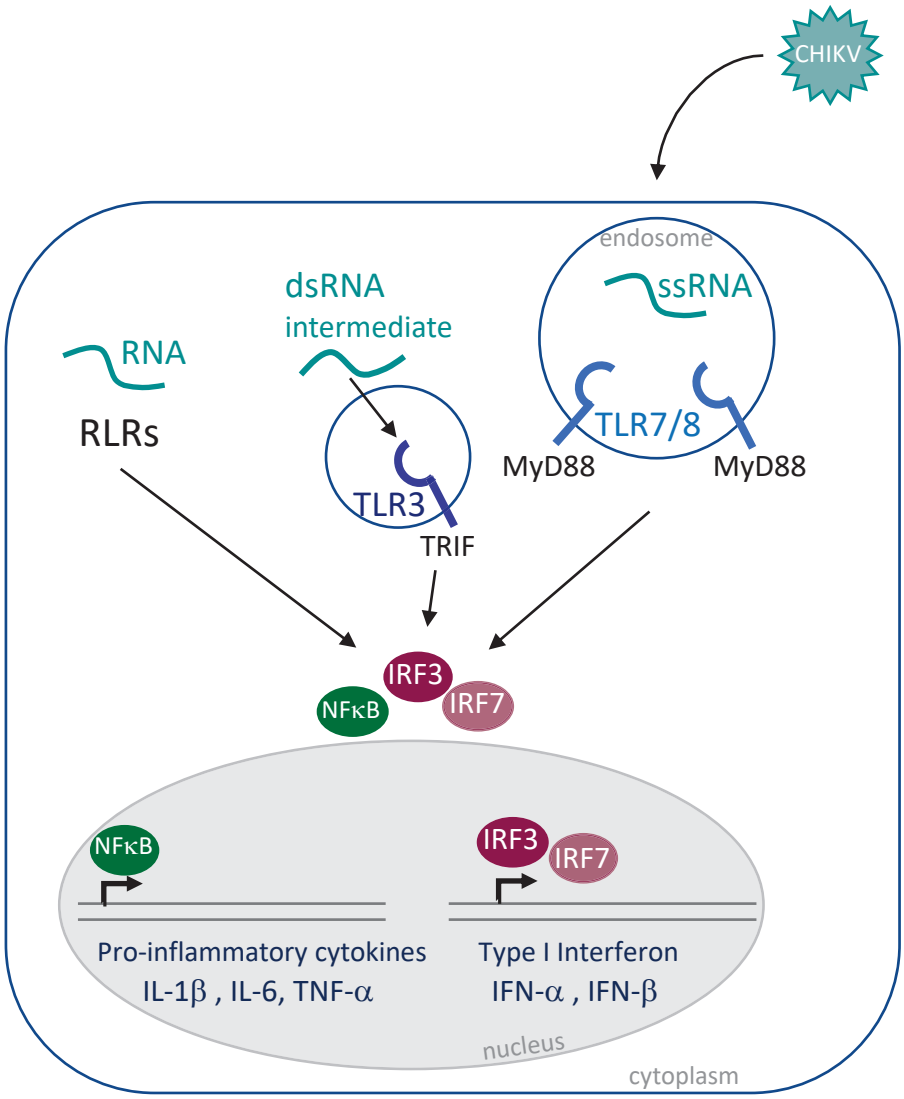

Figure 15: Innate immune control of CHIKV

MyD88: myeloid differentiation primary response protein 88, TRIF: TIR domain-containing adaptater-inducing IFN-β, IRF: IFN regulatory factor, NFκB: nuclear factor κB, IL: interleukin, TNF: Tumor Necrosis Factor.

e. Diagnostic

Chikungunya virus infection is diagnosed on the basis of clinical, epidemiological and laboratory criteria. Given similarities in clinical manifestations of CHIKV infection with other arboviruses like Dengue virus, the use of specific diagnosis assays is crucial.

The laboratory diagnosis assays of CHIKV infection are based on the kinetic of infection (Fig.16). Detection of viral RNA by molecular assays permits diagnosis during the acute viremic phase. Molecular assays include detection of viral RNA of E1 protein, nsp1 or nsp2 by reverse transcription-polymerase chain reaction (RT-PCR) (Pastorino et al., 2005, Carletti et al., 2007, Ho et al., 2010).

Diagnosis by viral isolation can be performed from the serum of infected individuals on insect cell lines or VeroE6 mammal cell line. It can also be useful for epidemiological studies, pathogenesis studies or molecular characterization. However, early antibody response limits virus isolation.

Other diagnosis assays rely on serological methods such as Enzyme-linked assays (ELISA) and indirect immunofluorescence assays (IFA), hemo-agglutination inhibition (HI) and microneutralization (MNt). zELISA and IFA can distinguish between IgM (acute phase) and IgG (late or after infection) antibodies. IgM appear 2-3 days after the onset of clinical illness and persist for several weeks to months while IgG antibodies are detected soon after IgM (day 7-8) and persist for years (Johnson et al., 2016).

f. Antiviral treatments and vaccines

No antiviral drugs or licensed vaccines are available against CHIKV and patients are symptomatically treated with anti-inflammatory drugs.
Chloroquine, commonly used as an anti-malaria drug, showed promising results on CHIKV infected patients in a study more than 30 years ago (Brighton, 1984). Although chloroquine shows a strong antiviral effect in cell culture, it has no effect on patients and seems, quite the opposite, to exacerbate the acute infection and to delay cellular and humoral response in non-human primate models and in patients (de Lamballerie et al., 2009, Roques et al., 2018).
Broad-spectrum anti-viral combination of ribavirin and interferon have been shown to inhibit CHIKV infection in cell culture, but further studies are required to support the clinical efficiency *in vivo* (Briolant et al., 2004, Gallegos et al., 2016). On the contrary, the small anti-inflammatory molecule bindarit has been shown to be effective to treat CHIKV infection induced arthritis (Rulli et al., 2011). Moreover, a drug used against influenza and other respiratory infections, called Arbidol, which impacts membrane remodeling and fusion, proved to efficiently inhibit CHIKV replication on a human cell line (Delogu et al., 2011).

Given recent CHIKV outbreaks, many research approaches were used to develop a vaccine triggering a high level of antibodies and providing lasting immunity. As of 2018,

about 40 vaccine candidates have been developed. These approaches include virus-like particle (VLP) vaccines, subunit vaccines, chimeric vaccines, nucleic acid vaccines and live attenuated vaccines (Powers et al., 2017). Some approaches are described below.

One of these approaches permits the generation of a vaccine candidate CHIKV/internal ribosome entry sequence (IRES) by manipulation of the structural protein expression of a wild type CHIKV (La Réunion strain) and the IRES of encephalomyocarditis virus (EMCV). This vaccine candidate has presented promising results in mice and it is being tested in nonhuman primates (Plante et al., 2011).

In parallel, another approach with a chimeric vaccine using the backbone of vascular stomatitis virus (VSV) and structural proteins of CHIKV showed an efficient induction of neutralizing antibody response in mice against CHIKV infection (Chattopadhyay et al., 2013).

A virus-like particle vaccine derived from a West African lineage strain (CHIKV strain 37997) has been shown to be immunogenic, safe and well tolerated in phase I and II of clinical trial (Chang et al., 2014).

In addition, a recombinant Measle virus-based chikungunya vaccine has been demonstrated to be safe and highly immunogenic in humans. Clinical evaluations are ongoing for this promising candidate vaccine against chikungunya fever (Gerke et al., 2019).

Nowadays, the predominant need for a vaccine is within low- and middle-income countries although it could be used by travelers and military. However, the cost of production and the requirement for immunization campaign may discourage widespread use in these countries where CHIKV is endemic, such as India, Bangladesh and southern Indian Ocean islands.

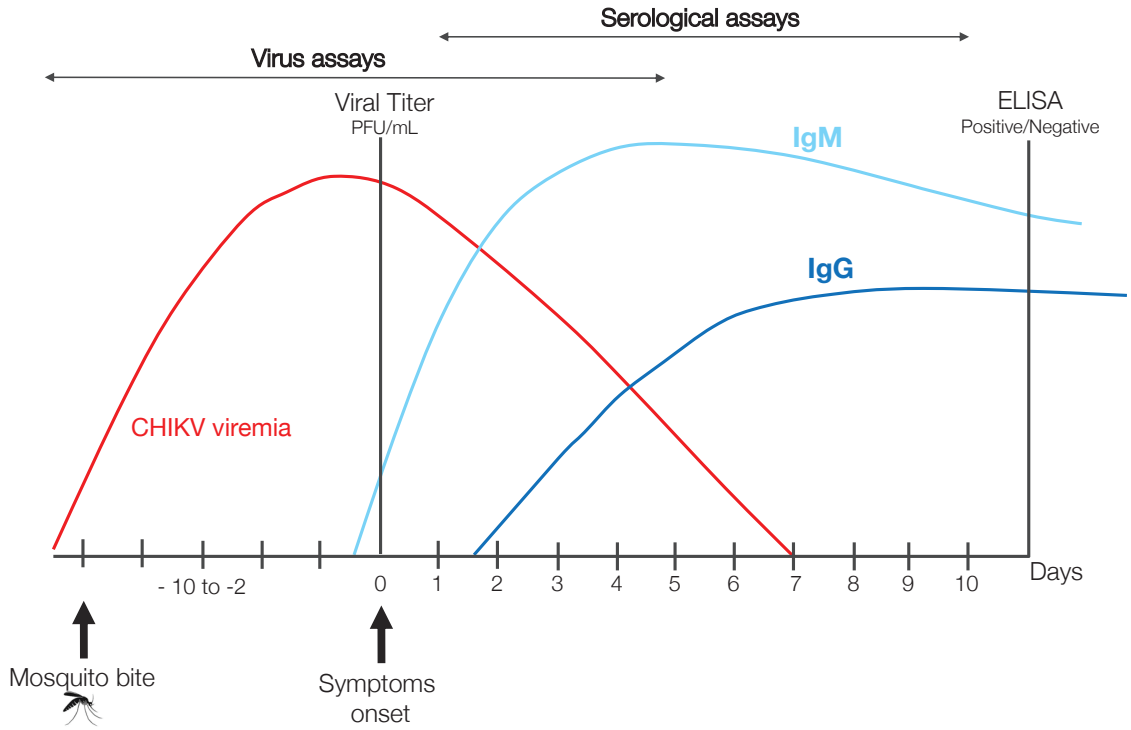

Figure 16: Chikungunya virus pathogenesis and diagnosis assays range.
Following transmission by mosquito bite, infected individuals present an acute onset of disease with an increasing viremia. Biomarkers used in diagnostic assays to detect CHIKV infection are shown on the timeline.

III - CRISPR/Cas9 gene editing scissors

1 - Traditional genetic tools

a. Homologous recombination

Since the discovery of the deoxyribonucleic acid (DNA) double helix, the possibility of genome modification run through the mind of researchers and scientists. One of the first techniques to modify DNA in eukaryotic cells is called gene targeting. This method enables to modify an endogenous gene by homologous recombination (HR). Nevertheless, HR was complicated to use routinely as it shows poor efficiency. Two studies have shown that introduction of double-strand break (DSB) could enhance the efficiency of gene targeting (Rouet et al., 1994; Rudin and Haber, 1988).

b. Zinc finger nuclease

During the 90's, the discovery of zinc finger-mediated DNA binding and the endonuclease domain of the FokI enzyme led to the development of Zinc Finger Nucleases (ZFNs) (Li et al., 1992; Pavletich and Pabo, 1991). ZFNs are fusion proteins composed of a DNA-sequence-specific zinc finger protein and a nuclease domain derived from the FokI restriction endonuclease. They are designed as a pair that recognizes DNA sequences flanking the target site, one on the forward strand and the other on the reverse strand. The binding of the two ZFNs permits the dimerization of FokI nucleases which generate a DSB of the DNA between the DNA binding sites (Fig.17). Such ZFNs were found to be effective at inducing genomic sequence changes in *Drosophila* and mammalian cells (Bibikova, 2003; Bibikova et al., 2002). Although ZFN efficacy was reported for genome editing, they were not widely used as designing and engineering proteins targeting a specific DNA site of interest was very challenging.

c. TALEN

Later, the DNA binding domain of the transcription activator–like effector (TALE) from *Xanthomonas,* a bacterial plant pathogen, was described (Boch et al., 2009; Moscou and Bogdanove, 2009). Similarly to ZFN, this domain can be coupled to the FokI nuclease to create transcription-activator-like effector nuclease (TALEN) (Miller et al., 2011). In this way, TALEN are programmable fusion nuclease composed of a DNA-sequence-specific transcription-activator-like effector (TALE) protein and a nuclease domain derived from the FokI restriction endonuclease (Fig.17).

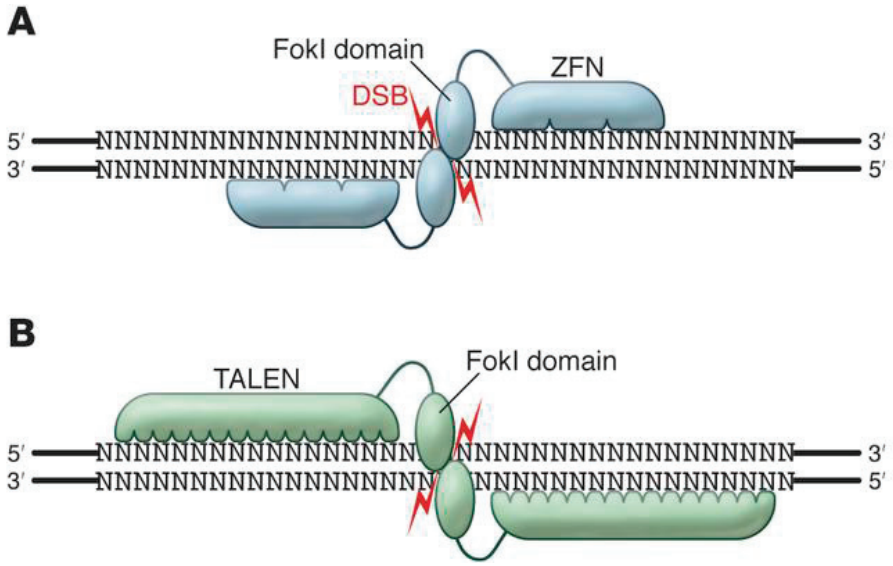

Figure 17: Schematic representation of ZFN and TALEN binding on DNA
(Gupta and Musunuru, 2014)

d. RNA interference (RNAi)

RNA interference (RNAi) has been discovered and described by Fire and Mello with their work on *Caenorhabditis elegans* in 1998 (Fire et al., 1998). The RNAi pathway used by cells for regulating gene expression is a well conserved process found in many eukaryotes described in figure 18. This discovery has rapidly resulted in the widespread use of synthetic small RNAs (Elbashir et al., 2001). Indeed, the cellular RNAi machinery can be redirected by introducing synthetic small RNAs into cells such as short-interfering RNAs (siRNAs) or short-hairpin RNAs (shRNAs). They target specific mRNA and promote their degradation which subsequently leads to the reduction of the protein level.

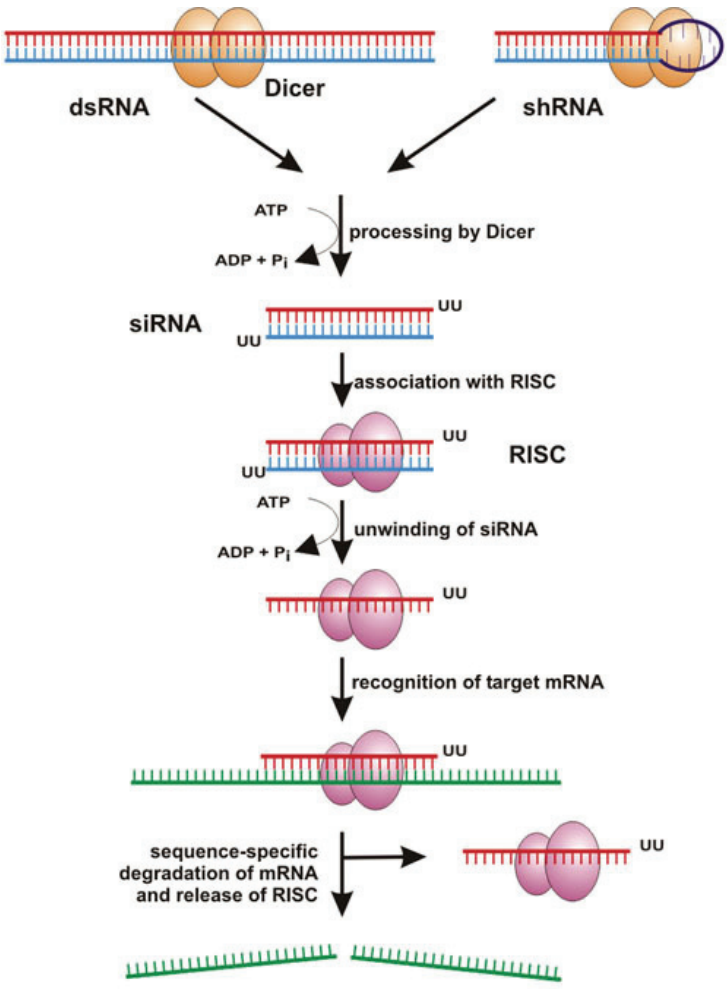

Figure 18: Gene silencing by RNA interference
Long dsRNA and shRNA are processed into siRNA by an enzyme called Dicer (in orange). The siRNA is recruited by an RNA-induced silencing complex (RISC, in pink) and the unwinding of the siRNA activates the complex. RISC targets a messenger RNA (mRNA, in green) leading to its cleavage and degradation. (Rutz and Scheffold, 2004)

2 - Discovery of the bacterial adaptive immunity system CRISPR/Cas

CRISPR acronym stands for Clustered Regularly Interspaced Short Palindromic Repeats. CRISPR/Cas systems are well-known acquired immunity systems that are widespread in archaea and bacteria. The first report of CRISPR was in 1987 when unusual repetitive sequences, later named CRISPR, were observed in *Escherichia coli* (Ishino et al., 1987). Similar sequences were then reported in an increasing number of distant bacterial and archaeal genomes suggesting an unknown but important function in prokaryotes (Mojica et al., 1993, 2000). These palindromic repeated sequences were shown to be interspaced with non-repetitive spacers. DNA repeated sequences were finally named CRISPR and genes associated with CRISPR

sequences were identified and called Cas genes for CRISPR-associated genes (Fig.19) (Jansen et al., 2002). In 2005, three different groups have reported that the spacers were similar to sequences of bacteriophages, archaeal viruses and plasmids suggesting a bacterial immune system role (Bolotin et al., 2005; Mojica et al., 2005; Pourcel et al., 2005). The demonstration that CRISPR/Cas systems are involved in acquired immunity against bacteriophages was quickly published (Barrangou et al., 2007). The following year, CRISPR RNAs (crRNAs) were then identified as guides in complex with Cas proteins to target specific DNA (Brouns et al., 2008).

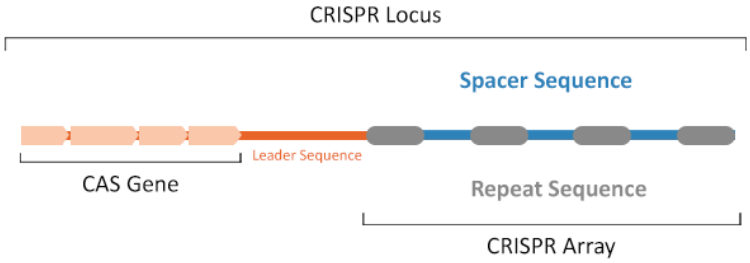

Figure 19: CRISPR/Cas locus
CRISPR/Cas loci consist of CRISPR array of identical repeats interspaced with invader DNA-targeting spacers encoding crRNA components and an operon of Cas genes encoding the Cas proteins.

In bacteria the CRISPR adaptive immunity process is divided into three stages: **acquisition**, **expression** and **interference** (Fig.20). During the immunization process or acquisition, exogenous DNA from virus or plasmid is recognized by a Cas complex. This complex cleaves DNA and incorporates a short sequence of the invading DNA as a spacer sequence into the CRISPR array. After a new insertion of exogenous DNA, the CRISPR array is transcribed into a precursor crRNA (pre-crRNA) that is processed to generate mature crRNAs, each composed of a repeat portion and an invader-targeting spacer portion. crRNA directs specific cleavage of foreign nucleic acid by Cas proteins for degradation (Fig.20).

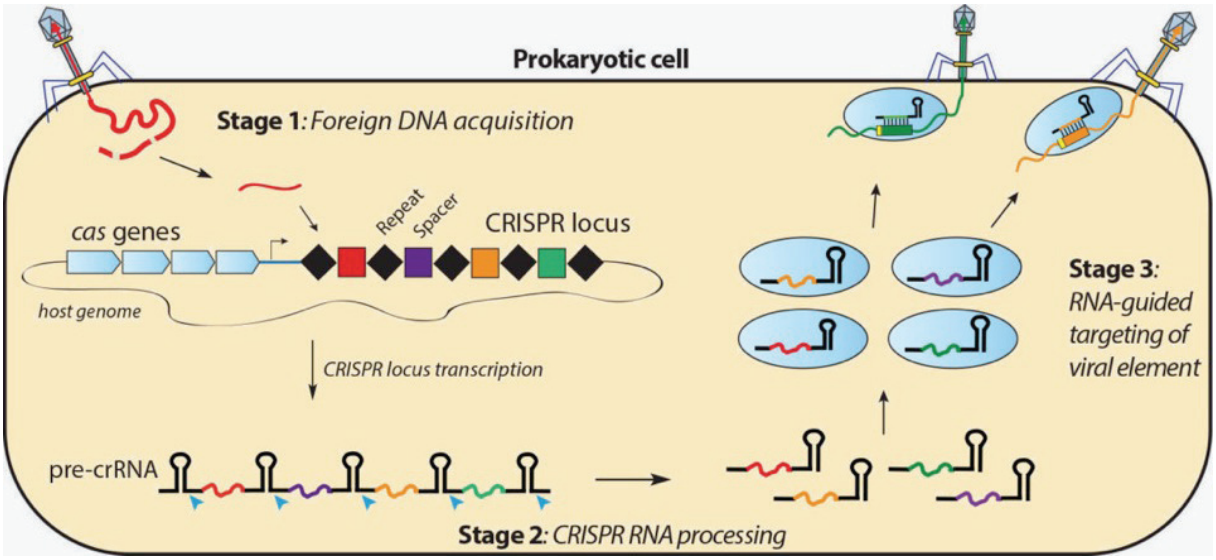

Figure 20: CRISPR acquisition process and immunity process
3 stages:
(1) acquisition: integration of exogeneous DNA into the CRISPR locus
(2) expression: transcription of pre-crRNA processed to crRNA
(3) interference: degradation of foreign DNA by Cas proteins directed by crRNA

3 - CRISPR/Cas mechanism

CRISPR systems have been classified into two major classes divided into six types and more than 30 subtypes (Koonin et al., 2017; Makarova et al., 2015). The conserved common feature of the different CRISPR systems is the acquisition mechanism by Cas1 and Cas2 proteins (Fig.21). These two proteins form a complex which captures about 30 base pairs (bp) of foreign DNA and integrates them into the CRISPR locus during the immunization process (Nuñez et al., 2014). However, the interference mechanism varies significantly among the different CRISPR systems. The class 1 systems (types I, III and IV) use specialized Cas endonucleases to process the pre-crRNAs and then mature crRNA assembles into a large multi-Cas protein complex capable of targeting and cleaving nucleic acids complementary to the crRNA (Makarova et al., 2011; Nishimasu and Nureki, 2017). In contrast, class 2 systems (types II, V and VI) involve a single effector Cas protein for interference process. The type II-A system is the most studied since a genome editing tool has been developed with the Cas9 from *Streptococcus pyogenes*.

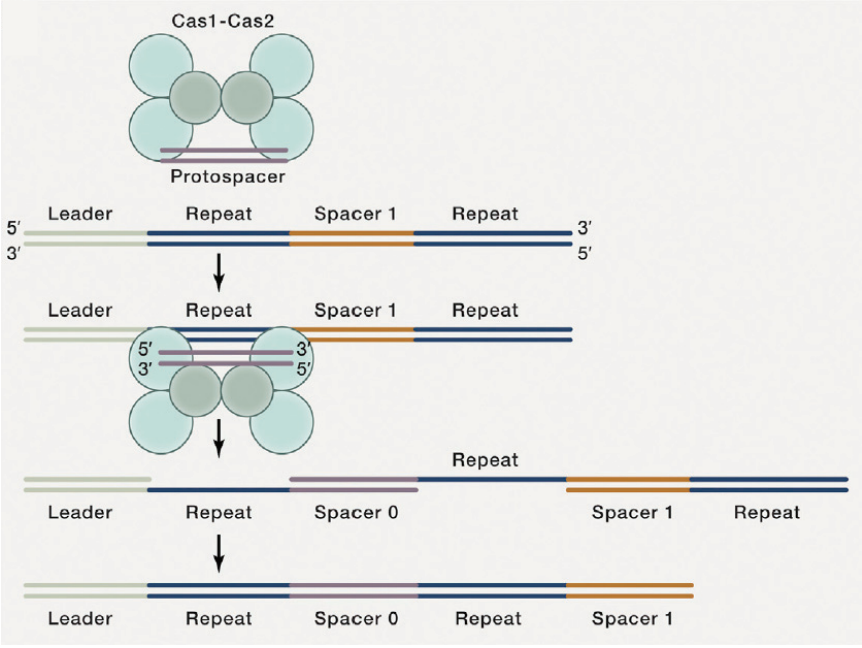

Figure 21: Acquisition mechanism by Cas1-Cas2 complex
The protospacer from exogenous DNA is incorporated into the CRISPR locus by the Cas1-Cas2 complex. (Wright et al., 2016)

Like for the other systems, the mechanism of action of the type II-A CRISPR system of *Streptococcus pyogenes* includes an acquisition mechanism involving Cas1 and Cas 2 proteins. Moreover, in this system, it has been reported that Cas9 and Csn2, a protein encoded by a gene of the Cas operon, also contribute to the acquisition of new spacers (Heler et al., 2015).

For the expression and interference mechanisms in this system, Cas9 protein requires a trans-activating crRNA (tracrRNA) (Chylinski et al., 2013; Jinek et al., 2012). Indeed, after pre-crRNA transcription, tracrRNAs complementary to the repeat sequences in pre-crRNA are recruited and trigger the processing of pre-crRNA into mature crRNA by the ribonuclease RNase III and the Cas9 protein (Fig. 22). In this way, there is a formation of a crRNA/tracrRNA/Cas9 complex. Then, each crRNA/tracrRNA/Cas9 complex will specifically bind to a target DNA sequence complementary to the crRNA (Fig.22). The target sequence contains a short motif called the Protospacer Adjacent Motif (PAM) directly after the target site of the crRNA. The PAM of *Streptococcus pyogenes* Cas9 is 5'-NGG but the motif differs between different strains and types of Cas protein. It has been shown that the complex initially binds to PAM to quickly screen for potential target sequences. If the complex finds an appropriate PAM, the complementarity between crRNA and target sequence is tested (Sternberg et al., 2014). After the complex stably binds, Cas9 separates the double stranded DNA

target and cleaves both strands near the PAM (Fig.22). Finally, the crRNA/tracrRNA/Cas9 complex unbinds after the double-strand break.

The Cas9 nuclease has two functional endonuclease domains, RuvC and HNH. The RuvC nuclease initiates cleavage of the DNA strand not complementary to the guide RNA while the HNH nuclease domain of Cas9 cleaves the DNA strand complementary to the RNA guide (Fig.22).

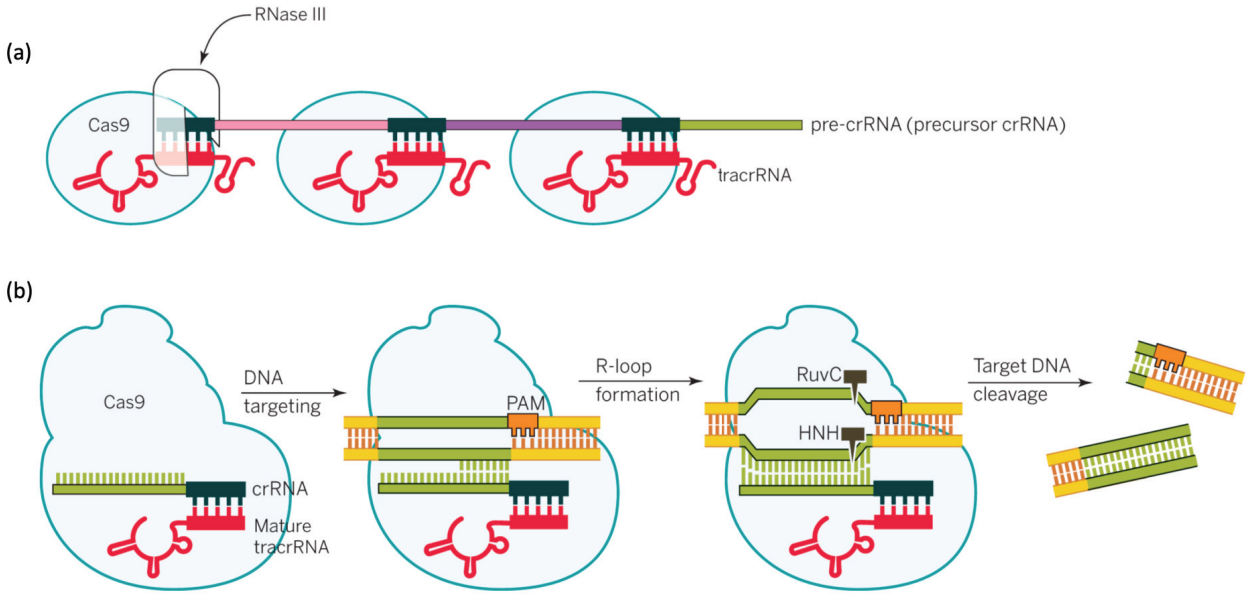

Figure 22: CRISPR/Cas9 system mechanism

(a) Association of Cas9 with tracrRNA and pre-crRNA and processing of pre-crRNA into mature crRNA by RNase III.

(b) crRNA/tracrRNA/Cas9 complex binds to the target sequence followed by PAM and induces DSB. (Doudna and Charpentier, 2014)

4 - CRISPR/Cas9 system as a gene editing tool

a. Mechanism

Jinek et al. have marked the beginning of CRISPR as a biotechnology tool, with the demonstration that Cas9 enzyme from *Streptococcus pyogenes* (*spCas9*) can be reprogrammed to target the desired DNA sequence in bacteria. They have also shown that Cas9 can be guided by a single chimeric RNA formed by the fusion of tracrRNA and crRNA, called single guide RNA (sgRNA) (Fig.23) (Jinek et al., 2012). This publication was quickly followed by revolutionary publications demonstrating that CRISPR can be adapted for *in vivo* genome editing in eukaryotic cells (Cong et al., 2013; Jinek et al., 2013; Mali et al., 2013).

The mechanism of targeting and cleavage of this two components system (sgRNA and Cas9) remains the same (Fig.24). The sgRNA/Cas9 complex identifies a PAM sequence in the genome, then the target-specific sequence of 20 nucleotides of the sgRNA hybridizes with the genomic DNA target sequence leading to a precise double-strand break 3 or 4 bp downstream of the PAM. The requirement of the PAM sequence directly after the 20 bp target sequence does not limit the targeting range in the human genome since the PAM sequence of spCas9 (5'-NGG) can be found in average every 8-12 bp. Regarding the design of sgRNA, many studies have been published to show how to optimize the design in order to maximize efficacy without reducing the specificity (Cui et al., 2018; Doench et al., 2016; Hsu et al., 2013).

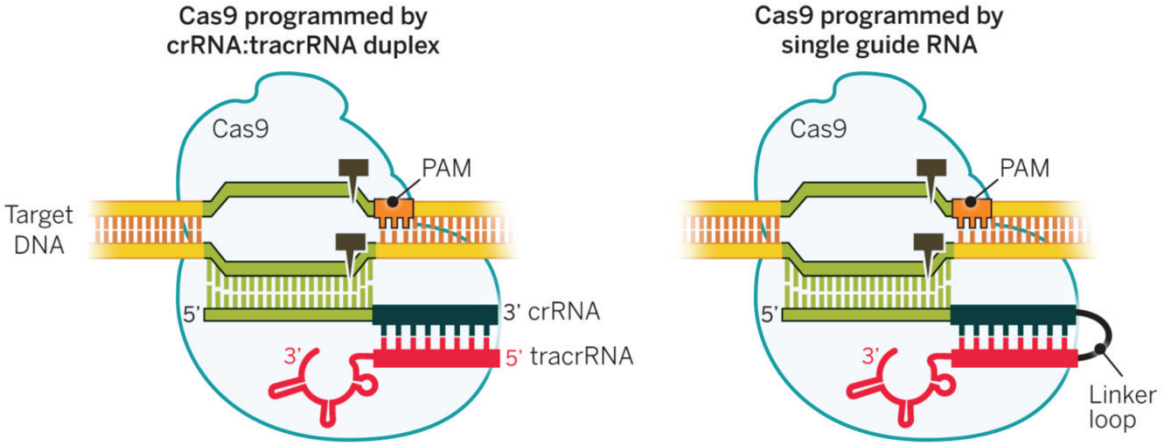

Figure 23: Programmed CRISPR/Cas9 systems with two RNAs or one single RNA ***Left:*** *Two-RNA complex formed by tracrRNA and crRNA guides Cas9 to cleave specific DNA target site.* ***Right:*** *Chimeric sgRNA generated by fusing the 3′ end of crRNA to the 5′ end of tracrRNA guides Cas9 nuclease. (Doudna and Charpentier, 2014)*

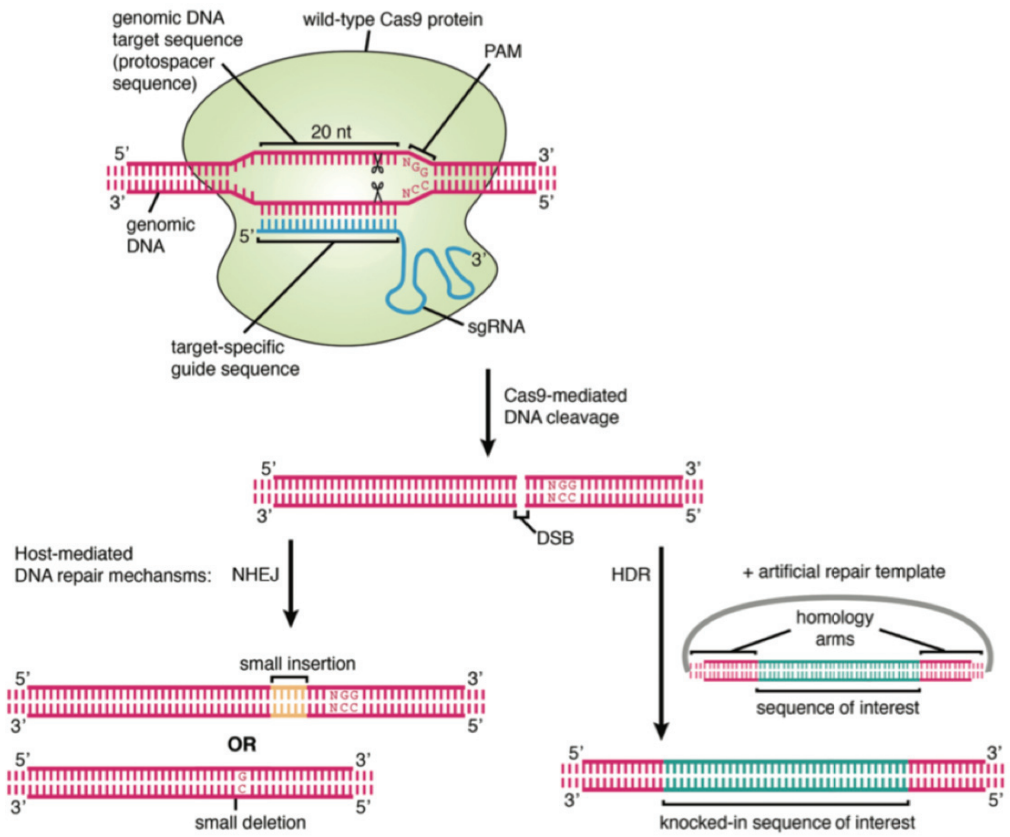

Figure 24: CRISPR/Cas9 mechanism with the single guide RNA (sgRNA)
The 20 nucleotides genomic DNA target sequence must be adjacent to a PAM sequence. Hybridation of sgRNA to the target specific sequence induces a double-strand break (DSB) of the target sequence generated by Cas9. DSB can be repaired by the non-homologous end-joining (NHEJ) mechanism or the homology-directed repair (HDR) process. (Agrotis and Ketteler, 2015)

b. DNA repair

The double strand break induced by Cas9 enzyme can be repaired by one of the two repair mechanisms: the non-homologous end-joining or the homology-directed repair (Fig.24).

The **non-homologous end-joining (NHEJ)** is an error-prone process used to repair DSB in absence of a repair template. This mechanism attempts to ligate the cleaved ends of the DSB together, but it often induces small insertion or deletion at the DSB site. This frequently causes frame shifts or introduces premature stop codons that permanently disrupt the open reading frame of the gene. It enables to generate specific gene knock-out.

The **homology-directed repair (HDR)** process can be used if a repair template is available or added. The DNA repair template has a high degree of homology to the sequence upstream and downstream of the DSB. The cell repairs the DSB by homologous recombination using the repair template. HDR permits to modify the target gene by introducing point mutation or by generating insertion or deletion of DNA fragments.

c. CRISPR/Cas9 limitation

Ideally, a sgRNA has a perfect homology to the target DNA with no homology elsewhere in the genome. Actually, unselective cleavages of DNA sequences that do not fully match the sgRNA have frequently been reported (Frock et al., 2015; Fu et al., 2013; Hsu et al., 2013; Kuscu et al., 2014; Lin et al., 2014b). These off-target events can introduce insertion or deletion mutation at sites in the genome other than the desired target site. Many different tools are available for designing sgRNA minimizing off-target effects based on prediction, but off-targets are challenging to predict (Bae et al., 2014a; Naito et al., 2015; Stemmer et al., 2015). To overcome the off-target effects *in vitro*, several distinct sgRNAs targeting different sequences of the same gene are usually used in separate assays.

In parallel, various strategies have been described to reduce genome off-target mutations.
A Cas9 nickase, a variant of the Cas9, has been developed by introducing a mutation in one of the two nuclease domains (Cong et al., 2013; Ran et al., 2013). This mutant cuts only one strand of DNA (nick) instead of inducing a DSB. A pair of sgRNAs, designed on opposite DNA strands, are required to permit gene editing (Fig.25). Since a single stranded break can be easily repaired by HDR using the non-cleaved complementary strand and the two sgRNAs need to work together to induce DSB, off-target effects are minimized.

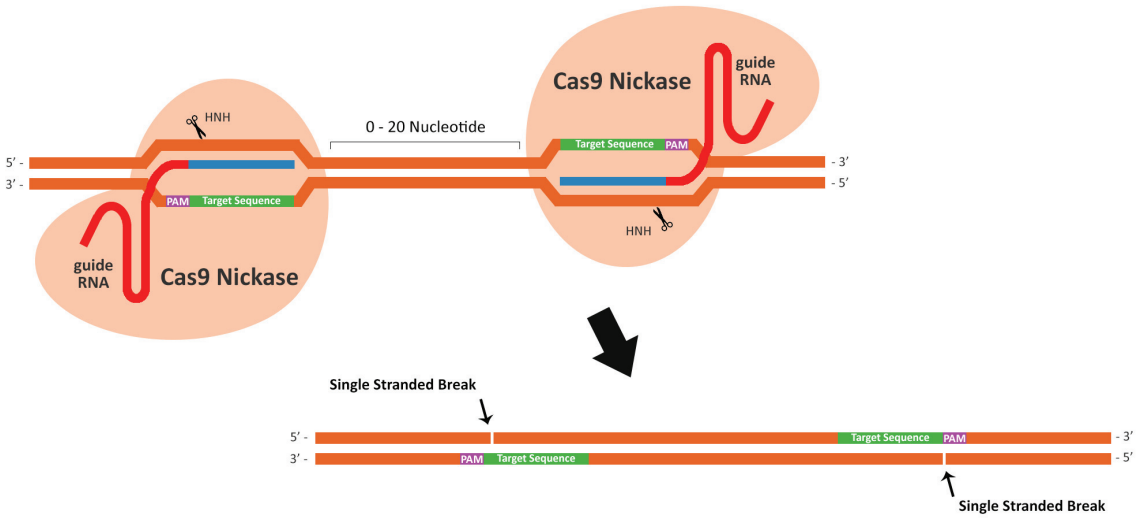

Figure 25: Use of Cas9 nickase recruited by a pair of sgRNAs for gene editing
(From Abm website)

The use of truncated sgRNAs has also been described to improve the Cas9 complex specificity (Fu et al., 2014). Moreover, several high fidelity nucleases such as the spCas9-HF and the HypaCas9, have been developed presenting very low off-target activity (Kleinstiver et al., 2016; Slaymaker et al., 2016).

In addition to the specificity, the efficiency of the CRISPR/Cas9 is another crucial point. The efficiency depends on the sgRNA sequence but is difficult to predict. These efficiency issues have been illustrated notably by the fact that *in vitro* CRISPR/Cas9 system is more efficient in haploid cells than in diploid cells and *in vivo* with mosaicism observations in mice.

5 - Applications

a. Gene knockout

As described above, CRISPR/Cas9 system can be used to generate gene knockout. In absence of a repair template, the DSB generated by Cas9 is repaired by NHEJ that usually induces small insertions or deletions. Thus, there is a shit of the reading frame or an introduction of a premature stop codon, leading to the gene disruption. To maximize the gene disruption, sgRNAs are generated to target the first or the second exon ensuring that frame shift mutations do not generate a partially functional gene product. In addition, a pair of sgRNAs can be used simultaneously to ensure gene knockout, to generate a larger deletion or to remove an exon (Cong et al., 2013). The microhomology-mediated end joining, an alternative NHEJ pathway, should be

avoided near the site of the DSB as they enhance deletion without shift of the reading frame (Bae et al., 2014b).

b. Gene editing

While NHEJ repair often leads to gene disruption, homology direct repair (HDR) mechanism can be used to induce mutations or insert a large fragment after Cas9-mediated DSB. In order to edit a gene, a DNA repair template is introduced with the sgRNA and the Cas9 into the cells. The DNA template must contain the sequence of interest flanked by homology arms. However, even in presence of sgRNA, Cas9 and a DNA template, the efficiency of HDR is generally low, with around 10% of modified alleles. Many studies have enabled to develop approaches to enhance HDR, some are presented below.

The use of small molecules that either inhibit NHEJ or upregulate HDR pathways have been reported to enhance HDR (Chu et al., 2015; Song et al., 2016).

Another approach to increase HDR efficiency is to synchronize cell cycle of all cells in order to introduce Cas9/sgRNA complex during the S/G2 phases of the cell cycle when HDR occurs (Lin et al., 2014a). In the same idea, a group has generated a modified Cas9 that allows a temporal control of Cas9 expression. The modified Cas9 is only expressed during the S/G2 phases of the cell cycle and thus induces DSB at the right time (Gutschner et al., 2016).

More recently, a strategy based on a covalent tethering of the donor DNA to Cas9/sgRNA ribonucleoprotein has been shown to increase HDR repair efficiency. This approach permits to spatially and temporally colocalize the DSB machinery and the template DNA (Aird et al., 2018).

Lastly, the DNA template can be optimized. It has been shown that a single strand DNA template with a length of around 70 nucleotides allows to enhance HDR efficiency (Yang et al., 2013). Moreover, the desired mutation should be as close as possible to the PAM sequence (Liang et al., 2017; Paquet et al., 2016). The 5'-NGG PAM is relatively abundant in the human genome but it may not be positioned correctly to target a specific gene for inducing mutation. Thus several teams have developed nuclease variant with different PAM sequence, for example the Cpf1 nuclease (Gao et al., 2017; Kleinstiver et al., 2015).

c. Base editing

Generation of deactived Cas9 (dCas9) with mutations in both nuclease domains permits the development of many tools. dCas9 is unable to cleave DNA but retains the ability to recognize and specifically bind to DNA when guided by a sgRNA. dCas9 fused with cytidine desaminase has been shown to mediate the conversion of cytidine to uridine within a window of around five nucleotides (Fig.26) (Komor et al., 2016).

d. Activation or repression of a target gene (CRISPRa and CRISPRi)

dCas9 has been also used to activate (CRISPRa) or repress (CRISPRi) target genes (Fig.26). By directly targeting dCas9 to the transcription site with a sgRNA, it permits to block RNA polymerase or disrupt transcription factor binding and thus inhibit gene expression (Dominguez et al., 2016). Many studies have described systems with dCas9 fused with transcriptional repressors or activators that result in robust transcriptional repression or activation of downstream target genes (Cheng et al., 2013; Gilbert et al., 2013; Lawhorn et al., 2014; Maeder et al., 2013; Perez-Pinera et al., 2013).

e. Epigenetic modification

Deactived Cas9 has also been fused to epigenetic modifiers to create programmable epigenome-engineering tools (Fig.26). These tools have the ability to induce histone acetylation, histone methylation or DNA methylation and thus modulate chromatin state and gene expression (Hilton et al., 2015; Thakore et al., 2015).

f. RNA targeting

Nuclease inactive Cas9 has also been fused to a fluorescent protein and programmed thanks to a specific sgRNA to target mRNA (Fig.26). This system offers a means to track RNA in living cells in a programmable manner (Nelles et al., 2016). Interestingly, another Cas protein, the Cas13 has been used to develop diagnostic assay that detects viral RNA of dengue virus and Zika virus (Gootenberg et al., 2017; Myhrvold et al., 2018).

g. Chromatin imaging and chromatin topology

Usually studied by fluorescent in-situ hybridization method (FISH), the organization of the chromatin structure can be studied by the use of fluorescently labeled dCas9 (Fig.26). This customizable DNA labeler permits to detect chromatin dynamics in living cells (Chen et al., 2013a). In addition, tools have been developed to manipulate chromatin topology (Fig.26). This involves the use of two sgRNA targeted dCas9 fused to two dimerizable protein domains. The dimerization of the two induces a forced

chromatin loop formation to understand the function of the chromatin structure and its contribution to gene expression (Morgan et al., 2017).

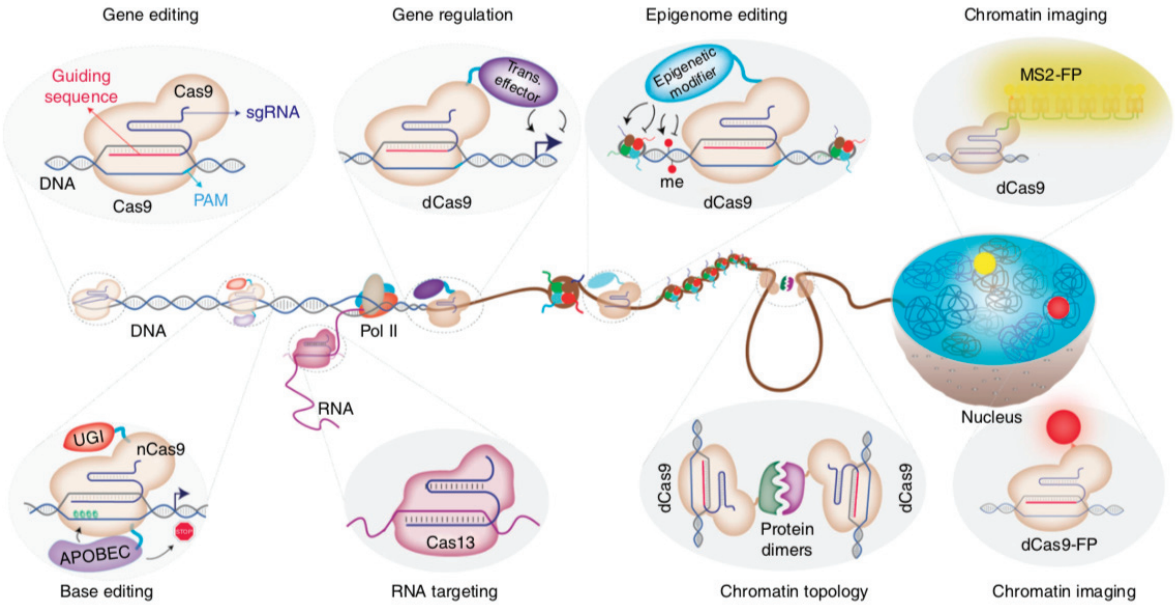

Figure 26: Different applications of the CRISPR/Cas9 system
(Adli, 2018)

6 - Particular application : CRISPR/Cas9 screens

a. Principle

CRISPR screens and genetic screens in general can be designed in two ways, an arrayed format or a pooled format which is mostly used.

In CRISPR arrayed screens, sgRNAs are separately introduced into wells in multi-well plates allowing direct monitoring of the phenotype. In contrast, pooled screens rely on the separation of cells into subpopulations either enriched or depleted for the phenotype of interest. They are based on the simultaneous targeting of a large number of genes in a pooled manner by using a library of sgRNAs. From this library, a library of lentiviruses is usually generated. Then lentiviral library is transduced into cells at a low multiplicity of infection to avoid co-infection by multiple lentiviruses and ensure that most cells receive only one stably-integrated sgRNA. After the screen is complete, genomic DNA of cells with the phenotype of interest is isolated and sgRNA sequences inserted into the genome are amplified by PCR. Finally, PCR amplicons are analyzed by next generation sequencing to determine sgRNA enrichment or depletion due to the applied screening selection pressure.

Many CRISPR screens take advantage of DNA cleavage process mediated by sgRNA-guided Cas9 that are subsequently repaired by the error-prone mechanism NHEJ to generate gene knockout (Shalem et al., 2014; Wang et al., 2014). In this way, a library of sgRNAs is used to generate a knockout library of cells. Many different libraries of sgRNAs are available. They vary in the target species (human, mice), the target genes (genome wide or a subpool of genes), the number of sgRNAs for each gene and the targeted position within the gene (Sanjana et al.; Shalem et al., 2014; Wang et al., 2015). Libraries are usually available as one-plasmid system with Cas9 and sgRNA encoded by the same plasmid or two-plasmids system in which sgRNA and Cas9 are encoded by two separate plasmids (see Part 2 Chapter 1). Cas9 expression can be stable, inducible or transient depending on the vector used.

A similar approach can be used to generate gene knockdown libraries by exploiting catalytically inactive Cas9 (dCas9). dCas9 targeted to the gene promoter or dCas9 fused to transcriptional repressor can be applied to modulate transcription without genome editing (Gilbert et al., 2014; Qi et al., 2013).

CRISPR screens have already been published for a wide range of approaches such as identification of genes essential for cell survival, identification of genes important for bacterial toxicity or viral replication and identification of genes responsible for drug resistance (McDougall et al., 2018; Shalem et al., 2014; Wang et al., 2014; Zhou et al., 2014).

b. Comparison with RNAi and haploid approaches for viral infection studies

Over the last several years, loss-of-function screens have played a major role in our understanding of how pathogenic viruses exploit cells to replicate. Indeed, the development of RNAi and haploid screens has led to the identification of cellular factors that promote viral replication for a large number of virus (Perreira et al., 2016). Compared to haploid and RNAi screens, the recent screens based on CRISPR/Cas9 system are more versatile and accurate. Among the major advantages of CRISPR screens over alternative technologies are the ability to generate null phenotypes and the possibility of using in any cell line. Indeed, RNAi approaches lead to a partial knockdown of gene expression while haploid screens are limited to cell types that have a haploid karyotype to achieve insertional mutagenesis of the allele. These haploid cells are not always permissive and susceptible to infection.
In addition, CRISPR approach has a high specificity with less off-target effects observed and a relative lack of false positives and false negatives (Puschnik et al.,

2017). Finally, CRISPR screens are relatively low cost and easily available. High levels of overlap between CRISPR screens involving the same virus were observed while low inter-screen overlaps between RNAi screens generated from different libraries have been noticed (Perreira et al., 2015; Savidis et al., 2016; Zhu et al., 2014).

c. Study of virus-host interactions by CRISPR screens

Last few years, several CRISPR pooled screens for virus-host interactions have been published.

A large majority of the studies relies on cytopathic viruses with cell survival as a phenotypic readout. The loss of particular cellular factors mediated by sgRNA makes cell resistant to viral infection and killing. These resistant cells are able to survive and expand leading to a relative prevalence of the sgRNAs they expressed. Similarly, several screens have been realized with labeled-virus that allow the enrichment for viral resistant cells by flow cytometry (Heaton et al., 2017; Park et al., 2017; Zhang et al., 2018).

Since the early CRISPR/Cas9 screen realized to identify host factors required for West Nile virus infection (Ma et al., 2015), screens have been achieved among others for human immunodeficiency virus, influenza virus, hepatitis C virus, chikungunya virus and several flaviviruses like Zika virus and dengue virus. A non-exhaustive table of some main CRISPR host-virus interaction screens is presented in figure 27.

Regarding the screen analysis and the ranking of candidate genes, different methods have been chosen in the published studies. Some teams have realized their analysis based on the number of reads for a specific sgRNA (Heaton et al., 2017; Ma et al., 2015; Park et al., 2017) while some others have ranked the candidates based on gene with the greatest number of unique sgRNAs (Savidis et al., 2016). On the other hand, some analyses were conducted with a RNAi screen analysis program adapted to CRISPR screen (Marceau et al., 2016), while others were realized with programs developed for CRISPR screening, like MAGeCK, that compare starting and ending sgRNA population to determine sgRNA enrichment or depletion (Li et al., 2014; Lin et al., 2017; Ma et al., 2017; Richardson et al., 2018; Zhang et al., 2016).

Many CRISPR screens to study flaviviruses replication cycle have been performed (Lin et al., 2017; Ma et al., 2015; Marceau et al., 2016; Richardson et al., 2018; Savidis et al., 2016; Zhang et al., 2016). The strong overlap of pathways and complexes identified in the different screens has permitted to attest the validity of the approach.

In addition, already known receptors or protein modifications essential for viral entry have been recovered in different CRISPR screens (Marceau et al., 2016; Park et al., 2017; Savidis et al., 2016). Thus CRISPR/Cas9 screen approach represents a powerful tool to study host-virus interactions.

Publication	Year of publication	Virus	Cell line	sgRNA library
Ma et al.	2015	WNV	293FT	Custom library: 77 406 sgRNAs targetting 20 121 genes (4 sgRNAs/gene)
Savidis et al.	2016	ZIKV	Hela	GeCKOv2 library: 123 411 sgRNAs targetting 19 050 genes (6 sgRNAs/gene)
Marceau et al.	2016	DENV-2 HCV_JFH1	Huh7.5.1	GeCKOv2 library
Orchard et al.	2016	MNoV	BV2	Asiago library: 120 462 sgRNAs targetting 20 077 genes (6 sgRNAs/gene)
Haga et al.	2016	MnoV-S7	RAW264.7 (mouse)	Yusa mouse library lentiviral CRISPR gRNA library v1: 87 897 sgRNAS targetting 19 150 genes
Zhang et al.	2016	WNV	293T	GeCKOv2 library
Kim et al.	2017	PV-1 EV-D68	Hela	Custom library: 30 840 sgRNAs targetting 10 280 genes (3 sgRNAs/gene)
Park et al.	2017	HIV-1 JR-CSF	GXRcas9 (CD4+ T cell)	Custom library: 187 536 sgRNAs targetting 18 543 genes (10 sgRNAs/gene)
Lin et al.	2017	DENV-2	Huh7.5.1	GeCKOv2 library
Ma et al.	2017	EBV	Burkitt Lymphoma - P3HR1	Avana library : 74 700 sgRNAs targetting 18 675 genes (4 sgRNAs/gene)
Zhang et al.	2018	CHIKV	3T3 (mouse)	GeCKOv2 mouse library: 130 209 sgRNAs targetting 20 611 genes
Han et al.	2018	IAV	A549	GeCKOv2 library A
Richardson et al.	2018	YFV-17D venus	Huh7.5	Brunello CRISPR knockout pooled library : 76 441 sgRNAs targetting 19 114 genes

Figure 27 : Comparative table of CRISPR/Cas9 host-virus interactions screens

Informations on virus, cell line and sgRNA library used in each CRISPR screen.

West Nile Virus (WNV), Zika virus (ZIKV), Dengue virus (DENV), Hepatitis C virus (HCV), Murine norovirus (MNoV), Poliovirus (PV), Enterovirus (EV), Human immunodeficiency virus (HIV), Epstein-Barr virus (EBV), Influenza A virus (IAV), Yellow Fever virus (YFV)

7 - The rise of CRISPR as a gene-editing technology

During the last 10 years, the study of the CRISPR mechanism in bacteria, the development and improvement of the genetic tool and its use for various applications have led to an increasing number of publications about CRISPR (Fig.28).

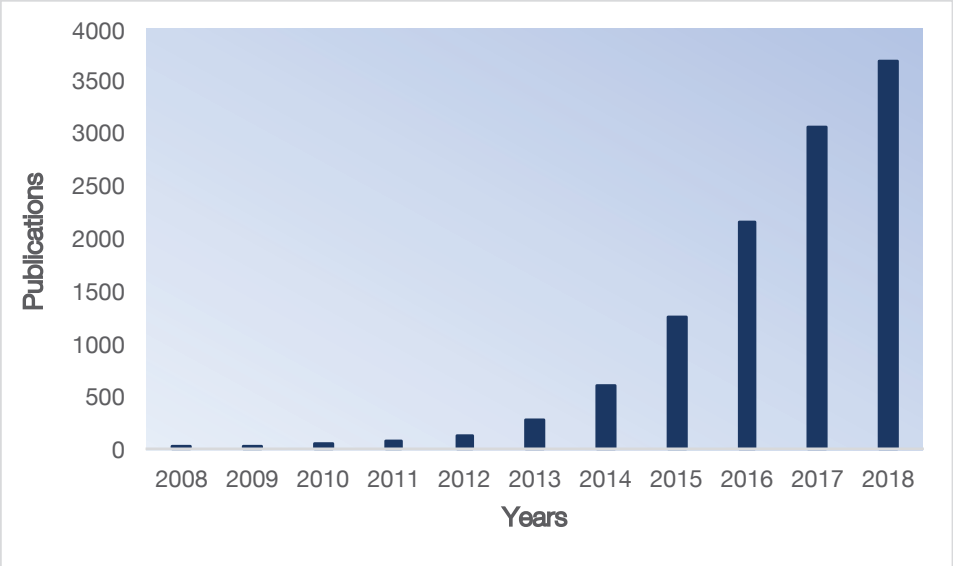

Figure 28: Mentions of the word CRISPR in Pubmed publications over the last 10 years

OBJECTIVES

Alphaviruses are emerging viruses representing a public health issue worldwide. Recent outbreaks of chikungunya virus across the world have caused debilitating diseases with fever and severe joint pains, resulting in a significant loss of life-quality and societal cost. Currently, there is no licensed cure for the disease. Acquired more knowledge of the virus biology is becoming crucial as it should enable the development of antiviral approaches, vaccines, and diagnostics as well. Nonetheless, chikungunya and alphavirus biology, in general, is poorly characterized and especially little is known about alphavirus entry. The main objective of my project was to better understand and characterize the chikungunya virus entry and the host factors used during replication steps.

The first key objective was mainly focused on alphavirus entry and early infection steps. In this way, we have made an interesting observation of infection decrease after treatment of cells with iron. Consequently, we have investigated the role of two iron-dependent proteins in chikungunya entry, the divalent metal transporter NRAMP2, and the transferrin receptor TFRC.
On the other hand, we have also studied the involvement in the entry of two totally distinct membrane proteins, CD46 and TM9SF2. These two proteins were highlighted as required for several viruses' entry in an RNAi screen realized previously in collaboration with other laboratories.

In parallel, in a second focal area, we have tried to gain a global understanding of host factors used during chikungunya virus replication by carrying out a genome-wide loss of function screen with the CRISPR/Cas9 technology. The selection of a relevant natural cell target for this screen (muscle cells) should have allowed a more physiological characterization of chikungunya virus cell cycle. In this approach, a cell library has been generated, in which each cell has a distinct knockout gene. As chikungunya virus normally induces cell death, this screen is based on the survival of cells in which the virus was not able to enter or replicate. Hits identified through the screen were tested individually in infection assays to study their involvement in the chikungunya replication cycle.

EXPERIMENTAL REPORT

PART 1

Iron effect on alphavirus infection and receptor candidates

Chapter 1: Iron effect on alphavirus infection

I - Context

- **Iron required for metabolic processes**

Iron is an essential nutrient for living cells and is required for cellular processes, such as DNA synthesis, energy metabolism, and electron transport in the respiratory chain (Anderson and Vulpe, 2009; Hentze et al., 2010). Deregulation of the iron status, both excess or deficiency, clearly affects the activity of iron-dependent proteins and disrupts cellular functions. Indeed, iron catalyzes the propagation of Reactive Oxygen Species (ROS) and the generation of reactive radicals that are toxic for the cell. Thus, a tightly regulated system has been developed to ensure an appropriate concentration of iron at the systemic and at the cellular levels.

Since viruses hijack the cellular machinery in order to replicate, iron homeostasis is also important for efficient viral replication. In the case of the human immunodeficiency virus and hepatitis C virus, viral infections can cause iron overload and exacerbate disease. In addition, it has been demonstrated that a decrease of intracellular iron concentration affects the viral replication of both viruses (Drakesmith and Prentice, 2008; Franchini et al., 2008). Regarding the arbovirus West Nile (WNV), it has been shown that iron treatment of mosquito vector cells increases WNV infection (Duchemin and Paradkar, 2017).

- **Antiviral effect of iron on several viruses**

Wang et al. have recently shown an antiviral effect of iron as ferric ammonium citrate (FAC) on several viruses including Influenza A virus, Human Immunodeficiency virus, Zika virus and Enterovirus 71 (Wang et al., 2018). It has been observed that HIV infection and associated innate immune response were decreased by FAC in human dendritic cells. In parallel, FAC has also been shown to inhibit Zika virus infection in green monkey Vero cells and in U251 mouse cell line. Finally, for enterovirus infection, FAC has been demonstrated to decrease genome amplification, induction of cytopathic effects and expression of a particular viral protein. In addition, a dose-dependent effect has been noticed on viral RNA level and new virions release. In the case of influenza A virus (IAV), viral infection was inhibited by FAC in a dose-dependent manner in human cell lines and co-inoculation of IAV and FAC in mice protects the animals from infection with a lower level of viral RNA and proinflammatory

cytokines. Treatment of cells with an iron chelator, deferoxamine, has been shown to rescue FAC-inhibited IAV infection, highlighting the iron requirement. Moreover, Wang et al. have demonstrated that both ferric ion and citrate ion of the complex were required for the antiviral activity.

Interestingly, the iron transporter Malvolio or dNRAMP has been proposed a few years ago as an entry receptor for another alphavirus, Sindbis virus, in *Drosophila* (Rose et al., 2011). dNRAMP is a member of a protein family that is well conserved from bacteria to humans (Nevo and Nelson, 2006). In mammals, two NRAMP genes are present, NRAMP1 and NRAMP2. NRAMP1 is mainly expressed in macrophages and monocytes, while NRAMP2 is ubiquitously expressed and is localized in endosomes and at the plasma membrane. High iron concentrations regulate NRAMP2 expression (Foot et al., 2008; Mackenzie et al., 2016). Rose et al. have used this response to iron to downregulate NRAMP2 in mammalian cells. Iron treatment with FAC has been shown to attenuate Sindbis virus infection in human U2OS, *Drosophila* DL1 and *Aedes aegypti* Aag2 cell lines. In parallel, depletion of NRAMP2 in mouse embryonic fibroblasts decreased Sindbis virus infection (Rose et al., 2011).

- **Role of NRAMP2 and transferrin receptor in iron transport**

NRAMP2 also known as DMT1 for divalent metal transporter 1, is a widely expressed metal transporter capable of transporting metals such as iron, zinc, and manganese (Gunshin et al., 1997). This iron transporter facilitates iron uptake at the apical cell membrane in duodenal enterocytes and transports iron across the endosomal membrane in almost all cell types after iron uptake via the transferrin pathway. There are two alternative transcripts of the 3’ untranslated regions (UTR), one with an Iron Responsive Element (+IRE) and one without IRE (-IRE), involved in NRAMP2 regulation at the mRNA level. There are also two transcripts 1A and 1B differing in the 5’ region (Hubert and Hentze, 2002). In total, this leads to four NRAMP2 isoforms namely 1A/+IRE, 1A/-IRE, 1B/+IRE and 1B/-IRE (Fig.29). 1A isoforms are predominantly found in duodenum and kidney tissues whereas 1B isoforms are ubiquitously expressed. In response to iron overload or deficiency, the conserved hairpin structure IRE permits mRNA stability or degradation thanks to iron-responsive proteins (IRP) (Fig.30) (Pantopoulos, 2004). NRAMP2 mRNA has only one IRE hairpin structure while other iron-regulated proteins may have several.
NRAMP2 expression and activity is not only regulated by IRE but also by a complex regulatory system at transcriptional, post-transcriptional and post-translational levels including, protein internalization by endocytosis, recycling of endosomal protein to

the plasma membrane, protein release by plasma membrane budding, ubiquitination and degradation of NRAMP2 protein or regulation of the transport activity by phosphorylation (Foot et al., 2008; Gunshin et al., 2001; Lam-Yuk-Tseung and Gros, 2006; Mackenzie et al., 2016; Seo et al., 2016).

Besides NRAMP2, the cellular iron-regulatory system involves various proteins including the transferrin and the transferrin receptor (TFRC). The transferrin receptor is also regulated by iron at the transcriptional and post-transcriptional level (Hentze et al., 2010) including a regulation mediated by IRE in the 3'UTR of the mRNA. The TFRC is the main receptor that mediates iron uptake in many cell types and is located on the plasma membrane. Hence, ferric iron is captured on transferrin which binds to the transferrin receptor leading to the uptake of the complex via clathrin-mediated endocytosis into endosomes (Fig.31). (Mayle et al., 2012). Subsequently, ferric iron taken up by transferrin is reduced in ferrous iron and NRAMP2 transports the iron across the endosomal membrane to be released into the cytosol (Gruenheid et al., 1999; Touret et al., 2003). Internalized iron is used for the synthesis of heme or iron-sulfur clusters, which are parts of several metalloproteins. Iron in excess is stored and detoxified in cytosolic ferritin (Hentze et al., 2010).

Given this broad antiviral effect of FAC, we have investigated an effect on alphavirus infection, in particular on chikungunya virus infection. We have observed a dose-dependent inhibition on chikungunya virus infection with FAC in human cell lines and sought to understand the mechanism. Since NRAMP2 and transferrin receptor proteins, both involved in iron uptake, are regulated by iron level and NRAMP2 has been proposed as the receptor for the alphavirus Sindbis, we investigated a potential role of NRAMP2 transporter and transferrin receptor in chikungunya virus entry.

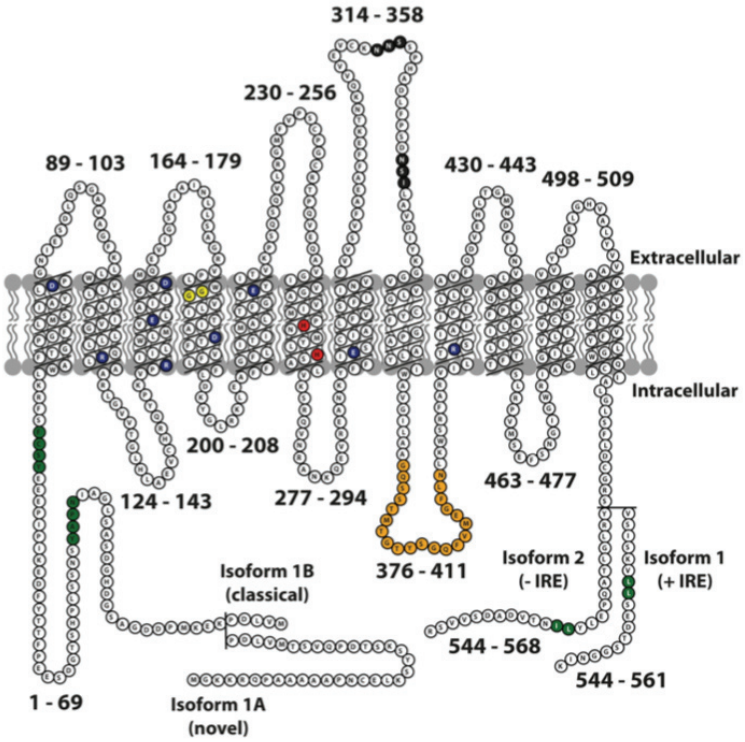

Figure 29: Schematic representation of mouse NRAMP2 with isoforms 1A and 1B +/- IRE, representative of mammal NRAMP2
(Skjørringe et al., 2015)

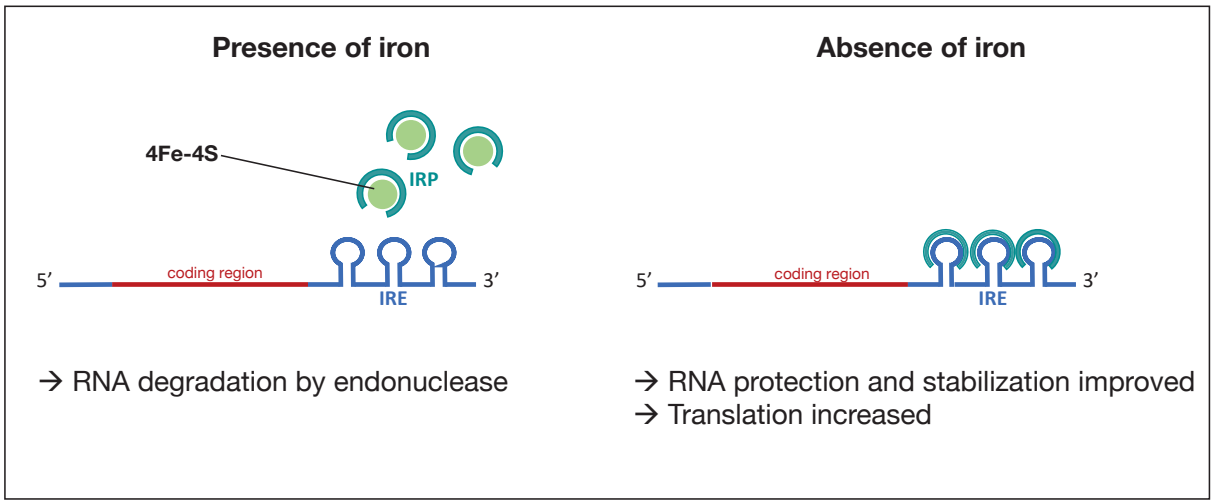

Figure 30: General mechanism of the Iron Responsive Element (IRE)

Presence of iron: *Iron, in form of iron-sulfur cluster, can bind to Iron Responsive Protein (IRP) leading to the dissociation of IRP from the IRE. Transcripts are more susceptible to endonuclease attack and degradation which down-regulate the translation.*

Absence of iron: *The IRP binds to the IRE in 3' UTR and protects transcripts against endonuclease degradation and therefore promotes the translation.*

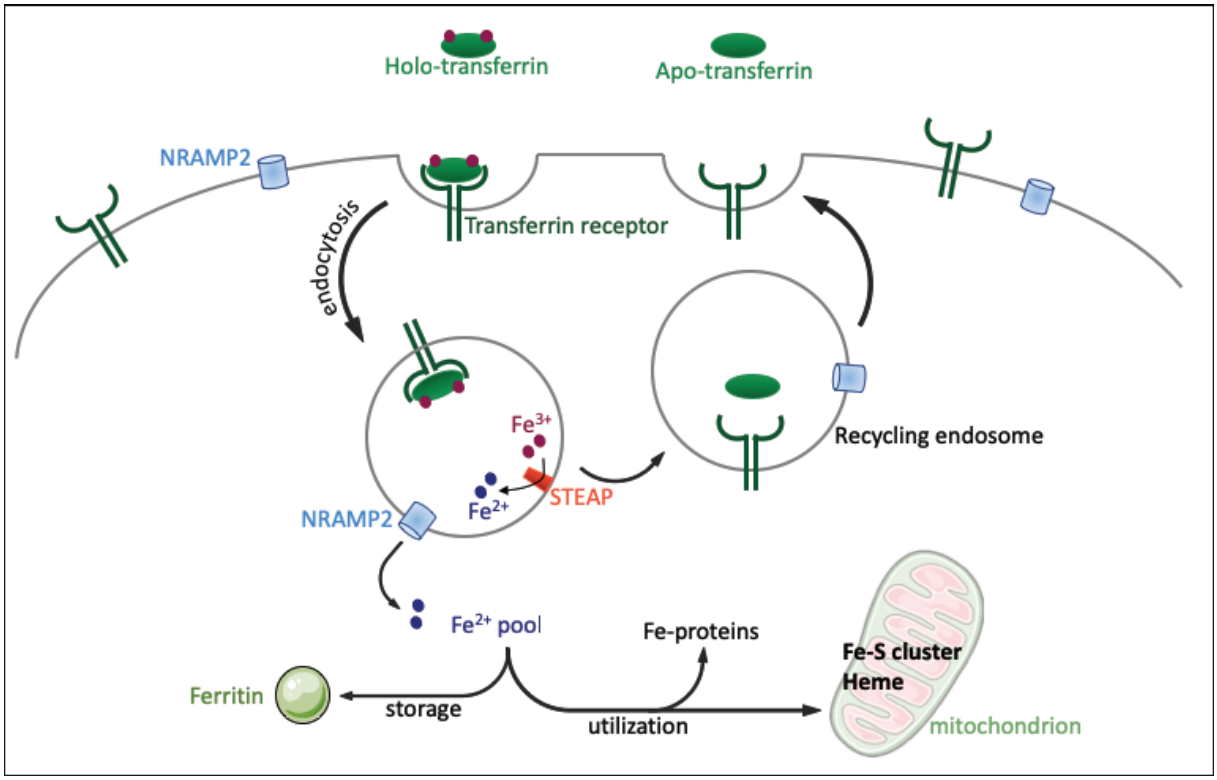

Figure 31: Scheme of iron transport by transferrin receptor and NRAMP2

Ferric iron Fe^{3+} binds to transferrin which subsequently binds to transferrin receptor (TFRC). The complex iron-transferrin-transferrin receptor is endocytosed. Ferric iron is reduced into ferrous iron Fe^{2+} by a metalloreductase STEAP and then transported to the cytoplasm by NRAMP2 transporter. Both molecules, TFRC and NRAMP2, are recycled back to the plasma membrane. Fe^{2+} pool, also called Labile Iron Pool (LIP) is utilized for direct incorporation into iron-proteins or transported to mitochondrion via mitoferrin, where the metal is inserted into Fe-S cluster and heme. Excess iron is stored in ferritin.

II - Material and Methods

1 - Cell lines and reagents

HEK 293T, BHK21, U2OS, and VeroE6 cells were cultured in Dulbecco's Modified Eagle Medium (DMEM; Gibco™ Thermo Scientific) supplemented with 10% fetal bovine serum (FBS; HyClone). LHCN-M2 (human skeletal myoblasts) were maintained in medium 4:1 DMEM/Medium 199 (Gibco™ Thermo Scientific) supplemented with 15% FBS, 0,02 M HEPES, 0,03 µg/mL Zinc sulfate (Sigma Aldrich), 1,4 µg/mL Vitamin B12 (Sigma Aldrich), 0,055 µg/mL Dexamethasone (Sigma Aldrich), 2,5 ng/mL recombinant human Hepatocyte Growth Factor (HGF, Peprotech), 10 ng/mL recombinant human FGF-basic (Peprotech).
Caco2 cells were cultured in Dulbecco's Modified Eagle Medium (DMEM; Gibco™ Thermo Scientific) supplemented with 20% FBS, 1% non-essential amino acids, 0,01 M HEPES (Gibco™ Thermo Scientific). All mammalian cell lines used were maintained at 37°C in the presence of 5% of CO_2 in a humidified incubator.
Aedes aegypti Aag2 cells were cultured in Leibovitz's L-15 medium (Gibco™ Thermo Scientific) supplemented with 10% FBS and 10% Tryptose Phosphate Broth (TPB, Gibco™ Thermo Scientific). Aag2 cells were maintained at 28°C in an insect cell incubator.

2 - Virus production and titration

Chikungunya La Réunion infectious molecular clone (CHIKV LRic, strain LR2006 OPY1, European Virus Archive; Marseille) and derived CHIKV-GFP were used to generate replicative chikungunya viruses in BioSafety level 3 (BSL3) laboratory. Starting from the infectious clone, viral RNA was generated by *in vitro* transcription (mMessage mMachine kit, Ambion) for subsequent electroporation in BHK-21 cells. After trypsinization and two washes with PBS 1X, 5.10^6 cells were resuspended into Opti-MEM medium (Gibco™ Thermo Scientific) and electroporated with viral RNA in a cuvette (0,4 cm gap width) using a Gene Pulser Xcell electroporation system (1 pulse, 270V, 950 µF). Electroporated cells were plated in DMEM supplemented with 10 % FBS and incubated for 20h at 37°C until medium change. The supernatant was harvested 24h and 48h later, clarified by centrifugation and then mixed with 0,5 M Sucrose (MP Biomedicals) and 50 mM HEPES (Gibco™ Thermo Scientific) for long time conservation at -80°C. SINV (Sindbis Virus) was produced in the same way using molecular clone from Toto 1101 strain. All viral stocks were titrated by TCID50 and plaque assay on VeroE6 cells.

3 - Production of pseudotyped retroviral particles

We have generated pseudotyped viruses consisting of a replication-deficient lentiviral backbone which displays viral envelope proteins at the surface and carries GFP reporter. These pseudotyped particles allow studying envelope-dependent entry in BSL2 conditions.

Different plasmids encoding the different viral envelopes were used: a plasmid encoding the chikungunya La Réunion infectious clone (LRic strain, LR2006 OPY1) viral envelope glycoproteins (the last 35 Capsid amino acids in frame with E3, E2, 6K and E1) under a CMV promoter, a plasmid encoding the Sindbis (strain Toto1101) viral envelope glycoproteins (the last 36 Capsid amino acids in frame with E3, E2, 6K and E1) under a CMV promoter and a plasmid encoding the Vesicular Stomatitis Virus g protein (VSVg) under a CMV promoter. In order to produce the VSV-, SINV-, CHIKV-pseudotyped retroviral particles, the 293T cells were transfected with expression vectors encoding the viral components, i.e. plasmids encoding the envelope glycoproteins (phCMV VSV-G, phCMV SINV, phCMV CHIKV), the retroviral core proteins (pTG5349 murine leukemia virus MLV gag-pol), and a packaging-competent GFP (pTG13077 expressing an MLV based RNA containing a CMV-GFP internal transcriptional unit). The 293T cells seeded the day before transfection, were transfected using calcium phosphate co-precipitation method with the gag-pol packaging construct (8,3 µg), the transfer vector construct (8 µg), and the glycoprotein-expressing construct. The medium was changed 16h after transfection. Supernatants were harvested and filtered through 0,45 µm pore-sized membranes 24 hours later.

4 - Cell viability assays after ferric ammonium citrate treatment

In order to monitor the effect of ferric ammonium citrate (FAC; generating Ferric iron Fe^{3+}) on cell fitness, cell viability assays were carried out. Cell viability was measured at different times after treatment with several concentrations of fresh ammonium iron (III, Fe^{3+}) citrate (Sigma Aldrich) using the CellTiter-Glo® luminescent cell viability assay kit (Promega) and a plate reader (Victor^2 plate reader, Perkin Elmer).

5 - Iron treatment and infection with replicative viruses

LHCN-M2, U2OS, and Aag2 cell lines were treated with different concentrations of fresh ammonium iron (III, Fe^{3+}) citrate for 24h prior to and throughout the infection. Cells were counted before infection to adapt the multiplicity of infection (MOI). The

different mammalian cell lines were infected at different MOI with CHIKV LRic (strain LR2006 OPY1) and SINV (Toto1101). After 1h of virus binding at 4°C without FAC, cells were washed with PBS 1X, fresh medium with FAC was added, and cells were incubated at 37°C. For infection of mosquito cells Aag2 with CHIKV LRic, an incubation without FAC at 28°C for 1h was realized, then cells were washed with PBS 1X and fresh appropriate medium with FAC was added. Twenty-four hours post-infection, cells were fixed with paraformaldehyde 4% at 4°C for 15 min. Intracellular immunostaining was realized with antibodies diluted in PBS 1X supplemented with 0,1% saponin for cell permeabilization and 10 % FBS. First, cells were incubated 1h at 4°C with primary antibody raised to Semliki Forest nucleocapsid protein (1/800), that reacts with CHIKV capsid protein (IgG2a C42 kindly provided by Dr. Irene Greiser-Wilke, School of Veterinary Medicine (Hannover, Germany)). After washes, cells were incubated 1h at 4°C with FITC conjugated secondary anti-mouse IgG antibody (1/200) (F0257, Sigma Aldrich), cells were analyzed using a flow cytometer (FACSCalibur, BD Biosciences).

6 - NRAMP2 expression after iron treatment – qPCR and Western Blot

LHCN-M2, U2OS and Caco2 cells were plated and treated the next day with 50 µg/mL of fresh ammonium iron (III) citrate (Sigma Aldrich). After 24h and 48h of iron treatment, cells were lysed to follow NRAMP2 mRNA and protein expression by RT-qPCR and western blot respectively.

Total RNA of cells was extracted using NucleoSpin® RNA kit (Macherey Nagel). RNA was reverse transcribed using PrimeScript™ RT-PCR kit (Takara). mRNA was quantified by qPCR amplification in AriaMx system (Agilent) using SYBR Premix Ex Taq II (Takara) with the following primers (Hubert and Hentze, 2002). Results were normalized by at least three different housekeeping genes (RPL27, RPL22, GUSB).

Oligo name		**Sequence 5'-3'**
hNRAMP2_1A	Forward	GGAGCTGGCATTGGGAAAGTC
	Reverse	GGAGATCTTCTCATTAAAGTAAG
hNRAMP2_1B	Forward	GTTGCGGAGCTGGTAAGAATC
	Reverse	GGAGATCTTCTCATTAAAGTAAG
hGUSB	Forward	GATTGCCAATGAAACCAGGTATC
	Reverse	ACACGCAGGTGGTATCAGTCTT
hRPL22	Forward	TCGCTCACCTCCCTTTCTAA
	Reverse	TCACGGTGATCTTGCTCTTG
hRPL27	Forward	ATCGCCAAGAGATCAAAGATAA
	Reverse	TCTGAAGACATCCTTATTGACG

For western blot analysis, cells were lysed with RIPA lysis buffer pH 8 supplemented with Phosphatase and Protease Inhibitor (PI) 1X (ThermoFisher Scientific), Ethylenediaminetetraacetic acid (EDTA) at 1 mM (ThermoFisher Scientific) and Dithiothreitol (DTT) at 1 mM. RIPA lysis buffer was composed of 20 mM Tris HCl pH 7,5, 1% Triton X-100 (Euromedex), 0,05% SDS, 0,5% NaDeoxycholate, 150 mM NaCl. Cell lysates were sonicated on ice (3 pulses, amplitude 30) then incubated 30 min on ice, centrifuged for 5 min at 4°C at 11 000 g and supernatants were transferred into a new tube. Bradford protein assay was realized to quantify proteins in cell lysates. Whole cell extracts were separated by SDS-PAGE and then transferred to nitrocellulose membranes using a transfer apparatus according to the manufacturer's protocols (Bio-Rad). After protein transfer, membranes were incubated with 10% milk in PBS 0,1% Tween 20 (PBST 0,1%) for 2 hours followed by overnight incubation at 4°C with NRAMP2 mouse monoclonal antibody clone G-5 sc-166884 (Santa Cruz Biotechnology) in 10% milk PBST 0,1%. Membranes were washed 3 times and incubated 1 hour with a Horseradish peroxidase anti-mouse IgG antibody (1/10 000, A5906, Sigma Aldrich). After 3 washes, proteins were revealed with SuperSignal™ chemiluminescent substrate (ThermoScientific) using ChemiDoc™ imaging system (BioRad).

7 - Generation of NRAMP2 and TFRC CRISPR-mediated knockout cell lines

In order to study the potential role of NRAMP2 and TFRC in chikungunya virus replication, we have generated knockout cell lines using the CRISPR/Cas9 technology. This required the design of a single-guide RNA (sgRNA) specific for the gene of interest which was then cloned into the lentiviral vector, lentiCRISPRv2 (Fig.32) (Addgene). This lentiviral vector construct was co-transfected with other vectors in 293T cells to generate lentiviral particles bearing the g envelope protein of the Vesicular Stomatitis Virus (VSVg). Given the broad tropism of VSV, lentiviral particles are able to enter in almost all cell types and thus allow the stable integration of sgRNA sequence, Cas9 gene, and puromycin resistance gene into the genome. Puromycin selection permitted to select only transduced cells which stably expressed the sgRNA and the Cas9 nuclease. Finally, CRISPR-mediated knockouts were validated by western blot or cell surface immunostaining followed by flow cytometry analysis.

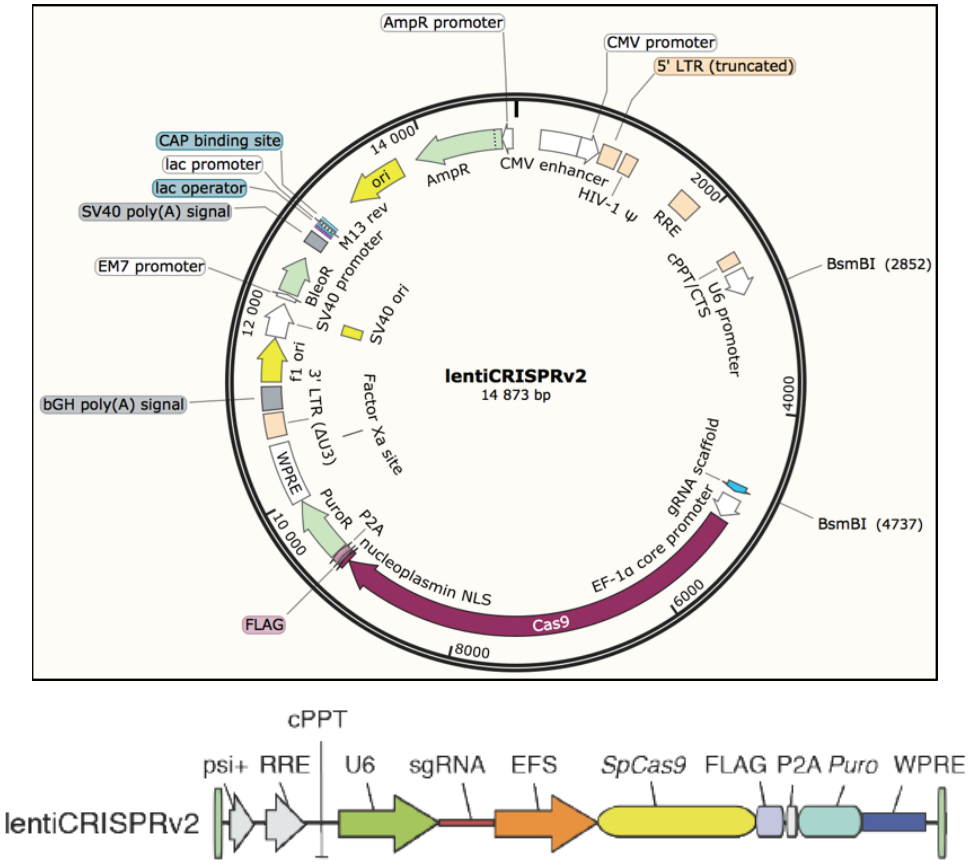

Figure 32: LentiCRISPRv2 cloning vector

Lentiviral expression vector for Streptococcus pyogenes Cas9 and sgRNA in a "one vector" system. Specific sgRNA sequence is cloned into the vector after digestion with BsmBI restriction enzyme. The sequence between the two Long Terminal Repeats (LTR) is transcribed and then packaged thanks to the Psi packaging signal (Ψ).
RRE: rev response element, cPPT: central polypurine tract, EF-1α: elongation factor-1α short promoter, P2A: 2A self-cleaving peptide, PuroR: puromycin selection marker, WPRE: post-transcriptional regulatory element.

a. sgRNA design

Sequences of single-guide RNAs (sgRNAs) for specific gene knockout were designed using different online tools. The sequence should be around 19-21 nucleotides and adjacent to a protospacer adjacent motif (PAM) sequence. Some compromises were made to select sgRNAs with the highest efficiency score, the highest out-of-frame score and the smallest risk of off-target. As lentiCRIPSRv2 (Addgene) used for cloning contains a U6 promoter, a G nucleotide (in blue) was added to increase transcription efficiency when primers start with another nucleotide. Finally, BsmBI restriction sites (in red) were added to the primers for cloning step.

The following primers were used:

Guide name		Sequence 5'-3'
sgRNA NRAMP2	Forward	CACCGCCAGTCTAGCTGCAAGCCGC
	Reverse	AAACGCGGCTTGCAGCTAGACTGGC
sgRNA_1 TFRC	Forward	CACCGAAATTCATATGTCCCTCGTG
	Reverse	AAACCACGAGGGACATATGAATTTC
sgRNA_2 TFRC	Forward	CACCGTGGAAACTGAGTGTGATTGA
	Reverse	AAACTCAATCACACTCAGTTTCCAC

b. Cloning

LentiCRISPRv2 vector was digested with BsmBI restriction enzyme and then purified from the agarose gel. Each pair of primers was annealed using an annealing buffer composed of 10 mM Tris-HCl pH 8, 50 mM NaCl and 1 mM EDTA. The mix was incubated for annealing for 3 min at 90°C following by incubation of 15 min at 37°C. Annealed primers were cloned into the linearized lentiCRISPRv2 using a ligation kit (Rapid DNA ligation kit, Roche) and then transformed into DH5α competent bacteria. Colony PCRs were realized for determining the presence or absence of insert DNA in the lentiCRISPRv2 plasmid. Clones were amplified and lentiCRISPRv2 plasmids containing the sequence for transcription of a specific sgRNA were purified and digested for verification.

c. Lentivirus production

In order to generate stable cell lines expressing the sgRNA and the Cas9 nuclease, lentiviruses were produced. For this, 293T cells seeded the day before transfection, were co-transfected using calcium phosphate co-precipitation method with the HIV packaging construct with a CMV promoter (8,3 µg, psPAX2 (AddGene 12260)), the gene specific lentiCRISPRv2 construct (8 µg), and the VSV glycoprotein-expressing construct under CMV control (2,5 µg, pVSVg (AddGene 8454)). The medium was changed 16 hours after transfection. Supernatants were harvested, filtered through 0,45 µm pore-sized membranes 24hours later and stored at -80°C.

d. Stable cell line generation by transduction

Cells were plated in 6-well plates and transduced the day after with lentivirus. Transduced cells were selected with different concentrations of puromycin depending on the cell type. Puromycin selection was maintained until non-transduced control cells are all dead, then selected cells were amplified.

e. Verification of gene knockout

Depending on the tools available, several strategies were used to confirm gene knockout in the different cell lines.

i. Western blot

Cells were lysed and sonicated as described above. Bradford protein assay was realized to quantify proteins in cell lysates. Whole cell extracts from CRISPR and control cell lines were separated by SDS-PAGE and then transferred to nitrocellulose membranes. After protein transfer, membranes were incubated with 10% milk in PBST 0,1% for 2 hours followed by overnight incubation at 4°C with NRAMP2/SLC11A2 monoclonal mouse antibody clone 4G2 (1/300, SAB1404146, Sigma Aldrich). Membranes were washed 3 times and incubated 1 hour with a Horseradish peroxidase anti-mouse IgG antibody (1/10 000, A5906, Sigma Aldrich). After 3 washes, proteins were revealed with SuperSignal™ chemiluminescent substrate (ThermoScientific) using ChemiDoc™ imaging system (BioRad).

ii. Flow cytometry

The sgRNA TFRC cells were directly stained for cell surface protein detection. Cells were incubated for 1h at 4°C with anti-TFRC CD71 antibody (DF1513, SantaCruz sc-7327) at 1 µg/mL in PBS 1X-2% FBS-0,1% NaN_3 (PBFA). After 3 washes with PBFA, cells were incubated with FITC conjugated anti-mouse IgG secondary antibody (1/200) (F0257, Sigma Aldrich) in PBFA. After 3 washes, immunostained cells were analyzed using a flow cytometer (Accuri C6 or FACSCalibur, BD Biosciences).

8 - Generation of NRAMP2 shRNA-mediated knockdown cell lines

NRAMP2 knockdown was generated using the following shRNA against NRAMP2: 5'-CCGGGCTATCAATCTTCTGTCTGTACTCGAGTACAGACAGAAGATTGATAGCTTTTTG-3' (TRCN0000043248, Sigma Aldrich). The lentiviral shRNA expressing plasmid was used to generate lentiviruses as described above. Caco2 cell line was transduced by lentiviruses packaging shRNA and selected with puromycin for several days. NRAMP2 knockdown cell line was validated by western blot analysis using a mouse monoclonal anti-NRAMP2 antibody (SAB1404146, Sigma Aldrich) followed by incubation with an anti-mouse IgG peroxidase antibody as described above.

9 - Infection of knockout and knockdown cell lines with replicative virus or pseudoparticles

The different cell lines were infected at different MOI with CHIKV LRic (strain LR2006 OPY1) and SINV (Toto1101) as a control. After 1h of virus binding at 4°C, cells were washed with PBS 1X and the medium was changed before incubation at 37°C. Twenty-four hours post-infection, cells were fixed with paraformaldehyde 4% at 4°C for 15 min. Intracellular immunostaining was realized with antibodies diluted in PBS 1X supplemented with 0,1% saponin for cell permeabilization and 10 % FBS. First, cells were incubated 1h at 4°C with a primary antibody raised to Semliki Forest nucleocapsid protein (1/800), that reacts with CHIKV capsid protein (IgG2a C42 kindly provided by Dr. Irene Greiser-Wilke, School of Veterinary Medicine (Hannover, Germany)). After washes, cells were incubated 1h at 4°C with FITC conjugated secondary anti-mouse IgG antibody (1/200) (F0257, Sigma Aldrich), cells were analyzed using a flow cytometer (FACSCalibur, BD Biosciences). For CHIKV-GFP infected cells, the percentage of infected cells was directly measured by flow cytometry analysis after fixation with paraformaldehyde (PFA).

In parallel, the different cell lines were infected with SINV-, CHIKV- and VSV-pseudotyped retroviral particles. After 1h of particles binding at 4°C, cells were washed with PBS 1X and the medium was changed before incubation at 37°C for three days. Cells were fixed with paraformaldehyde 4% at 4°C for 15 min and the percentage of GFP-positive cells was directly measured by flow cytometry.

10 - Study of correlation between NRAMP2 expression profile and CHIKV permissiveness of cell lines

The different following cell lines were lysed and whole cell lysates were separated by SDS-PAGE and transferred to nitrocellulose membranes for western blot analysis with NRAMP2/SLC11A2 monoclonal mouse antibody clone 4G2 (SAB1404146, Sigma Aldrich) as explained above in the western blot section. The nine different human cell lines are listed below:

Jurkat: CD4+ T lymphoid cell line
Raji: B lymphoid cell line
A431: epidermoid carcinoma epithelial cell line
HT1080: connective tissue fibrosarcoma epithelial cell line
HOS: bone osteosarcoma fibroblast/epithelial-like cell line

Caco2: colorectal adenocarcinoma epithelial-like cell line
Hela: cervical carcinoma epithelial cell line
LHCN-M2: immortalized human myoblast cell line
U2OS: bone osteosarcoma epithelial cell line.

In parallel, the different cell lines were infected with CHIKV LRic and level of infection was monitored by immunostaining followed by flow cytometry analysis as described above and/or titration of viral production in the cell supernatant by TCID50 on VeroE6.

III - Results

1 - Infection of LHCN-M2 and U2OS cell lines by alphaviruses

Our study relies on the use of two different cell lines, LHCN-M2 and U2OS. As alphaviruses infect muscle cell lines in humans, skeletal muscle cell line LHCN-M2 represents a suitable model for chikungunya study (Ozden et al., 2007). The second cell line, U2OS derived from bone osteosarcoma is frequently used in alphavirus studies like whole genome screens (Ooi et al., 2013; Rose et al., 2011; Stiles and Kielian, 2016). We infected cells with either CHIKV or SINV and looked at the percentage of infected cells over time. CHIKV and SINV infect and replicate efficiently in U2OS (Fig.33). In parallel, LHCN-M2 cells were also efficiently infected by CHIKV and began to die after 48h of infection.

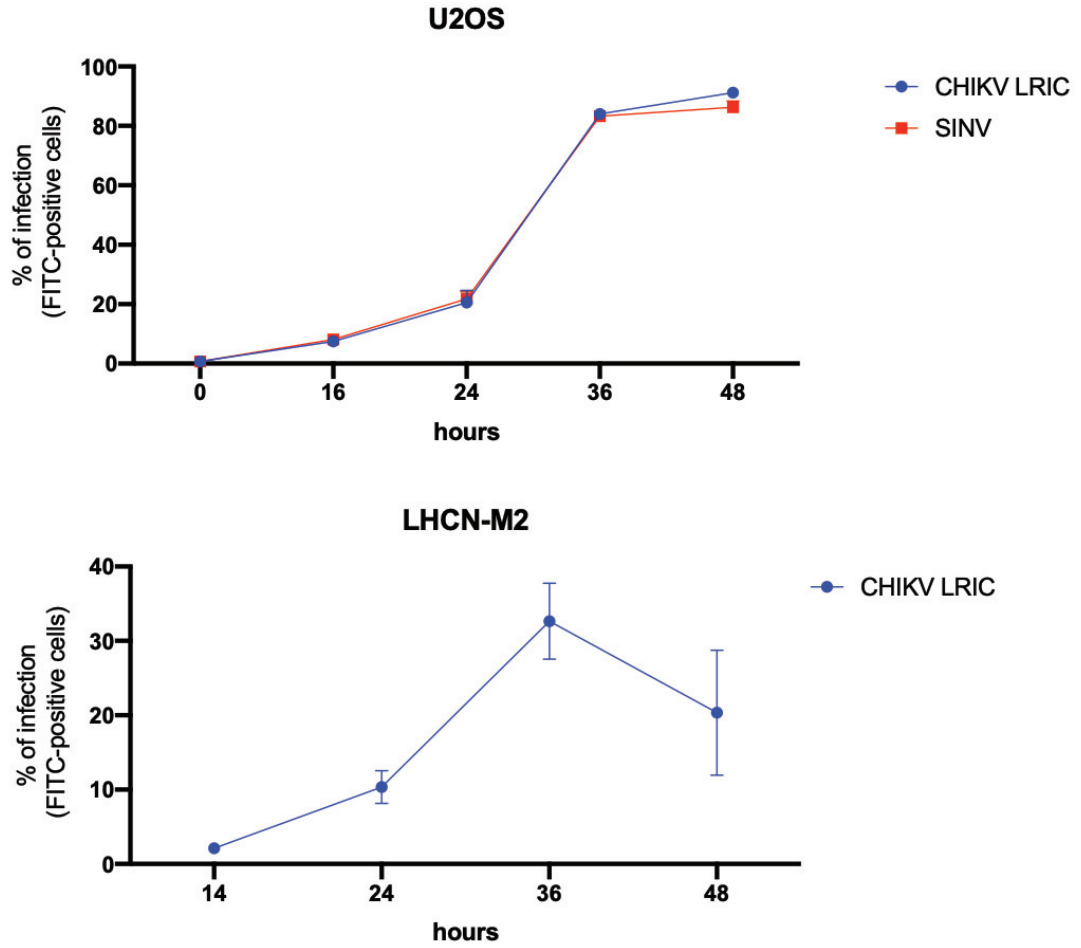

Figure 33: Infection kinetics in U2OS and LHCN-M2 cell lines
Cells were infected with CHIKV or SINV at MOI 0,1 and harvested at different time points after infection. Cells were fixed in PFA 4% before immunostaining with a primary antibody raised to Semliki Forest nucleocapsid protein, that reacts with CHIKV and SINV capsid protein (IgG2a C42) and then analyzed by flow cytometry analysis.

2 - Effect of ferric ammonium citrate (FAC) treatment on SINV and CHIKV infections

Due to the broad antiviral effect of ferric ammonium citrate described for different viruses, we tested whether ferric ammonium citrate (FAC) had an effect on SINV and CHIKV infection in U2OS. Many cell mechanisms - DNA replication, mitochondrial function - are regulated by iron. To make sure that FAC does not have a toxic effect on cells, we followed cell growth and survival after FAC treatment. We observed that U2OS cell viability and growth were not greatly affected by FAC (Fig.34). Cells treated with 10, 25 or 50 µg/mL grow similarly as untreated cells while the growth of cells treated with 100 µg/mL of FAC was slightly slowed. Regarding LHCN-M2 cells, the growth of cells treated with 10 µg/mL FAC was comparable to the growth of untreated cells. Treatment with 25 µg/mL FAC was shown to slow the growth and the greater doses to completely stop the growth. With 100 µg/mL of FAC, LHCN-M2 cells seem to die after 60 h of treatment. However, we did not use this high concentration and did not treat cells during more than 48h in our infection assays.

Subsequently, U2OS cells were treated with FAC and infected with CHIKV or SINV for 24h. We observed a substantial decrease of CHIKV infection in presence of FAC (Fig.35(a)) and also a decrease of SINV infection as it was previously described (Rose et al, 2011). Same results were obtained with a significant decrease of CHIKV infection in LHCN-M2 cells (Fig.35(b)). Using different concentrations of FAC, we observed a dose-response relationship with both SINV and CHIKV in U2OS cells with almost complete inhibition of infection at 100 µg/mL of FAC (Fig.35(c)).
Moreover, as *Aedes aegypti* is one of the natural mosquito vectors for both CHIKV and SINV, we examined the effect of FAC treatment on *Aedes Aegypti* cells Aag2. Cell count after iron treatment has demonstrated that cell viability and growth were not affected by FAC (data not shown). Iron treatment with 50 µg/mL of FAC on Aag2 cells attenuated CHIKV infection (Fig.36). In parallel, as we had difficulties to detect SINV by immunostaining in Aag2 cells, we have shown by supernatant titration (TCID50 assay on VeroE6 cells) that FAC also decreased SINV infection in Aag2 (data not shown).

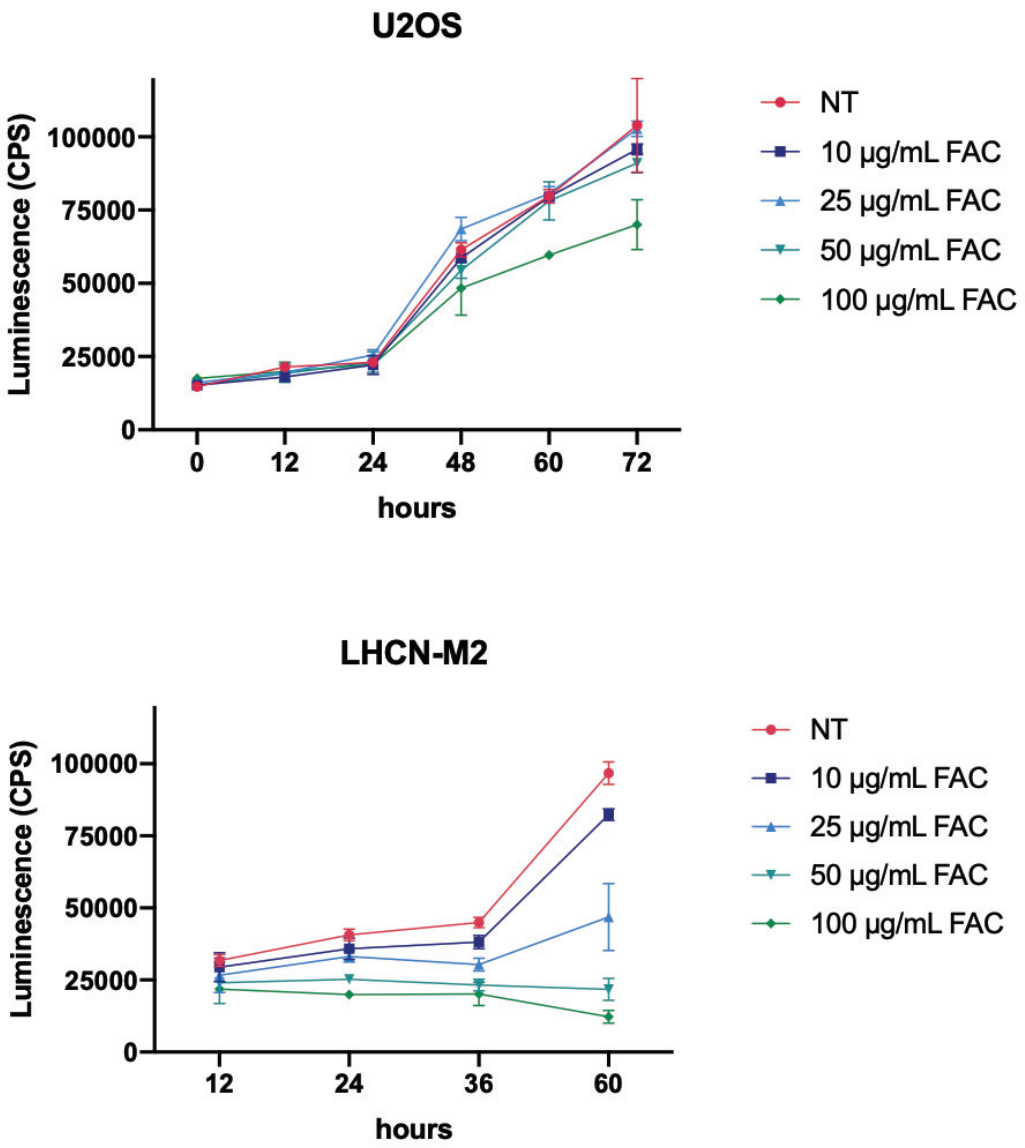

Figure 34: Cell viability after iron treatment with ferric ammonium citrate
Cell viability of both cell lines was measured at different times after treatment with several concentrations of ferric ammonium citrate (FAC) using the CellTiter-Glo® luminescent cell viability assay kit (Promega). NT = untreated, CPS = count per second

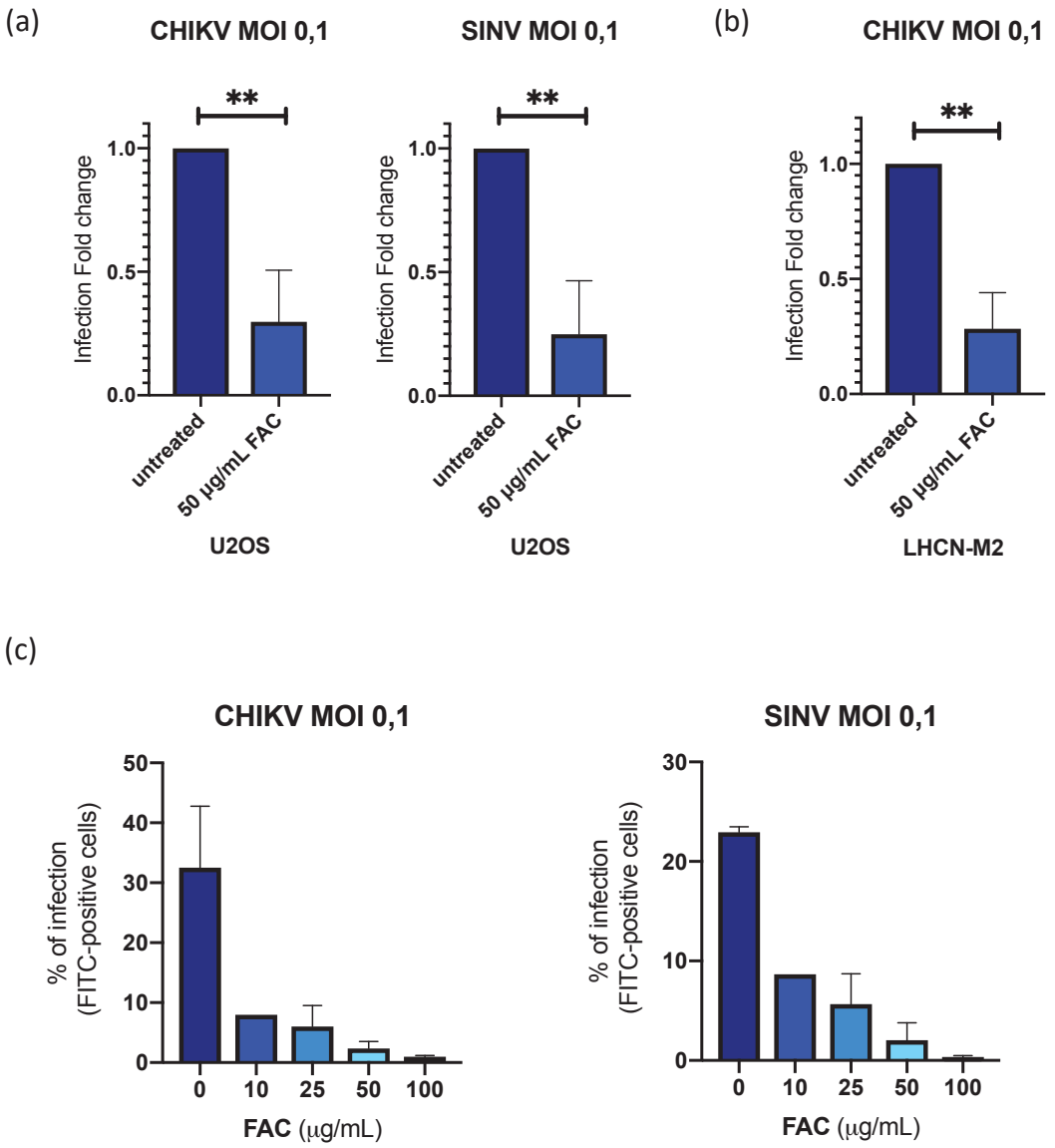

Figure 35: Effect of iron treatment on chikungunya virus and Sindbis virus infection in mammal cell lines

(a) Proportion of infected cells after 24h of SINV or CHIKV infection in presence of 50 µg/mL of FAC in U2OS cells (n=3). Infection on untreated cells was established at 1.

(b) Proportion of infected cells after 24h of CHIKV infection in presence of 50 µg/mL of FAC in LHCN-M2 cells (n=3). Infection on untreated cells was established at 1.

(c) Dose-dependent inhibition of SINV and CHIKV infection in U2OS cells by increasing dose of FAC (n=2).

Cells untreated or treated with FAC were infected with CHIKV or SINV at MOI 0,1 and harvested at different time points after infection. Cells were fixed in PFA 4% before immunostaining with a primary antibody raised to Semliki Forest nucleocapsid protein, that reacts with CHIKV and SINV capsid protein (IgG2a C42) and then analyzed by flow cytometry analysis. Statistical analyses were made with unpaired t-test with p-value < 0,05.

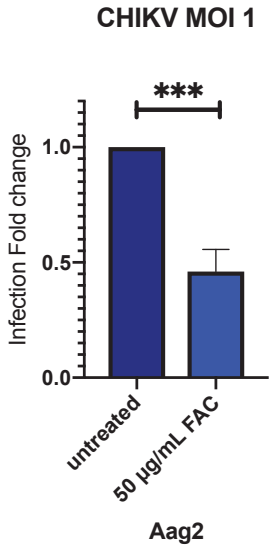

Figure 36: Effect of iron treatment on CHIKV infection in Aag2 mosquito cells
Proportion of infected cells after 24h of CHIKV infection in presence of 50 µg/mL of FAC (n=3).
Aag2 cells were infected with CHIKV at MOI 1 and harvested after 24h of infection. Cells were fixed in PFA 4% before immunostaining with a primary antibody raised to Semliki Forest nucleocapsid protein, that reacts with CHIKV capsid protein (IgG2a C42) and then analyzed by flow cytometry analysis. Infection on untreated cells was established at 1. Statistical analysis was made with unpaired t-test with p-value < 0,05.

3 - NRAMP2 transcriptional and post-translational regulations after FAC treatment

A decrease of CHIKV and SINV infections induced by FAC treatment has been observed in mammal and mosquito cells. Since iron regulates many processes and proteins, we have tried to identify a potential host factor regulated by iron which could explain the infection decrease. The iron transporter NRAMP2 has been published several years ago as a potential receptor of SINV in mammal cells (Rose et al., 2011). In this publication, it was notably shown that FAC treatment decreases SINV infection as we have also observed. Thus, we have investigated the potential role of NRAMP2 for CHIKV entry.

SLC11A2 gene encoding NRAMP2 protein produces multiple isoforms through alternative promoters (1A or 1B) and/or alternative splicing to produce transcripts with or without an iron regulatory element (+IRE or –IRE).
Here we have, as a first step, examined mRNA and protein expressions in different cell lines after 24h and 48h of iron treatment with 50 µg/mL of FAC. RT-qPCRs were realized using published primers that recognize isoform 1A and isoform 1B, without distinction between +IRE and -IRE (Hubert and Hentze, 2002). Besides the skeletal

muscle cell line (LHCN-M2) and the osteosarcoma cell line (U2OS), we have used a cell line derived from epithelial intestinal cells called Caco2.
The 1A isoforms are known to be expressed in duodenum and kidney, while 1B isoforms are ubiquitously expressed. As we expected from the literature, 1A isoform has been found in large amount in Caco2 cells compared to LHCN-M2 and U2OS cells (Fig.37(a)). Moreover, 1B isoform has been observed in comparable quantity in the three cell lines nonetheless with an expression more important in LHCN-M2 cells (Fig.37(a)). Regarding the effect of iron on NRAMP2 expression, 1A isoform was greatly reduced in Caco2 and LHCN-M2 after 24h in presence of iron and expressed again after 48h (Fig.37(b)). In U2OS cells, the iron response seems slower with a slight decrease of 1A isoform at 24h and a higher reduction at 48h (Fig.37(b)). Overall, 1A isoform appears to be sensitive to iron and its regulation by iron was clearly visible.
On the other hand, the 1B isoform detected in Caco2 was halved after 24h and 48h of iron treatment (Fig.37(b)). In LHCN-M2 cells, the quantity of 1B isoform was also halved after 24h but seemed to slightly re-increased at 48h (Fig.37(b)). Finally, 1B isoform expression did not seem to be impacted by iron treatment in U2OS cells. Our results show that 1A isoform is more sensitive to FAC treatment than 1B isoform.

In parallel, NRAMP2 protein expression after iron treatment was also monitored by western blot analysis on whole cell lysates. The NRAMP2 mouse monoclonal antibody (sc-166884, Santa Cruz Biotechnology) used is raised against amino acids 461-568 mapping at the C-terminus of NRAMP2 and recognizes both 1A and 1B isoforms. After western blot revelation, we did not observe any changes in NRAMP2 protein expression after 24h and 48h of FAC treatment in the three cell lines (Fig.38). The western blot presented below is representative of what we observed in three separate experiments.

From these analyses, we can conclude that, surprisingly, after FAC treatment, we observed regulation of NRAMP2 mRNA level but the total cellular NRAMP2 protein content does not appear to vary significantly.

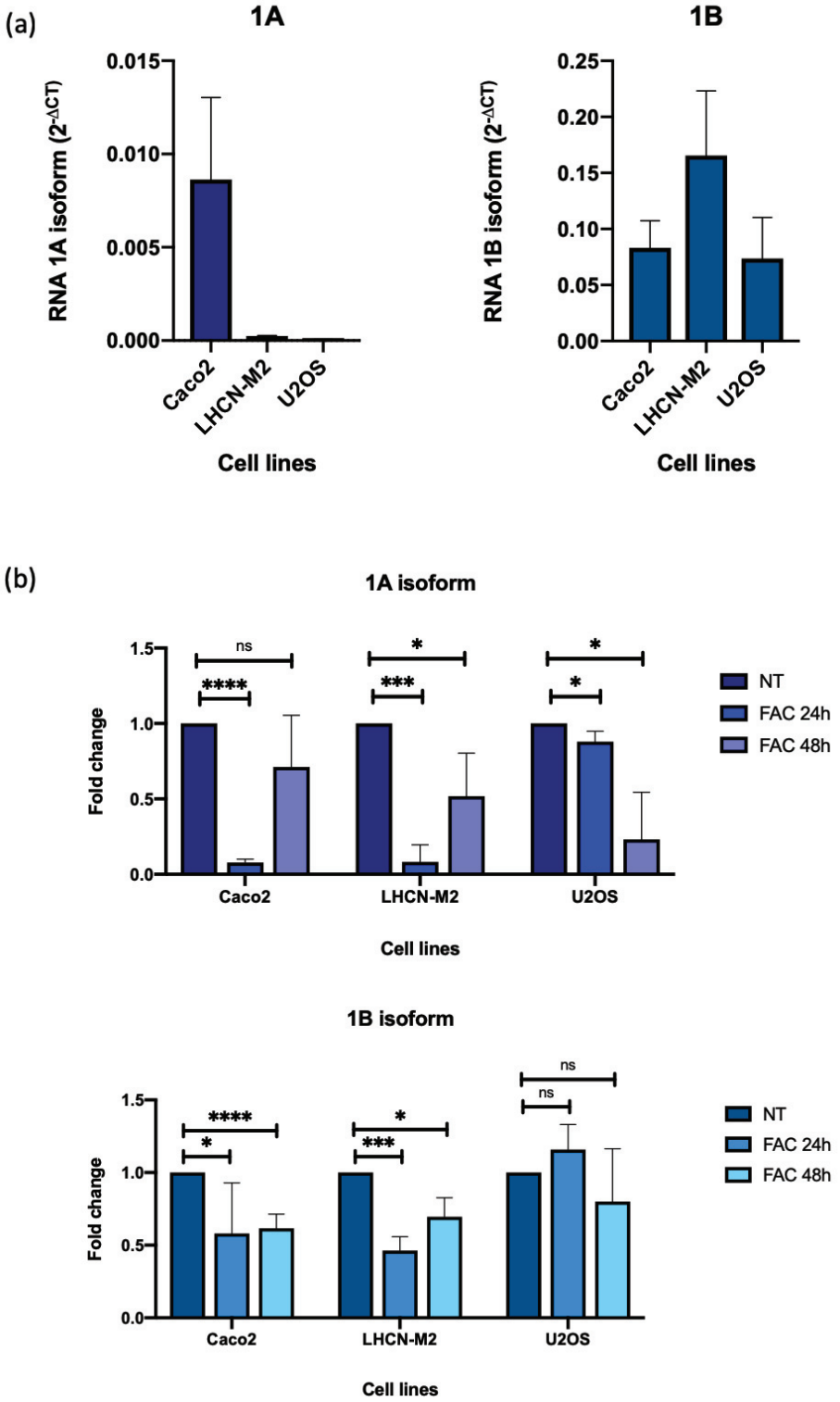

Figure 37: Monitoring RNA level of 1A and 1B isoforms of NRAMP2 by RT-qPCR

(a) Expression of 1A and 1B isoforms in the different cell lines (relative to 3 housekeeping genes)

(b) Effect of FAC treatment on both isoforms in the three cell lines. Cells were incubated for 24 h or 48 h after treatment with 50 μg/mL of FAC and RNA level monitored by RT-qPCR. (relative to 3 housekeeping genes) Expression on untreated cells was established at 1. NT= untreated control cells. n=3. Statistical analyses were made with unpaired t-test with p-value < 0,05.

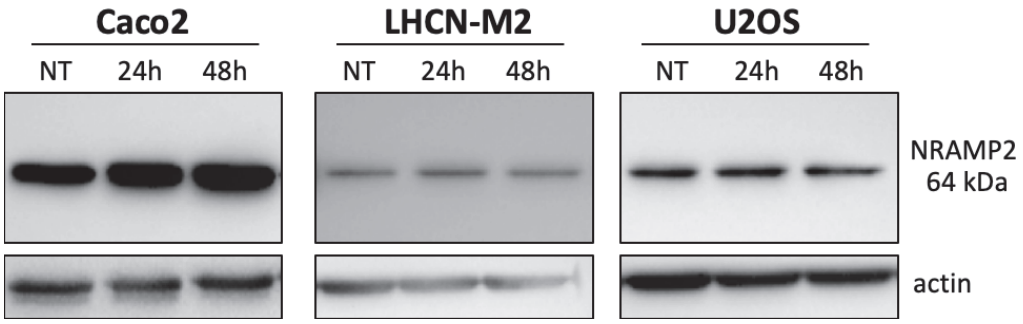

Figure 38: NRAMP2 protein expression in whole cell lysate after FAC treatment
Cells were treated with FAC and harvested 24h or 48h later. NRAMP2 mouse monoclonal antibody clone G-5 (sc-166884, Santa Cruz Biotechnology) was used to detect NRAMP2 protein. Antibody raised to housekeeping protein β-actin was used as an internal control.

4 - Effect of NRAMP2 downregulation and depletion on the entry of pseudotyped alphaviruses

As NRAMP2 is a transmembrane protein and suggested to be an alphavirus receptor (Rose et al., 2011), we chose to focus on viral entry. We decided to analyze the direct role of NRAMP2 in CHIKV entry by generating cell lines depleted for NRAMP2.
We generated NRAMP2 CRISPR-mediated knockout in U2OS and LHCN-M2 cell lines. NRAMP2 knockouts were confirmed by western blot analysis using an antibody recognizing all isoforms (Fig.39). For studying the viral entry, we used pseudotyped viruses consisting of a replication-deficient lentiviral backbone which displays CHIKV or SINV envelope proteins at the surface and carries GFP reporter. For most of virus families, their entry mimics perfectly the entry properties of wild type replicating virus. Pseudoparticles bearing envelope protein of Vesicular Stomatitis Virus (VSV) were used as a control. WT and NRAMP2 CRISPR-mediated knockout cell lines were infected with pseudoparticles as described earlier. Three days post-infection, pseudoparticles entry was assessed by GFP reporter gene expression. We checked that infection percentage never exceed 50 % to remain in the linear range. NRAMP2 knockout in LHCN-M2 did not seem to affect CHIKV and SINV pseudoparticles as the GFP level were equivalent to WT cells (Fig.39(a)). Same observations were made in U2OS cells infected CHIKV and SINV pseudoparticles (Fig.39(a)). As expected, no changes in infection by VSVg pseudotypes were observed as VSV was shown recently to use Low-Density Lipoprotein (LDL) receptor for entry.
In parallel, to verify that our protocol did not induce a bias in our analysis, we have realized shNRAMP2 mediated knockdown in the Caco2 cell line and carried out

infection with pseudoparticles in these cells. GFP levels in cells infected with CHIKV or SINV pseudoparticles were comparable between WT and shNRAMP2 Caco2 cells (Fig.39(b)).

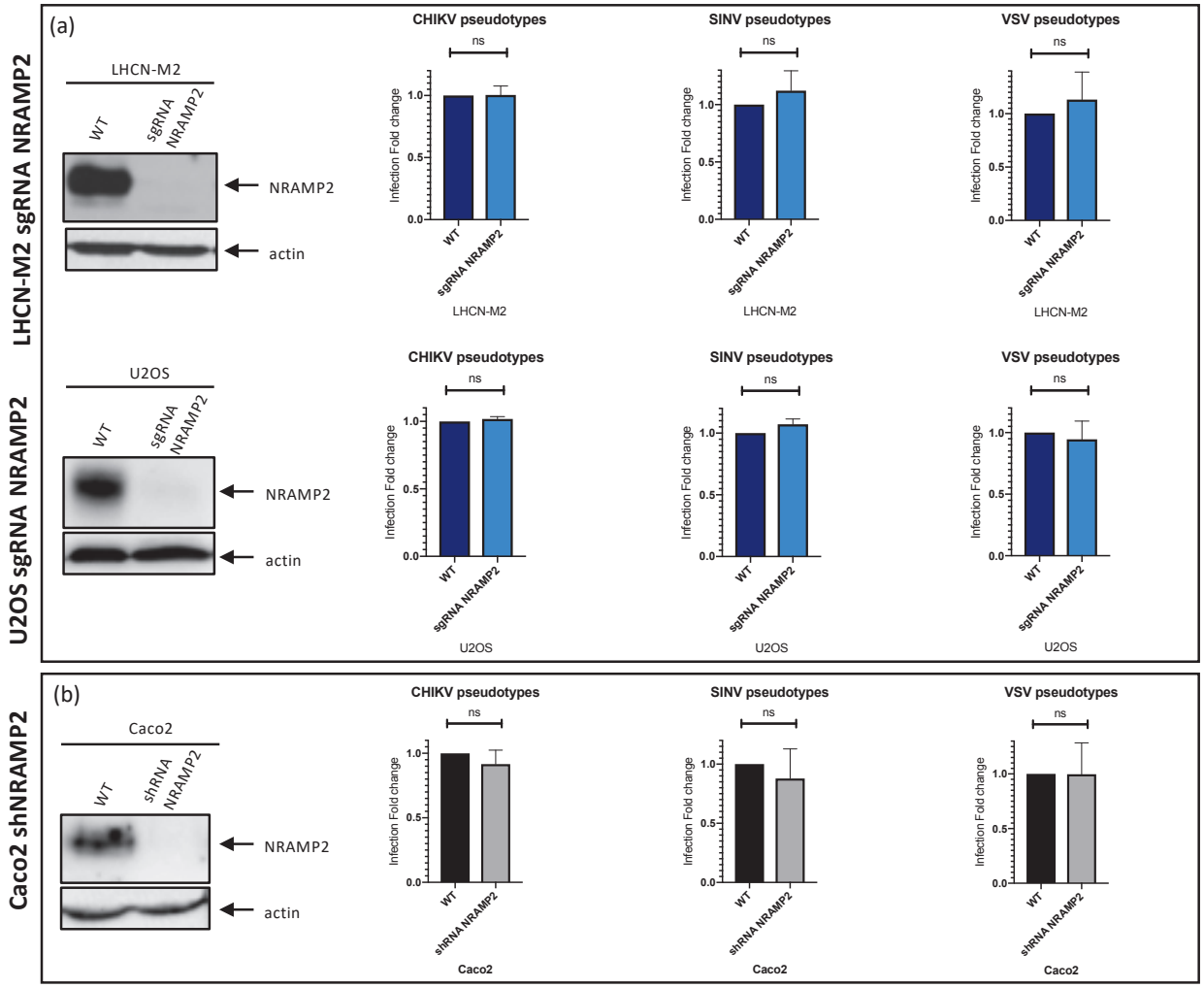

Figure 39: Infection with pseudotyped viruses in cells depleted or downregulated for NRAMP2

(a) NRAMP2 depletion (sgRNA) has no effect on infection with SINV and CHIKV pseudotyped viruses in U2OS and LHCN-M2 cell lines. n=3

(b) NRAMP2 knockdown (shRNA) has no effect on infection with SINV and CHIKV pseudotyped viruses in the Caco2 cell line. n=3

NRAMP2 expression was analyzed by western blot using NRAMP2/SLC11A2 mouse monoclonal antibody clone 4G2. Antibody raised against β-actin protein was used as an internal control.

Pseudoparticles entry was determined by measuring the percentage of GFP positive cells using a flow cytometer. Infection on naïve WT cells was established at 1. Statistical analysis was made with unpaired t-test with p-value < 0,05. ns= non significative

5 - Effect of NRAMP2 downregulation and depletion on SINV and CHIKV infection

As the NRAMP2 knockout and downregulation did not seem to have an impact on the entry of pseudotyped alphaviruses, we assumed that NRAMP2 might be important for another step in the viral cycle. Hence, we have carried out infection assays with replicative viruses in the cell lines with NRAMP2 knockout and knockdown. We found that NRAMP2 CRISPR-mediated knockout did not influence CHIKV infection in LHCN-M2 and U2OS cell lines (Fig.40(a)). Surprisingly, NRAMP2 knockout in U2OS cells did not seem to impact SINV infection either.
Despite clear downregulation of NRAMP2, infection rates for CHIKV at both MOI 1 and 0,1 were comparable between wild-type (WT) and shNRAMP2 Caco2 cells. Infection levels were also equivalent in both cell lines with SINV (Fig.40(b)).

6 - Study of the correlation between NRAMP2 expression profile and cell permissiveness for CHIKV

In parallel of infection assays, we have tested several cell lines for their permissiveness for CHIKV and simultaneously examined NRAMP2 protein expression in these cell lines. Whereas most of blood-derived cells are refractory to CHIKV (excepted macrophages and platelets), CHIKV is known to infect many different adherent cells including Hela (cervical carcinoma epithelial), 293T (kidney epithelial), MRC5 (primary lung fibroblasts), Vero (monkey kidney epithelial), BEAS-2B (bronchial epithelial) (Sourisseau et al., 2007). In our assay, different cell lines were infected with CHIKV and the level of infection was monitored by immunostaining followed by flow cytometry analysis and/or titration of viral production in the cell supernatant.
In parallel, whole cell lysate was loaded and separated by SDS-PAGE, then NRAMP2 protein was detected by western blot analysis using an antibody that recognizes all isoforms (Fig.41). For lymphoid Jurkat and Raji cell lines known to be refractory for CHIKV, we did not observe CHIKV-positive cells after infection as expected. Regarding NRAMP2 expression, Jurkat cells seem to express the protein while no NRAMP2 protein was detected in the Raji cell line. A431 cell line was shown as poorly sensitive to CHIKV although it expressed the NRAMP2 protein. HT1080 and HOS cell lines are mildly sensitive to CHIKV and do not express NRAMP2 at all. Finally, Caco2, Hela, LHCN-M2 and U2OS cell lines were demonstrated to be permissive for CHIKV and to express NRAMP2.
Although we observed NRAMP2 protein expression in cell lines sensitive to CHIKV, it seems difficult to establish a correlation between NRAMP2 protein expression and cell sensitivity to CHIKV infection.

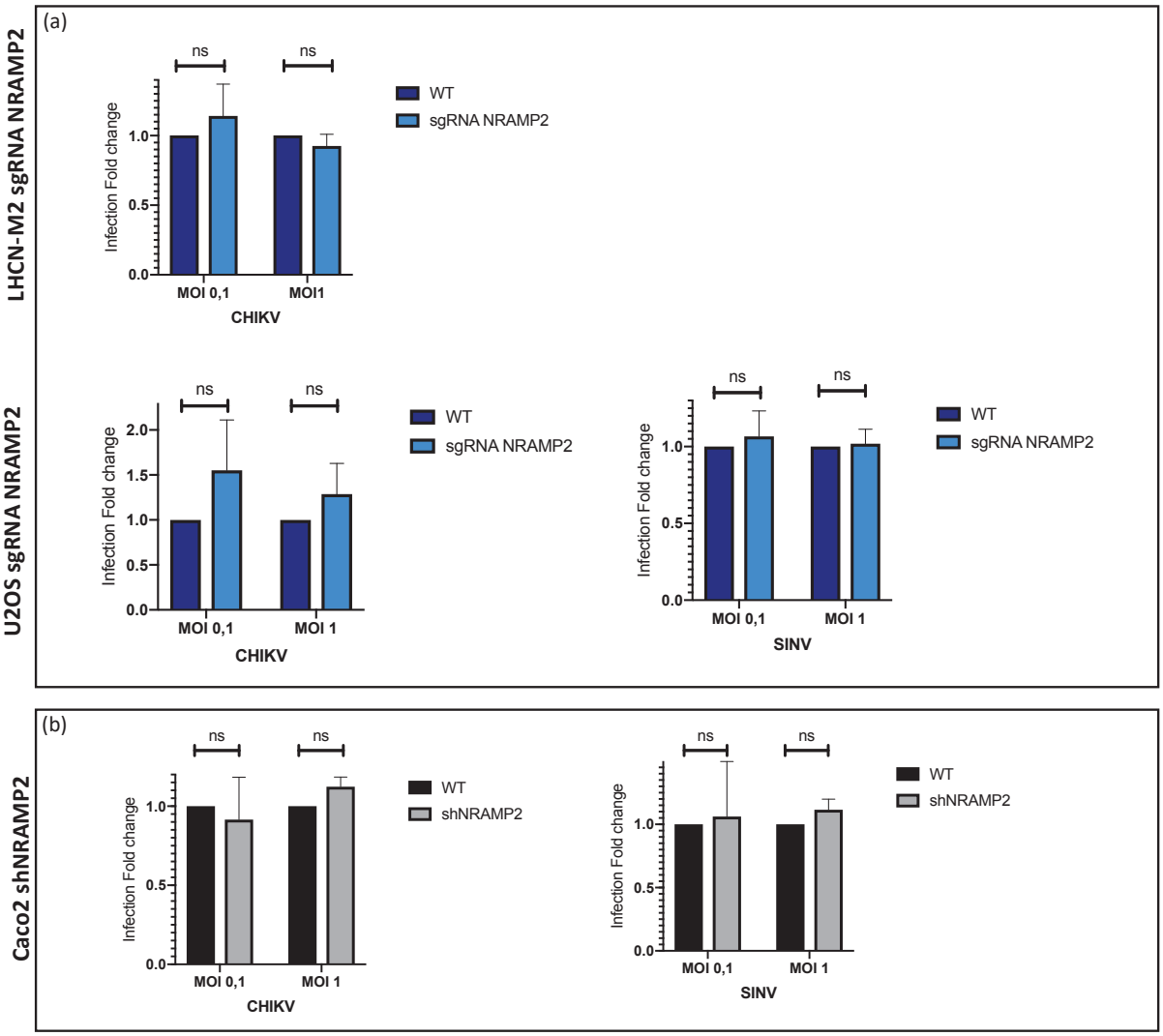

Figure 40: Replicative virus infection in cells depleted or downregulated for NRAMP2

(a) NRAMP2 depletion (sgRNA) has no effect on CHIKV infection in LHCN-M2 cells and on SINV and CHIKV infection in U2OS cells. n=3
(b) NRAMP2 knockdown (shRNA) has no effect on SINV and CHIKV infection in Caco2. n=3
Infection of knockout cells was measured by FACS using C42 antibody raised against SFV nucleocapsid protein. Infection on naïve WT cells was established at 1. Statistical analysis was made with unpaired t-test with p-value < 0,05.
ns= non significative

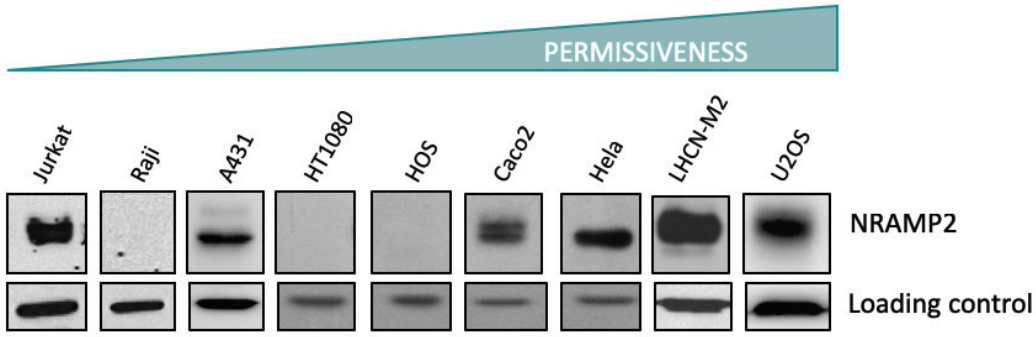

Figure 41: Study of cell permissiveness to CHIKV infection and NRAMP2 protein expression
***Jurkat**: CD4⁺ T lymphoid cell line, **Raji**: B lymphoid cell line, **A431**: epidermoid carcinoma epithelial cell line, **HT1080**: connective tissue fibrosarcoma epithelial cell line, **HOS**: bone osteosarcoma fibroblast/epithelial-like cell line, **Caco2**: colorectal adenocarcinoma epithelial-like cell line, **Hela**:* cervical carcinoma epithelial cell line, ***LHCN-M2**: immortalized human myoblast cell line, **U2OS**: bone osteosarcoma epithelial cell line.*
Cell permissiveness was assessed by infection assays and NRAMP2 protein was detected by western blot on whole cell lysate using SLC11A2 monoclonal mouse antibody clone 4G2 (SAB1404146, Sigma Aldrich). Antibody raised to housekeeping protein tubulin or β-actin was used as an internal control.

7 - Effect of Transferrin Receptor (TFRC) depletion on CHIKV and SINV infection

Two TFRC CRISPR-mediated knockout cell lines were generated using two distinct sgRNA targeting different sequences into the TFRC gene. The CRISPR-mediated knockout in 293T was validated by cell surface immunostaining with an anti-TFRC/CD71 antibody (DF1513, SantaCruz sc-7327) followed by flow cytometry analysis. Percentage of cells expressing TFRC in the WT population was around 80% while percentages were around 5% in both cell lines with sgRNA TFRC (Fig.42). As these two cell lines were indeed depleted for TFRC protein, we realized infection assays with either alphavirus derived pseudoparticles or replicative alphaviruses.

TFRC depleted and WT cells were transduced with pseudotyped virus harboring either CHIKV, SINV envelope proteins or VSV-g as a control. In regard to alphavirus pseudotyped viruses, TFRC depletion did not seem to alter entry of the different pseudoparticles (Fig.43). The entry of control VSV-pseudotyped viruses was not affected by TFRC depletion in 293T cells.

In parallel, TFRC knockout and WT cell lines were infected simultaneously with CHIKV or SINV at two different MOI for 24h. At MOI 0,1, we observed a small increase of

CHIKV infection in TFRC KO cell lines compared to WT cells (Fig.44) while infection levels between cell lines are similar at MOI 1. Regarding SINV, infection levels were comparable between WT and KO cell lines, except for CHIKV MOI 0,1 in sgRNA_2 TFRC cells but with large variability between replicates. Taken together, it seems that the depletion of TFRC protein has no impact on CHIKV and SINV infection in 293T cells. However, it is interesting to note that we observed variations between the two TFRC cell lines generated with different sgRNAs. It highlights the importance to work with independent replicates generated with different sgRNAs even if the population is a cellular pool. Despite the requirement of TFRC for the entry of other RNA viruses, our data enabled to demonstrate that the transferrin receptor is not required for CHIKV and SINV entry route.

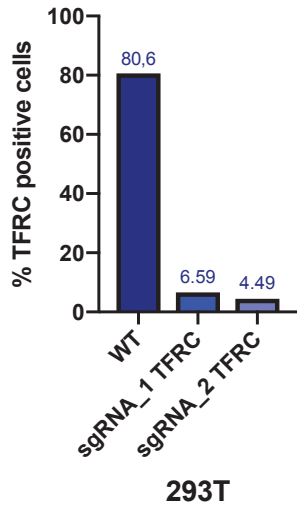

Figure 42: Validation of TFRC CRIPSR-mediated knockout in 293T by immunostaining and flow cytometry analysis.
TFRC protein expression was assessed by cell surface immunostaining with anti-TFRC CD71 antibody (DF1513, SantaCruz sc-7327) at 1 µg/mL in PBS 1X-2% FBS-0,1% NaN_3 and anti-mouse IgG coupled with FITC. Cells were analyzed on FACS calibur cytometer (BD Biosciences).

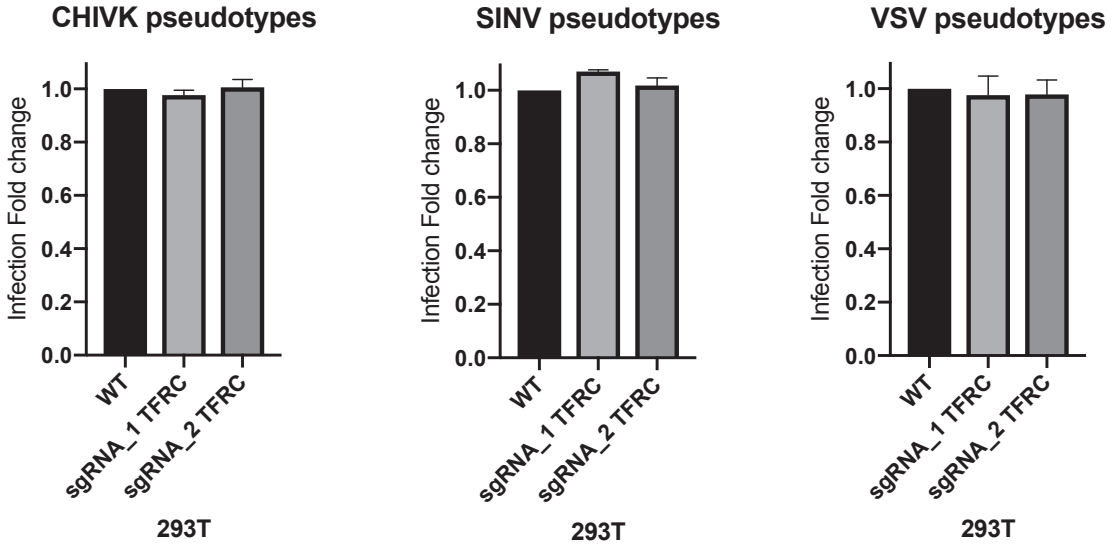

Figure 43: Infection assays in WT and sgRNA TFRC cell lines with pseudoparticles.
Cells were incubated with pseudoparticles 2 h at 37°C before medium change and then harvested 3 days post-infection and fixed in PFA 4%. Pseudoparticles entry was determined by measuring the percentage of GFP positive cells using a flow cytometer. Infection on naïve WT cells was established at 1. (n=2)

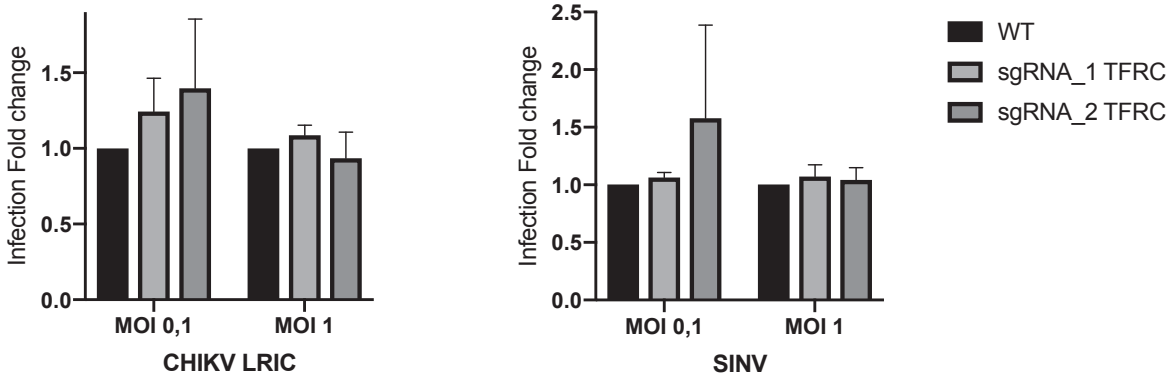

Figure 44: CHIKV and SINV infection assays in WT and sgRNA TFRC 293T cells.
Cells were infected with CHIKV or SINV at MOI 0,1 or MOI 1 for 24h and then harvested and fixed in PFA 4%. CHIKV and SINV infection was monitored by immunostaining using primary antibody raised to Semliki Forest nucleocapsid protein, that reacts with CHIKV and SINV capsid protein (IgG2a C42) and then analyzed by flow cytometry analysis. Infection on naïve WT cells was established at 1. (n=2)

IV - Discussion

As we mentioned earlier, iron is essential for cellular processes and activities and is probably important also for viruses as cell-dependent pathogens. However, it has recently been shown that iron in the form of ferric ammonium citrate (FAC) presents an antiviral effect on several diverse viruses (Wang et al., 2018). In our study, we have investigated and demonstrated an antiviral role of FAC treatment on alphavirus infection including CHIKV and SINV. Then we have studied a potential involvement of protein implicated in iron transport to explain this inhibition of infection and we have demonstrated that neither NRAMP2 or TFRC are required for CHIKV infection. This suggests that the antiviral effect of iron on alphavirus infection is dependent on another still unexplored mechanism.

We have initially observed a decrease of SINV and CHIKV infection in U2OS cells and a decrease of CHIKV infection in LHCN-M2 after treatment with FAC. Since iron catalyzes the formation of reactive oxygen species which can damage cells (Andrews, 2000), we have evaluated the toxicity of FAC treatment on U2OS and LHCN-M2 cells by realizing viability assays. It has permitted to show that iron does not affect U2OS cell viability even at high concentration while LHCN-M2 cells appear to be more sensitive to high iron concentration. We have then demonstrated that the FAC effect on alphavirus infection is dose-dependent. In parallel, as alphaviruses are transmitted by mosquitoes and are known to infect and replicate efficiently in the *Aedes aegypti* mosquito cell line, Aag2, we have investigated the FAC effect on mosquito cell line infection. We have demonstrated an antiviral activity of FAC on CHIKV and SINV infection in Aag2 cells. A decrease of SINV infection after FAC treatment in Aag2 has already been published but with a lower iron-concentration and a longer treatment duration (Rose et al., 2011).
We have sought a virus as a control which would not be affected by FAC treatment.
Two published experiments highlight the insensitivity of West Nile virus (WNV) to FAC treatment. In U2OS cell line, it has been shown that treatment with 160 µM (≈42 µg/mL) of FAC does not affect WNV infection and seems to even increase the infection level (Rose et al., 2011). In another study focusing on WNV infection of its *Culex* mosquito vector, it has been demonstrated that increasing iron levels increase viral titers (Duchemin and Paradkar, 2017). Thus, WNV appears to be a proper control virus for our infection assays. Preliminary promising results have allowed to observe similar infection levels with WNV in untreated and FAC treated U2OS cells. However,

infection levels were a bit low to clearly conclude. Further experiments with a higher MOI will be conducted.
It should be noticed that ferric ammonium citrate has an opposite effect on two viruses of the same genus of flavivirus. As we just mentioned above, FAC appears indeed to increase the infection of the flavivirus West Nile while Wang et al. have emphasized that infection of the flavivirus Zika was inhibited by FAC (Wang et al., 2018). These two flaviviruses are known to share a similar replication cycle in cells (Brinton, 2013; Medigeshi, 2011). Nonetheless, the distinct experiments seem difficult to compare as they have not been realized in the same cell line and the virus has been produced in cell lines from different species.

As NRAMP2 is a divalent metal transporter regulated by iron and has been reported as the receptor of Sindbis virus in mammals (Rose et al., 2011), we have studied its potential involvement in CHIKV entry.
Overall, we have observed a rapid regulation of NRAMP2 mRNA, isoforms 1A and 1B, after iron treatment in Caco2 and LHCN-M2 cells. In contrast, the regulation of 1A isoform is slower in U2OS cells after FAC treatment and the expression of 1B isoform transcript does not seem to be regulated. Our data suggest that 1A isoforms are more sensitive to FAC treatment than 1B isoforms. Interestingly, NRAMP2 1A/+IRE isoform is predominantly detected at the plasma membrane, whereas the 1A/−IRE, 1B/+IRE and 1B/−IRE isoforms are more abundant in intracellular compartments i.e. recycling endosomes (Seo et al., 2016). The iron-dependent regulation is linked to IRE harbored by mRNA in its 3' UTR (Lee et al., 1998). However, it was also shown that the exon 1A region adds an in-frame translation initiation codon extending the NRAMP2 open reading frame (ORF) by a sequence of 29-31 amino acids which participates in iron regulation of NRAMP2 expression (Hubert and Hentze, 2002). This could explain the higher iron susceptibility of 1A isoform compared to 1B isoform.

In parallel, we have realized western blot analysis to detect NRAMP2 protein in the whole cell lysate. Iron treatment with FAC did not seem to modify total abundance of expressed NRAMP2 protein and we did not observe a relationship between mRNA level variations and protein expression. Even if it may seem surprising as it is usually assumed that there is some correlation between the levels of mRNA and protein, several reasons might explain this poor correlation. First, there are many varied post-transcriptional mechanisms involved in turning mRNA into protein that are not yet sufficiently well-defined to be able to compute protein concentrations from mRNA. On the other hand, information regarding *in vivo* half-lives of NRAMP2 protein in our

different cell lines is poorly described. It is maybe the easiest explanation for the lack of correlation during 48 hours between mRNA level and protein level. Longer treatment associated with RNA and protein detection will be necessary to validate this hypothesis. On the other hand, regulation of NRAMP2 protein might occur in many different ways, including the relocalization of NRAMP2 transporter from cell membrane to recycling endosome by internalization (Lam-Yuk-Tseung and Gros, 2006). In addition, the transport-activity of NRAMP2 can be regulated *via* the phosphorylation of NRAMP2 (Seo et al., 2016). These types of regulation are not detectable by western blot on whole cell lysate but might be the mean used by the cell to rapidly control iron transport prior to RNA-dependent regulation. Finally, in regard to the methods employed, both western blot and qPCR are at risk of errors and noise and western blot analysis is hardly quantitative. In the end, these results do not highlight a link between FAC treatment, NRAMP2 protein expression and the decrease of viral infection.

We have then carried out infection assays in cell line knockout or knockdown for NRAMP2 to investigate more specifically a potential role of the protein in chikungunya virus infection.
Our data suggest that NRAMP2 is not required for chikungunya virus infection in Caco2, U2OS and LHCN-M2 cells. Our CRISPR approach will be validated in short-term experiments by adding a positive control in our infection assays. We have indeed planned to generate CRISPR-mediated knockout for the protein Mxra8 which has been recently described as a receptor for chikungunya virus in mammal cells (Zhang et al., 2018). As the first description of the role of NRAMP2 has used RNAi technologies, we also knockdown NRAMP2 in human cells using shRNA that targets the RNA (and not the genome directly as for CRISPR/Cas9 strategy). However, no effect of NRAMP2 reduction on the CHIKV and SINV entry or replication was observed neither. Since it's generally assumed that RNAi induces many off-target effects, cell lines with scramble shRNA are also going to be generated.

We sought to find out if there was a correlation between the permissiveness of cells to chikungunya virus and expression of NRAMP2 protein. In our experiments, cell lines refractory to CHIKV infection appear to express NRAMP2 protein while some cell lines which did not express NRAMP2 were susceptible to CHIKV infection. Thus, the permissiveness of cells to CHIKV does not seem to be strictly correlated with the presence of NRAMP2.

Taken together with infection assays in depleted cell lines, our data suggest that NRAMP2 is not required for CHIKV biology.

Surprisingly, in our hands, we did not either observe an effect of NRAMP2 depletion on SINV infection in U2OS cells as it was described (Rose et al., 2011). In this publication, the dNRAMP (*Drosophila* NRAMP) transporter was identified as required for SINV infection thanks to a genome-wide RNAi screen in *Drosophila* cells. The role of dNRAMP was confirmed in *Drosophila* cells by silencing gene with double-stranded RNA (dsRNA) *in vitro* and also *in vivo*. They took advantage of the sensitivity to iron of the transporter to study NRAMP involvement in SINV infection in mosquito vector and mammal cells. However, it should be noticed that the expression of many proteins and many cellular activities are modified upon iron treatment (Wang and Pantopoulos, 2011).

Rose et al. have shown that iron in form of FAC, decreased SINV infection in *Aedes aegypti* cells and they suggest that NRAMP is also required for viral entry into vector mosquitoes.

A study has recently identified new candidate iron transporters from the Zinc-regulated transporter/Iron-regulated transporter-like and Zinc transporters (ZIP and ZnT) gene families in the mosquito *Aedes aegypti,* but they were unable to identify an NRAMP2 ortholog in *Aedes aegypti* or other culicine mosquitoes (Tsujimoto et al., 2018). This suggests that the inhibition of SINV infection noticed in Aag2 cells after FAC treatment may not be correlated to NRAMP2, and a translation of results obtained in *Drosophila* insect model may not always be possible in other insects or mammals.

In human U2OS cells, Rose et al. have demonstrated that FAC decreased SINV infection as we also observed. Their data suggest that NRAMP2 co-precipitates with SINV and that this interaction is lost under high iron concentration. Finally, they have shown the requirement of NRAMP2 for SINV infection with Cre-Lox knockout in a different cellular model which are mouse embryonic fibroblasts (MEFs). It is nonetheless difficult to compare with our results because the origin of the cell line and the technique used to deplete gene are both different.

In a genome-wide RNAi screen conducted later in U2OS cells, Ooi et al. explained that they did not find NRAMP2 in their screen but they identified FBXL5 as an inhibitor of SINV infection (Ooi et al., 2013). The iron-sensing protein FBXL5 promotes the degradation of the iron regulatory proteins that stabilize the mRNAs of both NRAMP2 and transferrin receptor (TFRC) (Thompson and Bruick, 2012).

The sensitivity of CHIKV to iron has made of the transferrin receptor another interesting candidate for viral entry. Furthermore, TFRC has been identified as a cellular receptor for different viruses including haemorrhagic fever arenaviruses Machupo (MACV), Guanarito (GTOV), Junin (JUNV) (Radoshitzky et al., 2007), feline panleukopenia virus and canine parovirus (Parker et al., 2001). Lastly, a team has shown that TFRC was involved in Hepatitis C virus (HCV) particles internalization (Martin and Uprichard, 2013). Nonetheless, our data did not suggest a role of TFRC in CHIKV and SINV entry even if iron-sensing protein FBXL5 regulates TFRC and even if FAC inhibits infection.

To conclude, the two candidates tested, NRAMP2 and TFRC, did not appear to be required for infection in mammal cells. The inhibition of infection observed after iron treatment in mammal cells and insect cells might be linked to another unexplored mechanism.

The study from Rose et al. on NRAMP2, the publication on the antiviral effect of iron and our experiments share a common point which is the use of iron in the form of ferric ammonium citrate. As we discussed earlier, Wang et al. have demonstrated that FAC has an antiviral effect and that both ferric ion and citrate ion of the complex were required for the antiviral activity.

In their study, in order to understand the antiviral mechanism of FAC, they were focused first on viral entry and have shown by doing virus attachment assays that FAC does not inhibit viral binding on the cell surface but target early events (Wang et al., 2018). Indeed, the inhibitory effect of FAC is lost when it is added 3h post infection. It has been observed that FAC directly promotes the fusion of virions on the plasma membrane, which made the virions difficult to be endocytosed by the cell. In spite of this fusion induced by FAC, a part of virus particles was shown to still enter the cell. However, it has been found that FAC also enhances intracellular vesicle fusion thus preventing the release of viruses from the endosome and keeping them in endosomal compartments. Since FAC was shown to induce liposome aggregation as well, the authors have suggested that FAC binds to phosphate head group of phospholipid molecules of the viral membrane to explain the fusion of viruses and intracellular vesicles. Nonetheless, they do not exclude the possibility of FAC interference with intracellular proteins involved in vesicle traffic, fission or fusion.

This mechanism of action of FAC might explain the decrease in CHIKV and SINV infection observed in our experiments and the decrease of SINV infection in the experiments of Rose et al. as well. SINV and CHIKV might be indeed sensitive to FAC and particles could fuse together as it has been noticed for the other viruses. In

addition, since alphavirus entry is mainly mediated by endocytosis, FAC might also interfere with endosomes and enhance vesicles fusion thus preventing the delivery of alphavirus into the cytoplasm.
By treating cells with FAC at different time points of the infection (prior to infection, during viral incubation and/or after incubation time), we could understand which stage of the viral infection is affected by FAC. More specifically, binding assays could be realized to determine if FAC modifies viral attachment on cell surface by measuring viral RNA by RT-qPCR. Finally, we could carry out time course immunofluorescence of chikungunya virus after infection of cells with or without ferric ammonium citrate to compare viral replication in both conditions.

To sum up, we have highlighted the inhibition of chikungunya and Sindbis viruses infection by ferric ammonium citrate in human cells and in *Aedes aegypti* cells as well.
Our data suggest that the NRAMP2 transporter and the transferrin receptor, both regulated by iron, are not involved in chikungunya virus entry and early infection steps. We suggest a direct antiviral effect of iron as ferric ammonium citrate as it has been recently published for several viruses. Further experiments will be conducted to explore the mechanism of action of FAC on CHIKV and SINV infection.

Chapter 2 - Receptor candidates: infection assays of CRISPR-mediated knockout cells

I - Context

- **Alphavirus entry pathway**

Viral entry into host cells is a key step in viral infection. For enveloped viruses, after nonspecific attachment to different cell surface molecules, the primary step involves specific binding of the viral glycoproteins to cellular receptors and possibly co-receptors. Following this binding, the virus is internalized, and the viral material released into the cytoplasm thanks to the fusion of viral and endosomal membranes. Most viruses use receptor-mediated endocytosis, generally mediated by the formation of clathrin-coated pits and the transport to early endosomes where fusion is triggered by the low-pH environment. Alternatively, some viruses enter into cells via clathrin-independent pathways, such as caveolar/raft pathway or small GTPases dependent pathway (Mayor and Pagano, 2007).
Alphaviruses belong to enveloped viruses. Their nucleocapsid is surrounded by a lipid bilayer containing glycoproteins E1 and E2 organized in a trimer of heterodimers. It is established so far that E2 protein mediates virus attachment with protein receptors while E1 is responsible for low-pH mediated fusion of viral and endosomal membranes after clathrin-dependent endocytosis. Within endosomal vesicles, low-pH environment leads to the dissociation of E1-E2 heterodimer resulting in the liberation of E1 fusion loop and insertion in the membrane. This allows the rearrangement to a homotrimeric complex active for fusion. The fusion of alphavirus particles to membrane required also the presence of cholesterol (Kielian et al., 2010; Leung et al., 2011). This fusion of envelope with the membrane of endosome releases alphavirus nucleocapsid into the cytoplasm.

Despite many studies, factors required for alphavirus entry into cells remain poorly understood. Since Sindbis and chikungunya viruses are able to infect many different tissues and many different species, it suggests either the cell receptor is a ubiquitous class of molecules or alphaviruses utilize different or multiple receptors on different cells from different species.
Several molecule candidates have been suggested in the literature to act as alphavirus receptors and/or attachment factors in a non-specific manner, including

the high-affinity laminin receptor, the class I major histocompatibility antigen, α1ß1 integrin, cell surface glycosaminoglycan heparan sulfate, and C-type lectins (DC-SIGN and L-SIGN) (Kielian et al., 2010). As we discussed in the first chapter, NRAMP2 has been proposed as the receptor for Sindbis virus in mammal cells (Rose et al., 2011). More recently, Mxra8, a receptor for multiple arthritogenic alphaviruses including CHIKV and O'nyong nyong virus has been identified in a genome-wide CRISPR/Cas9 based screening in mice cells (Zhang et al., 2018).
Moreover, the human T-cell immunoglobulin and mucin-domain protein (TIM1) has been proposed as a mediator of the entry of a broad range of enveloped viruses including filovirus, flavivirus, New world arenavirus and alphavirus. Generally, TIM-family proteins specifically bind phosphatidylserine (PS) on apoptotic cells and promote their phagocytosis. TIM proteins have been suggested as an attachment factor for these viruses through binding PS residues exposed on the viral membrane (Jemielity et al., 2013; Moller-Tank et al., 2013).

Regarding the endocytosis stage, fuzzy homolog (FUZ) known to be involved in planar cell polarity and cilia biogenesis was identified as required for clathrin-dependent internalization of alphaviruses and endocytic ligand transferrin in human cells (Ooi et al., 2013). They also determined that TSPAN9, a member of the tetraspanin family, promotes infection by the alphaviruses Sindbis (SINV), Semliki Forest (SFV), and chikungunya (CHIKV) by using TSPAN9 siRNA in U2OS and Hela human cell lines (Ooi et al., 2013). TSPAN9 was shown to be localized at the plasma membrane and in early and late endosomes. TSPAN9 seems to be critical for efficient low pH-triggered fusion of alphavirus particles with the endosomal membrane by modulating early endosome compartment (Stiles and Kielian, 2016).

- **Potential entry factors identified in a preliminary screen**

A collaboration between several laboratories has focused on tetraspanin-enriched microdomains (TEM) as common pan-viral entry pathway. Using proteomic analysis, RNAi and viral pseudoparticles, the consortium and collaborators have identified cell membrane proteins of TEM as broad cell entry factors for pathogens of eight virus families (unpublished data). Among the identified cell membrane proteins, three candidates seem potentially important for chikungunya virus entry: **CD46, TM9SF2** and **PVR** (unpublished data, confidential).
CD46 receptor, also known as membrane cofactor protein (MCP), is a regulator of complement innate immunity system. CD46 is expressed in most human cells. It binds several viruses such as enveloped RNA measles virus (Dörig et al., 1993), enveloped

DNA human herpes virus 6 (HHV6), non-enveloped DNA adenoviruses B and D, and other pathogens like some serotypes of streptococcus bacteria (Cattaneo, 2004). CD46 seems to be a port of entry for many pathogens but the reasons for such an attractive molecule remain unclear. It might be linked to its capacity to drive T-cell differentiation via its cytoplasmic tail through which it connects innate and acquired immunity. This could allow pathogens to unbalance the immunity response (Cattaneo, 2004).

The second protein identified is **TM9SF2** which is a member of the transmembrane 9 superfamily with a little-known function. A study published meanwhile has shown that TM9SF2 knockout strongly affects the expression of N-sulfate of Heparan Sulfate (HS) because it is involved in the proper localization and stability of NDST1, the catalyzer of N-sulfation of HS (Tanaka et al., 2017).

Lastly, the third protein identified in the screen is **PVR** (also called CD155) which is a transmembrane glycoprotein belonging to the nectin-like molecule family. PVR was originally identified as a receptor for Poliovirus, a human neurotropic virus which invades the central nervous system (Mendelsohn et al., 1989). The external domain of PVR mediates cell attachment to the extracellular matrix, while its intracellular domain interacts with the dynein light chain DYNLT1 (Mueller et al., 2002). This interaction of PVR with DYNLT1 could explain how poliovirus reaches the neuronal cell body via retrograde axonal transport. As another dynein light chain, DYNLT3, was identified in our CRISPR genome-wide screen with CHIKV, this interaction aroused our interest. This topic and the study of PVR in chikungunya virus entry will be dealt in chapter 2 of Part 2 regarding the DYNLT3 protein candidate.

In this context, our aim was to study and characterize these first steps of infection for alphaviruses relying especially on these potential candidates. For this, we generated CRISPR-mediated knockout cells and realized infection assays to test a potential role of CD46 and TM9SF2 proteins in alphavirus early infection steps.

II - Material and methods

1 - Cell lines

HEK 293T, BHK21, and VeroE6 cells were cultured in Dulbecco's Modified Eagle Medium (DMEM; Gibco™ Thermo Scientific) supplemented with 10% fetal bovine serum (FBS; HyClone).
LHCN-M2 (human skeletal myoblasts) were maintained in medium 4:1 DMEM/Medium 199 (Gibco™ Thermo Scientific) supplemented with 15% FBS, 0,02 M HEPES, 0,03 µg/mL Zinc sulfate (Sigma Aldrich), 1,4 µg /mL Vitamin B12 (Sigma Aldrich), 0,055 µg /mL Dexamethasone (Sigma Aldrich), 2,5 ng/mL recombinant human Hepatocyte Growth Factor (HGF, Peprotech), 10 ng/mL recombinant human FGF-basic (Peprotech).
All cell lines used were maintained at 37°C in the presence of 5% of CO_2 in a humidified incubator.

2 - Generation of CRISPR-mediated knockout cell lines

a. sgRNA design

Sequences of single-guide RNA (sgRNA) for specific gene knockout were designed using different online tools as described in the previous chapter. The following primers were used for CD46 and TM9SF2 sgRNA:

Guide name		Sequence 5'-3'
sgRNA_1 CD46	Forward	CACCGTTTAAAGGATCCCGTATATA
	Reverse	AAACTATATACGGGATCCTTTAAAC
sgRNA_2 CD46	Forward	CACCGAACTCGTAAGTCCCATTTGC
	Reverse	AAACGCAAATGGGACTTACGAGTTC
sgRNA_1 TM9SF2	Forward	CACCGAACGTAAACTTATATGGTGA
	Reverse	AAACTCACCATATAAGTTTACGTTC
sgRNA_2 TM9SF2	Forward	CACCGTGGATAATATGCCTGTAACG
	Reverse	AAACCGTTACAGGCATATTATCCAC

b. Cloning, lentivirus production and cell line generation

As described in the previous chapter, sgRNAs were cloned into the lentiCRISPRv2 vector, then lentiCRISPRV2 constructs were used to generated lentivirus particles and

subsequently CRISPR-mediated knockout cell lines. We have tried to generate CD46 knockout in 293T and LHCN-M2 cells and TM9SF2 knockout in 293T cells only.

3 - Validation of gene knockout

Depending on the tools available, several strategies were used to confirm gene knockout in the different cell lines.

a. Flow cytometry immunostaining

The sgRNA CD46 cells were directly stained for cell surface protein detection. Cells were incubated 1h at 4°C with mouse monoclonal CD46 antibody (clone 13/42, kindly provided by C.Levy, ENS, Lyon) in PBS 1X-2% FBS-0,1% NaN_3 (PBFA). After 3 washes with PBFA, cells were incubated with an anti-mouse fluorochrome-conjugated secondary antibody in PBFA. After 3 washes with PBFA, immunostained cells were analyzed using a flow cytometer (Accuri C6 or FACSCalibur, BD Biosciences).

b. RNA detection by RT-qPCR

RT-qPCR analysis was used to detect TM9SF2 specific mRNA since no antibodies gave good results or were available. Total RNA of CRISPR and control cell lines were extracted using NucleoSpin® RNA kit (Macherey Nagel). RNA was reverse transcripted using PrimeScript™ RT-PCR kit (Takara). mRNAs were quantified by qPCR amplification in AriaMx system (Agilent) using SYBR Premix Ex Taq II (Takara) and the following primers: hTM9SF2/Fw 5'-CAGATGGGCGTCTAGATGGG-3', hTM9SF2/Rv 5'-CTGGGCATCTTCCGTAGAGTC-3'. Results were normalized by at least three different housekeeping genes (RPL27, RPL22, GUSB).

4 - Isolation of a clonal population

For sgRNA CD46 cell lines, a heterogeneous population was observed by flow cytometry showing cells with effective gene knockout and some with a wild type phenotype. Two different approaches were used. For 293T cells, single cell cloning by dilution in 96-well plate was realized to obtain a clonal population with a real knockout. Since LHCN-M2 cells do not tolerate single cell dilution even with conditioned media, cell sorting was established. LHCN-M2 cells were filtered through 70 µm pore-sized membranes prior to sorting. Cells were stained as described above

with CD46 antibody and fluorochrome-conjugated secondary antibody and then sorted using FACSAria cytometer (BD Biosciences).

5 - Production of alpha-pseudotyped viruses and infection assay

For infection assays, VSV- and CHIKV-pseudotyped retroviral particles were generated as described in the previous chapter.
One day before infection, CRISPR and control cell lines were plated in 48-well plates. Cells were transduced with pseudotyped viruses and incubated 2 h at 37°C before medium change. Cells were harvested 3 days post-infection and fixed in paraformaldehyde 4% at 4°C for 15 min. The cells were directly analyzed to measure the percentage of GFP positive cells using a flow cytometer (Accuri C6 or FACSCalibur, BD Biosciences).

6 - Production of replicative alphaviruses and infection assay

CHIKV LRic strain LR2006 OPY1 (European Virus Archive; Marseille) and Sindbis virus strain Toto1101 were produced as described in the previous chapter. Viral stocks were titrated by TCID50 and plaque assay on VeroE6 cells.

One day before viral infection, CRISPR and control cell lines were plated in 48-well plates. Cells were infected with replicative viruses at MOI 0,1 or MOI 1 and incubated 2 h at 37°C before medium change. Infected cells were harvested 24h post infection and fixed in paraformaldehyde 4% at 4°C for 15 min. The cells were permeabilized with saponin 0,1% for intracellular immunostaining and incubated at 4°C with a primary antibody raised to Semliki Forest nucleocapsid protein, that reacts with CHIKV and SINV capsid protein (IgG2a C42 kindly provided by Dr. Irene Greiser-Wilke, School of Veterinary Medicine (Hannover, Germany)). After washes, cells were incubated with anti-mouse IgG FITC conjugated secondary antibody (F0257, Sigma Aldrich), cells were analyzed using a flow cytometer (Accuri C6 or FACSCalibur, BD Biosciences).

III - Results and discussion

1 - Effect of CD46 depletion on entry of CHIKV-derived pseudoparticles

A cell surface immunostaining was realized with sgRNA CD46 293T cells and we observed a heterogeneous population of some cells with effective gene knockout and some with a wild type phenotype. Single cell cloning by dilution in 96-well plate was realized to obtain a clonal population with a real knockout. Each clone was subsequently tested for its CD46 expression status by cell surface immunostaining and we finally selected one clonal cell population depleted for CD46 protein (Fig.45). The wild-type (WT) 293T and clonal CD46 knockout cells were infected with pseudotyped viruses with CHIKV envelope proteins and GFP reporter gene. Level of pseudotyped viruses which entered the cells was monitored by measuring GFP-positive cells by flow cytometry. A slight decrease of GFP-positive cells was observed for cells with sgRNA targeting CD46, however, this diminution was not statistically significative (Fig.46). Comparison of clonal population with a WT pooled population is complex as clonal cell line might present a very distinct phenotype. Moreover, clonal cells might grow slower or faster than WT cells and as cells were not counted the day of infection, 24h after cell seeding, the MOI applied might vary from one cell line to another. Therefore, these results need to be taken with caution and we decided to develop another cell line.

sgRNA CD46 LHCN-M2 were also generated and like 293T cells, we observed a heterogeneous population of some cells with effective gene knockout and some with a wild type phenotype by flow cytometry analysis. As LHCN-M2 cell do not tolerate single cell cloning, we isolated a population depleted for CD46 by cell sorting (Fig.47). WT LHCN-M2 and CD46 knockout cells were infected with pseudotyped virus bearing either CHIKV envelope proteins or envelope of VSV (VSVg) as a control. The entry of CHIKV pseudotyped viruses and the entry of control VSV pseudotyped viruses were not impacted either by the CD46 knockout (Fig.48).
Altogether, even if a high variability was observed in 293T assays, we demonstrated that CD46 does not appear to be required for entry of CHIKV pseudotypes. Some exploratory infection assays performed with replicative viruses in 293T and LHCN-M2 cells knockout for CD46 (data not shown) did not bring evidence of an implication of CD46 for CHIKV infection neither. Experiments including Measle pseudotypes or virus should be added to validate the effect of CD46 KO.

Preliminary results from collaborators had shown that CD46 silencing with siRNA inhibits the entry of lentiviral pseudoparticles derived from CHIKV in Hela cells and the infection of Huh 7.5.1 cells with replicative CHIKV LRic strain (personal communication). CD46 protein might be involved in CHIKV entry in Hela cells and in Huh 7.5.1 but might be non-essential or used only as a cofactor in our cell lines. On the other hand, it is also possible that preliminary results obtained with siRNA are not reproducible with the CRISPR/Cas9 approach due to the high prevalence of off-target effects with RNAi reagents.

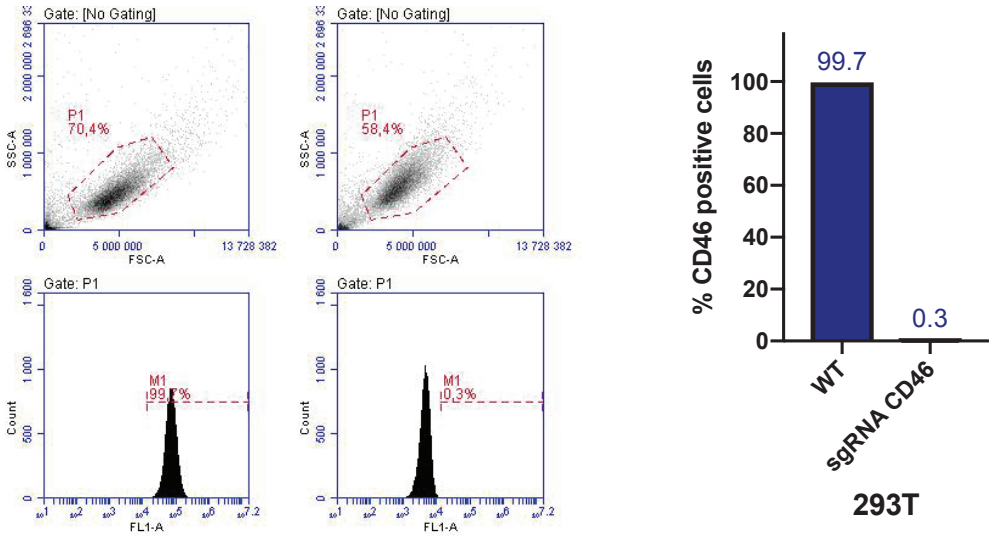

Figure 45: Validation of CD46 CRISPR-mediated knockout in clonal 293T population after serial dilution by immunostaining and flow cytometry analysis
Cell surface immunostaining was realized with CD46 antibody (clone 13/42, kindly provided by C.Levy, ENS, Lyon) in PBS 1X-2% FBS-0,1% NaN_3 and anti-mouse IgG coupled with FITC. Cells were analyzed on A6 accuri cytometer (BD Biosciences).

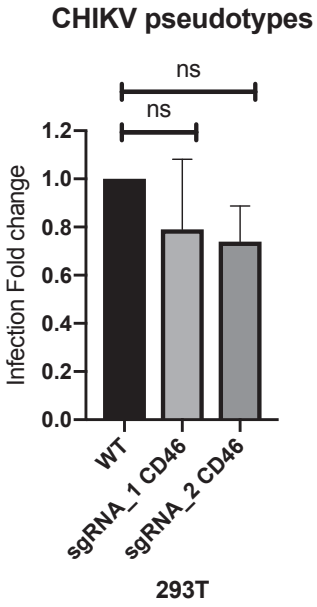

Figure 46: Infection assay in WT and clonal CD46 knockout 293T cell lines with CHIKV-derived pseudoparticles

Cells were incubated with pseudoparticles 2 h at 37°C before medium change. Cells were then harvested 3 days post-infection and fixed in PFA 4% before flow cytometry analysis (n=3). Statistical analyses were made with unpaired t-test with p-value < 0,05. Infection on naïve WT cells was established at 1.

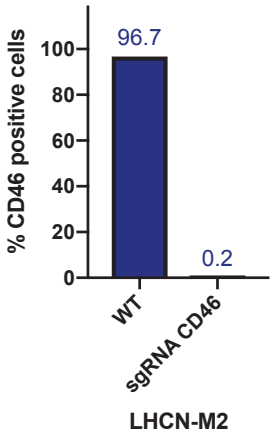

Figure 47: Validation of CD46 CRISPR-mediated knockout in LHCN-M2 population after cell sorting by immunostaining and flow cytometry analysis.

Cell surface immunostaining was realized with CD46 antibody (clone 13/42, kindly provided by C.Levy, ENS, Lyon) in PBS 1X-2% FBS-0,1% NaN_3 and anti-mouse IgG coupled with FITC. Cells were analyzed on A6 accuri cytometer (BD Biosciences).

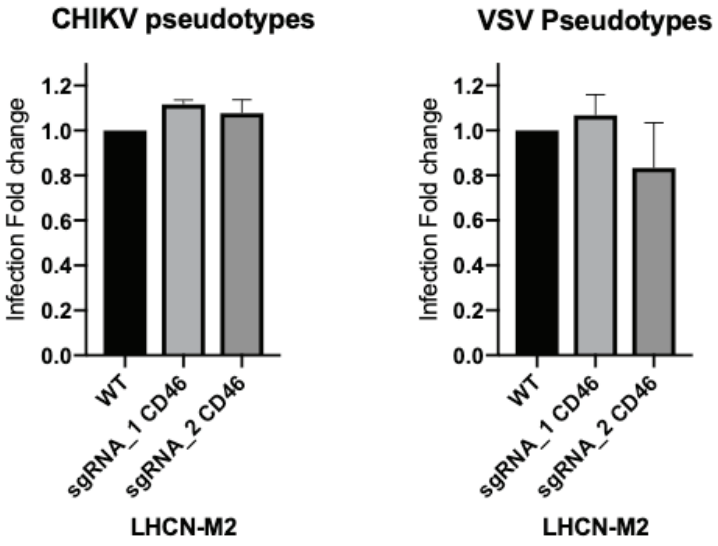

Figure 48: Infection assay in WT and CD46 knockout LHCN-M2 cell lines with CHIKV- and VSV-derived pseudoparticles.
Cells were incubated with pseudoparticles 2 h at 37°C before medium change. Cells were then harvested 3 days post-infection and fixed in PFA 4% before flow cytometry analysis (n=3). No significative differences observed with unpaired t-tests. Infection on naïve WT cells was established at 1.

2 - Effect of TM9SF2 depletion on SINV and CHIKV infection

As the antibody targeting the TransMembrane 9 SuperFamily member (TM9SF2) we had was not functional, we tried to confirm the disruption of TM9SF2 mRNA in 293T cells by RT-qPCR. Compared to WT cells, sgRNA TM9SF2 cells had 50% less TM9SF2 mRNAs meaning that at least one of both alleles has been altered (Fig.49). However, we were not able to conclude on the protein expression status for this cell line as we don't know if the remaining 50% of mRNAs are wild-type or altered and lead to translation of a correctly folded and active TMS9F2 protein or not.
Through preliminary data from collaboration, TM9SF2 silencing using siRNA had been shown to inhibit CHIKV derived pseudoparticles entry in both Hela and Huh 7.5.1 cells and replicative CHIKV infection in Huh 7.5.1 cells (data not shown).
In our study, infection assays were realized on WT and sgRNA TM9SF2 cells with replicative alphaviruses. A decrease of CHIKV infection was observed for both 1 and 0,1 MOI in sgRNA TM9SF2 cells compared to WT cells (Fig.50). The difference was significative only for infection at MOI 1. Regarding SINV infection, a slight non significative diminution was also detected with an MOI of 0,1 but a high variability was noticed among replicates (Fig.50). Lastly, no variations in infection levels were detected in sgRNA TM9SF2 cells compared to WT cells with SINV at MOI 1. During

the course of our study, it has been published that TM9SF2 is involved in the proper localization and stability of NDST1, a catalyzer of N-sulfation of Heparan Sulfate (Tanaka et al., 2017). Heparan sulfate was identified for the first time in 1998 as a receptor for alphaviruses. Tanaka et al. also illustrate that knockout of TM9SF2 reduced the susceptibility of HAP1 human haploid cells to CHIKV infection *via* a non-working N-sulfation activity. This result is in correlation with the slight decrease of CHIKV infection observed in our experiment. A cell line with complete depletion of TM9SF2 might be used as a control in future experiments.

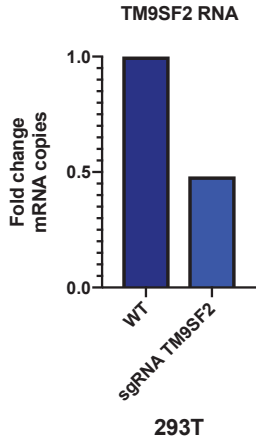

Figure 49: Quantification of TM9SF2 transcripts in WT and sgRNA TM9SF2 cells
RT-qPCR was realized on total RNA extracted to quantify TM9SF2 RNA in both cell lines.

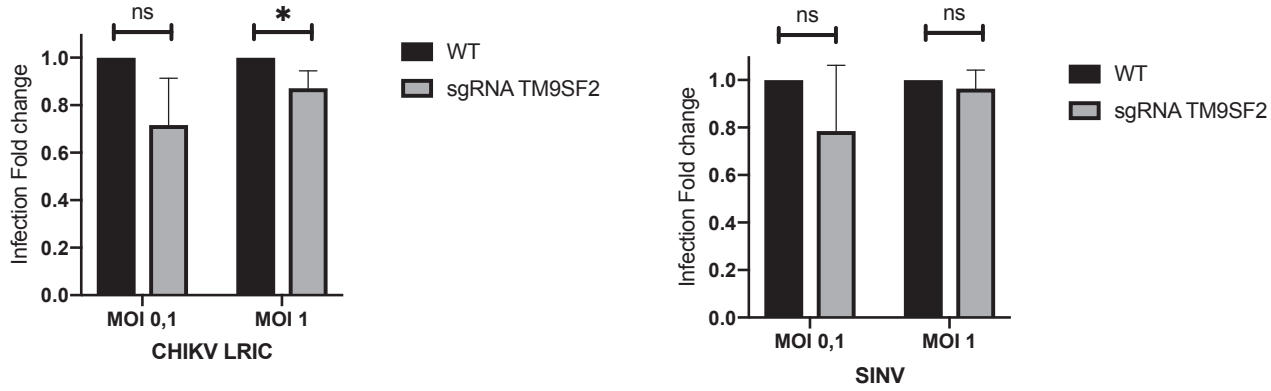

Figure 50: CHIKV, SINV and SFV infection assay in WT and sgRNA TM9SF2 cells
Cells were infected with CHIKV or SINV at MOI 0,1 or MOI 1 for 24h. Cells were harvested and fixed in PFA 4% before immunostaining and flow cytometry analysis (n=3). Statistical analyses were made with unpaired t-test with p-value < 0,05. Infection on naïve WT cells was established at 1.

PART 1 - Conclusion

To sum up this first part, we mainly focused on early steps of replication by studying the involvement in the viral entry of iron-dependent proteins, NRAMP2 and TFRC and then we have explored the role of CD46 and TM9SF2 proteins for chikungunya virus entry and replication.

Although we clearly observed an effect of iron on chikungunya virus infection, it appears that neither NRAMP2 nor TFRC were required for chikungunya virus infection of human cell lines. As it has been described for several viruses, we have suggested a direct antiviral effect of iron in the form of ferric ammonium citrate on chikungunya virus replication in mosquito and mammal cell lines. Further experiments should be realized to understand the mechanism of action of ferric ammonium citrate on viral replication as we discussed in the first chapter. In particular, we would like to determine if ferric ammonium citrate induces a non-specific fusion of virus particles and a fusion of intracellular vesicles or acts through a more complex pathway.

In parallel, two potential entry factors, CD46 and TM9SF2, had been identified through an RNAi screen in collaboration with other laboratories.
Preliminary results from collaborators had suggested an involvement of CD46 in CHIKV entry in Hela and Huh 7.5.1 cell lines. On the other hand, CD46 is known to be involved in several virus entry pathways such as Measle virus. However, using two CRISPR/Cas9 knockout cell lines, in our hands, CD46 protein does not appear to be required for CHIKV pseudoparticles entry. As we have suggested earlier, CD46 requirement for CHIKV entry might vary from a cell type to another and the use of different approaches to deplete protein could impact the reproducibility. However, it should be noticed that CD46 requirement has not been validated for any viruses identified in the screen so far (personal communication).

Preliminary data from collaboration had also highlighted a requirement of TM9SF2 for CHIKV entry. According to our data, we have also observed a small decrease of CHIKV infection in TM9SF2 CRISPR-mediated knockout cells although we were not able to characterize without ambiguity the knockout. Indeed, our cell line appears to be not fully knockout for TM9SF2 based on RNA analysis. TM9SF2 protein was poorly characterized at the time of its identification in the RNAi screen. A study published in the meantime, in 2017, highlighted the involvement of TM9SF2 in N-

sulfation of heparan sulfate and consequently the requirement of TM9SF2 for CHIKV infection (Tanaka et al., 2017). TM9SF2 candidate might serve as a positive control for our CHIKV infection assays by generating complete knockout.

PART 2

Genome-wide CRISPR/Cas9 mediated loss of function screen to identify host factors required for chikungunya virus infection

Chapter 1 - Realization of a genome-wide CRISPR/Cas9 screen

I - Context

- **Alphavirus studies with loss of function screens**

As described before, genome-wide screens are powerful tools to study virus-host interactions. Regarding alphaviruses, RNAi-mediated loss of function screens and haploid screenings have enabled the identification of host factors and pathways that either help (proviral) or limit (antiviral) viral replication.
A genome-wide RNAi screen in *Drosophila* cells has enabled the identification of a divalent metal ion transporter called natural resistance-associated macrophage (NRAMP2) and two related proteins, VCP and SEC61A, as factors required for SINV infection (Panda et al., 2013; Rose et al., 2011). Ooi et al. have realized a siRNA screen in human U2OS cells with SINV and identified Fuzzy homolog (FUZ) and tetraspanin membrane protein (TSPAN9) among others as required for SINV infection, but also for SFV and CHIKV infections (Ooi et al., 2013). Trafficking host factors used in human Hela cells by Venezuelan Equine Encephalitis Virus (VEEV) were identified by a siRNA screening (Radoshitzky et al., 2016). In parallel, a siRNA genome-wide loss of function screening was realized to find host factors implicated in CHIKV infection in human HEK-293 cells and to identify pathways possibly inhibited by effective chikungunya antiviral drugs (Karlas et al., 2016). Finally, a recent screen in human haploid cells HAP1 uncovered the importance of N-sulfation of heparan sulfate involving TM9SF2 protein for CHIKV infection (Tanaka et al., 2017).

In contrast to RNAi, which leads to partial depletion of expression for a specific gene, CRISPR/Cas9 enables a complete disruption of gene expression. CRISPR screens have allowed to study various viral infections with high fidelity and adaptability compared to RNAi and haploid screen approaches (cf. bibliographic synthesis). Recently, Rong Zhang et al. described Mxra8 as an entry mediator for multiple arthritogenic alphaviruses in humans including CHIKV. The cell adhesion molecule has been identified using a genome-wide CRISPR/Cas9-based screen in 3T3 mouse fibroblasts (Zhang et al., 2018).

- **Realization of a genome-wide loss of function screen with CRISPR/Cas9 to study chikungunya virus infection**

In order to identify cellular host factors important for chikungunya virus infection in humans, we carried out a genome-wide loss of function screen with CRISPR/Cas9 based on the stable knockout of genes. For this, each gene of the genome has been depleted using the CRISPR/Cas9 technology to identify which proteins, encoded by a gene, are required for the chikungunya virus infection.

Pooled screens rely on the physical separation of cells into subpopulations either enriched or depleted for the phenotype of interest. In our case, the phenotype of interest is cell viability. In the cell line used, chikungunya virus enters into the cell, replicates and induces strong cytopathic effects leading to cell death (Fig.51). This enables a straight selection of cells potentially resistant to the virus. Using a library of lentiviruses, a library of cells has been generated with one gene knockout in each cell. The principle is that majority of cells of the library die upon CHIKV infection and some cells survive and recover from CHIKV infection meaning that recovered mutant cells do not allow viral entry, translation, replication of viral genome or virus-induced cell death (Fig.51). Beforehand, practical considerations have to be taken into account to realize the screen, such as the choice of the cell line and of the CRISPR/Cas9 library.

Infection assays have been carried out to choose an appropriate cell line, efficiently infected by CHIKV and relevant for the study regarding the tropism in humans. Several human cell lines available in our lab were tested in CHIKV infection assays, including osteosarcoma cell line HOS, fibrosarcoma cell line HT1080, hepatocarcinoma cell line Huh7, melanoma cell line A375, epidermoid carcinoma cell line A431, adenocarcinoma cell line Caco2 and immortalized skeletal muscle cell line LHCN-M2. The immortalized human skeletal myoblasts were finally selected as they are able to produce a high virus titer and more than 99% of cells die after several days of infection. Immortalized cultured myoblasts consisted of a human myogenic cell line, called LHCN-M2, that had previously been obtained by introduction of human telomerase and cyclin-dependent protein kinase (Zhu et al., 2007). Different specific muscle cell markers have been well characterized in these cells. LHCN-M2 cells were known to be efficiently infected by CHIKV and likely to replicate the virus (Ozden et al., 2008). Given the cellular tropism of CHIKV for skeletal muscle cells among others (Ozden et al., 2007), LHCN-M2 cell line represents a relevant cellular model for CHIKV infection study. As LHCN-M2 cells are adherent cells which detach from the support when dying, this enables to easily keep the surviving cells and remove dead cells after viral infection.

The Zhang lab's GeCKOv2 sgRNA pooled library from the non-profit plasmid repository Addgene has been used for our screen. This library consists of over 100 000 unique sgRNAs for gene knockout in the human genome (Sanjana et al.). The library targets 19 050 genes and is split into two half-libraries called A and B, with each pool containing 3 sgRNAs against each gene, for a total of 6 sgRNAs per gene in the whole library. The library A also targets miRNAs (4 sgRNAs/miRNA). Both A and B libraries contain 1000 control sgRNAs designed not to target in the genome. The library is delivered as two pooled DNA plasmid half-libraries. Library's plasmids are based on a one vector expression system consisting of a lentiviral backbone containing both the *Streptococcus pyogenes* Cas9 nuclease and the single guide RNA (sgRNA) scaffold (Fig.52).

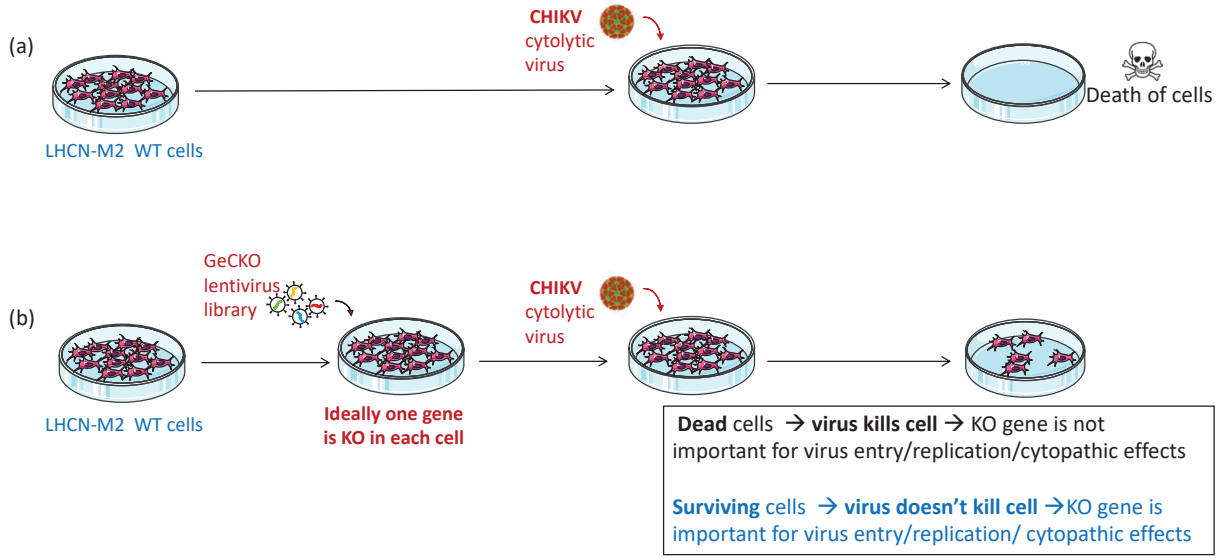

Figure 51: Principle of the genome-wide loss of function screen with CRISPR/Cas9 to identify important host factors for CHIKV infection

(a) Chikungunya virus enters and replicates efficiently in WT LHCN-M2 cells leading to the induction of cytopathic effects and cell death. Using a high MOI, all cells die after several days.

(b) Starting from LHCN-M2 WT cells, a library of cells with one gene knockout in each cell has been generated by transducing cells with the GeCKO lentivirus library. Infection with CHIKV enables a straightforward selection of virus-resistant cells. Majority of cells are dead, meaning that CHIKV killed them and that knockout genes in that particular cells were not important for viral entry or replication or for virus-induced cytopathic effects. In contrast, recovered mutants were not killed by virus meaning that knockout genes were genes involved in viral entry, translation of the viral genome, replication of the viral genome or virus-induced cell death.

(a)

Species	human
Number of genes targeted	19 050
Targeting constructs per gene	6 per gene (3 in library A, 3 in library B)
Number of miRNA targeted	1 864
Targeting constructs per miRNA	4 per miRNA
Control non-targeting sgRNAs	1 000
Total sgRNAs constructs	123 411 (65 383 in library A and 58 028 in library B)
Viral plasmid vector	Single vector lentiCRISPRv2

(b)

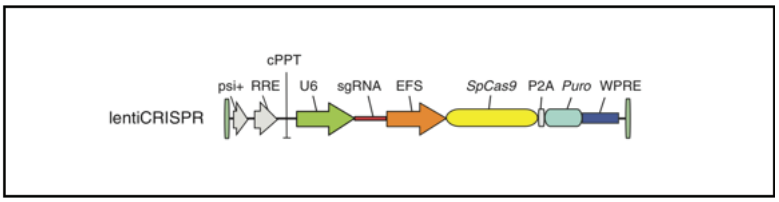

(c)

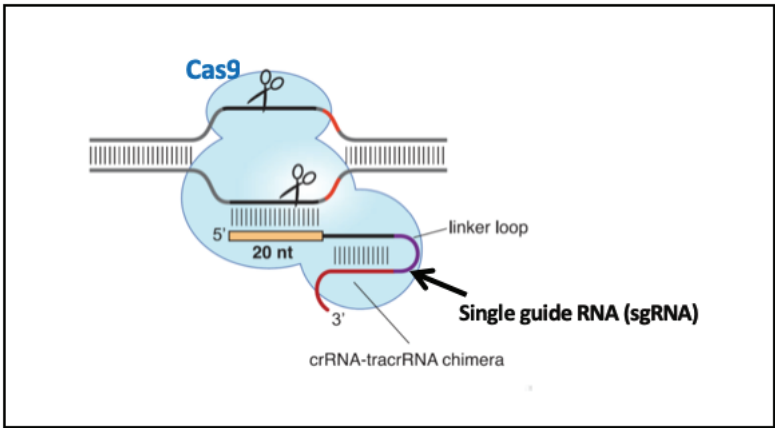

Figure 52: Genome-scale CRISPR Knock-Out (GeCKO) library

(a) Characteristics of the GeCKO v2 human library, adapted from Sanjana et al., 2014.
(b) Lentiviral expression vector for sgRNA and Streptococcus pyogenes Cas9 in one vector system. Psi+/Ψ : Psi packaging signal, RRE: rev response element, cPPT: central polypurine tract, U6: U6 promoter, sgRNA: sequence of sgRNA, EFS: elongation factor-1α short promoter, spCas9: Streptococcus pyogenes Cas9 gene, P2A: 2A self-cleaving peptide, Puro: puromycin selection marker, WPRE: post-transcriptional regulatory element.
(c) The lentiviral expression vector encodes Streptococcus pyogenes Cas9 protein which recognizes PAM sequence directly upstream of the target sequence and sgRNA which binds to the Cas9 enzyme and to the DNA target sequence. Both elements are expressed simultaneously in cells.

Starting from the library of lentiviral vectors, a library of lentivirus was generated and titrated precisely using the puromycin resistance. By transduction, a library of cells in which one gene is knocked out in each cell was created after selection. Subsequently, the library of cells was challenged twice with CHIKV. Finally, cell populations before and after viral challenge were sequenced. The genes driving cell survival were identified by comparing the relative abundance of corresponding sgRNAs in both fractions. The whole process is described in figure 53.

In this way, two screen replicates have been achieved separately and sgRNA enrichment analysis for both replicates has permitted to identify host factors potentially required for chikungunya virus infection. It should be noticed, however, that the two first steps, i.e. the amplification of plasmid library and the production of lentivirus, were common to both replicates.

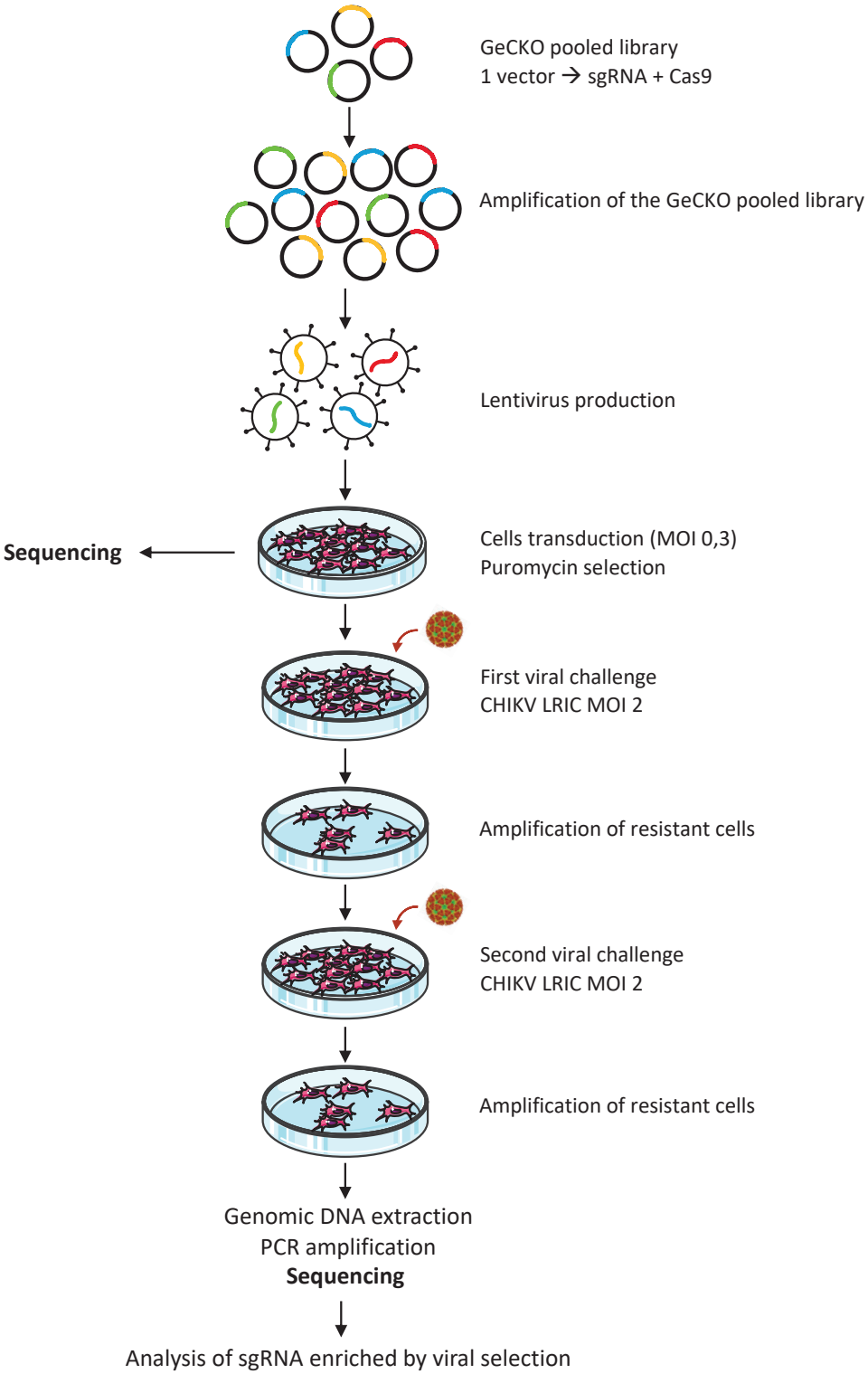

Figure 53: General workflow of the genome-wide screen

The library, delivered as two pooled DNA half-libraries, was amplified in competent bacteria cells. To ensure the sgRNA library's quality, it is important to maintain the complexity of the sgRNA pool when expanding the sgRNA plasmid pool in bacteria, during transduction of the target cells and during the extraction of genomic DNA from

cells for downstream analyses. Lentiviruses were produced by co-transfecting 293T cells with lentiviral vectors from the library, gag-pol packaging construct and glycoprotein-expressing construct. The use of lentivirus allows to obtain a stable cell line constitutively expressing a sgRNA and the Cas9 enzyme. LHCN-M2 cells were transduced with the library of lentiviruses with a low multiplicity of infection (MOI ~0,3) to ensure that only one integration event takes place per cell. Transduced cells were selected with puromycin treatment. A part of the whole cell library was used for next generation sequencing to determine sgRNA representation. The other part of the cell library was infected by replicative chikungunya virus using an MOI of 2. After several days, resistant cells from the infection were pooled and amplified for a second viral challenge. An MOI of 2 was also used for the second viral challenge with chikungunya virus. Surviving cells were amplified for subsequent genomic DNA extraction. PCRs were then realized to amplify the integrated sgRNA sequence and add at the same time adapters and barcode for the sequencing platform. After sequencing, sgRNA abundance between uninfected cells and surviving cells from viral challenges was compared.

II - Material and Methods

1 - Cell line and viral production

LHCN-M2 cells (immortalized human skeletal myoblasts) were used to generate the cell library of the genome-wide loss of function screen. HEK 293T cells were used for lentivirus production. BHK21 and VeroE6 cells were used for chikungunya virus production and titration respectively. Cell culture conditions were previously described in part 1. Chikungunya virus LRic strain was produced and titrated as previously described in part 1.

2 - Gecko library

The Zhang lab's Human CRISPR knockout pooled library (GeCKOv2 sgRNA library) was acquired from Addgene. The library targets 19 050 genes and is split into two half-libraries (A and B), with each pool containing 3 sgRNAs against each gene, for a total of 6 sgRNAs per gene in the whole library. The library A also targets miRNAs (4 sgRNAs/miRNA). The library includes 123 411 sgRNAs in total.

a. DNA amplification

Each lentiviral library (A and B) was amplified and prepared separately following the same protocol. Each library was diluted to 50 ng/µL in water and 2 µL of 50 ng/µL GeCKO library were electroporated in Endura electrocompetent cells (Lucigen). Electroporation in competent cells was made 4 times for each library. Cells were recovered in recovery media and placed in shaking incubator for 1 hour at 37°C. For each library, electroporated cells were plated on two pre-warmed 600 cm^2 LB agar plates with ampicillin and were grown for 16 hours at 37°C. In parallel, a 30 000-fold dilution of the full transformation was plated to estimate transformation efficiency to ensure that full library representation is preserved. The total number of colonies should be at least 3.10^6 corresponding approximatively to 50 colonies per construct in each GeCKO library. GeCKO library colonies were harvested by adding 10 mL of LB medium onto each plate and scrapped with a cell spreader. Liquid plus scrapped colonies were collected into a tube and the procedure was repeated a second time on the same plate with additional 10 mL of media. After centrifugation, bacterial pellets were weighed to determine the proper number of Maxiprep columns to use. Appropriated number of MaxiPrep (NucleoBond Xtra, Macherey Nagel) were performed and the concentration of each library was determined by NanoDrop

(NanoDrop 2000, Thermo Fischer Scientific). Plasmid libraries A and B were pooled in equimolar proportions for lentivirus production.

b. Lentivirus production and titration

HEK 293T cells were seeded at 5.10^6 cells per dish (15cm diameter) one day prior to transfection. Cells were transfected using Xtreme gene reagent (Roche) with three expression vectors, respectively, 10 µg of phCMV-VSV-g, 15 µg phCMV-Gag-Pol-HIV, 20 µg GeCKO plasmid library. The medium was changed with medium without antibiotic before incubation with DNA. Six hours after transfection, medium was replaced. Two viral harvests were collected at 40 hours and 60 hours after transfection. The two harvests were pooled, centrifuged and filtered through a 0.45 µm filter. Aliquots from the cleared supernatant were stocked at -80°C. Lentivirus production was titrated by infecting LHCN-M2 cells in 12-well plates with several different volumes of lentivirus. The next day, each well was split into duplicate: one replicate received a puromycin selection with a concentration determined earlier, the other one no puromycin. As soon as no surviving cells remained in the non-transduction control well under puromycin, cells were counted to calculate the percent of transduction and the viral titer.

c. Cell library generation

One day prior transduction, 10-10,5 millions of LHCN-M2 were plated in eight 12-well plates. Cells were transduced with a volume of GeCKO lentivirus library determined earlier for achieving an MOI of 0,3-0,5. LHCN-M2 cells were transduced by spin-infection during 1h30 at 37°C in complete LHCN-M2 medium supplemented with 8 µg polybrene. The next day, cells were trypsinized and seed into eight dishes (15 cm diameter) with puromycin at 0,8 µg/mL. Non-transduced cells were plated and treated with puromycin at 0,8 µg/mL in parallel as control of selection.

3 - Viral challenges

After several days of puromycin selection, a part of the cell library was lysed for genomic extraction and sequencing. The other part of the cell library was plated and infected with chikungunya virus (LRic strain LR2006 OPY1) at an MOI of 2. The medium was replaced 6 hours after infection. In parallel, a control dish with non-transduced LHCN-M2 cells was infected at MOI 2 with chikungunya virus. After several days, all surviving cells were pooled into three 15cm-dishes. When all cells were dead in the control dish, surviving cells of the library were plated into one 25cm-

dish for a second virus challenge. Cells were infected with chikungunya virus from the same production at an MOI of 2. A new control dish with non-transduced LHCN-M2 cells was infected in parallel. When all cells were dead in the control dish, surviving cells of the library were amplified for a few days and then lysed for genomic extraction and sequencing.

4 - Genomic extraction and DNA amplification

Preliminary tests were realized beforehand to estimate the DNA yield from a given number of cells and to calculate the maximum amount of starting material that can be loaded on spin columns without overloading them.
Genomic DNA (gDNA) was extracted from the cell library before chikungunya virus challenge and from surviving cells after chikungunya infection using Dneasy Blood&Tissue Kit (Qiagen).
The amplification of pooled sgRNA isolated from cell samples was carried out by one round of PCR using Clone Amp HiFi (Clontech Takara). Three separate PCRs with 250 ng of gDNA each were realized for each sample with fusion primers. Fusion primers used for the PCR contain a barcode for sample identification and an adapter complementary to the immobilized primers in the NGS flow cells (Fig.54). PCR products were purified with PCR Clean-up/Gel extraction kit (Macherey Nagel) then run on agarose gel following by a new purification step with PCR Clean-up/Gel extraction kit (Macherey Nagel). A last step of purification (AMPure, Beckman Coulter) was done by the sequencing platform (Sequencing platform IGFL).

5 - Next Generation Sequencing and analysis

Next Generation Sequencing was performed by the Sequencing platform at IGFL (Lyon) using Ion PI HiQ Chef Kit and Ion PI HiQ chip v3 (100pb-80M reads) on Ion Torrent platform (Thermo Fischer Scientific). The amplified samples of uninfected and challenged library conditions from both replicates were pooled together on the sequencing chip for the run. Afterward, thanks to barcode sequences added on PCR amplification primers, samples from uninfected and challenged conditions were sorted. Raw data from sequencing were processed to keep only the sequence of the sgRNA. In order to do so, data processing software was used to first eliminate incorrect sequences and then to trim sequences flanking the sequence of the sgRNA. The trimmed sequences were blasted against the GeCKO library database with determined parameters (95% identity on 90 % of the length (22 bp)) and only the first

hit was kept. Finally, a list was obtained with the number of reads for each sgRNA for each experimental condition.

For a given condition, the number of reads of each sgRNA was normalized by the total number of reads in this condition. Analyses were realized by comparing for each sgRNA, the number of reads in viral challenge condition to the number of reads in uninfected condition. Two different analyses were carried out, the first one based on genes (6 sgRNA/gene, 4sgRNA/miRNA) and the second one on sgRNAs.

(a)

Primer sequence: Adaptater-barcode-linker-lentiCRISPRv2

Samples		Primer sequence (5'-3')	
LIBRARY 1	Control uninfected library	Forward	CCATCTCATCCCTGCGTGTCTCCGACTCAGTACCAAGATCGATTGGACTATCATATGCTTACCGT
	Challenged library	Forward	CCATCTCATCCCTGCGTGTCTCCGACTCAGCTGCAAGTTCGATTGGACTATCATATGCTTACCGT
LIBRARY 2	Control uninfected library	Forward	CCATCTCATCCCTGCGTGTCTCCGACTCAGCAGAAGGAACGATTGGACTATCATATGCTTACCGT
	Challenged library	Forward	CCATCTCATCCCTGCGTGTCTCCGACTCAGTTCGTGATTCGATTGGACTATCATATGCTTACCGT
		Reverse	CCTCTCTATGGGCAGTCGGTGATAGTTGATAACGGACTAGCCT

(b)

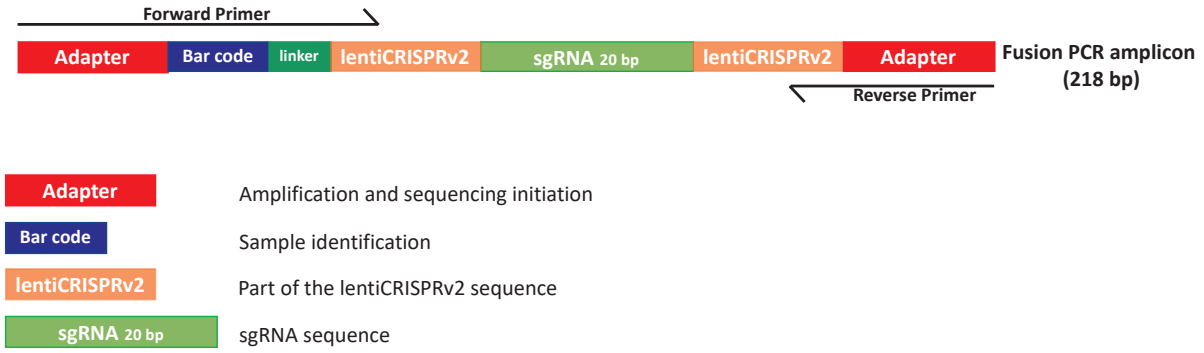

Figure 54: PCR amplification of sgRNA sequences from genomic DNA

(a) Table of fusion primers used for PCR amplification of sgRNA sequences from genomic DNA. For each condition (uninfected/challenged) and each library, a forward primer was designed. Reverse primer used was identical for all PCRs.
(b) Schematic representation of the PCR amplicon obtained and of the sequences recognized by primers. The primers allow the amplification of an amplicon with adapter sequences, a barcode, lentiCRISPRv2 sequences flanking sgRNA sequence and the sgRNA sequence.

III - Results

1 - General analysis of the screen

To identify host genes critical for CHIKV replication, we generated a GeCKO library with LHCN-M2 cells and performed a genome-scale loss of function genetic screen. To generate this library, several preliminary set-up experiments and intermediate controls were necessary. It is crucial to maintain the complexity of sgRNA pools at each step of the cell library generation.

The first control was realized when expanding the sgRNA plasmid pool in bacteria. A dilution of the full transformation was realized for both libraries to estimate transformation efficiency to ensure that the complexity of libraries was maintained. The library of lentiviruses was produced using validated sgRNA plasmid pools.

The lentivirus library was titrated beforehand in order to transduce cells with an MOI of about 0,3 to ensure that only one lentivirus enters per cell and that only one integration event takes place per cell. After discussion with collaborators from A. Ploss lab (Princeton University), we have chosen to transduce a number of cells 100-fold higher than the number of sgRNAs in the library to obtain a good sgRNA representation. After selection of transduced cells, a part of the cell library was kept for sequencing and the other part was plated for CHIKV challenge.

As a first step, after sequencing, the quality of the library of each replicate, called library 1 and library 2 thereafter, was observed. As a reminder, the library includes 6 sgRNAs for each gene for a total of 123 411 sgRNAs. In the library 1, 92% of total genes are represented but only 38% of sgRNAs are found (Fig.55). Regarding the library 2, 77% of all genes and 24% of sgRNAs are represented (Fig.55). In addition to negative selection of cells with a sgRNA targeting essential gene for cell survival, a lot of sgRNAs might have been lost during one or several steps of the process. Nevertheless, analysis of enrichment between the uninfected control cell line and challenged population in both replicates was examined in two different approaches. It should be noticed that the difference in total sgRNA counts between uninfected and challenged was not as important as we expected for both libraries (Fig.55). This small difference in sgRNA counts might suggest that our screen is not enough stringent.

	Uninfected		Challenged	
	Reads	sgRNA counts	Reads	sgRNA counts
LIBRARY 1	13 593 413	46 595 (41735)	15 632 558	29 126 (15 747)
LIBRARY 2	18 420 326	39 716 (28 005)	9 635 205	26 533 (17 937)

Figure 55: Recap chart of the number of reads for each library and condition and number of different sgRNAs counted

Numbers between parenthesis represent sgRNA counts with more than 10 reads/sgRNA.

2 - First analysis: analysis based on total sgRNA count per gene

As not so many sgRNAs were present in the uninfected library, we have chosen to realize the first analysis based on the number of reads per gene by taking account the 6 sgRNAs. All sgRNAs with less than 10 reads in uninfected or infected conditions were removed. Normalization was realized before focusing on gene enrichment by relating the number of reads per gene to the total number of reads in a given condition. Briefly, means of sgRNA counts of both libraries were calculated and DESeq2 algorithm was used in R software to generate a statistical analysis of differential sgRNA representation and the number of sgRNAs targeting each gene was integrated (Love et al., 2014). This analysis permitted to identify 142 enriched genes. Using the online tool PANTHER, we realized gene ontology analysis (Fig.56 and Fig.57) (Thomas, 2003).

Given the fact that CHIKV, and viruses in general, hijack the whole cellular machinery for their replication and for host-response shut down, we selected protein candidates with different cellular localization and favored proteins known to be required for replication of other viruses.

Several proteins localized at the plasma membrane were selected as we were particularly interested in chikungunya virus entry steps. In addition, as the team project also focuses on the role of apoptosis in alphavirus infection, several proteins related to apoptosis and p53 transcription factor were selected. The cellular localization of the nineteen hits selected from the screening analysis is displayed in figure 58. The candidates are presented below in alphabetical order with the number of sgRNAs (counted reads >10) present in challenged conditions, found either in the first replicate (library 1) or in the second replicate (library 2) or in both replicates.

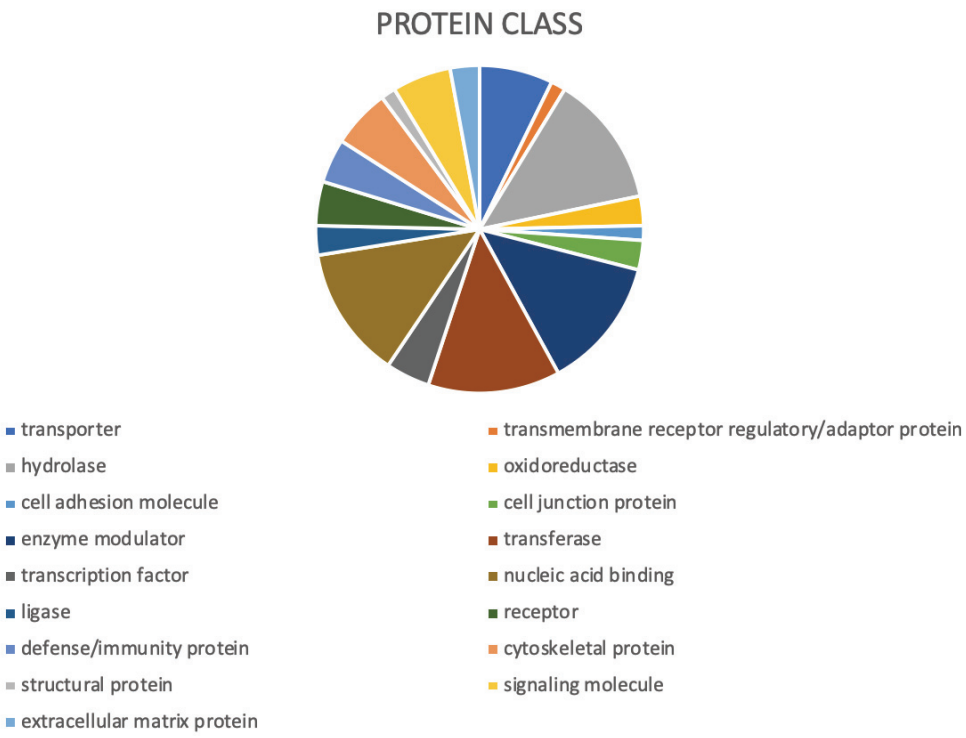

Figure 56: Gene ontology analysis of hits from the screen based on protein class

Analysis realized with the online tool PANTHER.

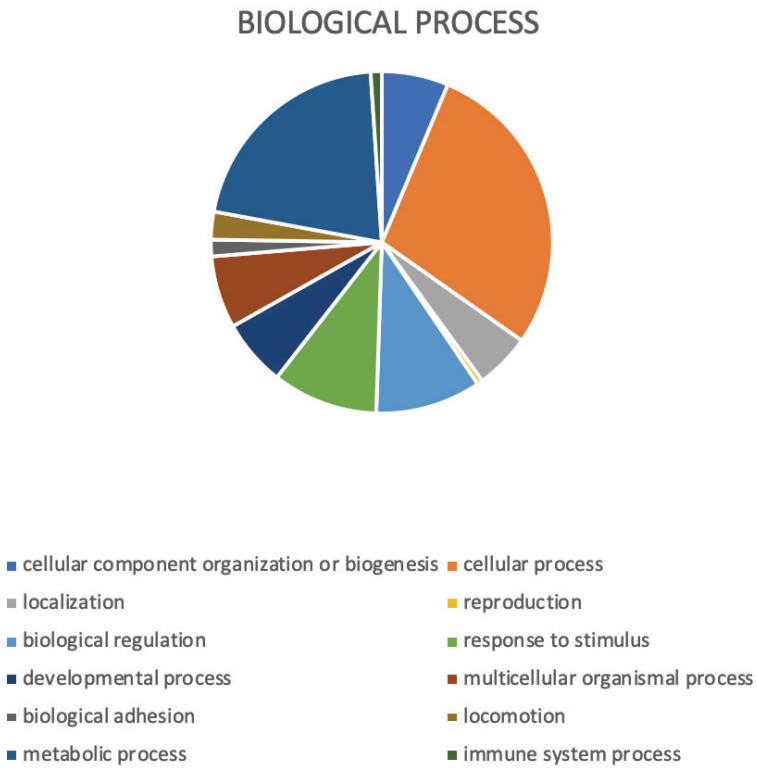

Figure 57: Gene ontology analysis of hits from the screen based on biological process

Analysis realized with the online tool PANTHER.

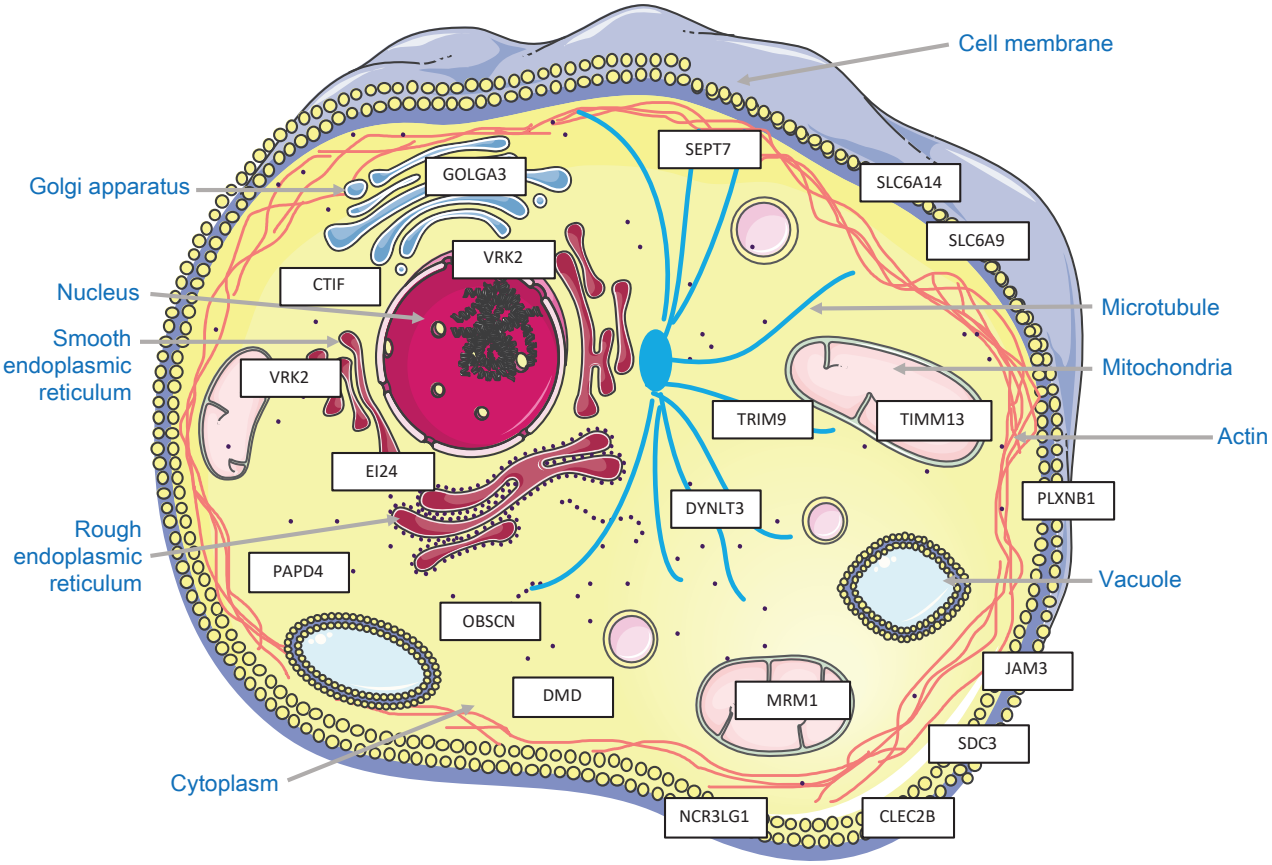

Figure 58: Cellular localization of the 19 hits selected from the screen analysis

The C-type lectin domain family 2 member B, **CLEC2B** (2 sgRNAs), is a member of the C-type lectin superfamily. Several C-type lectin receptors, e.g. DC-sign and L-sign, are important for viral infection by recognizing carbohydrate structures present on viral glycoproteins and functioning as attachment factors for several enveloped viruses (Lozach et al., 2007).

The cap-binding complex dependent translation initiation factor, **CTIF** (3 sgRNAs), is a component of the CBP80/CBP20 translation initiation complex. The translation initiation complex binds to the cap end of nascent mRNA and mediates translation (Kim et al., 2009).

The Duchenne muscular dystrophy gene, **DMD** (2 sgRNAs) encodes the dystrophin protein. This protein is found principally in muscles where it anchors the extracellular matrix to the cytoskeleton. Dystrophin is a part of the dystrophin-glycoprotein complex (DGC), which plays an important role as being a structural unit of muscle. DMD gene is mainly known for its implication in the inherited disease Duchenne muscular dystrophy (Gao and McNally, 2015).

DYNLT3 (4 sgRNAs) gene encodes the dynein light Tctex-type 3 which is a component of the dynein motor protein. Dynein motor complex protein has been shown to be involved in the transport of several viruses along microtubules. Moreover, DYNLT3 has been shown to interact directly with viral proteins (Milev et al., 2018). Involvement of dynein in viral infections is described in detail in chapter 2 of part 2.

Etoposide-induced protein 2,4kb transcript, **EI24** (3 sgRNAs) encodes a transmembrane protein localized in the endoplasmic reticulum, which is induced by the tumor suppressor protein p53. EI24 is known to be involved in apoptotic process by playing a pro-apoptotic role (Gu et al., 2000). Furthermore, EI24 is an essential autophagy gene and plays an important role in clearance of aggregated proteins (Zhao et al., 2012).

The Golgin subfamily A member 3, **GOLGA3** (3 sgRNAs) also called GCP170 is localized to the Golgi complex. It might be involved in the structural organization or stabilization of the Golgi complex (Misumi et al., 1997).

The junction adhesion molecule 3, **JAM3** (2 sgRNAs), also named JAM-C, belongs to the immunoglobulin superfamily with JAM-A, JAM-B and also Coxsackievirus and Adenovirus Receptor (CAR). JAM and CAR proteins span the membrane a single time and have a large extracellular domain and a short cytoplasmic C-tail. Several viruses including Reovirus, Rotavirus, Adenovirus, Coxsackievirus use members of this family as receptors (Bhella, 2014; Torres-Flores and Arias, 2015).

The **MRM1** (3 sgRNAs) gene encodes the mitochondrial rRNA methyltransferase 1 that is required for mitochondrial ribosome function in mammalian cells. MRM1 might participate in methylation of ribosomal RNA (Lee et al., 2013).

The **NCR3LG1** (4 sgRNAs) gene encodes the natural cytotoxicity triggering receptor 3 ligand 1 protein also known as B7-H6. NCR3LG1 is a ligand which triggers NCR3 (NKp30)-dependent natural killer cell activation.

The obscurin protein encoded by **OBSCN** (3 sgRNAs) gene plays important roles in myofibrillogenesis, cytoskeletal organization, and cell adhesion (Manring et al., 2017).

The poly(A) RNA polymerase **PAPD4** (4 sgRNAs), also called GLD2, is a cytoplasmic RNA polymerase that forms poly(A) tail by adding successive AMP monomers to the 3' end of selected cytoplasmic mRNAs (Kwak et al., 2004). A study has reported an effect of cytoplasmic polyadenylation of human papillomavirus type 16 (HPV-16) mRNAs by PAPD4 (Glahder et al., 2010).

The plexin-B1, **PLXNB1** (3 sgRNAs), has been identified as semaphorin receptors. Semaphorins play a role in axon guidance and in immune response. Activation of plexin results in the regulation of actin cytoskeleton by activating small GTPases (Driessens et al., 2001).

The syndecan 3**, SDC3** (2 sgRNAs), is a single-pass membrane heparan sulfate proteoglycan. SDC3 has been identified as a major HIV-1 attachment receptor on dendritic cells (de Witte et al., 2007). Moreover, it has been shown that syndecan 1 (SDC1) serves as a major receptor for attachment of Hepatitis C virus to hepatocytes while syndecan 2 (SDC2) is used as a receptor by Dengue 2 virus (Okamoto et al., 2012; Shi et al., 2013). Finally, both SDC1 and SDC2 have been shown to be involved in Herpes Simplex Virus type 1 (HSV1) infection (Bacsa et al., 2011).

The septin 7, **SEPT7** (3 sgRNAs), is a GTP-binding protein that associates with actin filaments and cellular membranes and that is required for many cellular processes including migration, division and membrane trafficking (Mostowy and Cossart, 2012). It has been demonstrated that septins inhibit bacterial infection by forming cage-like structures around intracellular pathogens such as *Shigella flexneri* bacteria and promote their targeting to autophagosomes (Mostowy et al., 2010; Sirianni et al., 2016). A high throughput small interfering RNA (siRNA) screen identified several septins as strong anti-viral factors against Vaccinia virus (VACV) (Beard et al., 2014). Another study confirms this role by demonstrating that septins suppress Vaccinia virus release from infected cells by "entrapping" the virus at the plasma membrane (Pfanzelter et al., 2018).

SLC6A14 (5 sgRNAs) and **SLC6A9** (2 sgRNAs) are two solute carrier (SLC) membrane transport proteins. SLCs control essential physiological functions, including ion transport, nutrient uptake and are relatively understudied (César-Razquin et al., 2015). Some solute carriers are receptors for viruses (retrovirus…) and their topology as multi-transmembrane protein are involved in tight binding of the virus to the cell

surface. Interestingly, the two transporters, SLC15A3 and SLC25A28, have been reported to inhibit CHIKV replication (Schoggins et al., 2011).

TIMM13 (3 sgRNAs) is a translocase of inner mitochondrial membrane that has been shown to participate in the import of protein into the mitochondrial inner membrane. This mitochondrial protein was selected notably since viruses are known to alter mitochondria functions, to influence energy production, metabolism, survival, and immune signaling.

TRIM9 (3 sgRNAs) is an E3 ubiquitin-ligase. TRIM9 short isoform has been shown to promote DNA and RNA virus-induced production of type I interferon (IFN) and expression of IFN-stimulated genes (Qin et al., 2016).

VRK2 (2 sgRNAs) is a serine-threonine kinase with two isoforms. VRK2A is anchored to the endoplasmic reticulum and mitochondria while VRK2B is detected free in nucleus and cytosol.
VRK2A isoform has been shown to be involved in the regulation of mitochondrial-mediated apoptosis (Monsalve et al., 2013). On the other hand, it has been published that VRK2B phosphorylates p53 and induces its stabilization (Blanco et al., 2006).

3 - Second analysis: analysis based on sgRNA

For comparison, a second analysis was realized based on counts for each sgRNA. The mean of count number in both replicates was calculated for each sgRNA in both conditions and was used to determine the log2 of fold change for each given sgRNA to study enrichment.
Genes highlighted in this second analysis were different from genes identified in the first analysis. A gene ontology analysis was also realized with the list of sgRNAs enriched (Fig.59 and Fig.60). From this second analysis, only one candidate has been selected for future assays.

AMBRA1 candidate presented one highly enriched sgRNA between uninfected and infected conditions. If we look at all sgRNAs targeting AMBRA1, four were presents in infected conditions with two sgRNAs found in both replicates.
However, for one screen replicate, only 1 of the 4 sgRNAs found in challenged conditions was present in uninfected conditions indicating as we presumed before that sgRNAs information have been lost during the process.

AMBRA1 has been identified as an important factor in regulating autophagy in vertebrates by promoting Beclin-1 interaction with its target kinase VPS34, thus mediating autophagosome nucleation (Maria Fimia et al., 2007). On the other hand, it has been shown that chikungunya virus triggers an autophagic process which promotes viral replication (Krejbich-Trotot et al., 2011). Thus, AMBRA1 might be involved in the autophagy process observed during chikungunya virus replication. Furthermore, it has been shown that AMBRA1 binds the dynein motor complex through direct interaction with the dynein light chain DLC1 (also called LC8). After autophagy induction, AMBRA1-DLC1 are released from the dynein complex upon ULK1-dependent phosphorylation, and relocalize to the endoplasmic reticulum, thus enabling autophagosome nucleation (Fig.61) (Di Bartolomeo et al., 2010). The presence of both AMBRA1 protein and a dynein light chain protein (DYNLT3) among the hits of the screen make them particularly interesting candidates.

Several candidates selected from the screen and presented above have been tested individually using CRISPR/Cas9 system to confirm or invalidate their role in chikungunya virus infection. Results from these assays are shown in the two following chapters.

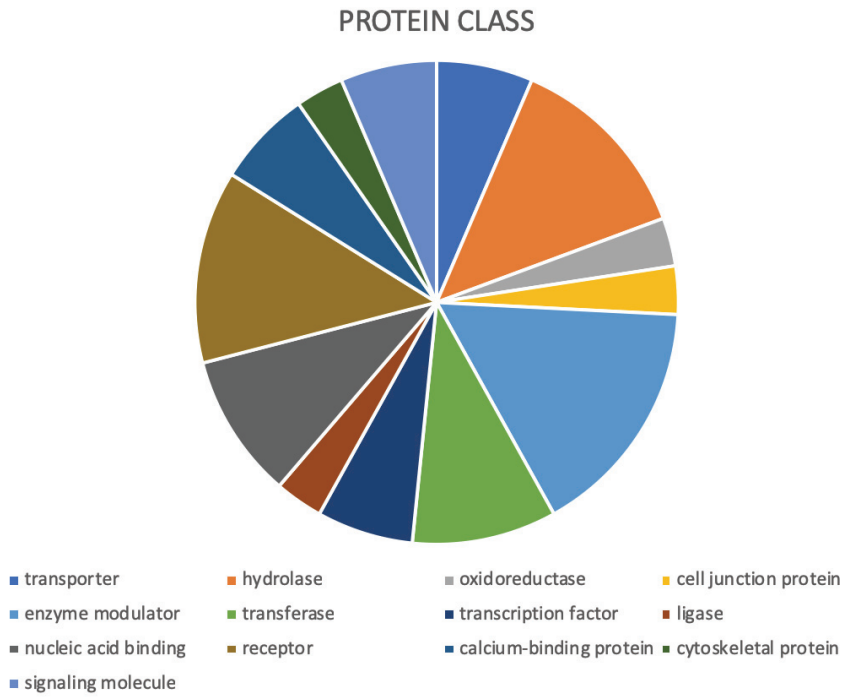

Figure 59: Gene ontology analysis of hits from the screen based on protein class
Analysis realized with the online tool Panther.

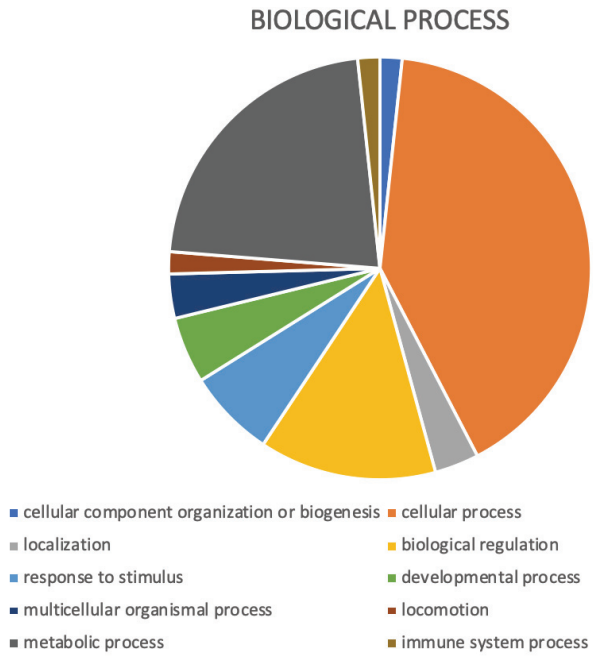

Figure 60: Gene ontology analysis of hits from the screen based on biological process

Analysis realized with the online tool Panther.

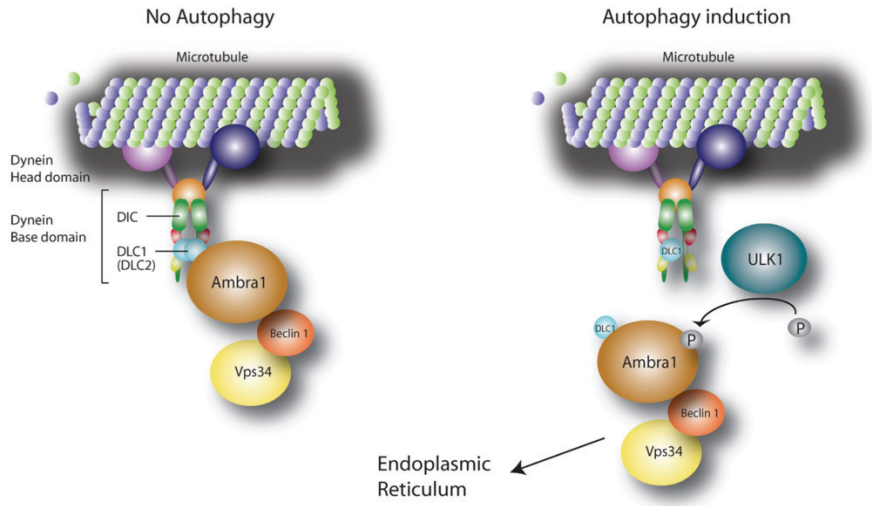

Figure 61: Model of AMBRA1 dynamic interaction with the dynein motor protein during autophagy induction

When the autophagic process is not induced, AMBRA1 is bound to the dynein light chain DLC1 of the dynein complex on microtubules. After autophagy induction, the phosphorylation of AMBRA1 by ULK1 allows the release and the translocation of AMBRA1 with Beclin-1 and Vps34 to the endoplasmic reticulum leading to autophagosome formation.

IV - Discussion

Identification and characterization of host factors involved in viral replication permit to bring new perspectives in understanding cellular biology and virus-host relationship and are also an important approach to develop potential therapeutics. Genetic screens are powerful tools that have been widely used to identify host factors that promote or restrict virus replication. Loss of function screens include RNAi approaches, haploid genetic screens and more recently CRISPR-mediated knockout screens.

By performing a loss of function screen, many critical aspects should be considered at different stages of the screen, from cell line choice to enrichment analysis.

A first critical step is the choice of a cell line. As viruses differ in their host range and tissue tropism, a cell line susceptible to the virus of interest and capable of efficiently replicating the virus has to be selected. CHIKV is known to infect the immortalized myoblast cell line, LHCN-M2, and also to replicate in these cells (Ozden et al., 2008). In addition, the choice of this cell line was relevant regarding the skeletal muscle tropism of CHIKV (Ozden et al., 2007). However, since the primary immortalized cell line could be considered as more normal compared to tumoral cell lines, they might have better DNA repair mechanisms. Consequently, cells might repair more efficiently double strand break induced by Cas9 and thus prevent the CRISPR-mediated loss of function. Another limitation of the use of this cell line is its poor tolerance to be seed at a very low density which makes it difficult to amplify after a strong cytolytic effect induced by CHIKV challenge. In spite of the strengths of LHCN-M2 cells, the use of a cell line that grows more easily should be considered for future screenings.

Regarding CRISPR sgRNA library, several CRISPR libraries are available with different features. The GeCKO library we used covers the whole genome and contains 6 sgRNAs per gene. This redundancy enables to control eventual low efficacy of sgRNA and off-target effects thus discriminate true and false positive hits. Indeed, genes that display high depletion or enrichment across multiple sgRNAs are more likely real. Another way to limit screen background and false positives is to include biological replicates of the viral transduction step. Our two screens were thus realized from independent libraries generated *via* two separate transduction steps.

Another crucial point is to maintain the complexity of the sgRNA pool to ensure the quality of the library. Library diversity should be preserved when expanding the

sgRNA plasmid pool, during lentiviral production, during transduction of target cells and during genomic DNA extraction and PCR amplification. High library diversity has a great impact on the robustness of the screen. High background noise is introduced by a too low representation, resulting in false positives due to random variations of the sgRNAs present in low numbers at the onset of the screen. Keep the diversity and identify all of the genes involved in viral replication is awkward as a proportion of genes are essential for cell viability and growth. Studies based on CRISPR screens and haploid screens have enabled the identification of a set of approximately 2 000 genes, so that's 10% of human genome, that are essential for cell growth and viability (Blomen et al., 2015; Wang et al., 2015). Nonetheless, this list includes genes which have only a moderate effect on cell growth and thus could be represented in the screening.

After sequencing, the quality and diversity of both cell libraries were analyzed. The genome coverage of the first library replicate was quite satisfactory with 92% of genes represented but the sgRNA diversity was very low with only 38% of total sgRNAs. For the second library, the genome coverage was acceptable with 77% of genes found but the sgRNA coverage was also very low with 24% of different sgRNAs identified. Determine at which stage sgRNA diversity was lost is a challenging point. We did not sequence plasmid library after amplification as it was not essential, but it might be interesting to sequence the pool of plasmids in order to estimate diversity at that stage. In the following steps, a loss of library complexity during lentivirus production is difficult to determine. However, sgRNA diversity might have been lost during cell line generation. Indeed, we have tried to achieve a 100-fold representation of the sgRNA library in our cell line but several studies published later highlight the requirement of a number of cells 500-fold to 1000-fold higher than the total number of sgRNAs in the library (McDougall et al., 2018; Perreira et al., 2016). Finally, information on present sgRNAs might have been lost during PCR amplification steps. Especially as we have observed sgRNAs present in challenged conditions but absent of the starting uninfected library, like for AMBRA1 gene. Genomic DNA quantity used or number of separate PCR might have been insufficient.

Our screen is based on phenotypic selection by selecting virus-resistant cells. In pooled screens, stringent selection leads to the selection of resistant cells for which gene depletion caused marked phenotype. The high stringency enables to be more confident of genes identified however genes with a less marked effect on viral infection may be missed. Indeed, in the case of highly cytopathic viruses which rapidly hijack the host cellular machinery after entry, only sgRNAs targeting factors involved

in the entry process are likely recovered (Kim et al., 2017). In contrast, the use of less aggressive viruses or the possibility to contain infection (e.g. with neutralizing antibodies) allow recovering factors that act at later stages of replication (Zhang et al., 2016, 2018).

Although the CHIKV challenge with an MOI of 2 seemed to induce strong cytopathic effects leading to cell death, we have observed a poor enrichment between unchallenged and challenged conditions. For future screening replicates, the selection should be more stringent, probably not in term of MOI, but with a longer selection period or with multiple rounds of virus challenge at low MOI. In a recent CRISPR screen with influenza virus, Julianna Han et al. have analyzed sgRNA enrichment during sequential influenza virus selection of five rounds. They observed a robust enrichment in the second round of infection with a progressive increase in enrichment occurring between round two and round five (Han et al., 2018).

The level of sgRNA enrichment in virus-resistant cells compared with that in unselected cells is determined by comparing the number of reads observed for each specific sgRNA in the different cell populations. Our first analysis based on the number of reads of all sgRNAs for a given gene enables to take into consideration the level of enrichment of multiple sgRNAs against the same gene. An important number of sgRNAs enriched for a given gene increases confidence in the candidate gene identified. In contrast, our second analysis based on the number of reads for a specific sgRNA is more susceptible to generate false positives mainly due to off-target effects of one specific sgRNA. Thus, our first analysis strategy seems more reliable. In parallel, it would have been interesting to realize a systematic comparison of the enriched genes in our screen with previous alphavirus or closely related virus screenings. This comparison would have been useful for the selection of candidates among the enriched genes.

All these different aspects and problems considered subsequent to the screen allow to take a critical look at these screen assays and to identify crucial points to improve future screens. These improvements include notably a higher number of cells for library generation for a better sgRNA representation, an optimized CHIKV challenge with several rounds of infection and a more adapted number of PCR reactions before sequencing.

Chapter 2: DYNLT3, a component of the cytoskeleton dynein motor complex

I - Context

- **Components of the cytoskeleton**

The cytoskeleton is a complex network of filaments regulated by many accessory proteins that extends throughout a cell. The cytoskeleton defines the cell shape and the internal organization. It also provides mechanical support that enables cells to carry out essential functions like motion and division. The cytoskeleton consists of three main components that differ in protein composition and in size. These components include actin filaments, microtubules and intermediate filaments (Fig.62).

Here we discuss more microtubules (MT) that are long hollow, straw-shaped cylinders with a diameter of about 25 nm. They are formed by the lateral association of between 12 and 17 protofilaments into a regular helical lattice. Each protofilament consists of repeating units of polymerized alpha (α) and beta (ß) tubulin monomers. MT are dynamic structures. Indeed, tubulin dimers are constantly added and subtracted at both ends of the filament. One end grows more rapidly and is called the plus end, whereas the other end is known as the minus end (Fig.63). Minus-ends are attached to the microtubule organizing center (MTOC) also called centrosome, usually located closed to the nucleus. Plus-ends are pointing in the direction of the cell periphery and the plasma membrane. MTOC creates the global organization of the microtubule network.

Main functions of MT are:

- Structural role by influencing the organization of the organelles, nucleus and cytoskeleton components.
- Formation of spindle structure which pulls the chromosome apart into daughter cells during cell division.
- Formation of an internal transport network for motors proteins called kinesins and dyneins which transport vesicles containing essential materials and other cargoes around the interior of the cell.

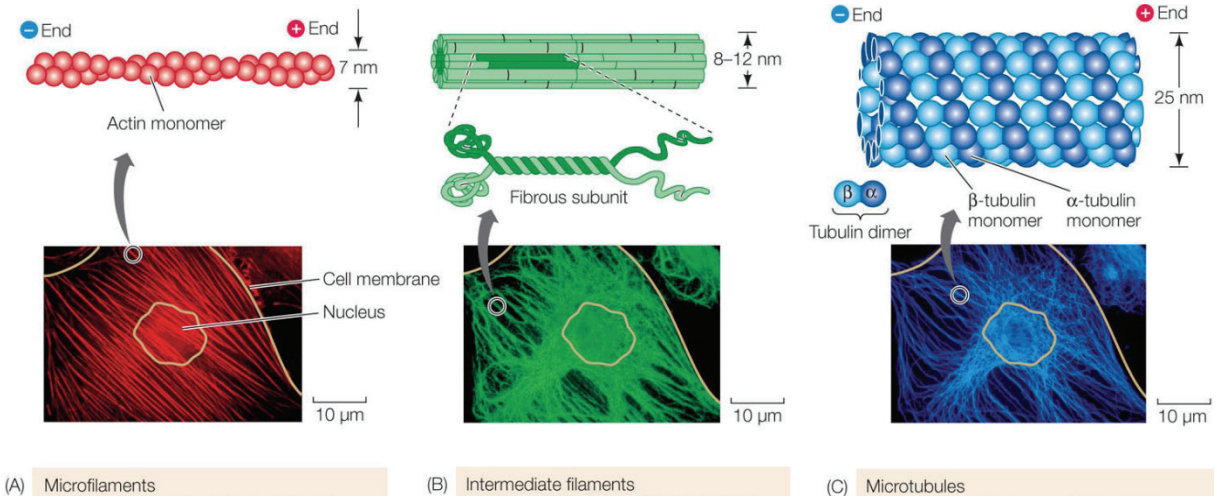

Figure 62: The three components of the cytoskeleton

(A) Actin filaments are the smallest type of filaments with a diameter of about 7 nanometers (nm), they are made up of strands of the protein actin and have plus and minus ends.
(B) Intermediate filaments are mid-sized with a diameter of 8 to 12 nm. Unlike microfilaments and microtubules, they are made of a number of different subunit proteins.
(C) Microtubules are the largest type of filament and are composed of a protein called tubulin.

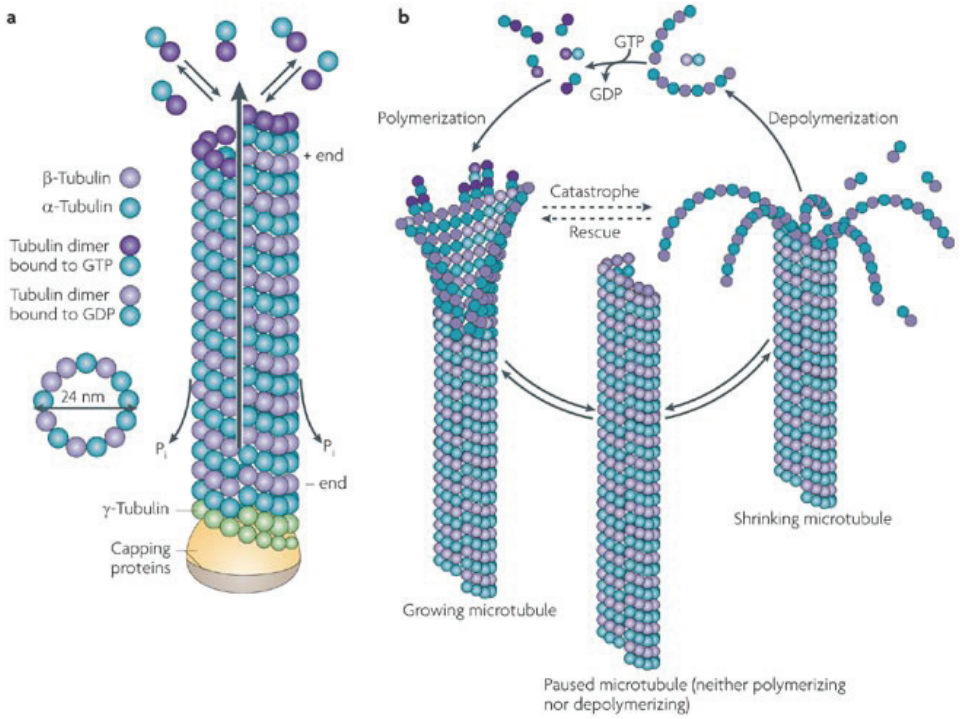

Figure 63: Microtubule dynamics

Microtubules are composed of two subunits, α-tubulin and β-tubulin, assembled into protofilaments. MT size can rapidly grow by polymerization or shrink by depolymerization. (Kaur et al., 2014)

- **The two motor proteins: kinesin and dynein**

Kinesin was the first plus-end directed microtubule motor to be identified. Kinesin catalyzes the anterograde transport in the cell (Fig.64). It is a heterotetramer composed of two heavy chains and two light chains (Fig.65). The head domain composed of heavy chains, which binds microtubules and ATP, is responsible for the motor activity of kinesin. Light chains are responsible for binding to membrane vesicles.

The second microtubule motor protein is the dynein protein. Two classes of dynein are identified: axonemal and cytoplasmic dynein. Axonemal dyneins are responsible for flagellar and ciliary beating while cytoplasmic dyneins are involved in intracellular transport, mitosis, cell polarization and directed cell movement.
Cytoplasmic dynein (called dynein afterward) powers the transport of cargoes - protein, membrane-bounded organelles, mRNA particles - towards MT minus ends by converting energy stored in ATP (Fig.64).
Dynein is a large protein complex (1,5 megaDalton) in the shape of a Y and consists of two dynein heavy chains (HCs), two intermediate chains (ICs), two light intermediate chains (LICs) and three families of light chains (Fig.66).
Dynein HCs contain at the C-terminal end the motor domain that composed of six ATPases of AAA+ superfamily and a binding stalk which mediates MT interaction (Carter et al., 2011; Kon et al., 2011). The N-terminus is involved in the homodimerization of the HC and contains the interaction sites for LICs and ICs. LICs contain binding sites for the Dynein Light Chains (LCs). ICs, LICs, and LCs are implicated in motor regulation and cargo binding. Cytoplasmic dynein requires help from a cofactor called dynactin to function in the cell (Kardon and Vale, 2009; Schroer, 2004). The dynactin complex interacts with dynein via binding sites on ICs.

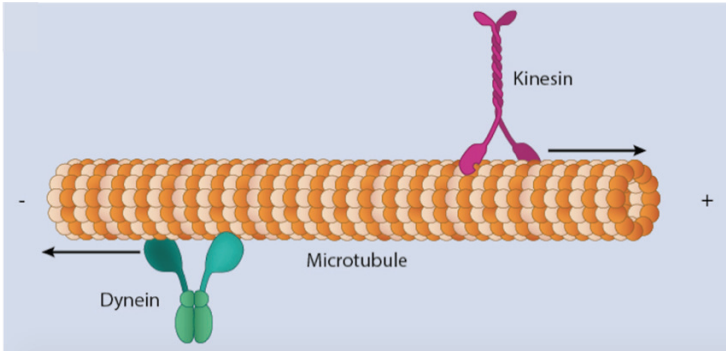

Figure 64: Dynein and Kinesin movement on microtubules

Dynein is a minus-end directed microtubule motor which enables cellular retrograde transport. Kinesin is a plus-end directed microtubule motor for anterograde transport in the cell.

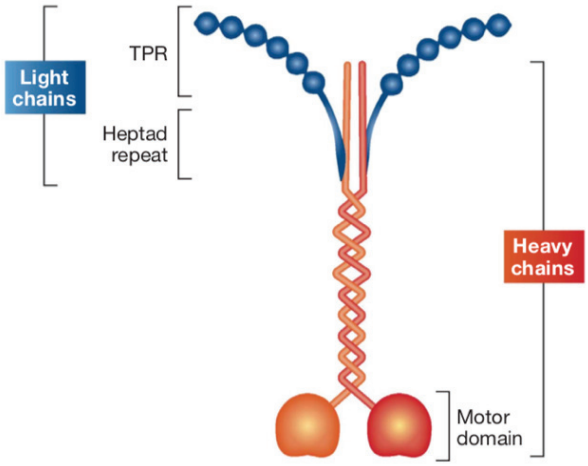

Figure 65: Schematic representation of kinesin motor protein

The two heavy chains (in orange) bind to the microtubules via a domain found in the N-terminus. Light chains (in blue) associate with heavy via heptad repeat motifs. The six Tetratricopeptide repeats (TPR) at the C-terminus of the light chains serve as cargo-binding domains. (Dodding and Way, 2011)

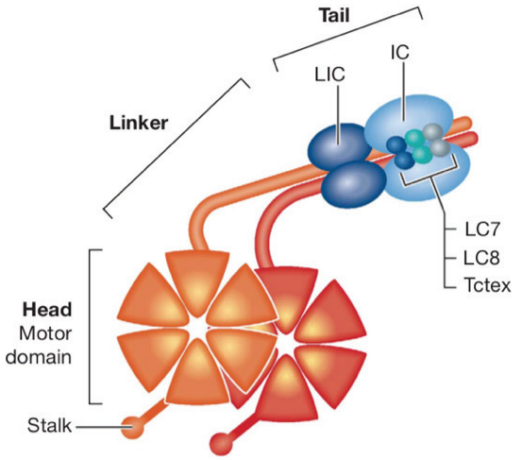

Figure 66: Schematic representation of dynein motor protein.

The dynein motor protein is composed of different subunits. The motor activity resides in the heavy chains (in orange). The six AAA ATPase domains are arranged in a hexameric ring from which an MT binding stalk sticks out. The N-terminal tail of heavy chains permits its dimerization and also the binding site for the intermediates chains (ICs) and light intermediates chains (LICs) (in blue). The three pairs of light chains (LC7, LC8, Tctex also called DYNLT) interact with ICs.(Dodding and Way, 2011)

- **Hijack of the cytoskeleton by viruses**

Viruses are intracellular parasites, this means that they use and manipulate the cellular machinery for trafficking, transcription, splicing and protein synthesis. Viruses or subviral particles are transported from the cell surface to the site of viral replication and from the site of synthesis to the assembly site and back to the plasma membrane for virus budding. They evolved to exploit the cellular cytoskeleton transport mechanisms since free diffusion of particles larger than 50 nm is restricted by the structural organization of the cytoplasm. This is especially true for neurotropic viruses that travel long distances through the cytoplasm in the axon during retrograde and anterograde transport (Bearer and Satpute-Krishnan, 2002).
Many arboviruses take advantage of cytoskeleton filaments as actin filaments as intermediate and microtubule filaments. Actin filaments were shown to contribute in the entry, production and release of the arbovirus dengue virus 2 (DENV2) by interacting with the viral protein E (Foo and Chee, 2015). It was also published that the actin motor, myosin, was involved in the release of DENV2 particles from HepG2 cells (Xu et al., 2009). In addition, the intermediate filament vimentin regulates the establishment of dengue virus replication complexes through interaction with non-structural protein ns4A (Teo and Chu, 2014). Concerning CHIKV, an interaction of vimentin with non-structural protein nsp3 of CHIKV was shown. Vimentin plays also an important role in CHIKV replication complexes by providing anchorage for the complexes (Issac et al., 2014).

Many viruses rely on microtubules for transport towards intracellular replication sites immediately after they have gained entry to the cell, this includes Herpes Simplex virus (HSV), human immunodeficiency virus (HIV), influenza virus, adenovirus, human cytomegalovirus, papillomavirus and rabies virus (RV) (Milev et al., 2018; Miranda-Saksena et al., 2018). Some viruses like herpes virus, HIV and several flaviviruses take advantage of microtubule network to move newly assembled particles to the plasma membrane to facilitate their egress (Brault et al., 2011; Ward, 2011). Microtubule cytoskeleton is also used by viruses to transport nucleic acids and protein components involved in virion assembly to specific cellular locations. In the case of CHIKV, it was shown that treatment with a MT polymerization inhibitor, called nocodazole, induces a decrease of CHIKV infection in HEK 293T cells (Bernard et al., 2010).

- **Involvement of the dynein complex in viral replication**

Research conducted over the past 10 years revealed that cytoplasmic dynein and kinesin are the two most common motor proteins involved in viral transport. For numerous viruses, interactions with microtubules occur through dynein interaction and in most cases, dynein light chains were identified as the dynein chains that interact with viral proteins (Fig.67). Herpes simplex virus type 1 (HSV1) transport along axons is mediated by cytoplasmic dynein (Döhner et al., 2002). Using a library of HSV capsid and tegument structural genes in a yeast two-hybrid system to identify dynein interactors, Douglas et al. have shown that the outer capsid protein VP26 interacts with dynein light chains DYNLT1 and DYNLT3. This interaction was confirmed by pull-down assays *in vitro* (Douglas et al., 2004). On the other hand, L2 capsid protein from DNA non-enveloped Human Papillomavirus 16 (HPV16) interacts with both dynein light chains DYNLT1 and DYNLT3 and depletion of both proteins by siRNAs inhibits HPV 16 infection (Schneider et al., 2011). These results suggest a likely requirement of the two proteins DYNLT1 and DYNLT3 for viral transport towards the nucleus.
A study on flaviviruses showed that DYNLT1 interacts with the ectodomain of membrane protein (M) of dengue viruses (serotypes 1-4), West Nile virus, and Japanese Encephalitis virus. Using RNA interference against DYNLT1, they demonstrated that interaction between M protein and DYNLT1 plays a role in late stages of virus replication, probably during the trafficking of flaviviral particles within infected cells (Brault et al., 2011).

Based on these different observations, the hijack of the dynein motor by many viruses has been proposed as a common mechanism for virus delivery near the cell nucleus replication site. Different models for viral retrograde transport presented in figure 68 have been proposed by Merino-Gracia et al..

Interestingly, an interaction between the Poliovirus Receptor (PVR) and the dynein light chain 1 (DYNLT1) has been highlighted (Mueller et al., 2002). This interaction enables the transport of the neurotropic poliovirus particles bound to PVR from the cell periphery to the neuronal cell body where the virus is uncoated and replicates. Model for retrograde transport of Poliovirus-PVR complex by dynein is presented in figure 68, model (C). This interaction has peaked our interest as PVR has been identified as a potential CHIKV receptor in the RNAi screen realized in collaboration (unpublished data) (described in Chapter 2 of Part 1).

In this context, we have tried to confirm a potential role of dynein light chain 3 (DYNLT3) identified in our CRISPR screen in CHIKV infection and investigated for a

potential interaction of DYNLT3 with a viral protein of CHIKV. Given the presence of DYNLT3 in our hits from the CRISPR screen, the presence of PVR in the RNAi screen and the described interaction between PVR and the other dynein light chain DYNLT1, we, therefore, decided to also investigate a potential role of PVR associated with dynein light chain in CHIKV entry steps.

Virus	Virus interaction domain	Dynein component involved in the interaction
Adeno-Associated virus	Capsid	dynein
Adenovirus	Capsid	LC and LIC
Adenovirus	FIP-1	LC (DYNLT1)
Africane Swine Fever virus	P54	LC (LC8)
Bovine Immunodeficiency virus	Capsid	LC (LC8)
Ebola virus	VP35	LC (LC8)
Hepatitis B virus	unknown	unknown
Hepatitis C virus	unknown	unknown
Hepatitis E virus	VP13	dynein
Herpes Simplex virus 1	VP26 capsid	RP3, DYNLT1
Equine Herpes virus	unknown	unknown
Kaposi's Sarcoma Herpes viurs (HHV-8)	unknown	unknown
Mason-Pfizer Simian virus	Matrix	LC (DYNLT1)
Bovine Immunodeficiency virus	Capsid	LC (LC8)
Human Foamy virus	Capsid	LC (LC8)
Human Papillomavirus	minor capsid L2	LCs (DYNLT1 and DYNLT3)
Poliovirus	Receptor PVR	LC (DYNLT1)
Rabies virus	P Phosphoprotein	LC (LC8)
Sirevirus	Hopie Gag extension	LC (LC8)
Rabies virus	polymerase L	LC (LC8)
Porcine circovirus	Capsid	IC and LC (LC8)
Human Immunodeficiency virus type 1	VPR	LC (DYNLT1) and DHC
Human Immunodeficiency virus type 1	Integrase	LC (DYNLT1)
Influenza A virus	unknown	dynein
Mouse polyomavirus (MPyV)	unknown	dynein
Rhesus rhadinovirus (RRV)	unknown	dynein
Japanese Encephalitis (JEV)	M protein	DYNLT1
Dengue virus (DENV) serotypes 1-4	M protein	DYNLT1
West Nile virus (WNV)	M protein	DYNLT1

Figure 67: Viruses interacting with dynein complex
For each interaction, viral protein and dynein component are specified when they are known. (adapted from Milev et al. 2018)

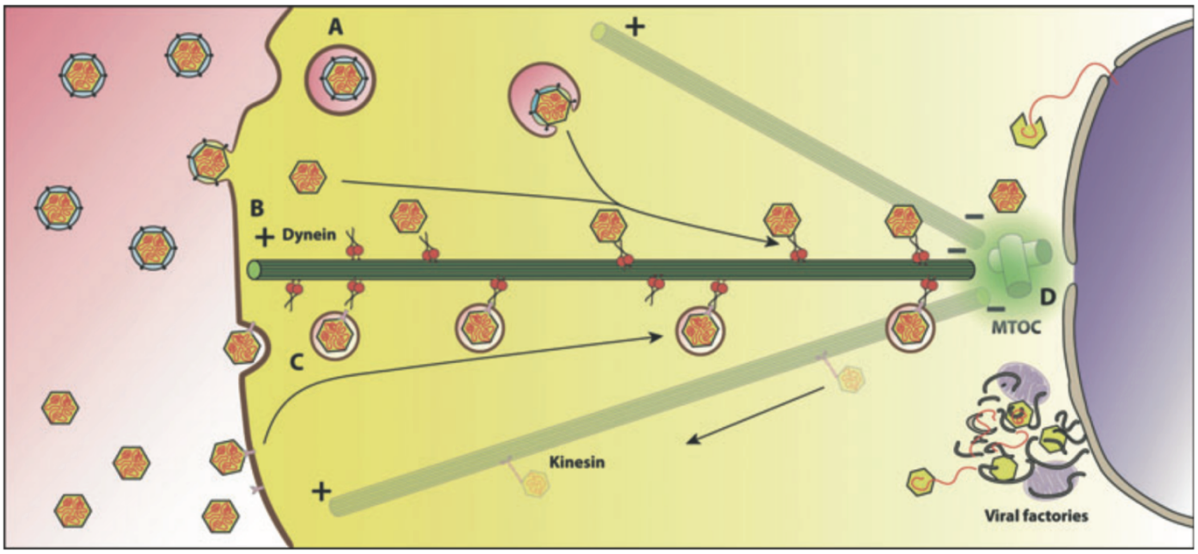

Figure 68: Model for retrograde transport of viruses proposed by Merino-Gracia et al., 2011

Both the entry of the viral particle through the endosome pathway (A, C) and the direct fusion of the viral envelope to the plasma membrane (B) might lead to the retrograde transport along microtubules using the cytoplasmic dynein motor.
After viral entry by endocytosis (A) or direct membrane fusion (B), viral capsid might associate to dynein directly leading to the retrograde transport along microtubules using the dynein motor protein.
After viral entry by endocytosis, cellular receptor might bind simultaneously to a viral protein and the dynein protein (C).
Viruses reach the MicroTubules Organizing Center (MTOC) at the minus end of MT (D) where they are uncoated and directed to the sites of replication, production and, assembly. The newly assembled viral particles might be transported to the cell periphery by the anterograde transport machinery. (Merino-Gracia et al., 2011)

II - Material and Methods

1 - Generation of CRISPR-mediated knockout cell lines

SgRNA design, cloning and lentivirus production were realized as described previously in part 1 using the following primers. Two sgRNAs were designed for the DYNLT3 gene and one sgRNA was designed for both DYNLT1 and PVR genes. In addition, a sgRNA targeting luciferase (sgRNA luc) was designed as a control.

Guide name		Sequence 5'-3'
sgRNA_1 DYNLT3	Forward	CACCGCCACTATGCTTGCAGTCCAC
	Reverse	AAACGTGGACTGCAAGCATAGTGGC
sgRNA_2 DYNLT3	Forward	CACCGTTTTCGAGGCCCGCCCGGT
	Reverse	AAACACCGGGCGGGCCTCGAAAAC
sgRNA DYNLT1	Forward	CACCGTTAACGCACACGGTGCCGAT
	Reverse	AAACATCGGCACCGTGTGCGTTAAC
sgRNA PVR	Forward	CACCGTGAGTGACCCCCGCGCAGTC
	Reverse	AAACGACTGCGCGGGGGTCACTCAC
sgRNA luc	Forward	CACCGGGCATTTCGCAGCCTACCG
	Reverse	AAACCGGTAGGCTGCGAAATGCCC

For cell line generation, LHCN-M2 cells were plated in 6-well plate and transduced the day after by lentiviruses. Transduced cells were selected with 0,8 µg/mL puromycin. Puromycin selection was maintained until non-transduced control cells are all dead.

2 - Verification of gene knockout by qPCR

Total RNA of CRISPR and control cells was extracted using NucleoSpin® RNA kit (Macherey Nagel). RNA was reverse transcripted using PrimeScript™ RT-PCR kit (Takara). mRNAs were quantified by qPCR amplification in AriaMx system (Agilent) using SYBR Premix Ex Taq II (Takara) with the following primers. Results were normalized by at least three different housekeeping genes (GUSB, RPL22, RPL27).

Oligo name		Sequence 5'-3'
hDYNLT3	Forward	AGTGGACTGCAAGCATAGTG
	Reverse	GGTACAGGTTCCATCAGATGTG
hDYNLT1	Forward	AACGCTTATCAACACAGCAAAGTGAAC
	Reverse	CAGTGCAGCTCCCGTCAGT
hGUSB	Forward	GATTGCCAATGAAACCAGGTATC
	Reverse	ACACGCAGGTGGTATCAGTCTT
hRPL22	Forward	TCGCTCACCTCCCTTTCTAA
	Reverse	TCACGGTGATCTTGCTCTTG
hRPL27	Forward	ATCGCCAAGAGATCAAAGATAA
	Reverse	TCTGAAGACATCCTTATTGACG

3 - Production of alpha-pseudotyped viruses and infection assays

Pseudoparticles bearing alphavirus envelopes and carrying GFP reporter were produced and infection assays carried out as described previously in part 1.

4 - Production of replicative alphaviruses and infection assays

CHIKV LRic strain LR2006 OPY1 and derived CHIKV-GFP were produced as mentioned before in chapter 1 of Part 1. For infection assays, two different protocols were successively used. First cells were plated for infection assay 4 days after transduction by CRISPR lentiviruses. In a second phase, cells were amplified after transduction at least one-week before infection assay. Procedure for infection assay was realized as explained in chapter 1 of part 1.

5 - Infection of LHCN-M2 cells overexpressing DYNLT3 protein

a. Generation of LHCN-M2 cells overexpressing DYNLT3 and characterization

LHCN-M2 cells were transduced by DYNLT3 packaging lentiviruses. As described above in part 1, lentiviruses were produced by co-transfecting three vectors in 293T cells: gag-pol packaging construct derived from HIV, VSV glycoprotein-expressing construct and lentiviral DYNLT3-expressing construct from Addgene (pLX307, Addgene). The DYNLT3 construct permits the expression of DYNLT3 protein with a V5 tag at the C-terminal end. LHCN-M2 cells were plated in 6-well plate and transduced the day after by lentiviruses. Transduced cells were selected with a concentration of 0,8 µg/mL puromycin. Puromycin selection was maintained until

non-transduced control cells are all dead and then selected cells were amplified. In order to monitor the effect of DYNLT3 overexpression on cell fitness, a cell viability assay was carried out. WT and DYNLT3 overexpressing LHCN-M2 cells were plated in 96-well plate at 3000 cells per well. Cell viability was measured at different time points (0, 18, 24, 48 and 72 hours) using the CellTiter-Glo® Luminescent cell viability assay kit (Promega) and a plate reader (Victor^2 plate reader, Perkin Elmer). It allows to determine the number of viable cells in culture based on the generation of a luminescent signal proportional to the amount of ATP present, which signals the presence of metabolically active cells.

b. Infection assay

One day before viral infection, cells overexpressing DYNLT3 and WT control cells were plated at 50 000 cells/well in 48-well plates. Cell lines were counted before infection to adapt the MOI. Cells were infected with replicative viruses at an MOI 0,1 or MOI 1 and incubated 1h at 4°C before medium change. Infected cells were harvested 24h post-infection and fixed in paraformaldehyde 4% at 4°C for 15 min. Intracellular immunostaining was realized with antibodies diluted in PBS 1X supplemented with 0,1% saponin for cell permeabilization and 10 % FBS. First, cells were incubated 1h at 4°C with a primary antibody raised to Semliki Forest nucleocapsid protein (1/800), that reacts with CHIKV capsid protein (IgG2a C42 kindly provided by Dr. Irene Greiser-Wilke, School of Veterinary Medicine (Hannover, Germany)). After washes, cells were incubated 1h at 4°C with FITC conjugated anti-mouse IgG secondary antibody (1/200) (F0257, Sigma Aldrich), cells were analyzed using a flow cytometer (FACSCalibur, BD Biosciences). For CHIKV-GFP infected cells, the percentage of infected cells was directly measured by flow cytometry analysis after paraformaldehyde fixation.

6 - Co-immunoprecipitation assay

The potential interaction between the capsid of chikungunya virus (CHIKV-capsid) and the DYNLT3 protein was studied in two different approaches:

- In the first approach, CHIKV-capsid and DYNLT3 protein with V5 tag (DYNLT3-V5) were overexpressed in LHCN-M2 cells (**a** and **b**).
- In the second model, LHCN-M2 cells overexpressing DYNLT3-V5 were infected with CHIKV to study the potential interaction under conditions of infection (**c**).

a. Generation of CHIKV-capsid stable and inducible cell line

For stable and inducible expression, CHIKV-capsid gene was cloned in the tetracycline-inducible lentiviral pCW57.1 vector (Addgene). Using CHIKV LRic molecular clone as a template, CHIKV capsid was cloned in frame with a FLAG tag into the vector using In-Fusion®HD Cloning kit (Clontech).

Lentiviruses were produced, as described above in part 1, by co-transfecting three vectors in 293T cells: gag-pol packaging construct derived from HIV, VSV glycoprotein-expressing construct and CHIKV-capsid inducible expressing construct. LHCN-M2 were transduced by lentiviruses and selected with 0,8 µg/mL puromycin. Puromycin selection was maintained until non-transduced control cells are all dead and then selected cells were amplified.

In order to verify CHIKV-capsid expression in transduced cells, LHCN-M2 cells were plated and capsid expression was induced by doxycycline (tetracycline analog) treatment at a concentration of 2 µg/mL determined beforehand. After 48h of doxycycline treatment, cells were lysed and whole-cell extracts were separated by SDS-PAGE and then transferred to nitrocellulose membranes using a transfer apparatus according to the manufacturer's protocols (Bio-Rad). After protein transfer, membranes were incubated with 10% milk in PBST 0,1% for 2 hours followed by overnight incubation at 4°C with primary antibody (1/300, PBST 0,1% with 5% milk) raised to Semliki Forest nucleocapsid protein, that reacts with CHIKV capsid protein (IgG2a C42). Membranes were washed 3 times and incubated 1 hour with anti-mouse IgG coupled with Horseradish Peroxidase (1/10 000, A5906, Sigma Aldrich). After 3 washes, proteins were revealed with SuperSignal™ chemiluminescent substrate (ThermoScientific) using ChemiDoc™ imaging system (BioRad).

b. Generation of a DYNLT3-V5/CHIKV-capsid inducible cell line

Stable LHCN-M2 cells with inducible CHIKV capsid gene were transduced with a high MOI of DYNLT3-V5 packaging lentiviruses to guarantee that each cell has been transduced and expresses DYNLT3-V5 protein. Finally, this cell line expresses constitutively the protein DYNLT3-V5, and the CHIKV-capsid expression can be induced by doxycycline treatment. For the co-immunoprecipitation assay, 1.10^6 cells were plated in 10 cm dish and CHIKV-capsid expression was induced by 2 µg/mL of doxycycline for 48h before cell lysis.

c. Chikungunya virus infection of LHCN-M2 cells overexpressing DYNLT3-V5

LHCN-M2 cells overexpressing DYNLT3-V5 and WT LHCN-M2 cells were plated in parallel in 10 cm dish for chikungunya virus infection the next day. Cells were infected by CHIKV LRic strain with an MOI of 1 and lysed 24h after infection.

d. Co-immunoprecipitation

Cells were lysed with RIPA lysis buffer (pH 8) supplemented with Protease Inhibitor (PI) 1X (Thermo), Ethylenediaminetetraacetic acid (EDTA) 1mM and Dithiothreitol (DTT) 1mM, called afterward supplemented RIPA buffer. Cell lysates were sonicated on ice three times then incubated 30 min on ice and centrifuged for 5 min at 4°C at 11 000 g and supernatants transferred to a new tube. Bradford protein assay was realized to quantify proteins in cell lysates using protein assay dye reagent (Bio-Rad).

For the co-immunoprecipitation assay, the antibody raised to SFV capsid that reacts with CHIKV capsid was used to form immunocomplex (antibody C-SFV, IgG2a C42 kindly provided by Dr. Irene Greiser-Wilke, School of Veterinary Medicine (Hannover, Germany)). 500 μg of proteins in 500 μL of supplemented RIPA buffer were incubated with 2 μL of antibody C-SFV with rotation for 2 h at 4°C. A volume of 20 μL of protein G magnetic beads (Cell signaling #70024) was pre-washed four times with supplemented RIPA buffer using a magnetic separation rack. The lysate and antibody (immunocomplex) solution were transferred to the tube containing the pre-washed magnetic bead pellet and then incubated with rotation overnight at 4°C. Beads were pelleted using magnetic separation rack and washed four times with 400 μL of supplemented RIPA buffer for 10 min with rotation. For elution step, 30 μL of Laemmli 2x-supplemented RIPA buffer were added directly on beads. Samples were centrifuged for 2 min at 4°C at 500g, gently mixed and then heated for 5min at 95°C. A new centrifugation step (2min, 4°C, 500g) was realized to pellet beads and eluate was transferred to a new tube stored at -20°C until western-blot analysis.

After heat denaturation, proteins were separated by electrophoretic migration on SDS-PAGE and then transferred onto nitrocellulose membranes using a transfer apparatus according to the manufacturer's protocols (Bio-Rad). After protein transfer, membranes were incubated with 10% milk in PBST 0,1% for 2 h at room temperature followed by overnight incubation at 4°C with following primary antibodies to detect respectively DYNLT3-V5 and CHIKV-capsid.

Protein	Antibodies	Reference	Source	Working dilution
DYNLT3-V5	antibody anti-V5	V5 probe (C9) Sc-271944 SantaCruz	mouse	1/1000 PBST 0,1% 10% milk
CHIKV-Capsid	Antibody anti-C-SFV	IgG2a C42 provided by Dr.Greiser-Wilke (Hannover, Germany)	mouse	1/300 PBST 0,1% 5% milk

After three washes with PBST 0,1%, membranes were incubated for 2 h at room temperature with anti-mouse IgG coupled with horseradish peroxidase (A5906, Sigma Aldrich) diluted at 1/5000 in PBST 0,1%, milk 10%. Detection of β-actin was performed as a loading control for input samples. After 3 washes, immunoreactive bands were revealed with SuperSignal™ chemiluminescent substrate (ThermoScientific) using ChemiDoc™ imaging system (BioRad).

III - Results

1 - Generation of CRISPR-mediated knockout cell lines: DYNLT3, DYNLT1 and PVR genes

We looked into a direct role of DYNLT3 in CHIKV infection by generating cell lines with two different sgRNAs targeting DYNLT3: sgRNA_1 DYNLT3 and sgRNA_2 DYNLT3. We tried to confirm knockout of DYNLT3 by western-blot analysis using two different antibodies raised to DYNLT3 protein (SAB #45950 and Proteintech 11687-1-AP), but unfortunately, we were not able to detect endogenous DYNLT3 protein in LHCN-M2 cells. Using specific primers, we realized RT-qPCR to quantify DYNLT3 mRNAs in cells (Fig.69). Compared to wild-type (WT) cells, sgRNA_1 DYNLT3 cells had 50% fewer DYNLT3 mRNAs but we cannot know if the remaining 50% of mRNAs lead to the translation of a correctly folded and active DYNLT3 protein or not. In parallel, we tried to study also the role of DYNLT1 and PVR in CHIKV infection by generating cell lines with sgRNA targeting both genes. qPCR assays have shown that cells with sgRNA DYNLT1 had also 50% less DYNLT1 mRNA (Fig.69). However, we were not able to confirm the protein status in sgRNA PVR cell line due to a lack of tools.

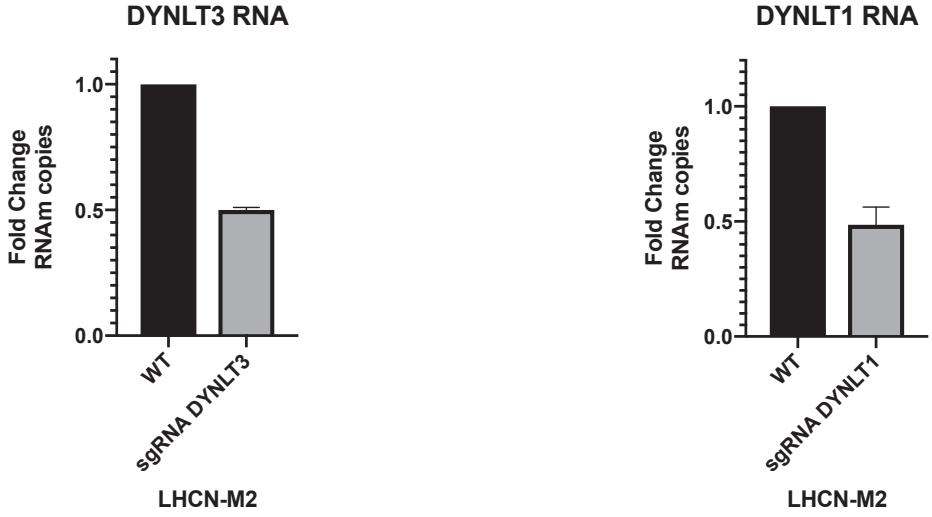

Figure 69: Quantification of DYNLT3 and DYNLT1 transcripts in WT and sgRNA DYNLT3 or sgRNA DYNLT1 cells

RT-qPCR was realized on total RNA extracted to quantify DYNLT3 and DYNLT1 RNA in cell lines. Results were normalized by three different housekeeping genes (GUSB, RPL22, RPL27). RNA level on naïve WT cells was established at 1.

2 - Study of chikungunya virus infection in lentivirus-generated cell lines

Chikungunya virus infection levels in cells with sgRNA_1 and sgRNA_2 DYNLT3, sgRNA DYNLT1 and sgRNA PVR were compared to infection level in WT LHCN-M2 cells. For the first infection assays, cells were plated 4 days after transduction by CRISPR lentiviruses and infected with CHIKV the day after (Fig.70).

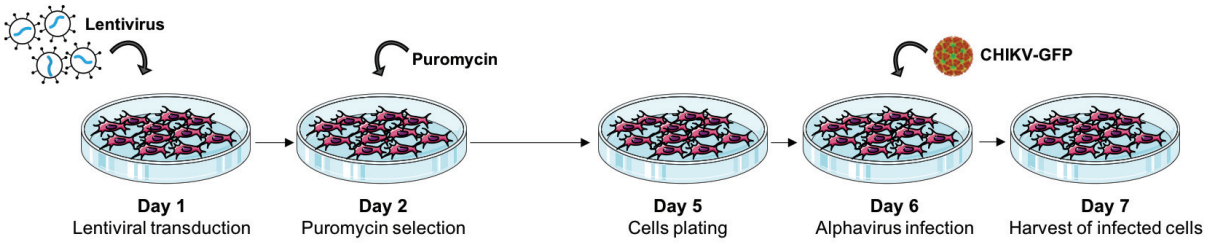

Figure 70: Schematic workflow of the first infection assay

Day 1: *LHCN-M2 cells were transduced by CRISPR lentiviruses.* ***Day 2****: Transduced cells were selected with puromycin.* ***Day 5****: After 3 days of selection, cells were plated for infection assay.* ***Day 6:*** *Cells were infected with replicative CHIKV-GFP.* ***Day 7****: Cells were harvested for flow cytometry analysis.*

Cells were infected at two different MOI with CHIKV-GFP making possible to directly determine the percentage of infected cells by flow cytometry. After 24h of infection, we observed a huge decrease of CHIKV infection in LHCN-M2 with either sgRNA_1 DYNLT3 or sgRNA_2 DYNLT3 at both MOI compared to the WT cells (Fig.71 (a) and (b)). In sgRNA DYNLT1 and sgRNA PVR LHCN-M2 cell lines, we also detected a considerable diminution of CHIKV-GFP infection compared to wild type cells (Fig.71 (c) and (d)).

As the lentiviral transduction and the stable expression of Cas9 protein and sgRNA might alter the cell fitness, we generated a control sgRNA targeting the luciferase gene (sgRNA luc) which is not naturally present in the LHCN-M2. LHCN-M2 cells with sgRNA Luc were used as control cells for new infection assays realized following the same procedure. WT, sgRNA luc, and sgRNA DYNLT3 cells were infected simultaneously with CHIKV-GFP for 24h allowing direct assessment of infection level by flow cytometry. We observed a huge decrease of CHIKV infection compared to WT cells in sgRNA DYNLT3 cells, from 50% of infected cells to less than 5%, but surprisingly we also observed this decrease in sgRNA luc cells with less than 10% of GFP-positive cells (Fig.72 (a)). In parallel, we monitored CHIKV infection by TCID50 titration of viral production in the supernatant of the three cell lines. Viral production

in both sgRNA cell lines was significantly decreased (Fig.72 (b)). As a control the sgRNA luc should not impact gene expression in cells and therefore should not modify CHIKV infection, we hypothesized that cell transduction itself might modify cell fitness. Nonetheless, a decrease of viral production was observed in sgRNA DYNLT3 cells compared to control sgRNA luc cells (> 1 log decrease).

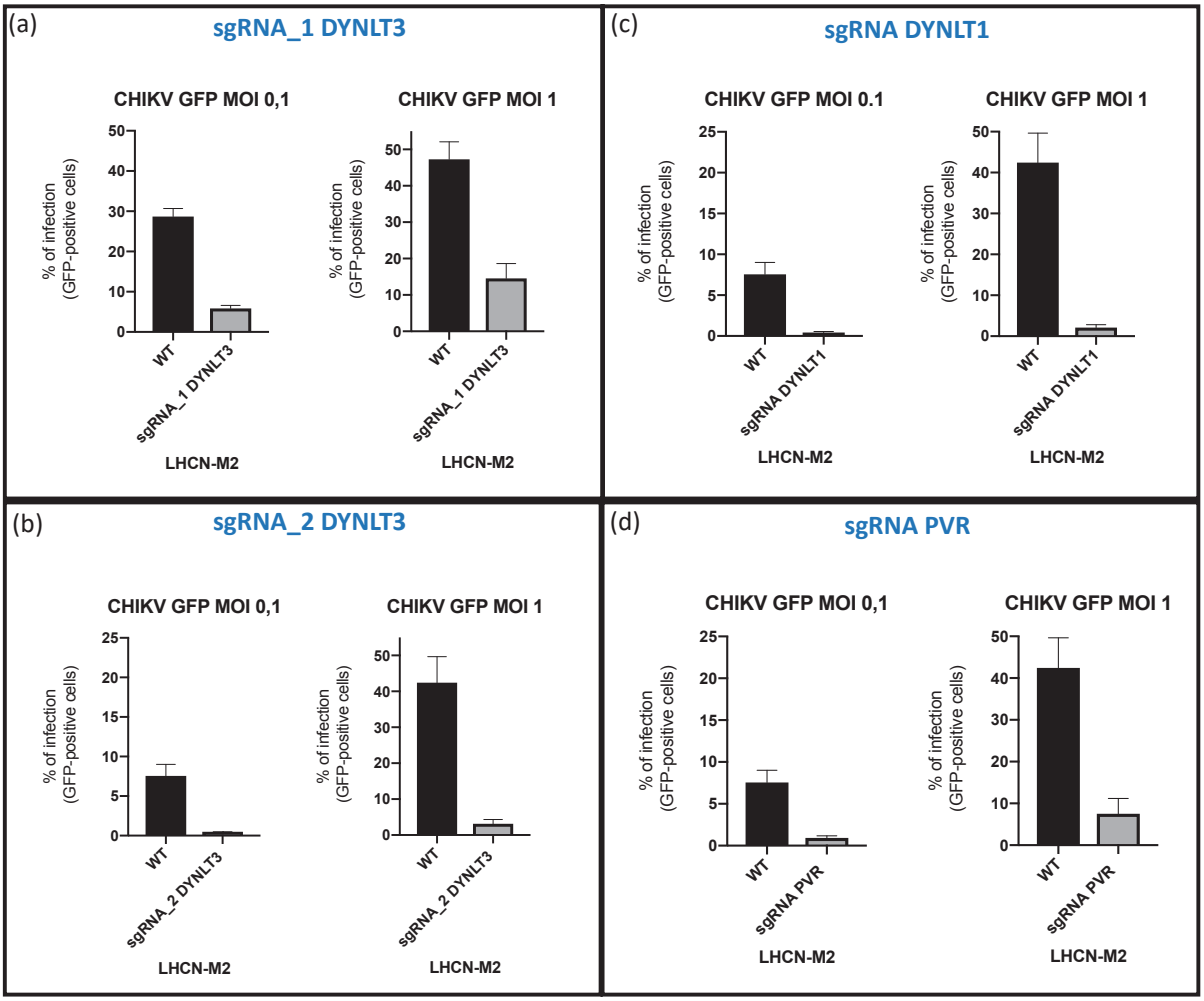

Figure 71: CHIKV-GFP infection assays in WT, sgRNA_1 DYNLT3 (a), sgRNA_2 DYNLT (b), sgRNA DYNLT1 (c) and sgRNA PVR (d) LHCN-M2 cells

Cells were infected 4 days after lentiviral transduction with CHIKV-GFP at MOI 0,1 or MOI 1 for 24h. Cells were harvested and fixed in PFA 4% before flow cytometry analysis (n=2).

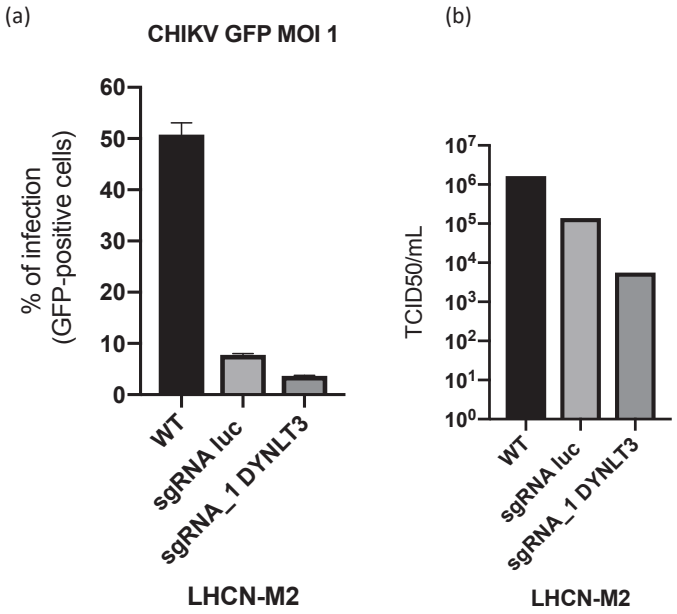

Figure 72: CHIKV-GFP infection assays in WT, sgRNA luc and sgRNA_1 DYNLT3 LHCN-M2 cells

(a) Monitoring of GFP positive cells for the three cell lines.
Cells were infected 4 days after lentiviral transduction with CHIKV-GFP at MOI 1 for 24h. Cells were harvested and fixed in PFA 4% before flow cytometry analysis (n=2).
(b) Titration of viral production in the supernatant of the three cell lines.
Supernatants were titrated by serial dilution (TCID50) on VeroE6 cells (n=2).

3 - Chikungunya infection assays in cells with sgRNAs against DYNLT3, DYNLT1, and PVR after long culture period

For this second round of infection assays, cells were amplified at least one week after transduction by CRISPR lentiviruses for subsequent CHIKV infection (Fig.73).

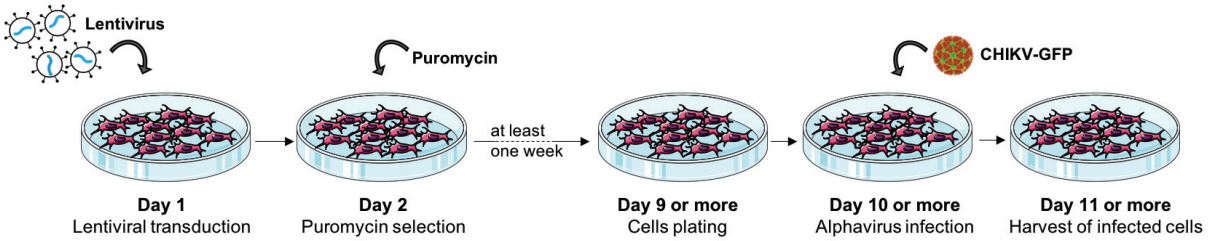

Figure 73: Schematic workflow of infection assay

Day 1: *LHCN-M2 cells were transduced by CRISPR lentiviruses.* ***Day 2****: Transduced cells were selected with puromycin (3 days) and amplified at least one week before CHIKV-infection.* ***Day 9 or more****: Cells were plated for infection assay.* ***Day 10 or more:*** *Cells were infected with replicative CHIKV-GFP.* ***Day 11 or more****: Cells were harvested for flow cytometry analysis.*

sgRNA_1 DYNLT3 cells were infected with CHIKV-GFP at two different MOI for 24h. The other cell lines (sgRNA_2 DYNLT3, sgRNA DYNLT1, and sgRNA PVR LHCN-M2) were only infected with CHIKV-GFP at MOI 1 for 24h. After 24h of infection, we observed a slight decrease of CHIKV infection in LHCN-M2 with sgRNA_1 DYNLT3 at both MOI compared to the WT cells (Fig.74(a)). However, no difference in CHIKV infection level was observed in sgRNA_2 DYNLT3 cells (Fig.74 (b)). A slight decrease of CHIKV infection was shown for sgRNA DYNLT1 cells compared to WT cells (Fig.74 (c)). A small increase of infection level is observed in sgRNA PVR cells, but it might be due to a problem of cell number at the moment of infection (Fig.74 (d)). Nonetheless, these observations have been made on only two experiments. Replicate experiments should be realized once the protein status has been properly validated. In addition, like in the previous experiment, sgRNA luc cells should be infected in parallel and viral production in the supernatant should be titrated.

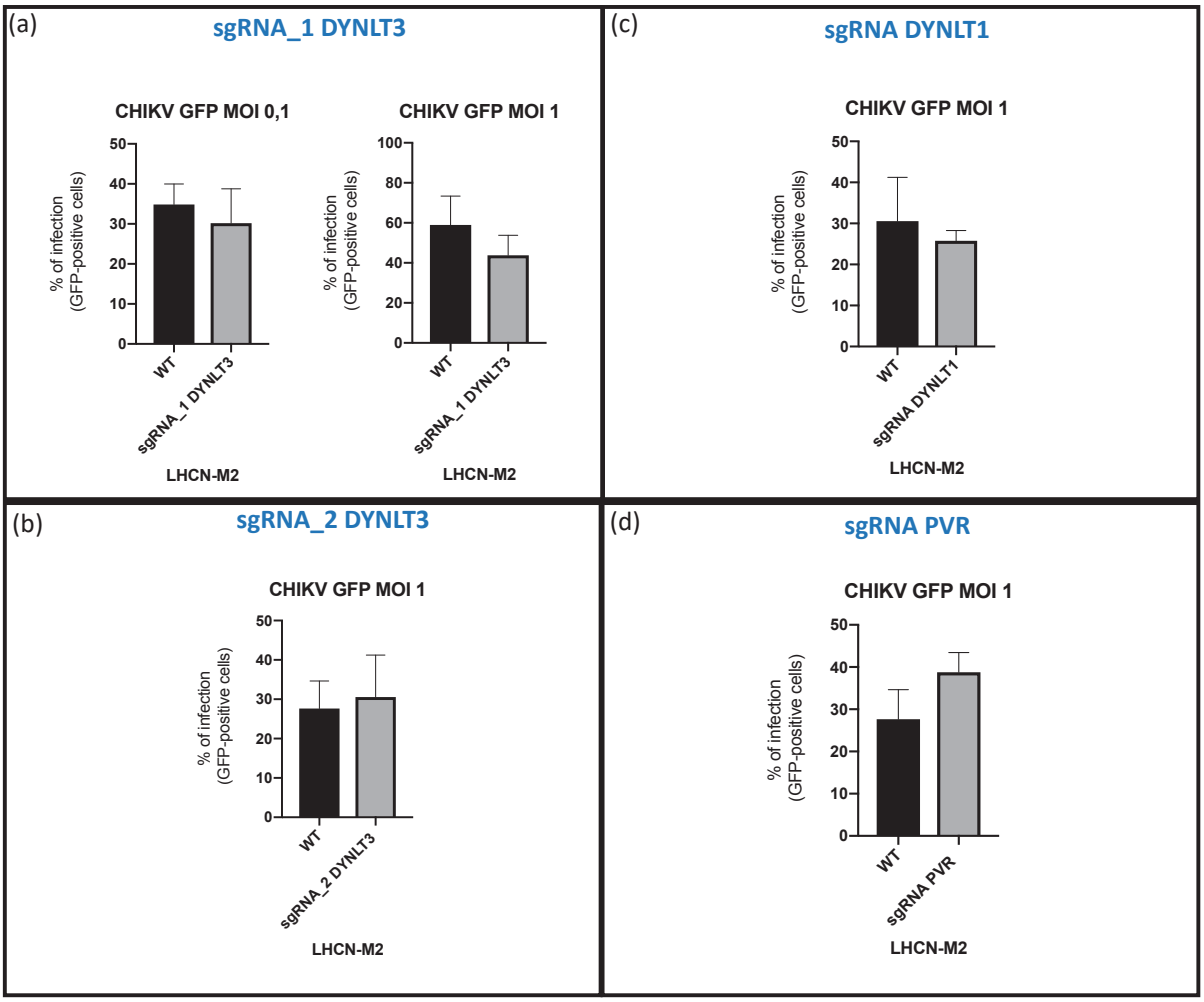

Figure 74: CHIKV-GFP infection assays in WT, sgRNA_1 DYNLT3 (a), sgRNA_2 DYNLT3 (b), sgRNA DYNLT1 (c) and sgRNA PVR (d) LHCN-M2 cells

Cells were infected with CHIKV-GFP at MOI 0,1 or MOI 1 for 24h. Cells were harvested and fixed in PFA 4% before flow cytometry analysis (n=2).

Subsequently, we tried to generate CRISPR-mediated knockout of DYNLT3 in another cell line as efficient CRISPR depletion might vary from cell to cell. We used U2OS cell line to generate sgRNA luc U2OS and sgRNA DYNLT3 U2OS. Cells were transduced, selected with puromycin and amplified at least one week before infection assays. Cells were infected with CHIKV-GFP at MOI 0,1 or 1 for 24h. Luciferase sgRNA appears to generate a small effect on CHIKV infection compared to WT cells (Fig.75). We did not observe a decrease of infection in sgRNA DYNLT3 U2OS cells but even a slight increase (Fig.75). However, this experiment has been realized only once and, for this cell line neither, we were not able to confirm the knockout due to the lack of antibodies.

Generally, this CRISPR approach was considerably penalized by the lack of performant characterization tools to validate protein status. It represents an important issue that needs to be overcome before carrying out further infection assays.

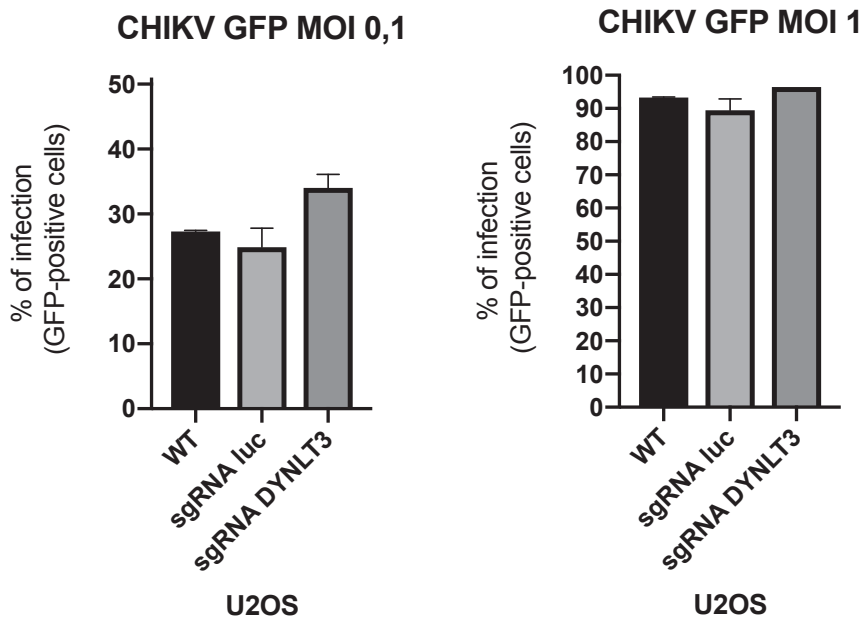

Figure 75: CHIKV-GFP infection assays in WT, sgRNA luc and sgRNA DYNLT3 U2OS cells

Cells were infected with CHIKV-GFP at MOI 0,1 or MOI 1 for 24h. Cells were harvested and fixed in PFA 4% before flow cytometry analysis (n=1).

4 - Effect of DYNLT3 protein overexpression on CHIKV infection

Another way to look into the role of DYNLT3 in CHIKV infection was to overexpress DYNLT3 protein in LHCN-M2 cells. Lentiviruses carrying the DYNLT3 gene were produced for transducing LHCN-M2 cells. Overexpression of DYNLT3 in transduced

cells was confirmed by western-blot analysis with antibodies against DYNLT3 (Fig.76 (a)). However, as before, the two different DYNLT3 antibodies tested were not able to detect endogenous DYNLT3 protein in WT cells. Cell viability over time was monitored for WT cells and cells overexpressing DYNLT3 (called thereafter LHCN-M2 hDYNLT3) to make sure that overexpression does not modify too much cell fitness. Cell viability of both cell lines was similar 18h and 24h after cells were plated (Fig.76 (b)). After 48h and 72h, it appears that the cell viability of LHCN-M2 hDYNLT3 is higher than the viability of WT cells (Fig.76 (b)). Since we observed that LHCN-M2 hDYNLT3 grow a little bit slower than WT cells, the lower viability of WT at 72 h especially might be explained by a more confluent state in the well.

Subsequently, WT and hDYNLT3 cells were infected with CHIKV-GFP at two different MOI for 24h. The level of CHIKV-GFP in hDYNLT3 cells was significantly lower than in WT cells at MOI 0,1 and also at MOI 1 (Fig.76 (c)).
To explain this effect, one hypothesis was that the dynein might interact with a protein of CHIKV during infection. This hypothesis is supported by the numerous studies published on interactions between dynein light chains and viral proteins. Thus, we suggested that DYNLT3 might interact with the capsid protein of CHIKV. The infection decrease observed in cells overexpressing DYNLT3 might be due to the DYNLT3 protein present in high amount which catches capsid proteins. To test this hypothesis, we realized a co-immunoprecipitation assay.

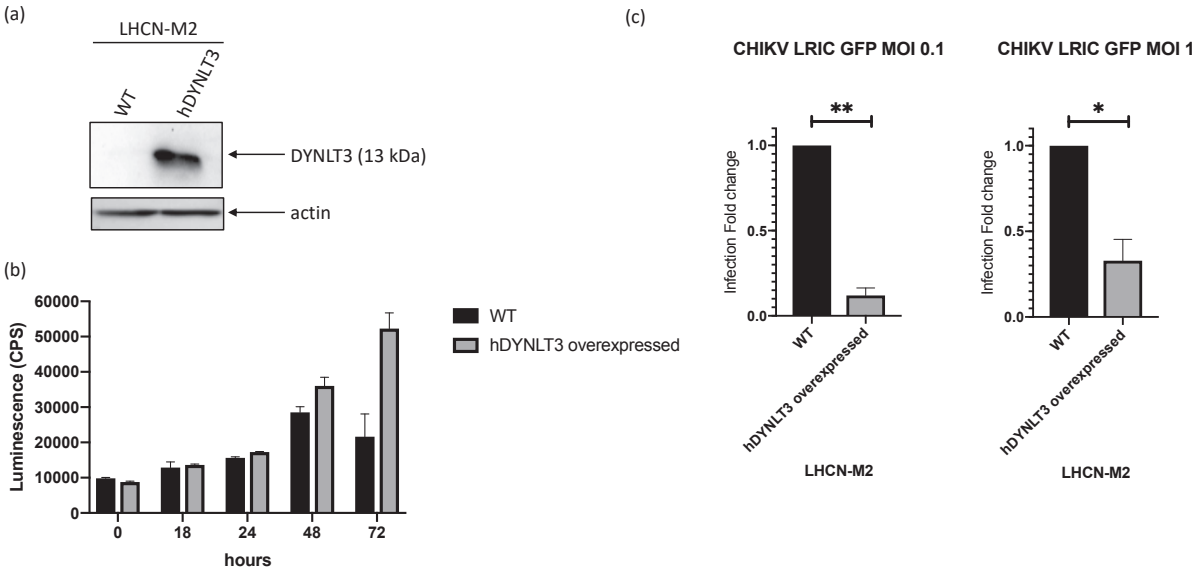

Figure 76: Overexpression of DYNLT3 protein in LHCN-M2 cells

(a) Expression of DYNLT3 protein in cells overexpressing DYNLT3 and in WT cells. DYNLT3 rabbit antibody (11687-1-AP, Proteintech) was used to detect DYNLT3 protein. Antibody raised to housekeeping protein β-actin was used as an internal control.

(b) Cell viability over time of WT cells and cells overexpressing DYNLT3.

Cells were plated in 96-well plate and the number of viable cells in culture was monitored at different time points by using a kit which quantifies the ATP present in the well.

(c) CHIKV-GFP infection assay in WT and hDYNLT3 overexpressing LHCN-M2 cells.

LHCN-M2 WT and LHCN-M2 hDYNLT3 cells were infected with CHIKV-GFP at MOI 0,1 or MOI 1 for 24h (n=3). Cells were harvested and fixed in PFA 4% before flow cytometry analysis. Statistical analyses were made with unpaired t-test with p-value <0,05. Infection on naïve WT cells was established at 1.

5 - Study of a potential interaction between CHIKV-capsid and DYNLT3 protein

Two separate co-immunoprecipitation (Co-IP) assays were carried out to study a potential interaction between CHIKV-capsid and DYNLT3 protein.

Both proteins were overexpressed in LHCN-M2 cells for the first assay. DYNLT3 with a V5 tag was constitutively expressed while CHIKV-capsid protein was only expressed after induction with doxycycline to avoid toxicity. The antibody anti-Capsid (C-SFV) that reacts with CHIKV capsid was used to form immunocomplexes and to co-immunoprecipitate proteins.

Input samples and Co-IP samples were analyzed by western-blot with antibodies targeting V5 tag of DYNLT3 and capsid protein respectively. On the western blot membranes with input samples, as expected we saw that CHIKV-capsid is not expressed in cells not treated with doxycycline (Fig.77). CHIKV-capsid theoretical

molecular weight is about 30 kDa and in the past, we already detected the capsid by western-blot around this size from lysates of CHIKV infected cells.
In lysates from cells treated with doxycycline, we observed one weak signal and a stronger one (Fig.77). We suggested that the weak signal corresponds to the CHIKV-capsid as it is at the expected molecular weight. The stronger signal is either a non-specific signal or it might come from an unexplained cleaved form of the capsid protein. On the membrane with Co-IP samples, the two signals were also detected meaning that both forms were recognized by the antibody and successfully captured on magnetic beads (Fig.77).

Regarding DYNLT3 in input samples, the protein was detected using an antibody directed to the V5 tag of the protein. DYNLT3-V5 was detected as the expected size of about 13 kDa on both samples with or without doxycycline (Fig.77).
However, on the membrane with Co-IP samples, DYNLT3-V5 protein was not detected in the condition with doxycycline treatment meaning that no interaction between CHIKV-capsid and DYNLT3 was found in this assay. It might signify that no physical interaction exists between the two proteins but given the weak signal for CHIKV-capsid protein and the presence of the strong unexplained signal we were not able to openly conclude.

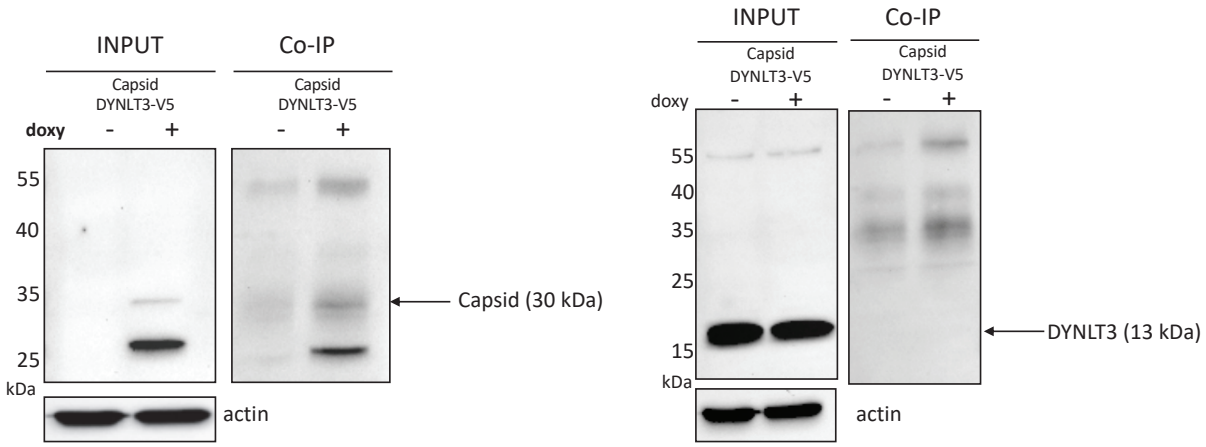

Figure 77: Input and co-immunoprecipitation samples from the overexpression system analyzed by western-blot
Cells were treated or not with doxycycline (doxy) for 48 h before cell lysis. The antibody anti-Capsid (C-SFV) was used to form immunocomplexes and to co-immunoprecipitate proteins. Input and co-IP samples were analyzed by western-blot using anti-Capsid (C-SFV) and anti-V5 (sc-271944, SantaCruz) antibodies. Antibody raised to housekeeping protein β-actin was used as an internal control.

In order to overcome these two signals observation in our overexpression system, we infected LHCN-M2 hDYNLT3 with chikungunya replicative virus, permitting the capsid expression in a context of infection. As a control, we infected WT LHCN-M2 cells in parallel. CHIKV-capsid was clearly detected in our input sample with the majority of the signal around 30 kDa (Fig.78). After the co-IP assay, CHIKV-capsid was also distinctly observed by western-blot analysis (Fig.78).
In parallel, DYNLT3-V5 was detected with the anti-V5 antibody in cells overexpressing the protein (Fig.78). Unfortunately, DYNLT3-V5 protein was not observed on the membrane with samples from the Co-IP (Fig.78) which implies that CHIKV-Capsid and DYNLT3 proteins do not seem to interact.

In addition, we have also reversed the co-immunoprecipitation assay by using anti-V5 tag antibody to form immunocomplexes and to co-immunoprecipitate proteins, but it appeared that the CHIKV-capsid binds in an unspecific manner to magnetic beads (data not shown).

To conclude these assays do not permit to identify an interaction between the two proteins and the potential relationship between CHIKV-Capsid and DYNLT3 might be studied by other approaches.

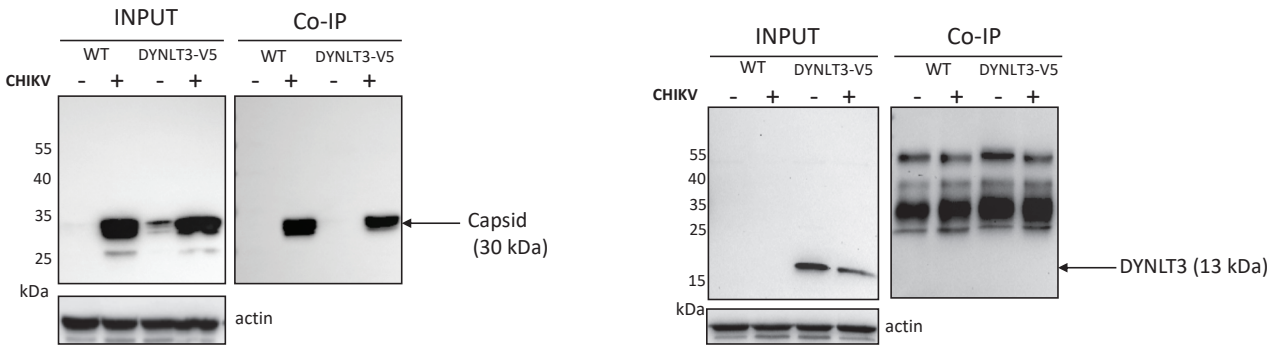

Figure 78: Input and co-immunoprecipitation samples from infected conditions
Cells were infected or not with CHIKV for 24h before cell lysis. The antibody anti-Capsid (C-SFV) was used to form immunocomplexes and to co-immunoprecipitate proteins. Input and co-IP samples were analyzed by western-blot using anti-Capsid (C-SFV) and anti-V5 (sc-271944, SantaCruz) antibodies. Antibody raised to housekeeping protein β-actin was used as an internal control

IV - Discussion

In the past few years, a lot of studies have demonstrated the role of microtubules and in particular dynein motor for transport during virus infection (Milev et al., 2018). In addition, direct interactions between viral proteins and dynein light chains have been identified including HSV L2 capsid protein, HPV16 capsid, Ebola virus VP35 protein, HIV Vpr protein and M protein of several flaviviruses (Brault et al., 2011; Caly et al., 2016; Douglas et al., 2004; Kubota et al., 2009; Schneider et al., 2011). The presence of the dynein light chain, DYNLT3, among the hits of our CRISPR-mediated screening, suggests a potential role of the dynein motor for CHIKV infection. Our CRISPR-based approach to study a potential implication of DYNLT3 protein in CHIKV infection has encountered technical difficulties which will be discussed there. On the other hand, we will present and discuss hypotheses to explain the decrease of CHIKV infection observed in DYNLT3 overexpression system.

Given the fact that we focused on many different protein candidates, as many tools as proteins were necessary to study these candidates. The critical and crucial point is the validation of knockout in CRISPR-mediated knockout cell lines by western-blot or immunostaining using specific antibodies. When specific antibodies were not available or not functional, a RT-qPCR strategy was used to quantify specific mRNA in cells. However, this approach does not always allow to conclude about the protein expression status in our cell lines. One solution, adopted by several other laboratories, is to generate clonal cell lines which are then sequenced. As one clonal cell line might represent a given phenotype, it implies to realize experiments on several clonal cell lines in parallel. Nevertheless, the clonal cell line option was hardly conceivable with LHCN-M2 cells as they don’t really tolerate to be seeded at very low density. More experiments will be needed to validate or not knockout.

An important decrease in the level of CHIKV infected cells was observed when viral infection was realized shortly after cell line generation but not when cells were amplified several days after transduction. We suggested a potential effect of the transduction on cell fitness and consequently on CHIKV infection. Lentiviral transduction might induce an innate immune response which limits the CHIKV infection 5 days later. After entry into the cell, the single-stranded RNA (ssRNA) of lentivirus is released, reverse transcribed into viral cDNA and transported to the nuclear genome for integration. Indeed, RNA from lentiviruses and reverse-transcribed viral DNA might be recognized by Toll-like receptors (TLRs) and cytosolic

DNA sensors (CDSs). TLR7 and TLR8 recognize ssRNA while TLR9 targets viral cDNA due to the presence of high frequency of CpG motifs. Ligand binding to TLRs triggers intracellular signaling pathways leading to the secretion of type 1 interferons (IFNs) and pro-inflammatory cytokines (Borsotti et al., 2016; Follenzi et al., 2007).
By doing RT-qPCR experiments throughout infection assays, IFN-β RNAs were detected 24h but not 96 h after lentiviral transduction and then strongly induced 24h after CHIKV infection (data not shown). In parallel, we also monitored RNAs of two interferon-stimulated Genes (ISGs), Mx and IFIT1 (data not shown). RNAs of both genes were detected 24h and 96h after lentiviral transduction and also after 24h of CHIKV infection. These data highlight the immune response triggered by the lentiviral transduction which could limit the subsequent CHIKV infection and might be an explanation of the observed effect.

Regarding cells with sgRNA DYNLT3 in the second round of infection assays, it might be difficult to conclude on a potential role of DYNLT3 for CHIKV infection as we were not confident in DYNLT3 protein status in both cell lines. In parallel, a cell line with a sgRNA targeting the other dynein light chain, DYNLT1, was generated as the two dynein light chains might have a redundant function in dynein activity or both be required for CHIKV infection. Indeed, in the case of human papillomavirus type-16, both DYNLT1 and DYNLT3 light chains are required for infection and the viral capsid protein interacts in fact with both DYNLT1 and DYNLT3 (Schneider et al., 2011).

On the other hand, the poliovirus receptor (PVR) has been shown to associate strongly and specifically with the dynein light chain DYNLT1. Data indicate that DYNLT1 interacts with a particular motif in the cytoplasmic domain of PVR closed to the membrane. In the case of the neurotropic poliovirus, the interaction might explain how poliovirus reaches motor neurons via retrograde transport. In the proposed model for infection, poliovirus binds to its receptor PVR and is subsequently endocytosed. The cytoplasmic tail of PVR displayed at the surface of endosomes associate with DYNLT1 and the virus/receptor complex is transported along microtubules by retrograde axonal transport (cf. figure 68 model C) (Mueller et al., 2002). Interestingly though, PVR has been identified in a collaborative RNAi screen project as an entry factor for CHIKV (unpublished data from collaboration, confidential). In order to validate the impact of PVR for entry of CHIKV and study an eventual PVR/dynein association, a cell line with a sgRNA targeting PVR was generated. However, it was difficult to conclude for both DYNLT1 and PVR impact on infection since protein status was unknown for lack of characterization tools. Cell lines should be

characterized using specific tools in future experiments and new infection assays should be realized.

With regard to the CRISPR-mediated knockout system, it's a recent technology, but it rapidly appears that control/scramble sgRNAs are primordial for experimental studies particularly regarding off-target effects. However, information obtained from such control is limited to off-target effects due to Cas9 but not to off-target effects derived from specific sgRNA used. Moreover, as sgRNA and Cas9 protein are integrated into the genome and constitutively active, it might clearly affect cell fitness. Indeed, it has been shown that double strand break induced by Cas9 activates p53, leading to a growth arrest (Haapaniemi et al., 2018). In our experiments, it also seems that the control sgRNA (targeting luciferase gene) might have an impact on cells as we almost always observed a slightly lower level of CHIKV infection in cells with sgRNA luciferase compared to WT cells.

Interestingly, overexpression of DYNLT3 protein in LHCN-M2 cells induces an important decrease of CHIKV infection level. A cell viability assay has been realized to ensure that overexpression does not alter cell survival. Further experiments could be realized to better characterize this cell line such as cell cycle assay. It could be also interesting to set up microscopy assays to observe the cellular localization of the overexpressed DYNLT3 protein. In addition, for infection assays, an overexpression control cell line should be added as well as a control virus (not affected by DYNLT3 overexpression).

Several hypotheses could be proposed to illustrate the CHIKV infection diminution. Many virus-dynein interactions occur *via* an association of a dynein component with the viral capsid. It can be illustrated by the interaction with dynein of, among others, HSV capsid, L2 capsid protein of HPV, capsid of adenovirus, capsid of bovine immunodeficiency virus (Bremner et al., 2009; Douglas et al., 2004; Kelkar et al., 2004; Su et al., 2010). With this in mind, we have studied the alphavirus replication cycle to suggest steps during which DYNLT3 protein might interact with CHIKV-capsid.

During the alphavirus replication cycle, after receptor binding and endocytosis, the fusion of viral envelope with the endosomal membrane allows the release of nucleocapsid into the cytoplasm. The capsid proteins of the nucleocapsid associate with 60S ribosomal subunit, facilitating the uncoating and disassembly of the nucleocapsid and the release of viral RNA for initiation of the protein synthesis

(SINGH' and HELENIUS, 1992; Wengler et al., 1992). We have suggested that nucleocapsid might be transported by dynein to a particular localization inside the cell for disassembly and RNA release for subsequent protein synthesis. When overexpressed, the dynein light chain might disrupt dynein complex formation or correct dynein function and consequently inhibit dynein-dependent transport of the nucleocapsid. Some data published on dynactin that act as a co-factor for the microtubule motor dynein show that overexpression of one dynactin subunit, dynamitin, disrupts the complex, resulting in dissociation of cytoplasmic dynein in mammalian cells (Echeverri, 1996). Also, transport of HSV1 capsid by dynein along microtubules has been shown to be inhibited by dynamitin overexpression leading to dynactin complex disruption (Döhner et al., 2002).

Following the translation from subgenomic RNA, the alphavirus polyprotein is autocatalytically processed at the N-terminal end by the capsid protease and the alphavirus capsid protein is released into the cytoplasm. Capsid protein binds to genomic RNA promoting nucleocapsid formation. Finally, 240 copies of capsid proteins assemble to encapsidate the viral RNA and form nucleocapsid core (NC). A study suggests that NC assembles near cytopathic vacuole type I (CPV I) that are the sites of viral RNA synthesis and then traffic to the plasma membrane for budding. In parallel, few of NC were found attached to cytopathic vacuole type II (CPV-II) originated from the trans-Golgi network, and the rest of NC transported by unknown host transport machinery (Bremner et al., 2009; Douglas et al., 2004; Kelkar et al., 2004). It has also been shown that distinct capsid and NC pools are formed during infection with only a fraction of total capsid produced that is incorporated into new virions. Regarding what we know about nucleocapsid formation, we have suggested that after translation of new capsid proteins, a potential association between capsid and the dynein light chain DYNLT3 might permit to transport capsid monomer to the site of nucleocapsid assembly. Overexpressed DYNLT3 in our assays might bind to CHIKV-capsid and catch a large amount of monomeric capsid protein preventing the assembly of new nucleocapsid.

As positive-strand RNA viruses, alphaviruses replication cycle occurs within the cytoplasm of infected cells. However, several RNA viruses and alphaviruses target a number of viral proteins to the nucleus (Garmashova et al., 2007a; Jakob, 1993; Walker and Ghildyal, 2017; Weidman et al., 2003). CHIKV-capsid has been reported to possess one nuclear import signal (NLS) and two nuclear export signals (NES) (Jacobs et al., 2017; Thomas et al., 2013). Little is known about the importance of

capsid nuclear transport and localization for CHIKV and other arthritogenic alphaviruses. On the other hand, it has been shown that nuclear localization of the non structural protein nsp2 of old world alphaviruses CHIKV, SINV and SFV induces a transcriptional shutoff while new world alphaviruses VEEV and EEEV transcription inhibition is dependent on the capsid protein (Garmashova et al., 2007b). Finally, it has also been demonstrated that mutation in the nuclear localization sequence of CHIKV-capsid attenuates viral replication in mammalian cells (Taylor et al., 2017). Based on these data, our last hypothesis suggests the transport of CHIKV-capsid by the dynein motor near the nucleus thus enabling its trafficking into the nucleus. CHIKV-capsid in the nucleus might play an unknown role or might be involved a transcriptional shutoff. Free DYNLT3 in excess in our overexpression system might interact with CHIKV-Capsid stopping its nuclear trafficking.

To investigate a potential interaction between the dynein light chain DYNLT3 and the capsid of CHIKV, a cell line expressing constitutively DYNLT3 and CHIKV-capsid protein under induction was generated. An unexpected strong signal has been observed on the western-blot realized for capsid detection with a lower molecular weight than the expected CHIKV-capsid signal. As this signal has not been observed in the same cell line but without doxycycline induction, we have suggested that it might be a cleaved form of the capsid protein although no study has reported such a cleaved form of the protein. This assay did not permit to conclude about the interaction. In the second assay realized with the capsid protein expressed from CHIKV infection, a strong signal corresponding to the 30 kDa capsid protein has been observed. Despite this, no results for CHIKV-capsid and DYNLT3 interaction was observed in this assay nor in the reverse co-immunoprecipitation assay either. These results seem to suggest either the dynein light DYNLT3 does not interact with the capsid protein or not directly. It would be interesting to realize further experiments to study eventual proximity or colocalization of the two proteins such as proximity ligation, immunofluorescence or confocal microscopy assays. It will be also possible with the tagged DYNLT3 to pool down cellular protein of infected *versus* non infected cells to identify any virus protein/DYNLT3 interactions.

On the other hand, the DYNLT3 protein might be involved indirectly in the chikungunya virus infection. Indeed, it has been shown that autophagosomes are transported by dynein motor proteins along microtubules towards lysosomes near the microtubule-organizing center (Jahreiss et al., 2008; Ravikumar et al., 2005) and that inhibition of autophagy dramatically decreases chikungunya virus infection (Krejbich-

Trotot et al., 2011). Overexpression or depletion of DYNLT3 might increase the level of non-functional or disrupted dynein complex inside the cell that might inhibit the autophagy process and subsequently the chikungunya virus infection. It will be interesting to quantify autophagy in infected cells overexpressing or not DYNLT3.

To conclude, several pieces of evidence suggest the involvement of DYNLT3 in chikungunya virus replication: DYNLT3 has been identified in our CRISPR screen, DYNLT3 is required for the infection of numerous viruses and DYNLT3 overexpression has an impact on CHIKV infection. Thus, it would be interesting to realize, among others, new infection assays in validated CRISPR-mediated knockout cell lines and to set up microscopy assays to observe the cellular localization of the viral components in WT cells, cells overexpressing DYNLT3 and cells knockout for DYNLT3.

Chapter 3: Candidates from the screen

I - Material and Methods

Generation of CRISPR-mediated knockout cell lines and infection assays were realized as described in Part 1. The following primers were used to generate the different CRISPR vectors.

Guide name		Sequence 5'-3'
sgRNA CLEC2B	Forward	CACCGAGAGTTTATGCCCCTATGAT
	Reverse	AAACATCATAGGGGCATAAACTCTC
sgRNA JAM3	Forward	CACCGATTCGCAGACAAGTGACCCC
	Reverse	AAACGGGGTCACTTGTCTGCGAATC
sgRNA PAPD4	Forward	CACCGATTGTGCATCTATAAGCTGC
	Reverse	AAACGCAGCTTATAGATGCACAATC
sgRNA SLC6A14	Forward	CACCGAATGATGAGAATCAGGACCG
	Reverse	AAACCGGTCCTGATTCTCATCATTC
sgRNA_1 AMBRA1	Forward	CACCGCAGACATCCGGGCATTGCG
	Reverse	AAACCGCAATGCCCGGATGTCTGC
sgRNA_2 AMBRA1	Forward	CACCGACCGAGCTCCACGCAATGCC
	Reverse	AAACGGCATTGCGTGGAGCTCGGTC

II - Results

Cloning of sgRNAs into lentiCRISPRv2 and lentiviral production were achieved for the nineteen selected candidates from the first analysis based on gene counts. In addition to DYNLT3 assays, test of protein expression status and infection assays were executed for some of the nineteen candidates, including CLEC2B, JAM3, SLC6A14, PAPD4. In parallel, infection assays were also realized for the candidate AMBRA1 coming from the guide-based analysis. For infection assays, cells were amplified at least one week after CRISPR lentivirus transduction.

1 - CLEC2B

We tried to validate CLEC2B knockout by immunohistochemistry, however, the antibody used for the staining did not permit to obtain an exploitable signal. Infection assays were realized without a confirmed status of CLEC2B expression. SgRNA CLEC2B and WT were infected with replicative CHIKV at two different MOI. A decrease of CHIKV infection was observed with an MOI of 0,1 in sgRNA CLEC2B cells compared to WT cells (Fig.79) while infection levels were almost similar between the two cell lines at MOI 1. Experiments need to be replicated to confirm the decrease observed at MOI 0,1 in sgRNA CLEC2B cells. In addition, sgRNA luc cells should be infected in parallel as a control. Concurrently, sgRNA CLEC2B and WT cells were also infected with pseudotyped viruses harboring either CHIKV, SINV envelope proteins or envelope of VSV as a control. No significative differences were observed with CHIKV and SINV pseudotypes (Fig.80).

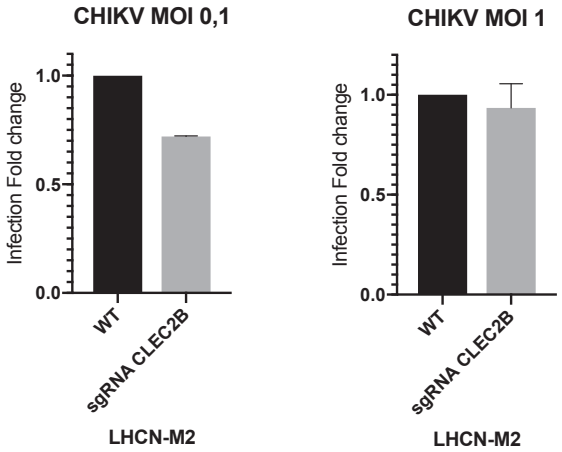

Figure 79: CHIKV infection assay in WT and sgRNA CLEC2B cell lines

Cells were infected with CHIKV at MOI 0,1 or MOI 1 for 24h. Cells were harvested and fixed in PFA 4% before immunostaining and flow cytometry analysis (n=2). Infection on naïve WT cells was established at 1.

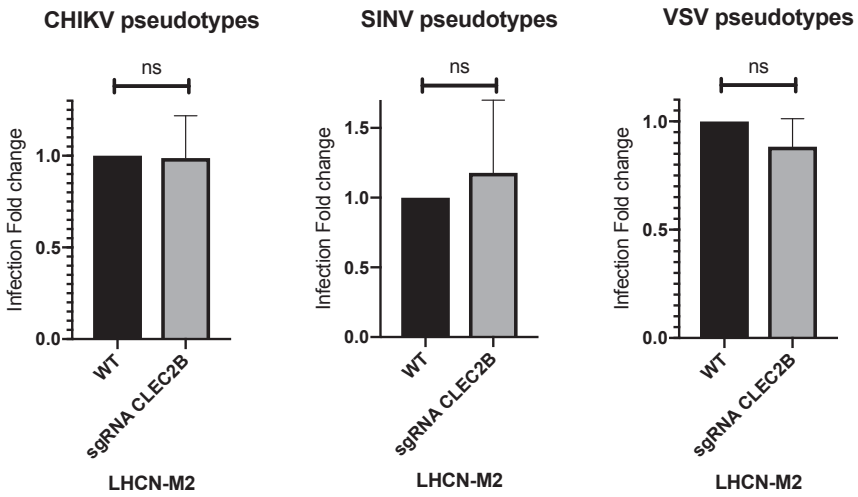

Figure 80: Infection assay in WT and sgRNA CLEC2B cells with pseudoparticles

Cells were incubated with pseudoparticles 2 h at 37°C before medium change. Cells were then harvested 3 days post-infection and fixed in PFA 4% before flow cytometry analysis (n=3). Infection on naïve WT cells was established at 1.

2 - JAM3

A cell surface immunostaining was realized with sgRNA JAM3 pooled cells followed by flow cytometry analysis as described in Part 1 (antibody CD323, 356703, Biolegend). It appears that 84% of cells were negative for JAM3. Infection assays with CHIKV-GFP were carried out using this knockout cell line. Infection levels were nearly equivalent between WT and sgRNA JAM3 cell lines (Fig.81). This result needs to be confirmed by other replicates and with control sgRNA luc cell line in parallel.

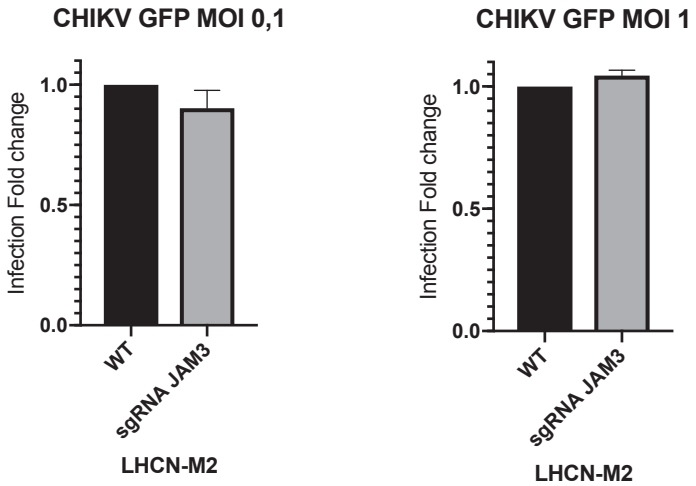

Figure 81: CHIKV-GFP infection assay in WT and sgRNA JAM3 LHCN-M2 cells

Cells were infected with CHIKV-GFP at MOI 0,1 or MOI 1 for 24h. Cells were harvested and fixed in PFA 4% before flow cytometry analysis (n=2). Infection on naïve WT cells was established at 1.

3 - SLC6A14

We tried to validate SLC6A14 knockout by immunohistochemistry and western-blot however the antibody used did not permit to obtain exploitable results (SLC6A14 polyclonal antibody, E-AB-33363, Elabscience). The SLC6A14 protein expression status needs to be confirmed. Infection assays with replicative CHIKV-GFP and pseudotyped viruses were carried out twice. By considering the standard deviation in each assay, we did not observe any difference in infection levels either with CHIKV-GFP (Fig.82) or pseudotyped viruses (Fig.83).

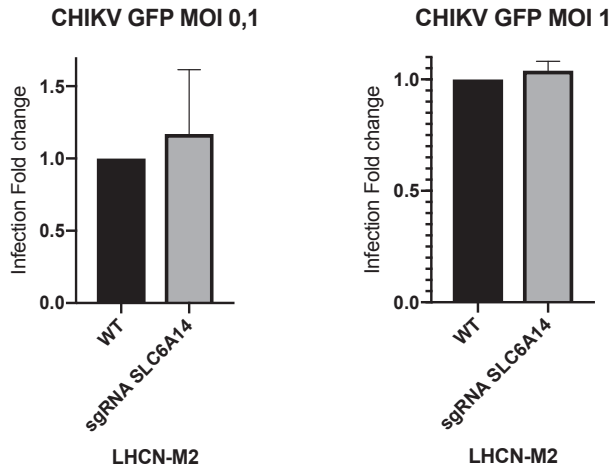

Figure 82: CHIKV-GFP infection assay in WT and sgRNA SLC6A14 cells

Cells were infected with CHIKV-GFP at MOI 0,1 or MOI 1 for 24h. Cells were harvested and fixed in PFA 4% before flow cytometry analysis (n=2). Infection on naïve WT cells was established at 1.

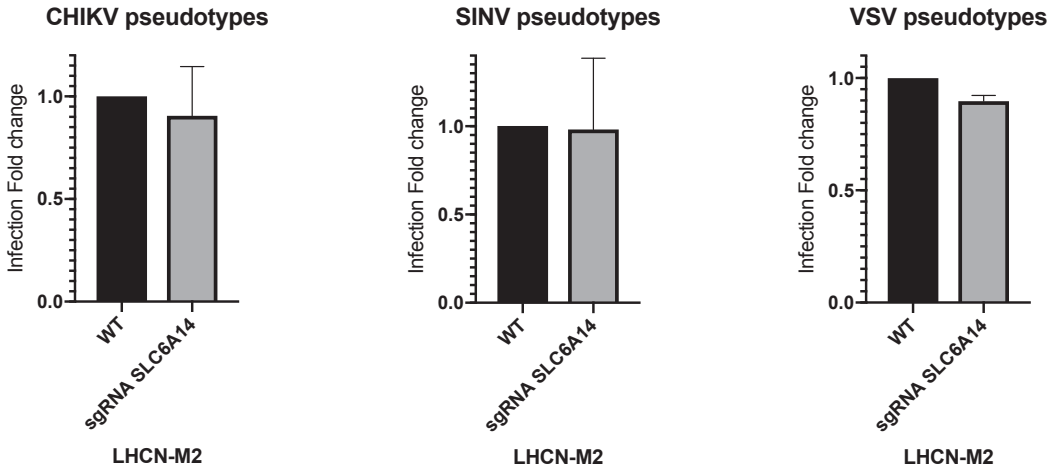

Figure 83: Infection assay in WT and sgRNA SLC6A14 cells with pseudoparticles

Cells were incubated with pseudoparticles 2h at 37°C before medium change. Cells were then harvested 3 days post-infection and fixed in PFA 4% before flow cytometry analysis (n=2). Infection on naïve WT cells was established at 1.

4 - AMBRA1

AMBRA1 CRISPR-mediated knockout in LHCN-M2 cells was validated by western blot analysis (Fig.84). Cell lines depleted for AMBRA1 were infected by CHIKV LRic in parallel with WT cells and control cell line with sgRNA luciferase (sgRNA luc). Unfortunately, we did not notice any significative difference in CHIKV infection level between the control cell line and AMBRA1 knockout cell lines either at MOI 0,1 or MOI 1 (Fig.85).

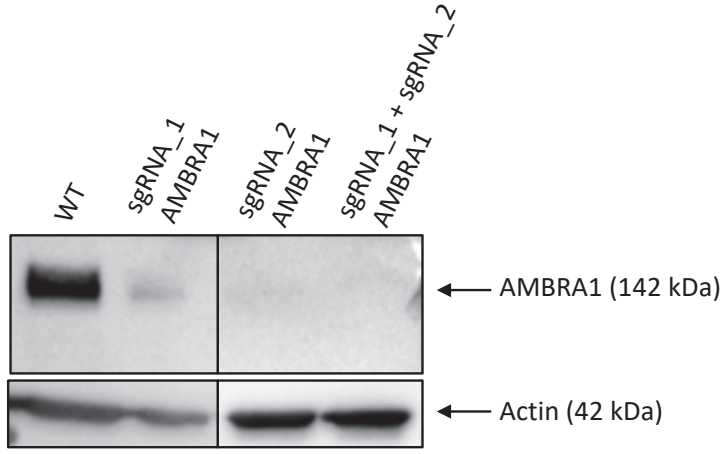

Figure 84: Validation of AMBRA1 knockout by western blot analysis

AMBRA1 mouse monoclonal antibody clone G6 (SantaCruz sc-398204) was used to detect AMBRA1 protein in cell lysates (1/1000 in 10% milk PBST 0,1%, overnight incubation, 4°C). Secondary anti-mouse IgG antibody was used as described previously. Antibody raised to β-actin was used as an internal control.

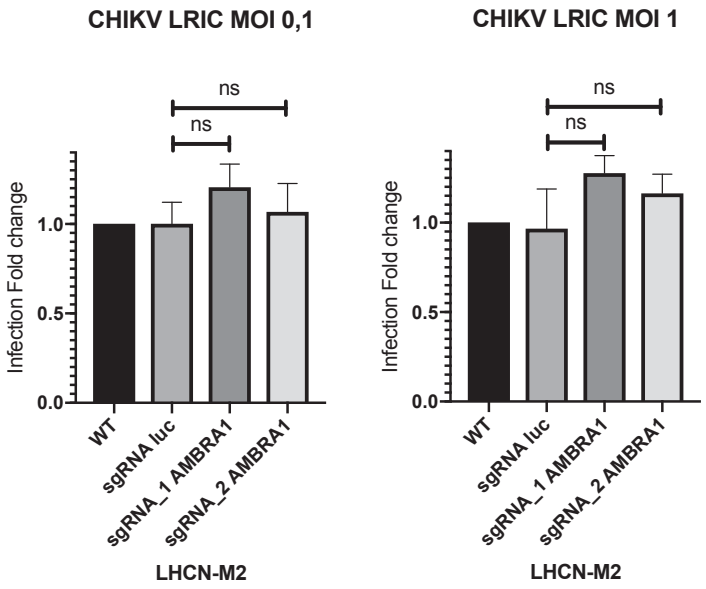

Figure 85: Infection assay in WT, sgRNA luc and sgRNA AMBRA1 cells

WT, sgRNA luc, and sgRNA AMBRA cells were infected with CHIKV LRic at MOI 0,1 or MOI 1 for 24h and then harvested in PFA 4%. Cells were immunostained with a primary antibody raised to Semliki Forest nucleocapsid protein, that reacts with CHIKV capsid protein (IgG2a C42) and then analyzed by flow cytometry analysis. (n=3) Statistical analyses were made with unpaired t-test with p-value < 0,05. Infection on naïve WT cells was established at 1.

Finally, very preliminary data were obtained in sgRNA PAPD4 cells (expression status not confirmed). We observed a slight decrease of CHIKV-GFP infection in sgRNA PAPD4 cells, from 40% of infected cells in WT to 32% in CRISPR cells. Replicates experiment needs to be realized to confirm the observed tendency since infection assay has been made only once. As we have already observed and mentioned in the previous chapter, our approach was limited by the need of numerous and performant antibodies to validate protein status.

Part 2 - General discussion

Over the past decade, loss of function screens have provided a powerful tool for investigating virus-host biology. The discovery of CRISPR/Cas9 system has enabled the expansion of CRISPR/Cas9 screen as a new tool to identify host factors that are important for viral replication. In parallel, face to the recent re-emergence of arboviruses including Zika, dengue and chikungunya viruses causing large outbreaks, more virus-cell interaction studies were needed and have been conducted. However, the replication of chikungunya virus and other alphaviruses remains poorly characterized and the efforts to understand the virus biology and the pathogenesis need to progress.

In order to understand the chikungunya replication cycle and identify host factors required for the infection, a genome-wide CRISPR/Cas9 loss of function screen has been realized. Besides problems of library diversity raised earlier, we have faced difficulties to confirm the role of the hits identified through the screen. These difficulties are associated with the validation of specific-gene knockout, the actual efficiency of CRISPR/Cas9 *in vivo* and the presence of false positives.

An important issue already mentioned is the requirement of multiple functioning tools to validate gene knockout in the different generated cells lines. The use of antibodies for western-blot, flow cytometry or microscopy immunostaining permits to confirm with certainty the protein status and the efficient knockout. However, their use is tricky as antibodies are generally quite expensive and as their efficacy and quality cannot be assured prior to testing them.

We used an alternative approach by doing RT-qPCR assays to monitor transcript level in CRISPR cell lines compared to the WT cell line. These assays are informative when transcript level is actually null in CRISPR cell line but since transcripts are detected it is difficult to conclude on protein knockout.

Other strategies are used to estimate or validate the presence of mutations and might be considered for future experiments.

The generation of clonal cell lines and sequencing of the region of interest might be one of the best alternatives although our LHCN-M2 model cell line is hardly clonable and multiple sequencing can be quite expensive and highly time-consuming.

Nuclease mismatch detection assay is a widely used method which exploits the properties of mismatch-specific endonucleases to detect and cleave mismatches (Vouillot et al., 2015). After PCR amplification of the region of interest and denaturation followed by formation of DNA duplex by heating and slow cooling, mismatch

nucleases (T7E1) or Surveyor nucleases can be used to recognize and cleave heteroduplexed DNA amplicons containing mismatched base-pairs. Visualization of cleaved DNA products on electrophoresis agarose gel permits to determine the frequency of mutations induced by the CRISPR/Cas9 system.
Another approach to estimate mutation frequency is the use of digital PCR assays. In digital PCR (dPCR), the sample is split up into thousands of physically isolated partitions (such as droplets or wells on a chip), such that most partitions will contain either one or no copies of the target DNA. The assay consists of a reference PCR with primers binding to sequences distant from the target site and then a second PCR is realized with the same forward primer, but a reverse primer designed to bind directly at the Cas9 target site. If the target site is mutated, the primer is not capable of binding and the corresponding amplicon is not amplified (Findlay et al., 2016). Observations of the different amplicons on agarose gel permit to identify mutated samples. Finally, approaches to monitoring gene editing are multiple and enabled a systemic screening of mutated samples, nevertheless, verification of protein expression remains crucial.
In the end, another alternative to validate hits will be to use siRNA or shRNA that target the mRNA and to measure the level of mRNA by RT-qPCR. However, this technic can have other bias like more frequent off-target effect, reduction in particular but not all spliced mRNA.

Surprisingly, for genes for which we had functioning characterization tools, it often appears that protein expression remains unchanged in CRISPR-edited cell lines. It means either no modification has been introduced in the genome or the introduced mutation(s) do not lead to protein disruption. The efficiency of sgRNAs is a major concern in the CRISPR field. Several publications have shown that sgRNA efficiency varies widely. Indeed, it has been reported that the level of insertion/deletion creation varies between 5% to 65% with an average between 10 to 40% (Cong et al., 2013; Fu et al., 2013). Chromatin structure, particular sequence elements and stability of sgRNA-target DNA complex might avoid efficient sgRNA binding and activity (Chen et al., 2017; Xu et al., 2017).
Efforts have been made to develop algorithms that predict sgRNA activity and efficiency. Nevertheless, through our CRISPR experience, we have often observed that even if the *in silico* predicted efficiency is high, two or three sgRNAs have to be tested *in vitro* to successfully generated a knockout. For the candidates from the screen, we did not design our own specific sgRNAs targeting candidate genes, but we used sgRNAs from the library highlighted in the screen. Given our results, it suggests a variable efficiency among the sgRNAs of the library. The question arises

of whether variable efficiency seen using CRISPR/Cas9 is sufficient to generate a desired phenotype in the screening assay. In theory, this is in part offset by the presence of multiple sgRNAs targeting the same gene. We may design ourselves other sgRNA targeting the selected genes using other software and test them.

The cell line might also influence gene editing efficiency. Indeed, the ploidy of the gene locus of interest and the DNA repair status of the target cell might affect the efficiency of the knockout. Double strand break of only one allele of a gene can be easily repaired by HDR with a second allele as a template. To improve the chances of generating protein depletion, two sgRNAs targeting the same gene can be used for instance to generate large deletion easily detectable by PCR and likely to disrupt protein expression. In addition, as discussed previously, the LHCN cells might be more prone to DNA repair that cell lines derived from tumor cells. Even if initially our goal was to select a relevant target cell closest of the real tissue *in vivo*, finally, our screen may be improved by using another cancer cell line.

In parallel of our screening, another library in a different cell line (HCT116 epithelial cells from colorectal carcinoma) was generated for a collaboration with another team working on dependence receptors and cancer (Team P.Mehlen, CRCL, Lyon). Except for their screen challenge which was drug-triggered cell death, their screen and our screen were generated and processed following the same process. We have used the same lentiviral library for generating both modified cell lines and they have realized PCR amplification from both genomic DNA samples in the same way. After the analysis of their screen, they observed a low library representation and several false positives among their enriched candidates as well.

In our screen, we have also observed a low library representation as discussed earlier. Moreover, even among the cell lines with a validated knockout, none of the screen candidates have been clearly confirmed as required for CHIKV infection assays suggesting the presence of many false positives.

As already mentioned earlier, the low library representation might greatly impact the robustness of both screens. Indeed, random variations of sgRNAs present in low numbers introduce high background noise. Moreover, a high representation allows to avoid depletion by random chance leading to false negatives. Based on what we knew at that time, cell libraries were realized with a 100-fold representation of sgRNA library, but it appears with the different screens and studies published later than a higher

representation is preferred to maintain the diversity. However, it also appeared that the genomic DNA quantity used for PCR amplification prior sequencing was insufficient to maintain the representation. In the screen of the other team, indeed, many sgRNAs were present among hits of the challenged condition although they were not detected in the non-challenged control library. It means that certain sgRNAs were present in the cell library, but they have not been detected during the sequencing, certainly because the genomic DNA quantity used for PCR did not preserve the representativeness of the library. This too low DNA quantity might greatly impact the library representativeness and the presence of false positives. PCR amplification was realized with less than 1 μg of genomic DNA while quantities used in other studies are generally higher than 5 μg (Han et al., 2018; Richardson et al., 2018). Nevertheless, it's hardly comparable since the quantity of genomic DNA for PCR should be adapted to the number of lysed cells. We have tried to find a way to calculate the amount of genomic DNA required. As it is generally agreed that the genome of diploid cells has a mass of 6,6 picograms, we suggested that the quantity of genomic DNA required for PCR amplification might be calculated by taking into account the number of cells with a lentiviral integration and the mass per genome. Thus, by multiplying the number of cells by the mass per genome, it might be possible to calculate the amount of genomic DNA required to maintain fold representativeness.

In addition, as we already discussed earlier, we have also noticed a poor enrichment in our screen after the challenge although two rounds of viral infection have been realized. This not-enough-stringent challenge can considerably increase the number of false positives among the hits. As we mentioned earlier through a CRISPR screen with the influenza virus, the multiplication of the number of rounds of selection permits a progressive increase in sgRNA enrichment (Han et al., 2018). Thus, multiple rounds of chikungunya virus challenge in our future screens might reduce the number of false positives among the hits.

Presence of false positives might also be linked to the specificity of the CRISPR/Cas9 system. It has been described that CRISPR/Cas9 induces less off-target effects than RNAi, nevertheless, several studies have highlighted a quite high frequency of off-target mutagenesis in human cells (Fu et al., 2013). Notably, it has been revealed sequence flexibility and tolerance up to five mismatches and tolerance for bulges of sgRNAs (Carroll, 2013). The observed virus-resistant phenotype might be linked to off-target effects rather than the specific-knockout effect. In CRISPR screens,

multiple sgRNAs for each gene are included to overcome specificity and efficiency issues and in order to observe redundancy of phenotype.
The issue of the specificity is also raised as we have noticed the presence of control non-targeting sgRNAs which are supposed to target nothing in the human genome, in our lists of enriched sgRNAs and in other published screens.

In this screen, our approach is based on the genomic DNA isolation from a pool of virus-resistant cells and on the sequencing of sgRNA sequence integrated into the genome. The first questionable aspect of this approach is that a pool of cells is recovered without knowing if every single cell is really resistant to the virus. The second point of criticism is the fact that we cannot know if the virus-resistant phenotype is truly caused by the specific knockout generated by the integrated sgRNA or by an off-target effect. Other approaches described below that might be explored, could permit to significantly decrease the number of false positives.
After one or several virus challenges, surviving cells might be isolated by serial dilution in a multi-well plate to obtain ideally one single clone in each well. After cell expansion, a new virus challenge permits to confirm or invalidate the virus-resistant phenotype of every single clone. The genome of resistant single clones can be sequenced and compared with the genome of WT cells to identify mutations conferring the resistance. On the other hand, by using virus with a fluorescent reporter, non-infected cells or cells with low levels of virus can be isolated and their resistant-phenotype can be confirmed with a new virus challenge as described above (Heaton et al., 2017; Park et al., 2017).

To conclude, this screen has enabled us to observe the limitations of the CRISPR/Cas9 technology and to identify the defaults of our approach. Screenings with CRISPR/Cas9 are powerful tools, provided that the library representation is high, and the phenotypic selection is stringent.

In short-term prospects, it might be valuable to redo PCRs with the appropriate quantity of DNA starting from the remaining extracted genomic DNA of both screens, then to realize a new sequencing with this amplified DNA. By doing this for our screen in LHCN-M2 cells and the other screen in HCT116 cells, this will enable to gain insight into the source of the problem.
Indeed, if after PCR amplification in adapted conditions and sequencing, the library representation is clearly better for both screens (LHCN-M2 cells and HCT116 cells), it will suggest that the low representation was linked to PCR amplification.

In the other hand, if library representation is better but still not so high, it might mean that adapted PCR amplification improved the diversity but that the number of cells used at the beginning (100-fold library) was probably not enough and should be increased. However, it might also be linked to a loss of sgRNAs during DNA amplification, lentivirus production or during any other step of the process. That is why the sequencing of the DNA plasmid library should also be considered before any replicate. Lastly, if the library representation is improved for the screen in HCT116 cells but not for our screen in LHCN-M2 cells, it might suggest that the LHCN-M2 cell line is not totally suitable for a CRISPR/Cas9 screen approach.

In a long-term perspective, based on the observations made from our data and the new sequencing, we could carry out a new screen by using a cell library with a better sgRNA diversity, realizing multiple rounds of virus challenge (with tagged virus or not), and adapting genomic DNA quantity used for PCR amplification to increase the signal-to-noise ratio. Finally, we might also consider collaborating with a bioinformatician to analyze in greater detail the sequencing data using notably CRISPR-specific analysis software.

GENERAL CONCLUSION

Alphaviruses are arboviruses typically disseminated to humans by mosquitoes such as *Aedes aegypti* and *Aedes albopictus*. In recent years, chikungunya virus has spread from endemic areas of Africa and Asia to new populations in Europe and the Americas, making chikungunya virus a global threat and the most common alphavirus infecting humans. It is generally accepted that the global spread of alphaviruses and especially CHIKV is a combination of expanding mosquito populations, the adaptation of alphaviruses to new mosquito vectors and increased international travel (Kraemer et al., 2015; Tsetsarkin et al., 2007). Chikungunya virus is an alphavirus capable of causing long term debilitating joint and muscle pain. Millions of individuals were infected in the last 10 years, resulting in a significant loss of life-quality, high societal cost, and thousands of deaths. Currently, there are no licensed vaccines or treatments for CHIKV infection justifying the importance to continue research and gain insight into chikungunya virus biology. Despite the numerous studies, host factors involved in chikungunya virus entry and replication cycle remain poorly characterized.

The main objective of my project was to better understand and characterize the chikungunya virus entry and the host factors used during replication steps.

The first key objective was mainly focused on alphavirus entry and early infection steps. Working with CHIKV and SINV, we have demonstrated that iron treatment of cells prior to and throughout the infection has an effect on viral infection of both viruses. This effect appears to be dose-dependent. Impact of iron on SINV infection had already been described in a study in which the divalent metal ion transporter NRAMP2 has been identified as a receptor for SINV in mammals (Rose et al., 2011). Given the fact that SINV and CHIKV are closely-related viruses belonging to the same genus of Alphavirus, we have hypothesized that NRAMP2 could also be involved in CHIKV entry. By generating cell lines depleted for NRAMP2 protein, we have demonstrated that the protein is required neither for the entry of CHIKV-derived pseudotypes and nor for the infection with replicative viruses. Finally, we have shown that there is no clear correlation between cell permissiveness for CHIKV and NRAMP2 expression profile. This combination of arguments allows to rule out the involvement of NRAMP2 in CHIKV infection. In term of analysis of arbovirus entry, it is an important conclusion that suggests that the use of orthologs is not the obvious way to identify receptors in different species. In addition to our work, it has also been shown that

Malvolio or NRAMP2 orthologs do not exist in *Aedes aegypti* mosquitoes (Tsujimoto et al., 2018). Clearly, more work is needed to understand the broad tropism of alphavirus and arboviruses in general.
Following the idea of receptor regulated by iron, we have then highlighted that the transferrin receptor is neither involved in CHIKV infection although TFRC is also iron-regulated and known to be a receptor for several viruses. Finally, our current hypothesis is that iron in form of ferric ammonium citrate might have an antiviral effect as it has been recently described for several viruses. Relying on this latter, future experiments will be focused on the understanding of the antiviral effect of iron treatment in our model.

Regarding the two proteins identified previously in an RNAi screen, we have demonstrated that CD46 is not required for CHIKV entry while TM9SF2 appears to be required for CHIKV efficient infection. However, the role of the latter has been published in the meantime by another laboratory. TM9SF2 has been shown to be involved in the localization and stability of another protein called NDST1 known to be required for the N-sulfation of heparan sulfate. Since CHIKV uses heparan sulfate as attachment factors, the depletion of TM9SF2 in cells has an indirect impact on CHIKV infection.

In the last focal area, our goal was to obtain a global understanding of host factors used during chikungunya virus replication by carrying out a genome-wide loss of function screen with the CRISPR/Cas9 technology.
The difficulties experienced have been analyzed and discussed in order to determine short-term experiments to realize and to optimize future screens.

Among the candidates identified through the screen, we focused on the DYNLT3 protein, a light chain of the dynein motor complex involved in cargo binding. Since cytoskeleton is commonly used by viruses and the dynein motor often hijacked by viruses for intracellular transport, DYNLT3 protein represents a good candidate. Unfortunately, we did not observe an effect of sgRNA against DYNLT3 in our infection experiments, but the protein expression status was not clearly characterized. However, we have shown that the DYNLT3 overexpression induces a decrease of the CHIKV infection. Our hypothesis of an interaction between DYNLT3 and CHIKV-capsid protein has not been validated by the co-immunoprecipitation experiments. More work remains to be done to understand and to characterize a potential role of DYNLT3 in CHIKV infection. In parallel, the study of the potential implication in infection of the other hits identified in the screen should be continued. Indeed, the

CRISPR/Cas9 system has been validated by many studies of virus-cell interaction. For Hepatitis C virus for example, in one screen, three receptors, namely CD81, Claudin 1 and Occludin, have been confirmed, whereas with previous technics, it took 11 years for scientists to discover them all from the first one CD81 (1998) to Occludin (2009). Very recently, the Mxra8 receptor has been discovered for arthritogenic alphaviruses (CHIKV, O'nyong nyong virus, Mayaro virus) using a CRISPR/Cas9 screen in mice cells. However, CRISPR/Cas9 screens in human cells are still of high importance. In addition, Mxra8 protein is not the receptor for encephalitogenic alphaviruses. Therefore, other screen using other alphaviruses will be valuable and the setting up will lead to important knowledge of alphavirus biology.

REFERENCES

Adli, M. (2018). The CRISPR tool kit for genome editing and beyond. Nature Communications *9*.

Agarwal, A., Dash, P.K., Singh, A.K., Sharma, S., Gopalan, N., Rao, P.V.L., Parida, M.M., and Reiter, P. (2014). Evidence of Experimental Vertical Transmission of Emerging Novel ECSA Genotype of Chikungunya Virus in Aedes aegypti. PLoS Neglected Tropical Diseases *8*, e2990.

Agrotis, A., and Ketteler, R. (2015). A new age in functional genomics using CRISPR/Cas9 in arrayed library screening. Frontiers in Genetics *6*.

Aird, E.J., Lovendahl, K.N., St. Martin, A., Harris, R.S., and Gordon, W.R. (2018). Increasing Cas9-mediated homology-directed repair efficiency through covalent tethering of DNA repair template. Communications Biology *1*.

Anderson, G.J., and Vulpe, C.D. (2009). Mammalian iron transport. Cellular and Molecular Life Sciences *66*, 3241–3261.

Andrews, N.C. (2000). Iron homeostasis: insights from genetics and animal models. Nature Reviews Genetics *1*, 208–217.

Bacsa, S., Karasneh, G., Dosa, S., Liu, J., Valyi-Nagy, T., and Shukla, D. (2011). Syndecan-1 and syndecan-2 play key roles in herpes simplex virus type-1 infection. Journal of General Virology *92*, 733–743.

Bae, S., Park, J., and Kim, J.-S. (2014a). Cas-OFFinder: a fast and versatile algorithm that searches for potential off-target sites of Cas9 RNA-guided endonucleases. Bioinformatics *30*, 1473–1475.

Bae, S., Kweon, J., Kim, H.S., and Kim, J.-S. (2014b). Microhomology-based choice of Cas9 nuclease target sites. Nature Methods *11*, 705–706.

Barrangou, R., Fremaux, C., Deveau, H., Richards, M., Boyaval, P., Moineau, S., Romero, D.A., and Horvath, P. (2007). CRISPR Provides Acquired Resistance Against Viruses in Prokaryotes. Science *315*, 1709–1712.

Beard, P.M., Griffiths, S.J., Gonzalez, O., Haga, I.R., Pechenick Jowers, T., Reynolds, D.K., Wildenhain, J., Tekotte, H., Auer, M., Tyers, M., et al. (2014). A Loss of Function Analysis of Host Factors Influencing Vaccinia virus Replication by RNA Interference. PLoS ONE *9*, e98431.

Bearer, E., and Satpute-Krishnan, P. (2002). The Role of the Cytoskeleton in the Life Cycle of Viruses and Intracellular Bacteria: Tracks, Motors, and Polymerization Machines. Current Drug Target - Infectious Disorders *2*, 247–264.

Bernard, E., Solignat, M., Gay, B., Chazal, N., Higgs, S., Devaux, C., and Briant, L. (2010). Endocytosis of Chikungunya Virus into Mammalian Cells: Role of Clathrin and Early Endosomal Compartments. PLoS ONE *5*, e11479.

Bernard, K.A., Klimstra, W.B., and Johnston, R.E. (2000). Mutations in the E2 Glycoprotein of Venezuelan Equine Encephalitis Virus Confer Heparan Sulfate Interaction, Low Morbidity, and Rapid Clearance from Blood of Mice. Virology *276*, 93–103.

Bhella, D. (2014). The role of cellular adhesion molecules in virus attachment and entry. Philosophical Transactions of the Royal Society B: Biological Sciences *370*, 20140035–20140035.

Bibikova, M. (2003). Enhancing Gene Targeting with Designed Zinc Finger Nucleases. Science *300*,

764–764.
Bibikova, M., Golic, M., Golic, K.G., and Carroll, D. Targeted Chromosomal Cleavage and Mutagenesis in Drosophila Using Zinc-Finger Nucleases. 7.

Blanco, S., Klimcakova, L., Vega, F.M., and Lazo, P.A. (2006). The subcellular localization of vaccinia-related kinase-2 (VRK2) isoforms determines their different effect on p53 stability in tumour cell lines: Differential stabilization of p53 by VRK2 isoforms. FEBS Journal *273*, 2487–2504.

Blomen, V.A., Majek, P., Jae, L.T., Bigenzahn, J.W., Nieuwenhuis, J., Staring, J., Sacco, R., van Diemen, F.R., Olk, N., Stukalov, A., et al. (2015). Gene essentiality and synthetic lethality in haploid human cells. Science *350*, 1092–1096.

Boch, J., Scholze, H., Schornack, S., Landgraf, A., Hahn, S., Kay, S., Lahaye, T., Nickstadt, A., and Bonas, U. (2009). Breaking the Code of DNA Binding Specificity of TAL-Type III Effectors. Science *326*, 1509–1512.

Borsotti, C., Borroni, E., and Follenzi, A. (2016). Lentiviral vector interactions with the host cell. Current Opinion in Virology *21*, 102–108.

Brault, J.-B., Kudelko, M., Vidalain, P.-O., Tangy, F., Desprès, P., and Pardigon, N. (2011). The interaction of flavivirus M protein with light chain Tctex-1 of human dynein plays a role in late stages of virus replication. Virology *417*, 369–378.

Bremner, K.H., Scherer, J., Yi, J., Vershinin, M., Gross, S.P., and Vallee, R.B. (2009). Adenovirus Transport via Direct Interaction of Cytoplasmic Dynein with the Viral Capsid Hexon Subunit. Cell Host & Microbe *6*, 523–535.

Brinton, M. (2013). Replication Cycle and Molecular Biology of the West Nile Virus. Viruses *6*, 13–53.

Brouns, S.J.J., Jore, M.M., Lundgren, M., Westra, E.R., Slijkhuis, R.J.H., Snijders, A.P.L., Dickman, M.J., Makarova, K.S., Koonin, E.V., and van der Oost, J. (2008). Small CRISPR RNAs Guide Antiviral Defense in Prokaryotes. Science *321*, 960–964.

Caly, L., Kassouf, V.T., Moseley, G.W., Diefenbach, R.J., Cunningham, A.L., and Jans, D.A. (2016). Fast track, dynein-dependent nuclear targeting of human immunodeficiency virus Vpr protein; impaired trafficking in a clinical isolate. Biochemical and Biophysical Research Communications *470*, 735–740.

Carroll, D. (2013). Staying on target with CRISPR-Cas. Nature Biotechnology *31*, 807–809.

Carter, A.P., Cho, C., Jin, L., and Vale, R.D. (2011). Crystal Structure of the Dynein Motor Domain. Science *331*, 1159–1165.

Cattaneo, R. (2004). Four Viruses, Two Bacteria, and One Receptor: Membrane Cofactor Protein (CD46) as Pathogens' Magnet. Journal of Virology *78*, 4385–4388.

César-Razquin, A., Snijder, B., Frappier-Brinton, T., Isserlin, R., Gyimesi, G., Bai, X., Reithmeier, R.A., Hepworth, D., Hediger, M.A., Edwards, A.M., et al. (2015). A Call for Systematic Research on Solute Carriers. Cell *162*, 478–487.

Chang, L.-J., Dowd, K.A., Mendoza, F.H., Saunders, J.G., Sitar, S., Plummer, S.H., Yamshchikov, G., Sarwar, U.N., Hu, Z., Enama, M.E., et al. (2014). Safety and tolerability of chikungunya virus-like particle vaccine in healthy adults: a phase 1 dose-escalation trial. The Lancet *384*, 2046–2052.

Charlier, C., Beaudoin, M.-C., Couderc, T., Lortholary, O., and Lecuit, M. (2017). Arboviruses and pregnancy: maternal, fetal, and neonatal effects. The Lancet Child & Adolescent Health *1*, 134–146.

Chen, B., Gilbert, L.A., Cimini, B.A., Schnitzbauer, J., Zhang, W., Li, G.-W., Park, J., Blackburn, E.H., Weissman, J.S., Qi, L.S., et al. (2013a). Dynamic Imaging of Genomic Loci in Living Human Cells by an

Optimized CRISPR/Cas System. Cell *155*, 1479–1491.

Chen, R., Wang, E., Tsetsarkin, K.A., and Weaver, S.C. (2013b). Chikungunya Virus 3′ Untranslated Region: Adaptation to Mosquitoes and a Population Bottleneck as Major Evolutionary Forces. PLoS Pathogens *9*, e1003591.

Chen, X., Liu, J., Janssen, J.M., and Gonçalves, M.A.F.V. (2017). The Chromatin Structure Differentially Impacts High-Specificity CRISPR-Cas9 Nuclease Strategies. Molecular Therapy - Nucleic Acids *8*, 558–563.

Cheng, A.W., Wang, H., Yang, H., Shi, L., Katz, Y., Theunissen, T.W., Rangarajan, S., Shivalila, C.S., Dadon, D.B., and Jaenisch, R. (2013). Multiplexed activation of endogenous genes by CRISPR-on, an RNA-guided transcriptional activator system. Cell Research *23*, 1163–1171.

Chu, V.T., Weber, T., Wefers, B., Wurst, W., Sander, S., Rajewsky, K., and Kühn, R. (2015). Increasing the efficiency of homology-directed repair for CRISPR-Cas9-induced precise gene editing in mammalian cells. Nature Biotechnology *33*, 543–548.

Chylinski, K., Le Rhun, A., and Charpentier, E. (2013). The tracrRNA and Cas9 families of type II CRISPR-Cas immunity systems. RNA Biology *10*, 726–737.

Coffey, L., Failloux, A.-B., and Weaver, S. (2014). Chikungunya Virus–Vector Interactions. Viruses *6*, 4628–4663.

Cong, L., Ran, F.A., Cox, D., Lin, S., Barretto, R., Habib, N., Hsu, P.D., Wu, X., Jiang, W., Marraffini, L.A., et al. (2013). Multiplex Genome Engineering Using CRISPR/Cas Systems. Science *339*, 819–823.

Cui, Y., Xu, J., Cheng, M., Liao, X., and Peng, S. (2018). Review of CRISPR/Cas9 sgRNA Design Tools. Interdisciplinary Sciences: Computational Life Sciences *10*, 455–465.

Di Bartolomeo, S., Corazzari, M., Nazio, F., Oliverio, S., Lisi, G., Antonioli, M., Pagliarini, V., Matteoni, S., Fuoco, C., Giunta, L., et al. (2010). The dynamic interaction of AMBRA1 with the dynein motor complex regulates mammalian autophagy. The Journal of Cell Biology *191*, 155–168.

Dodding, M.P., and Way, M. (2011). Coupling viruses to dynein and kinesin-1: Coupling viruses to dynein and kinesin-1. The EMBO Journal *30*, 3527–3539.

Doench, J.G., Fusi, N., Sullender, M., Hegde, M., Vaimberg, E.W., Donovan, K.F., Smith, I., Tothova, Z., Wilen, C., Orchard, R., et al. (2016). Optimized sgRNA design to maximize activity and minimize off-target effects of CRISPR-Cas9. Nature Biotechnology *34*, 184–191.

Döhner, K., Wolfstein, A., Prank, U., Echeverri, C., Dujardin, D., Vallee, R., and Sodeik, B. (2002). Function of Dynein and Dynactin in Herpes Simplex Virus Capsid Transport. Molecular Biology of the Cell *13*, 2795–2809.

Dominguez, A.A., Lim, W.A., and Qi, L.S. (2016). Beyond editing: repurposing CRISPR–Cas9 for precision genome regulation and interrogation. Nature Reviews Molecular Cell Biology *17*, 5–15.

Dörig, R.E., Marcil, A., Chopra, A., and Richardson, C.D. (1993). The human CD46 molecule is a receptor for measles virus (Edmonston strain). Cell *75*, 295–305.

Doudna, J.A., and Charpentier, E. (2014). The new frontier of genome engineering with CRISPR-Cas9. Science *346*, 1258096–1258096.

Douglas, M.W., Diefenbach, R.J., Homa, F.L., Miranda-Saksena, M., Rixon, F.J., Vittone, V., Byth, K., and Cunningham, A.L. (2004). Herpes Simplex Virus Type 1 Capsid Protein VP26 Interacts with Dynein Light Chains RP3 and Tctex1 and Plays a Role in Retrograde Cellular Transport. Journal of Biological Chemistry *279*, 28522–28530.

Drakesmith, H., and Prentice, A. (2008). Viral infection and iron metabolism. Nature Reviews Microbiology *6*, 541–552.

Driessens, M.H.E., Hu, H., Nobes, C.D., Self, A., Jordens, I., Goodman, C.S., and Hall, A. (2001). Plexin-B semaphorin receptors interact directly with active Rac and regulate the actin cytoskeleton by activating Rho. Current Biology *11*, 339–344.

Duchemin, J.-B., and Paradkar, P.N. (2017). Iron availability affects West Nile virus infection in its mosquito vector. Virology Journal *14*.

van Duijl-Richter, M., Hoornweg, T., Rodenhuis-Zybert, I., and Smit, J. (2015). Early Events in Chikungunya Virus Infection—From Virus CellBinding to Membrane Fusion. Viruses *7*, 3647–3674.

Echeverri, C.J. (1996). Molecular characterization of the 50-kD subunit of dynactin reveals function for the complex in chromosome alignment and spindle organization during mitosis. The Journal of Cell Biology *132*, 617–633.

El Maadidi, S., Faletti, L., Berg, B., Wenzl, C., Wieland, K., Chen, Z.J., Maurer, U., and Borner, C. (2014). A Novel Mitochondrial MAVS/Caspase-8 Platform Links RNA Virus-Induced Innate Antiviral Signaling to Bax/Bak-Independent Apoptosis. The Journal of Immunology *192*, 1171–1183.

Elbashir, S.M., Harborth, J., Lendeckel, W., Yalcin, A., Weber, K., and Tuschl, T. (2001). Duplexes of 21-nucleotide RNAs mediate RNA interference in cultured mammalian cells. Nature *411*, 494–498.

Findlay, S.D., Vincent, K.M., Berman, J.R., and Postovit, L.-M. (2016). A Digital PCR-Based Method for Efficient and Highly Specific Screening of Genome Edited Cells. PLOS ONE *11*, e0153901.

Fire, A., Xu, S., Montgomery, M.K., Kostas, S.A., Driver, S.E., and Mello, C.C. (1998). Potent and specific genetic interference by double-stranded RNA in. *391*, 6.

Follenzi, A., Santambrogio, L., and Annoni, A. (2007). Immune Responses to Lentiviral Vectors. Current Gene Therapy *7*, 306–315.

Foo, K.Y., and Chee, H.-Y. (2015). Interaction between *Flavivirus* and Cytoskeleton during Virus Replication. BioMed Research International *2015*, 1–6.

Foot, N.J., Dalton, H.E., Shearwin-Whyatt, L.M., Dorstyn, L., Tan, S.-S., Yang, B., and Kumar, S. (2008). Regulation of the divalent metal ion transporter DMT1 and iron homeostasis by a ubiquitin-dependent mechanism involving Ndfips and WWP2. Blood *112*, 4268–4275.

Franchini, M., Targher, G., Capra, F., Montagnana, M., and Lippi, G. (2008). The effect of iron depletion on chronic hepatitis C virus infection. Hepatology International *2*, 335–340.

Frock, R.L., Hu, J., Meyers, R.M., Ho, Y.-J., Kii, E., and Alt, F.W. (2015). Genome-wide detection of DNA double-stranded breaks induced by engineered nucleases. Nature Biotechnology *33*, 179–186.

Fu, Y., Foden, J.A., Khayter, C., Maeder, M.L., Reyon, D., Joung, J.K., and Sander, J.D. (2013). High-frequency off-target mutagenesis induced by CRISPR-Cas nucleases in human cells. Nature Biotechnology *31*, 822–826.

Fu, Y., Sander, J.D., Reyon, D., Cascio, V.M., and Joung, J.K. (2014). Improving CRISPR-Cas nuclease specificity using truncated guide RNAs. Nature Biotechnology *32*, 279–284.

Gao, Q.Q., and McNally, E.M. (2015). The Dystrophin Complex: Structure, Function, and Implications for Therapy. In Comprehensive Physiology, R. Terjung, ed. (Hoboken, NJ, USA: John Wiley & Sons, Inc.), pp. 1223–1239.

Gao, L., Cox, D.B.T., Yan, W.X., Manteiga, J.C., Schneider, M.W., Yamano, T., Nishimasu, H., Nureki,

O., Crosetto, N., and Zhang, F. (2017). Engineered Cpf1 variants with altered PAM specificities. Nature Biotechnology *35*, 789–792.

Gardner, C.L., Choi-Nurvitadhi, J., Sun, C., Bayer, A., Hritz, J., Ryman, K.D., and Klimstra, W.B. (2013). Natural Variation in the Heparan Sulfate Binding Domain of the Eastern Equine Encephalitis Virus E2 Glycoprotein Alters Interactions with Cell Surfaces and Virulence in Mice. Journal of Virology *87*, 8582–8590.

Garmashova, N., Atasheva, S., Kang, W., Weaver, S.C., Frolova, E., and Frolov, I. (2007a). Analysis of Venezuelan Equine Encephalitis Virus Capsid Protein Function in the Inhibition of Cellular Transcription. Journal of Virology *81*, 13552–13565.

Garmashova, N., Gorchakov, R., Volkova, E., Paessler, S., Frolova, E., and Frolov, I. (2007b). The Old World and New World Alphaviruses Use Different Virus-Specific Proteins for Induction of Transcriptional Shutoff. Journal of Virology *81*, 2472–2484.

Gerke, C., Frantz, P.N., Ramsauer, K., and Tangy, F. (2019). Measles-vectored vaccine approaches against viral infections: a focus on chikungunya. Expert Review of Vaccines.

Gilbert, L.A., Larson, M.H., Morsut, L., Liu, Z., Brar, G.A., Torres, S.E., Stern-Ginossar, N., Brandman, O., Whitehead, E.H., Doudna, J.A., et al. (2013). CRISPR-Mediated Modular RNA-Guided Regulation of Transcription in Eukaryotes. Cell *154*, 442–451.

Gilbert, L.A., Horlbeck, M.A., Adamson, B., Villalta, J.E., Chen, Y., Whitehead, E.H., Guimaraes, C., Panning, B., Ploegh, H.L., Bassik, M.C., et al. (2014). Genome-Scale CRISPR-Mediated Control of Gene Repression and Activation. Cell *159*, 647–661.

Glahder, J.A., Kristiansen, K., Durand, M., Vinther, J., and Norrild, B. (2010). The early noncoding region of human papillomavirus type 16 is regulated by cytoplasmic polyadenylation factors. Virus Research *149*, 217–223.

Gomez de Cedrón, M., Ehsani, N., Mikkola, M.L., García, J.A., and Kääriäinen, L. (1999). RNA helicase activity of Semliki Forest virus replicase protein NSP2. FEBS Letters *448*, 19–22.

Gootenberg, J.S., Abudayyeh, O.O., Lee, J.W., Essletzbichler, P., Dy, A.J., Joung, J., Verdine, V., Donghia, N., Daringer, N.M., Freije, C.A., et al. (2017). Nucleic acid detection with CRISPR-Cas13a/C2c2. Science *356*, 438–442.

Gruenheid, S., Canonne-Hergaux, F., Gauthier, S., Hackam, D.J., Grinstein, S., and Gros, P. (1999). The Iron Transport Protein NRAMP2 Is an Integral Membrane Glycoprotein That Colocalizes with Transferrin in Recycling Endosomes. The Journal of Experimental Medicine *189*, 831–841.

Gu, Z., Flemington, C., Chittenden, T., and Zambetti, G.P. (2000). ei24, a p53 Response Gene Involved in Growth Suppression and Apoptosis. Molecular and Cellular Biology *20*, 233–241.

Gunshin, H., Mackenzie, B., Berger, U.V., Gunshin, Y., Romero, M.F., Boron, W.F., Nussberger, S., Gollan, J.L., and Hediger, M.A. (1997). Cloning and characterization of a mammalian proton-coupled metal-ion transporter. Nature *388*, 482–488.

Gunshin, H., Allerson, C.R., Polycarpou-Schwarz, M., Rofts, A., Rogers, J.T., Kishi, F., Hentze, M.W., Rouault, T.A., Andrews, N.C., and Hediger, M.A. (2001). Iron-dependent regulation of the divalent metal ion transporter. FEBS Letters *509*, 309–316.

Gupta, R.M., and Musunuru, K. (2014). Expanding the genetic editing tool kit: ZFNs, TALENs, and CRISPR-Cas9. Journal of Clinical Investigation *124*, 4154–4161.

Gutschner, T., Haemmerle, M., Genovese, G., Draetta, G.F., and Chin, L. (2016). Post-translational Regulation of Cas9 during G1 Enhances Homology-Directed Repair. Cell Reports *14*, 1555–1566.

Haapaniemi, E., Botla, S., Persson, J., Schmierer, B., and Taipale, J. (2018). CRISPR–Cas9 genome editing induces a p53-mediated DNA damage response. Nature Medicine *24*, 927–930.

Han, J., Perez, J.T., Chen, C., Li, Y., Benitez, A., Kandasamy, M., Lee, Y., Andrade, J., tenOever, B., and Manicassamy, B. (2018). Genome-wide CRISPR/Cas9 Screen Identifies Host Factors Essential for Influenza Virus Replication. Cell Reports *23*, 596–607.

Hardy.W Strauss J. (1989) Processing the nonstructural polyproteins of sindbis virus:nonstructural proteinase is in the C-terminal half of nsp2 and functions both in cis and trans. Journal of virology

Heaton, B.E., Kennedy, E.M., Dumm, R.E., Harding, A.T., Sacco, M.T., Sachs, D., and Heaton, N.S. (2017). A CRISPR Activation Screen Identifies a Pan-avian Influenza Virus Inhibitory Host Factor. Cell Reports *20*, 1503–1512.

Heler, R., Samai, P., Modell, J.W., Weiner, C., Goldberg, G.W., Bikard, D., and Marraffini, L.A. (2015). Cas9 specifies functional viral targets during CRISPR–Cas adaptation. Nature *519*, 199–202.

Hentze, M.W., Muckenthaler, M.U., Galy, B., and Camaschella, C. (2010). Two to tango: regulation of Mammalian iron metabolism. Cell *142*, 24–38.

Her, Z., Teng, T.-S., Tan, J.J., Teo, T.-H., Kam, Y.-W., Lum, F.-M., Lee, W.W., Gabriel, C., Melchiotti, R., Andiappan, A.K., et al. (2015). Loss of TLR3 aggravates CHIKV replication and pathology due to an altered virus-specific neutralizing antibody response. EMBO Molecular Medicine *7*, 24–41.

Higgs, S., and Vanlandingham, D. (2015). Chikungunya Virus and Its Mosquito Vectors. Vector-Borne and Zoonotic Diseases *15*, 231–240.

Hilton, I.B., D'Ippolito, A.M., Vockley, C.M., Thakore, P.I., Crawford, G.E., Reddy, T.E., and Gersbach, C.A. (2015). Epigenome editing by a CRISPR-Cas9-based acetyltransferase activates genes from promoters and enhancers. Nature Biotechnology *33*, 510–517.

Hsu, P.D., Scott, D.A., Weinstein, J.A., Ran, F.A., Konermann, S., Agarwala, V., Li, Y., Fine, E.J., Wu, X., Shalem, O., et al. (2013). DNA targeting specificity of RNA-guided Cas9 nucleases. Nature Biotechnology *31*, 827–832.

Hubert, N., and Hentze, M.W. (2002). Previously uncharacterized isoforms of divalent metal transporter (DMT)-1: Implications for regulation and cellular function. Proceedings of the National Academy of Sciences *99*, 12345–12350.

Hyde, J.L., Chen, R., Trobaugh, D.W., Diamond, M.S., Weaver, S.C., Klimstra, W.B., and Wilusz, J. (2015). The 5′ and 3′ ends of alphavirus RNAs – Non-coding is not non-functional. Virus Research *206*, 99–107.

Ishino, Y., Shinagawa, H., Makino, K., Amemura, M., and Nakata, A. (1987). Nucleotide sequence of the iap gene, responsible for alkaline phosphatase isozyme conversion in Escherichia coli, and identification of the gene product. Journal of Bacteriology *169*, 5429–5433.

Issac, T.H.K., Tan, E.L., and Chu, J.J.H. (2014). Proteomic profiling of chikungunya virus-infected human muscle cells: Reveal the role of cytoskeleton network in CHIKV replication. Journal of Proteomics *108*, 445–464.

Jacobs, S., Taylor, A., Herrero, L., Mahalingam, S., and Fazakerley, J. (2017). Mutation of a Conserved Nuclear Export Sequence in Chikungunya Virus Capsid Protein Disrupts Host Cell Nuclear Import. Viruses *9*, 306.

Jahreiss, L., Menzies, F.M., and Rubinsztein, D.C. (2008). The Itinerary of Autophagosomes: From Peripheral Formation to Kiss-and-Run Fusion with Lysosomes. Traffic *9*, 574–587.
Jakob, R. (1993). Nucleolar accumulation of core protein in cells naturally infected with Semliki Forest

virus. Virus Research *30*, 145–160.

Jansen, R., Embden, J.D.A. van, Gaastra, W., and Schouls, L.M. (2002). Identification of genes that are associated with DNA repeats in prokaryotes. Molecular Microbiology *43*, 1565–1575.

Jemielity, S., Wang, J.J., Chan, Y.K., Ahmed, A.A., Li, W., Monahan, S., Bu, X., Farzan, M., Freeman, G.J., Umetsu, D.T., et al. (2013). TIM-family Proteins Promote Infection of Multiple Enveloped Viruses through Virion-associated Phosphatidylserine. PLoS Pathogens *9*, e1003232.

Jinek, M., Chylinski, K., Fonfara, I., Hauer, M., Doudna, J.A., and Charpentier, E. (2012). A Programmable Dual-RNA-Guided DNA Endonuclease in Adaptive Bacterial Immunity. Science *337*, 816–821.

Jinek, M., East, A., Cheng, A., Lin, S., Ma, E., and Doudna, J. (2013). RNA-programmed genome editing in human cells. ELife *2*.

Jose, J., Snyder, J.E., and Kuhn, R.J. (2009). A structural and functional perspective of alphavirus replication and assembly. Future Microbiology *4*, 837–856.

Jose, J., Taylor, A.B., and Kuhn, R.J. (2017). Spatial and Temporal Analysis of Alphavirus Replication and Assembly in Mammalian and Mosquito Cells. MBio *8*, e02294-16.

Judith, D., Mostowy, S., Bourai, M., Gangneux, N., Lelek, M., Lucas-Hourani, M., Cayet, N., Jacob, Y., Prévost, M.-C., Pierre, P., et al. (2013). Species-specific impact of the autophagy machinery on Chikungunya virus infection. EMBO Reports *14*, 534–544.

Kardon, J.R., and Vale, R.D. (2009). Regulators of the cytoplasmic dynein motor. Nature Reviews Molecular Cell Biology *10*, 854–865.

Karlas, A., Berre, S., Couderc, T., Varjak, M., Braun, P., Meyer, M., Gangneux, N., Karo-Astover, L., Weege, F., Raftery, M., et al. (2016). A human genome-wide loss-of-function screen identifies effective chikungunya antiviral drugs. Nat Commun *7*, 11320.

Kaur, R., Kaur, G., Gill, R.K., Soni, R., and Bariwal, J. (2014). Recent developments in tubulin polymerization inhibitors: An overview. European Journal of Medicinal Chemistry *87*, 89–124.

Kelkar, S.A., Pfister, K.K., Crystal, R.G., and Leopold, P.L. (2004). Cytoplasmic Dynein Mediates Adenovirus Binding to Microtubules. Journal of Virology *78*, 10122–10132.

Kielian, M.C., and Helenius, A. Role of Cholesterol in Fusion of Semliki Forest Virus with Membranes. 3.

Kielian, M., Chanel-Vos, C., and Liao, M. (2010). Alphavirus Entry and Membrane Fusion. Viruses *2*, 796–825.

Kim, H.S., Lee, K., Bae, S., Park, J., Lee, C.-K., Kim, M., Kim, E., Kim, M., Kim, S., Kim, C., et al. (2017). CRISPR/Cas9-mediated gene knockout screens and target identification via whole-genome sequencing uncover host genes required for picornavirus infection. Journal of Biological Chemistry *292*, 10664–10671.

Kim, K.M., Cho, H., Choi, K., Kim, J., Kim, B.-W., Ko, Y.-G., Jang, S.K., and Kim, Y.K. (2009). A new MIF4G domain-containing protein, CTIF, directs nuclear cap-binding protein CBP80/20-dependent translation. Genes & Development *23*, 2033–2045.

Kleinstiver, B.P., Prew, M.S., Tsai, S.Q., Topkar, V.V., Nguyen, N.T., Zheng, Z., Gonzales, A.P.W., Li, Z., Peterson, R.T., Yeh, J.-R.J., et al. (2015). Engineered CRISPR-Cas9 nucleases with altered PAM specificities. Nature *523*, 481–485.

Kleinstiver, B.P., Pattanayak, V., Prew, M.S., Tsai, S.Q., Nguyen, N.T., Zheng, Z., and Joung, J.K. (2016). High-fidelity CRISPR–Cas9 nucleases with no detectable genome-wide off-target effects. Nature *529*, 490–495.
Klimstra, W.B., Ryman, K.D., and Johnston, R.E. (1998). Adaptation of Sindbis Virus to BHK Cells Selects for Use of Heparan Sulfate as an Attachment Receptor. J. VIROL. *72*, 10.

Klimstra, W.B., Nangle, E.M., Smith, M.S., Yurochko, A.D., and Ryman, K.D. (2003). DC-SIGN and L-SIGN can act as attachment receptors for alphaviruses and distinguish between mosquito cell- and mammalian cell-derived viruses. J. Virol. *77*, 12022–12032.

Kolokoltsov, A.A., Fleming, E.H., and Davey, R.A. (2006). Venezuelan equine encephalitis virus entry mechanism requires late endosome formation and resists cell membrane cholesterol depletion. Virology *347*, 333–342.

Komor, A.C., Kim, Y.B., Packer, M.S., Zuris, J.A., and Liu, D.R. (2016). Programmable editing of a target base in genomic DNA without double-stranded DNA cleavage. Nature *533*, 420–424.

Kon, T., Sutoh, K., and Kurisu, G. (2011). X-ray structure of a functional full-length dynein motor domain. Nature Structural & Molecular Biology *18*, 638–642.

Koonin, E.V., Makarova, K.S., and Zhang, F. (2017). Diversity, classification and evolution of CRISPR-Cas systems. Current Opinion in Microbiology *37*, 67–78.

Kraemer, M.U., Sinka, M.E., Duda, K.A., Mylne, A.Q., Shearer, F.M., Barker, C.M., Moore, C.G., Carvalho, R.G., Coelho, G.E., Van Bortel, W., et al. (2015). The global distribution of the arbovirus vectors Aedes aegypti and Ae. albopictus. ELife *4*.

Krejbich-Trotot, P., Gay, B., Li-Pat-Yuen, G., Hoarau, J.-J., Jaffar-Bandjee, M.-C., Briant, L., Gasque, P., and Denizot, M. (2011). Chikungunya triggers an autophagic process which promotes viral replication. Virol. J. *8*, 432.

Kubota, T., Matsuoka, M., Chang, T.-H., Bray, M., Jones, S., Tashiro, M., Kato, A., and Ozato, K. (2009). Ebolavirus VP35 Interacts with the Cytoplasmic Dynein Light Chain 8. Journal of Virology *83*, 6952–6956.

Kuscu, C., Arslan, S., Singh, R., Thorpe, J., and Adli, M. (2014). Genome-wide analysis reveals characteristics of off-target sites bound by the Cas9 endonuclease. Nature Biotechnology *32*, 677–683.

Kwak, J.E., Wang, L., Ballantyne, S., Kimble, J., and Wickens, M. (2004). Mammalian GLD-2 homologs are poly(A) polymerases. Proceedings of the National Academy of Sciences *101*, 4407–4412.

La Linn, M., Gardner, J., Warrilow, D., Darnell, G.A., McMahon, C.R., Field, I., Hyatt, A.D., Slade, R.W., and Suhrbier, A. (2001). Arbovirus of Marine Mammals: a New Alphavirus Isolated from the Elephant Seal Louse, Lepidophthirus macrorhini. Journal of Virology *75*, 4103–4109.

Lam-Yuk-Tseung, S., and Gros, P. (2006). Distinct Targeting and Recycling Properties of Two Isoforms of the Iron Transporter DMT1 (NRAMP2, Slc11A2) †. Biochemistry *45*, 2294–2301.

Lawhorn, I.E.B., Ferreira, J.P., and Wang, C.L. (2014). Evaluation of sgRNA Target Sites for CRISPR-Mediated Repression of TP53. PLoS ONE *9*, e113232.

Lee, K.-W., Okot-Kotber, C., LaComb, J.F., and Bogenhagen, D.F. (2013). Mitochondrial Ribosomal RNA (rRNA) Methyltransferase Family Members Are Positioned to Modify Nascent rRNA in Foci near the Mitochondrial DNA Nucleoid. Journal of Biological Chemistry *288*, 31386–31399.

Lee, P.L., Gelbart, T., West, C., Halloran, C., and Beutler, E. (1998). The human Nramp2 gene: characterization of the gene structure, alternative splicing, promoter region and polymorphisms. Blood

Cells, Molecules, and Diseases *24*, 199–215.

Leung, J.Y.-S., Ng, M.M.-L., and Chu, J.J.H. (2011). Replication of alphaviruses: a review on the entry process of alphaviruses into cells. Adv Virol *2011*, 249640.

Li, L., Wv, L.P., and Chandrasegaran, S. (1992). Functional domains in Fok I restriction endonuclease. Proc. Natl. Acad. Sci. USA 5.

Li, L., Jose, J., Xiang, Y., Kuhn, R.J., and Rossmann, M.G. (2010). Structural changes of envelope proteins during alphavirus fusion. Nature *468*, 705–708.

Li, W., Xu, H., Xiao, T., Cong, L., Love, M.I., Zhang, F., Irizarry, R.A., Liu, J.S., Brown, M., and Liu, X.S. (2014). MAGeCK enables robust identification of essential genes from genome-scale CRISPR/Cas9 knockout screens. 12.

Liang, X., Potter, J., Kumar, S., Ravinder, N., and Chesnut, J.D. (2017). Enhanced CRISPR/Cas9-mediated precise genome editing by improved design and delivery of gRNA, Cas9 nuclease, and donor DNA. Journal of Biotechnology *241*, 136–146.

Lim, E., Lee, W., Madzokere, E., and Herrero, L. (2018). Mosquitoes as Suitable Vectors for Alphaviruses. Viruses *10*, 84.

Lin, D.L., Cherepanova, N.A., Bozzacco, L., MacDonald, M.R., Gilmore, R., and Tai, A.W. (2017). Dengue Virus Hijacks a Noncanonical Oxidoreductase Function of a Cellular Oligosaccharyltransferase Complex. *8*, 16.

Lin, S., Staahl, B.T., Alla, R.K., and Doudna, J.A. (2014a). Enhanced homology-directed human genome engineering by controlled timing of CRISPR/Cas9 delivery. ELife *3*.

Lin, Y., Cradick, T.J., Brown, M.T., Deshmukh, H., Ranjan, P., Sarode, N., Wile, B.M., Vertino, P.M., Stewart, F.J., and Bao, G. (2014b). CRISPR/Cas9 systems have off-target activity with insertions or deletions between target DNA and guide RNA sequences. Nucleic Acids Research *42*, 7473–7485.

Love, M.I., Huber, W., and Anders, S. (2014). Moderated estimation of fold change and dispersion for RNA-seq data with DESeq2. Genome Biology *15*.

Lozach, P.-Y., Kühbacher, A., Meier, R., Mancini, R., Bitto, D., Bouloy, M., and Helenius, A. (2011). DC-SIGN as a Receptor for Phleboviruses. Cell Host & Microbe *10*, 75–88.

Lozach, P.-Y., Burleigh, L., Staropoli, I., and Amara, A. The C Type Lectins DC-SIGN and L-SIGN. 18.

Ma, H., Dang, Y., Wu, Y., Jia, G., Anaya, E., Zhang, J., Abraham, S., Choi, J.-G., Shi, G., Qi, L., et al. (2015). A CRISPR-Based Screen Identifies Genes Essential for West-Nile-Virus-Induced Cell Death. Cell Reports *12*, 673–683.

Ma, Y., Walsh, M.J., Bernhardt, K., Ashbaugh, C.W., Trudeau, S.J., Ashbaugh, I.Y., Jiang, S., Jiang, C., Zhao, B., Root, D.E., et al. (2017). CRISPR/Cas9 Screens Reveal Epstein-Barr Virus-Transformed B Cell Host Dependency Factors. Cell Host & Microbe *21*, 580-591.e7.

Mackenzie, K., Foot, N.J., Anand, S., Dalton, H.E., Chaudhary, N., Collins, B.M., Mathivanan, S., and Kumar, S. (2016). Regulation of the divalent metal ion transporter via membrane budding. Cell Discovery *2*.

Maeder, M.L., Linder, S.J., Cascio, V.M., Fu, Y., Ho, Q.H., and Joung, J.K. (2013). CRISPR RNA–guided activation of endogenous human genes. Nature Methods *10*, 977–979.

Makarova, K.S., Haft, D.H., Barrangou, R., Brouns, S.J.J., Charpentier, E., Horvath, P., Moineau, S., Mojica, F.J.M., Wolf, Y.I., Yakunin, A.F., et al. (2011). Evolution and classification of the CRISPR–Cas

systems. Nature Reviews Microbiology *9*, 467–477.

Makarova, K.S., Wolf, Y.I., Alkhnbashi, O.S., Costa, F., Shah, S.A., Saunders, S.J., Barrangou, R., Brouns, S.J.J., Charpentier, E., Haft, D.H., et al. (2015). An updated evolutionary classification of CRISPR–Cas systems. Nature Reviews Microbiology *13*, 722–736.

Mali, P., Yang, L., Esvelt, K.M., Aach, J., Guell, M., DiCarlo, J.E., Norville, J.E., and Church, G.M. (2013). RNA-Guided Human Genome Engineering via Cas9. Science *339*, 823–826.

Manring, H.R., Carter, O.A., and Ackermann, M.A. (2017). Obscure functions: the location–function relationship of obscurins. Biophysical Reviews *9*, 245–258.

Marceau, C.D., Puschnik, A.S., Majzoub, K., Ooi, Y.S., Brewer, S.M., Fuchs, G., Swaminathan, K., Mata, M.A., Elias, J.E., Sarnow, P., et al. (2016). Genetic dissection of Flaviviridae host factors through genome-scale CRISPR screens. Nature *535*, 159–163.

Maria Fimia, G., Stoykova, A., Romagnoli, A., Giunta, L., Di Bartolomeo, S., Nardacci, R., Corazzari, M., Fuoco, C., Ucar, A., Schwartz, P., et al. (2007). Ambra1 regulates autophagy and development of the nervous system. Nature.

Martin, D.N., and Uprichard, S.L. (2013). Identification of transferrin receptor 1 as a hepatitis C virus entry factor. Proceedings of the National Academy of Sciences *110*, 10777–10782.

Mayle, K.M., Le, A.M., and Kamei, D.T. (2012). The intracellular trafficking pathway of transferrin. Biochimica et Biophysica Acta (BBA) - General Subjects *1820*, 264–281.

Mayor, S., and Pagano, R.E. (2007). Pathways of clathrin-independent endocytosis. Nature Reviews Molecular Cell Biology *8*, 603–612.

.McDougall, W.M., Perreira, J.M., Reynolds, E.C., and Brass, A.L. (2018). CRISPR genetic screens to discover host–virus interactions. Current Opinion in Virology *29*, 87–100.

McInerney, G.M., Smit, J.M., Liljeström, P., and Wilschut, J. (2004). Semliki Forest virus produced in the absence of the 6K protein has an altered spike structure as revealed by decreased membrane fusion capacity. Virology *325*, 200–206.

McLoughlin, M.F., and Graham, D.A. (2007). Alphavirus infections in salmonids ? a review. Journal of Fish Diseases *30*, 511–531.

Medigeshi, G.R. (2011). Mosquito-borne flaviviruses: overview of viral life-cycle and host–virus interactions. Future Virology *6*, 1075–1089.

Mellman, I., Fuchs, R., and Helenius, A. Acidification of the Endocytic and Exocytic Pathways. 38.
Mendes, A., and Kuhn, R. (2018). Alphavirus Nucleocapsid Packaging and Assembly. Viruses *10*, 138.
Merino-Gracia, J., García-Mayoral, M.F., and Rodríguez-Crespo, I. (2011). The association of viral proteins with host cell dynein components during virus infection: Viral proteins and host cell dynein components. FEBS Journal *278*, 2997–3011.

Mendelsohn C., Wimmer E., Racaniello V. (1989) Cellular Receptor for poliovirus: molecular cloning, nucleotide sequence, and expression of new member of the immunoglobulin superfamily. Cell

Milev, M.P., Yao, X., Berthoux, L., and Mouland, A.J. (2018). Impacts of virus-mediated manipulation of host Dynein. In Dyneins, (Elsevier), pp. 214–233.

Miller, J.C., Tan, S., Qiao, G., Barlow, K.A., Wang, J., Xia, D.F., Meng, X., Paschon, D.E., Leung, E., Hinkley, S.J., et al. (2011). A TALE nuclease architecture for efficient genome editing. Nature Biotechnology *29*, 143–148.

Miranda-Saksena, M., Denes, C., Diefenbach, R., and Cunningham, A. (2018). Infection and Transport of Herpes Simplex Virus Type 1 in Neurons: Role of the Cytoskeleton. Viruses *10*, 92.

Misumi, Y., Sohda, M., Yano, A., Fujiwara, T., and Ikehara, Y. (1997). Molecular Characterization of GCP170, a 170-kDa Protein Associated with the Cytoplasmic Face of the Golgi Membrane. Journal of Biological Chemistry *272*, 23851–23858.
Mojica, F.J.M., Juez, G., and Rodriguez-Valera, F. (1993). Transcription at different salinities of Haloferax mediterranei sequences adjacent to partially modified PstI sites. Molecular Microbiology *9*, 613–621.

Mojica, F.J.M., Diez-Villasenor, C., Soria, E., and Juez, G. (2000). Biological significance of a family of regularly spaced repeats in the genomes of Archaea, Bacteria and mitochondria. Molecular Microbiology *36*, 244–246.

Mojica, F.J.M., D□ez-Villase□or, C., Garc□a-Mart□nez, J., and Soria, E. (2005). Intervening Sequences of Regularly Spaced Prokaryotic Repeats Derive from Foreign Genetic Elements. Journal of Molecular Evolution *60*, 174–182.

Moller-Tank, S., Kondratowicz, A.S., Davey, R.A., Rennert, P.D., and Maury, W. (2013). Role of the Phosphatidylserine Receptor TIM-1 in Enveloped-Virus Entry. Journal of Virology *87*, 8327–8341.
Monsalve, D.M., Merced, T., Fernández, I.F., Blanco, S., Vázquez-Cedeira, M., and Lazo, P.A. (2013). Human VRK2 modulates apoptosis by interaction with Bcl-xL and regulation of BAX gene expression. Cell Death & Disease *4*, e513–e513.

Morgan, S.L., Mariano, N.C., Bermudez, A., Arruda, N.L., Wu, F., Luo, Y., Shankar, G., Jia, L., Chen, H., Hu, J.-F., et al. (2017). Manipulation of nuclear architecture through CRISPR-mediated chromosomal looping. Nature Communications *8*, 15993.

Moscou, M.J., and Bogdanove, A.J. (2009). A Simple Cipher Governs DNA Recognition by TAL Effectors. Science *326*, 1501–1501.

Mostowy, S., and Cossart, P. (2012). Septins: the fourth component of the cytoskeleton. Nature Reviews Molecular Cell Biology *13*, 183–194.

Mostowy, S., Bonazzi, M., Hamon, M.A., Tham, T.N., Mallet, A., Lelek, M., Gouin, E., Demangel, C., Brosch, R., Zimmer, C., et al. (2010). Entrapment of Intracytosolic Bacteria by Septin Cage-like Structures. Cell Host & Microbe *8*, 433–444.

Mueller, S., Cao, X., Welker, R., and Wimmer, E. (2002). Interaction of the Poliovirus Receptor CD155 with the Dynein Light Chain Tctex-1 and Its Implication for Poliovirus Pathogenesis. Journal of Biological Chemistry *277*, 7897–7904.

Münz, C. (2013). Macroautophagy—friend or foe of viral replication? EMBO Reports *14*, 483–484.
Myhrvold, C., Freije, C.A., Gootenberg, J.S., Abudayyeh, O.O., Metsky, H.C., Durbin, A.F., Kellner, M.J., Tan, A.L., Paul, L.M., Parham, L.A., et al. (2018). Field-deployable viral diagnostics using CRISPR-Cas13. Science *360*, 444–448.

Naito, Y., Hino, K., Bono, H., and Ui-Tei, K. (2015). CRISPRdirect: software for designing CRISPR/Cas guide RNA with reduced off-target sites. Bioinformatics *31*, 1120–1123.

Nelles, D.A., Fang, M.Y., O'Connell, M.R., Xu, J.L., Markmiller, S.J., Doudna, J.A., and Yeo, G.W. (2016). Programmable RNA Tracking in Live Cells with CRISPR/Cas9. Cell *165*, 488–496.

Nevo, Y., and Nelson, N. (2006). The NRAMP family of metal-ion transporters. Biochim. Biophys. Acta *1763*, 609–620.

Nishimasu, H., and Nureki, O. (2017). Structures and mechanisms of CRISPR RNA-guided effector nucleases. Current Opinion in Structural Biology *43*, 68–78.

Nuñez, J.K., Kranzusch, P.J., Noeske, J., Wright, A.V., Davies, C.W., and Doudna, J.A. (2014). Cas1–Cas2 complex formation mediates spacer acquisition during CRISPR–Cas adaptive immunity. Nature Structural & Molecular Biology *21*, 528–534.

Okamoto, K., Kinoshita, H., Parquet, M. d. C., Raekiansyah, M., Kimura, D., Yui, K., Islam, M.A., Hasebe, F., and Morita, K. (2012). Dengue virus strain DEN2 16681 utilizes a specific glycochain of syndecan-2 proteoglycan as a receptor. Journal of General Virology *93*, 761–770.

Ooi, Y.S., Stiles, K.M., Liu, C.Y., Taylor, G.M., and Kielian, M. (2013). Genome-Wide RNAi Screen Identifies Novel Host Proteins Required for Alphavirus Entry. PLoS Pathogens *9*, e1003835.

Owen, K.E., and Kuhn, R.J. (1997). Alphavirus Budding Is Dependent on the Interaction between the Nucleocapsid and Hydrophobic Amino Acids on the Cytoplasmic Domain of the E2 Envelope Glycoprotein. Virology *230*, 187–196.

Ozden, S., Huerre, M., Riviere, J.-P., Coffey, L.L., Afonso, P.V., Mouly, V., de Monredon, J., Roger, J.-C., El Amrani, M., Yvin, J.-L., et al. (2007). Human muscle satellite cells as targets of Chikungunya virus infection. PLoS ONE *2*, e527.

Ozden, S., Lucas-Hourani, M., Ceccaldi, P.-E., Basak, A., Valentine, M., Benjannet, S., Hamelin, J., Jacob, Y., Mamchaoui, K., Mouly, V., et al. (2008). Inhibition of Chikungunya Virus Infection in Cultured Human Muscle Cells by Furin Inhibitors: IMPAIRMENT OF THE MATURATION OF THE E2 SURFACE GLYCOPROTEIN. Journal of Biological Chemistry *283*, 21899–21908.

Panda, D., Rose, P.P., Hanna, S.L., Gold, B., Hopkins, K.C., Lyde, R.B., Marks, M.S., and Cherry, S. (2013). Genome-wide RNAi Screen Identifies SEC61A and VCP as Conserved Regulators of Sindbis Virus Entry. Cell Reports *5*, 1737–1748.

Pantopoulos, K. (2004). Iron Metabolism and the IRE/IRP Regulatory System: An Update. Annals of the New York Academy of Sciences *1012*, 1–13.

Paquet, D., Kwart, D., Chen, A., Sproul, A., Jacob, S., Teo, S., Olsen, K.M., Gregg, A., Noggle, S., and Tessier-Lavigne, M. (2016). Efficient introduction of specific homozygous and heterozygous mutations using CRISPR/Cas9. Nature *533*, 125–129.

Park, R.J., Wang, T., Koundakjian, D., Hultquist, J.F., Lamothe-Molina, P., Monel, B., Schumann, K., Yu, H., Krupzcak, K.M., Garcia-Beltran, W., et al. (2017). A genome-wide CRISPR screen identifies a restricted set of HIV host dependency factors. Nature Genetics *49*, 193–203.

Parker, J.S.L., Murphy, W.J., Wang, D., O'Brien, S.J., and Parrish, C.R. (2001). Canine and Feline Parvoviruses Can Use Human or Feline Transferrin Receptors To Bind, Enter, and Infect Cells. Journal of Virology *75*, 3896–3902.

Pavletich, N., and Pabo, C. (1991). Zinc finger-DNA recognition: crystal structure of a Zif268-DNA complex at 2.1 A. Science *252*, 809–817.

Perez-Pinera, P., Kocak, D.D., Vockley, C.M., Adler, A.F., Kabadi, A.M., Polstein, L.R., Thakore, P.I., Glass, K.A., Ousterout, D.G., Leong, K.W., et al. (2013). RNA-guided gene activation by CRISPR-Cas9–based transcription factors. Nature Methods *10*, 973–976.

Perreira, J.M., Aker, A.M., Savidis, G., Chin, C.R., McDougall, W.M., Portmann, J.M., Meraner, P., Smith, M.C., Rahman, M., Baker, R.E., et al. (2015). RNASEK Is a V-ATPase-Associated Factor Required for Endocytosis and the Replication of Rhinovirus, Influenza A Virus, and Dengue Virus. Cell Reports *12*, 850–863.

Perreira, J.M., Meraner, P., and Brass, A.L. (2016). Functional Genomic Strategies for Elucidating Human–Virus Interactions. In Advances in Virus Research, (Elsevier), pp. 1–51.

Pfanzelter, J., Mostowy, S., and Way, M. (2018). Septins suppress the release of vaccinia virus from infected cells. The Journal of Cell Biology *217*, 2911–2929.

Powers, A.M., Brault, A.C., Shirako, Y., Strauss, E.G., Kang, W., Strauss, J.H., and Weaver, S.C. (2001). Evolutionary Relationships and Systematics of the Alphaviruses. Journal of Virology *75*, 10118–10131.
Puschnik, A.S., Majzoub, K., Ooi, Y.S., and Carette, J.E. (2017). A CRISPR toolbox to study virus–host interactions. Nature Reviews Microbiology *15*, 351–364.

Qi, L.S., Larson, M.H., Gilbert, L.A., Doudna, J.A., Weissman, J.S., Arkin, A.P., and Lim, W.A. (2013). Repurposing CRISPR as an RNA-Guided Platform for Sequence-Specific Control of Gene Expression. Cell *152*, 1173–1183.

Qin, Y., Liu, Q., Tian, S., Xie, W., Cui, J., and Wang, R.-F. (2016). TRIM9 short isoform preferentially promotes DNA and RNA virus-induced production of type I interferon by recruiting GSK3β to TBK1. Cell Research *26*, 613–628.

Radoshitzky, S.R., Abraham, J., Spiropoulou, C.F., Kuhn, J.H., Nguyen, D., Li, W., Nagel, J., Schmidt, P.J., Nunberg, J.H., Andrews, N.C., et al. (2007). Transferrin receptor 1 is a cellular receptor for New World haemorrhagic fever arenaviruses. Nature *446*, 92–96.

Radoshitzky, S.R., Pegoraro, G., Chī, X., Dǒng, L., Chiang, C.-Y., Jozwick, L., Clester, J.C., Cooper, C.L., Courier, D., Langan, D.P., et al. (2016). siRNA Screen Identifies Trafficking Host Factors that Modulate Alphavirus Infection. PLOS Pathogens *12*, e1005466.

Ran, F.A., Hsu, P.D., Lin, C.-Y., Gootenberg, J.S., Konermann, S., Trevino, A.E., Scott, D.A., Inoue, A., Matoba, S., Zhang, Y., et al. (2013). Double Nicking by RNA-Guided CRISPR Cas9 for Enhanced Genome Editing Specificity. Cell *154*, 1380–1389.

Ravikumar, B., Acevedo-Arozena, A., Imarisio, S., Berger, Z., Vacher, C., O'Kane, C.J., Brown, S.D.M., and Rubinsztein, D.C. (2005). Dynein mutations impair autophagic clearance of aggregate-prone proteins. Nature Genetics *37*, 771–776.

Rebecca Brown, Judy Wan, and Margaret Kielian (2018). The Alphavirus Exit Pathway: What We Know and What We Wish We Knew. Viruses *10*, 89.

Richardson, R.B., Ohlson, M.B., Eitson, J.L., Kumar, A., McDougal, M.B., Boys, I.N., Mar, K.B., De La Cruz-Rivera, P.C., Douglas, C., Konopka, G., et al. (2018). A CRISPR screen identifies IFI6 as an ER-resident interferon effector that blocks flavivirus replication. Nature Microbiology *3*, 1214–1223.

Rose, P.P., Hanna, S.L., Spiridigliozzi, A., Wannissorn, N., Beiting, D.P., Ross, S.R., Hardy, R.W., Bambina, S.A., Heise, M.T., and Cherry, S. (2011). Natural Resistance-Associated Macrophage Protein Is a Cellular Receptor for Sindbis Virus in Both Insect and Mammalian Hosts. Cell Host & Microbe *10*, 97–104.

Rouet, P., Smih, F., and Jasin, M. (1994). Introduction of double-strand breaks into the genome of mouse cells by expression of a rare-cutting endonuclease. Molecular and Cellular Biology *14*, 8096–8106.

Rudin, N., and Haber, J.E. (1988). Efficient repair of HO-induced chromosomal breaks in Saccharomyces cerevisiae by recombination between flanking homologous sequences. Molecular and Cellular Biology *8*, 3918–3928.

Rutz, S., and Scheffold, A. Towards in vivo application of RNA interference – new toys, old problems. Arthritis Research *6*, 8.

Sanjana, N.E., Shalem, O., and Zhang, F. Improved vectors and genome-wide libraries for CRISPR screening. 22.

Savidis, G., McDougall, W.M., Meraner, P., Perreira, J.M., Portmann, J.M., Trincucci, G., John, S.P., Aker, A.M., Renzette, N., Robbins, D.R., et al. (2016). Identification of Zika Virus and Dengue Virus Dependency Factors using Functional Genomics. Cell Reports *16*, 232–246.

Schneider, M.A., Spoden, G.A., Florin, L., and Lambert, C. (2011). Identification of the dynein light chains required for human papillomavirus infection: Role of dynein light chains in HPV infection. Cellular Microbiology *13*, 32–46.

Schoggins, J.W., Wilson, S.J., Panis, M., Murphy, M.Y., Jones, C.T., Bieniasz, P., and Rice, C.M. (2011). A diverse range of gene products are effectors of the type I interferon antiviral response. Nature *472*, 481–485.

Schroer, T.A. (2004). DYNACTIN. Annual Review of Cell and Developmental Biology *20*, 759–779.

Schwartz, O., and Albert, M.L. (2010). Biology and pathogenesis of chikungunya virus. Nature Reviews Microbiology *8*, 491–500.

Seo, Y.A., Kumara, R., Wetli, H., and Wessling-Resnick, M. (2016). Regulation of divalent metal transporter-1 by serine phosphorylation. Biochemical Journal *473*, 4243–4254.

Shalem, O., Sanjana, N.E., Hartenian, E., Shi, X., Scott, D.A., Mikkelsen, T.S., Heckl, D., Ebert, B.L., Root, D.E., Doench, J.G., et al. (2014). Genome-Scale CRISPR-Cas9 Knockout Screening in Human Cells. Science *343*, 84–87.

Shi, Q., Jiang, J., and Luo, G. (2013). Syndecan-1 Serves as the Major Receptor for Attachment of Hepatitis C Virus to the Surfaces of Hepatocytes. Journal of Virology *87*, 6866–6875.

Shirako, Y., and Strauss, J.H. Regulation of Sindbis Virus RNA Replication: Uncleaved P123 and nsP4 Function in Minus-Strand RNA Synthesis, whereas Cleaved Products from P123 Are Required for Efficient Plus-Strand RNA Synthesis. 12.

SINGH', I., and HELENIUS, A. (1992). Role of Ribosomes in Semliki Forest Virus Nucleocapsid Uncoating. J. VIROL. *66*, 10.

Sirianni, A., Krokowski, S., Lobato-Márquez, D., Buranyi, S., Pfanzelter, J., Galea, D., Willis, A., Culley, S., Henriques, R., Larrouy-Maumus, G., et al. (2016). Mitochondria mediate septin cage assembly to promote autophagy of *Shigella*. EMBO Reports *17*, 1029–1043.

SkjÃ¸rringe, T., Burkhart, A., Johnsen, K.B., and Moos, T. (2015). Divalent metal transporter 1 (DMT1) in the brain: implications for a role in iron transport at the blood-brain barrier, and neuronal and glial pathology. Frontiers in Molecular Neuroscience *8*.

Slaymaker, I.M., Gao, L., Zetsche, B., Scott, D.A., Yan, W.X., and Zhang, F. (2016). Rationally engineered Cas9 nucleases with improved specificity. Science *351*, 84–88.

Smit, J.M., Waarts, B.-L., Kimata, K., Klimstra, W.B., Bittman, R., and Wilschut, J. (2002). Adaptation of Alphaviruses to Heparan Sulfate: Interaction of Sindbis and Semliki Forest Viruses with Liposomes Containing Lipid-Conjugated Heparin. Journal of Virology *76*, 10128–10137.

Snyder, A.J., and Mukhopadhyay, S. (2012). The Alphavirus E3 Glycoprotein Functions in a Clade-Specific Manner. Journal of Virology *86*, 13609–13620.

Song, J., Yang, D., Xu, J., Zhu, T., Chen, Y.E., and Zhang, J. (2016). RS-1 enhances CRISPR/Cas9- and TALEN-mediated knock-in efficiency. Nature Communications *7*.

Sourisseau, M., Schilte, C., Casartelli, N., Trouillet, C., Guivel-Benhassine, F., Rudnicka, D., Sol-Foulon, N., Le Roux, K., Prevost, M.-C., Fsihi, H., et al. (2007). Characterization of reemerging chikungunya

virus. PLoS Pathog *3*, e89.

Stemmer, M., Thumberger, T., del Sol Keyer, M., Wittbrodt, J., and Mateo, J.L. (2015). CCTop: An Intuitive, Flexible and Reliable CRISPR/Cas9 Target Prediction Tool. PLOS ONE *10*, e0124633.

Sternberg, S.H., Redding, S., Jinek, M., Greene, E.C., and Doudna, J.A. (2014). DNA interrogation by the CRISPR RNA-guided endonuclease Cas9. Nature *507*, 62–67.

Stiles, K.M., and Kielian, M. (2016). The Role of TSPAN9 in Alphavirus Entry and Early Endosomes. J. Virol. JVI.00018-16.

Strauss, J.H., and Strauss, E.G. (1994). The alphaviruses: gene expression, replication, and evolution. Microbiological Reviews *58*, 491–562.

Su, Y., Qiao, W., Guo, T., Tan, J., Li, Z., Chen, Y., Li, X., Li, Y., Zhou, J., and Chen, Q. (2010). Microtubule-dependent retrograde transport of bovine immunodeficiency virus: Microtubule-dependent transport of BIV. Cellular Microbiology *12*, 1098–1107.

Tanaka, A., Tumkosit, U., Nakamura, S., Motooka, D., Kishishita, N., Priengprom, T., Sa-ngasang, A., Kinoshita, T., Takeda, N., and Maeda, Y. (2017). Genome-Wide Screening Uncovers the Significance of N-Sulfation of Heparan Sulfate as a Host Cell Factor for Chikungunya Virus Infection. Journal of Virology *91*, e00432-17.

Taylor, A., Liu, X., Zaid, A., Goh, L.Y.H., Hobson-Peters, J., Hall, R.A., Merits, A., and Mahalingam, S. (2017). Mutation of the N-Terminal Region of Chikungunya Virus Capsid Protein: Implications for Vaccine Design. MBio *8*.

Teo, C.S.H., and Chu, J.J.H. (2014). Cellular Vimentin Regulates Construction of Dengue Virus Replication Complexes through Interaction with NS4A Protein. Journal of Virology *88*, 1897–1913.

Thakore, P.I., D'Ippolito, A.M., Song, L., Safi, A., Shivakumar, N.K., Kabadi, A.M., Reddy, T.E., Crawford, G.E., and Gersbach, C.A. (2015). Highly specific epigenome editing by CRISPR-Cas9 repressors for silencing of distal regulatory elements. Nature Methods *12*, 1143–1149.

Thomas, P.D. (2003). PANTHER: A Library of Protein Families and Subfamilies Indexed by Function. Genome Research *13*, 2129–2141.

Thomas, S., Rai, J., John, L., Schaefer, S., Pützer, B.M., and Herchenröder, O. (2013). Chikungunya virus capsid protein contains nuclear import and export signals. Virology Journal *10*, 269.

Thompson, J.W., and Bruick, R.K. (2012). Protein degradation and iron homeostasis. Biochimica et Biophysica Acta (BBA) - Molecular Cell Research *1823*, 1484–1490.

Torres-Flores, J., and Arias, C. (2015). Tight Junctions Go Viral! Viruses *7*, 5145–5154.

Touret, N., Furuya, W., Forbes, J., Gros, P., and Grinstein, S. (2003). Dynamic Traffic through the Recycling Compartment Couples the Metal Transporter Nramp2 (DMT1) with the Transferrin Receptor. Journal of Biological Chemistry *278*, 25548–25557.

Tsetsarkin, K.A., Vanlandingham, D.L., McGee, C.E., and Higgs, S. (2007). A Single Mutation in Chikungunya Virus Affects Vector Specificity and Epidemic Potential. PLoS Pathogens *3*, e201.

Tsetsarkin, K.A., McGee, C.E., and Higgs, S. (2011). Chikungunya virus adaptation to Aedes albopictus mosquitoes does not correlate with acquisition of cholesterol dependence or decreased pH threshold for fusion reaction. Virology Journal *8*.

Tsujimoto, H., Anderson, M.A.E., Myles, K.M., and Adelman, Z.N. (2018). Identification of Candidate Iron Transporters From the ZIP/ZnT Gene Families in the Mosquito Aedes aegypti. Frontiers in

Physiology *9*.

Vasiljeva, L., Merits, A., Auvinen, P., and Kääriäinen, L. (2000). Identification of a Novel Function of the *Alphavirus* Capping Apparatus: RNA 5′-TRIPHOSPHATASE ACTIVITY OF Nsp2. Journal of Biological Chemistry *275*, 17281–17287.

Villoing, S., Bearzotti, M., Chilmonczyk, S., Castric, J., and Bremont, M. (2000). Rainbow Trout Sleeping Disease Virus Is an Atypical Alphavirus. Journal of Virology *74*, 173–183.

Vouillot, L., Thélie, A., and Pollet, N. (2015). Comparison of T7E1 and Surveyor Mismatch Cleavage Assays to Detect Mutations Triggered by Engineered Nucleases. G3: Genes|Genomes|Genetics *5*, 407–415.

Walker, E.J., and Ghildyal, R. (2017). Editorial: Viral Interactions with the Nucleus. Frontiers in Microbiology *8*.

Wang, J., and Pantopoulos, K. (2011). Regulation of cellular iron metabolism. Biochemical Journal *434*, 365–381.

Wang, E., Brault, A.C., Powers, A.M., Kang, W., and Weaver, S.C. (2003). Glycosaminoglycan Binding Properties of Natural Venezuelan Equine Encephalitis Virus Isolates. Journal of Virology *77*, 1204–1210.

Wang, H., Li, Z., Niu, J., Xu, Y., Ma, L., Lu, A., Wang, X., Qian, Z., Huang, Z., Jin, X., et al. (2018). Antiviral effects of ferric ammonium citrate. Cell Discovery *4*.

Wang, T., Wei, J.J., Sabatini, D.M., and Lander, E.S. (2014). Genetic screens in human cells using the CRISPR-Cas9 system. Science *343*, 80–84.

Wang, T., Birsoy, K., Hughes, N.W., Krupczak, K.M., Post, Y., Wei, J.J., Lander, E.S., and Sabatini, D.M. (2015). Identification and characterization of essential genes in the human genome. Science *350*, 1096–1101.

Ward, B.M. (2011). The taking of the cytoskeleton one two three: How viruses utilize the cytoskeleton during egress. Virology *411*, 244–250.

Weaver, S.C., and Lecuit, M. (2015). Chikungunya Virus and the Global Spread of a Mosquito-Borne Disease. New England Journal of Medicine *372*, 1231–1239.

Weber, C., Berberich, E., von Rhein, C., Henß, L., Hildt, E., and Schnierle, B.S. (2017). Identification of Functional Determinants in the Chikungunya Virus E2 Protein. PLOS Neglected Tropical Diseases *11*, e0005318.

Weidman, M.K., Sharma, R., Raychaudhuri, S., Kundu, P., Tsai, W., and Dasgupta, A. (2003). The interaction of cytoplasmic RNA viruses with the nucleus. Virus Research *95*, 75–85.

Wengler, G. (2004). During entry of alphaviruses, the E1 glycoprotein molecules probably form two separate populations that generate either a fusion pore or ion-permeable pores. Journal of General Virology *85*, 1695–1701.

Wengler, G., Würkner, D., and Wengler, G. (1992). Identification of a sequence element in the alphavirus core protein which mediates interaction of cores with ribosomes and the disassembly of cores. Virology *191*, 880–888.

de Witte, L., Bobardt, M., Chatterji, U., Degeest, G., David, G., Geijtenbeek, T.B.H., and Gallay, P. (2007). Syndecan-3 is a dendritic cell-specific attachment receptor for HIV-1. Proceedings of the National Academy of Sciences *104*, 19464–19469.

Wright, A.V., Nuñez, J.K., and Doudna, J.A. (2016). Biology and Applications of CRISPR Systems:

Harnessing Nature's Toolbox for Genome Engineering. Cell *164*, 29–44.

Xu, X., Duan, D., and Chen, S.-J. (2017). CRISPR-Cas9 cleavage efficiency correlates strongly with target-sgRNA folding stability: from physical mechanism to off-target assessment. Scientific Reports *7*.

Xu, X.-F., Chen, Z.-T., Gao, N., Zhang, J.-L., and An, J. (2009). Myosin Vc, a Member of the Actin Motor Family Associated with Rab8, Is Involved in the Release of DV2 from HepG2 Cells. Intervirology *52*, 258–265.

Yang, L., Guell, M., Byrne, S., Yang, J.L., De Los Angeles, A., Mali, P., Aach, J., Kim-Kiselak, C., Briggs, A.W., Rios, X., et al. (2013). Optimization of scarless human stem cell genome editing. Nucleic Acids Research *41*, 9049–9061.

Zhang, R., Hryc, C.F., Cong, Y., Liu, X., Jakana, J., Gorchakov, R., Baker, M.L., Weaver, S.C., and Chiu, W. (2011). 4.4 Å cryo-EM structure of an enveloped alphavirus Venezuelan equine encephalitis virus: 4.4 Å cryo-EM structure of an enveloped alphavirus. The EMBO Journal *30*, 3854–3863.

Zhang, R., Miner, J.J., Gorman, M.J., Rausch, K., Ramage, H., White, J.P., Zuiani, A., Zhang, P., Fernandez, E., Zhang, Q., et al. (2016). A CRISPR screen defines a signal peptide processing pathway required by flaviviruses. Nature *535*, 164–168.

Zhang, R., Kim, A.S., Fox, J.M., Nair, S., Basore, K., Klimstra, W.B., Rimkunas, R., Fong, R.H., Lin, H., Poddar, S., et al. (2018). Mxra8 is a receptor for multiple arthritogenic alphaviruses. Nature *557*, 570–574.

Zhao, H., and Lindqvist, B. A tyrosine-based motif in the cytoplasmic domain of the alphavirus envelope protein is essential for budding. 8.

Zhao, Y.G., Zhao, H., Miao, L., Wang, L., Sun, F., and Zhang, H. (2012). The p53-induced Gene *Ei24* Is an Essential Component of the Basal Autophagy Pathway. Journal of Biological Chemistry *287*, 42053–42063.

Zhou, Y., Zhu, S., Cai, C., Yuan, P., Li, C., Huang, Y., and Wei, W. (2014). High-throughput screening of a CRISPR/Cas9 library for functional genomics in human cells. Nature *509*, 487–491.

Zhu, C.-H., Mouly, V., Cooper, R.N., Mamchaoui, K., Bigot, A., Shay, J.W., Di Santo, J.P., Butler-Browne, G.S., and Wright, W.E. (2007). Cellular senescence in human myoblasts is overcome by human telomerase reverse transcriptase and cyclin-dependent kinase 4: consequences in aging muscle and therapeutic strategies for muscular dystrophies. Aging Cell *6*, 515–523.

Zhu, J., Davoli, T., Perriera, J.M., Chin, C.R., Gaiha, G.D., John, S.P., Sigiollot, F.D., Gao, G., Xu, Q., Qu, H., et al. (2014). Comprehensive Identification of Host Modulators of HIV-1 Replication using Multiple Orthologous RNAi Reagents. Cell Reports *9*, 752–766.

PUBLICATION

Received: 22 November 2018 | Revised: 21 January 2019 | Accepted: 23 January 2019

DOI: 10.1002/jmv.25420

RESEARCH ARTICLE

WILEY JOURNAL OF MEDICAL VIROLOGY

Detection of chikungunya virus-specific IgM on laser-cut paper-based device using pseudo-particles as capture antigen

Gerald Theillet[1,2] | Gilda Grard[2,3] | Mathilde Galla[2,3] | Carine Maisse[4] | Margot Enguehard[5,6] | Marie Cresson[6,7] | Pascal Dalbon[1] | Isabelle Leparc Leparc-Goffart[2,3] | Frederic Bedin[1]

[1]bioMérieux, Innovations New Immuno-Concepts department, Chemin de l'Orme, Marcy-l'Etoile, France

[2]Unité des Virus Emergents (UVE: Aix-Marseille Univ, IRD 190, Inserm 1207, IHU Méditerranée Infection), Marseille, France

[3]IRBA, Unité de virologie, CNR des Arbovirus, HIA Laveran, Marseille, France

[4]Infections Virales et Pathologie Comparée, UMR754, INRA, Univ Claude Bernard Lyon1, Lyon, France

[5]Ecologie Microbienne CNRS UMR 5557, INRA UMR1418, Villeurbanne, France

[6]CAS Key Laboratory of Molecular Virology and Immunology, Unit of Interspecies transmission of arboviruses and antivirals, Institut Pasteur of Shanghai, Shanghai Institutes for Biological Sciences, Chinese Academy of Sciences, Shanghai, China

[7]IVPC UMR754, INRA, Univ Lyon, Université Claude Bernard Lyon 1, EPHE, PSL Research University, Lyon, France

Correspondence
Frederic Bedin, bioMérieux, Innovations New Immuno-Concepts department, Chemin de l'Orme, 69280 Marcy-l'Etoile, France.
Email: frederic.bedin@biomerieux.com

Funding information
This study was funded by BioMerieux SA and Agence Nationale de la Recherche et de la Technologie, Grant/Award Number: G. Theillet's grant CIFRE no 2015/0514

Abstract

The incidence of arbovirus infections has increased dramatically in recent decades, affecting hundreds of millions of people each year. The *Togaviridae* family includes the chikungunya virus (CHIKV), which is typically transmitted by *Aedes* mosquitoes and causes a wide range of symptoms from flu-like fever to severe arthralgia. Although conventional diagnostic tests can provide early diagnosis of CHIKV infections, access to these tests is often limited in developing countries. Consequently, there is an urgent need to develop efficient, affordable, simple, rapid, and robust diagnostic tools that can be used in point-of-care settings. Early diagnosis is crucial to improve patient management and to reduce the risk of complications. A glass-fiber laser-cut microfluidic device (paper-based analytical device [PAD]) was designed and evaluated in a proof of principle context, for the analysis of 30 µL of patient serum. Biological raw materials used for the functionalization of the PAD were first screened by MAC-ELISA (IgM capture enzyme-linked immunosorbent assay) for CHIKV Immunoglobulin M (IgM) capture and then evaluated on the PAD using various human samples. Compared with viral lysate traditionally used for chikungunya (CHIK) serology, CHIKV pseudo-particles (PPs) have proven to be powerful antigens for specific IgM capture. The PAD was able to detect CHIKV IgM in human sera in less than 10 minutes. Results obtained in patient sera showed a sensitivity of 70.6% and a specificity of around 98%. The PAD showed few cross-reactions with other tropical viral diseases. The PAD could help health workers in the early diagnosis of tropical diseases such as CHIK, which require specific management protocols in at-risk populations.

KEYWORDS
arbovirus, chikungunya, diagnosis, paper analytical device, pseudotyped virus, virus-like particles

1 | INTRODUCTION

Chikungunya (CHIK) is an infectious disease caused by the chikungunya virus (CHIKV), an arbovirus (arthropod-borne virus) transmitted by infected *Aedes* mosquitos.[1] CHIKV belongs to the *Togaviridae* family (*Alphavirus* genus), which also includes Ross River, Mayaro, Semliki Forest, and O'Nyong-Nyong viruses.[2,3] CHIKV was first isolated in Tanzania in 1952 [4,5] and became endemic in large areas of Africa, the Middle East, India, and Southeast Asia.[6,7] Between 2005 and 2007, CHIKV caused a massive epidemic on Reunion Island.[8] Since 2013, the rapid spread of the virus has been reported in the Caribbean and Central and South America. CHIK is an

acute highly symptomatic illness characterized by strong fever, headache, intense asthenia, rash, myalgia, and severe arthralgia.[9] Severe arthralgia that mainly affects hands, wrists, elbows, ankles, and knees can evolve to chronicity. To date, there is no specific and efficient treatment.

Arboviruses are mainly prevalent in developing countries of tropical and subtropical areas and represent a serious public health concern for these countries.[10] Diagnostic assays, such as reverse-transcriptase polymerase chain reaction (RT-PCR), plaque reduction neutralization test (PRNT) or enzyme-linked immunosorbent assay (ELISA) can provide sensitive results and help to optimize patient care.[11-15] However, these assays are time-consuming, rarely affordable, and require infrastructure and qualified operators, making them accessible to relatively few low-income countries.[16]

The development of rapid and affordable diagnostics tests can be an interesting alternative to the use of traditional diagnostic tests. Lateral flow assays (LFAs) for arboviruses diagnostics have been developed and are to date commercially available, both for the detection of viral proteins and for the serological of type M Immunoglobulins (IgM) and/or type G Immunoglobulins (IgG).[15,17,18] However, although the use of these tests is in principle suitable for low-income countries,[19] some issues have been reported, notably in terms of reliability, performance, quality, and regulatory approval.[20-24] Moreover, even with a regulated market price, they remain expensive and therefore relatively inaccessible to a great majority of the population living in the poorest countries.

Paper-based analytical devices (PADs) provide an alternative technology to traditional diagnostic devices. They are simple, low-cost, and suitable not only for infectious disease diagnosis but also for food quality control and environmental monitoring.[25,26] PADs are good candidates to fulfill the ASSURED criteria [27] as defined in 2003 by the World Health Organization (WHO). These criteria specify the ideal characteristics of a test that can be used at all levels of the health system, and are defined as: (i) affordable, (ii) sensitive, (iii) specific, (iv) user-friendly, (v) rapid and robust, (vi) equipment-free, (vii) delivered to those who need them.[27-29]

PAD manufacturing has been intensively explored and described in the literature. Techniques involving laser cutting, wax printing or photolithography are often cited.[30-34] PADs were originally developed for the separation of plasma from whole blood - notably by using glass-fiber paper,[35] for the detection of heavy metal ions [36,37] or for the detection of biomolecules such as uric acid and glucose in various biological samples.[38,39] PADs have also been used for bacterial diagnostics (eg *Mycobacterium tuberculosis*).[40] More recently, PADs have been developed for arboviruses diagnostics, including Zika and dengue.[34,41,42] To date, few data are available concerning CHIK diagnostic.

The presence of CHIKV-specific IgM that appears early in the disease is indicative of a recent infection. Assaying for their presence is recommended from the 5th-day onset after onset. Historically, the IgM capture enzyme-linked immunosorbent assay (MAC-ELISA) developed by the Centers for Disease Control and Prevention (CDC, Atlanta, GA) for the serological diagnosis of chikungunya used either a chemically inactivated chikungunya viral lysate (CHIK VL),[43] or a CHIKV envelope recombinant protein.[44]

In the present paper, a laser-cut glass-fiber PAD using chikungunya pseudo-particles (PPs) and virus-like-particles (VLPs) as alternative antigens to the viral lysate, was evaluated as a proof of concept for CHIKV IgM serology in human samples. PPs and VLPs are multiprotein structures that mimic the organization and conformation of the native virus but lack the viral genome and are therefore noninfectious.[45]

2 | MATERIALS AND METHODS

2.1 | Materials and specimens

Anti-E2 monoclonal antibody (3E10A5) was internally produced. 3E10A5 was directed against a conformational epitope of E2. If needed, it can be labeled with alkaline phosphatase (AP) following conventional procedures. CHIK VL was produced and purified by the Centre National de Reference des arbovirus (CNR Arbovirus, Institut de Recherche Biomédicale des Armées/IRBA, Marseille, France) using standard procedures.[46]

CHIK-negative sera and whole blood specimens were obtained from healthy donors from the French National Blood Bank (Etablissement Français du Sang, Lyon, France). Patient serum specimens were obtained from Biomnis, ABO (Lyon, France) and IRBA (Marseille, France) through specific contracts with bioMérieux SA (Lyon, France). Informed consent was obtained for all experimentation. All experiments were performed in compliance with relevant laws and institutional guidelines and in accordance with the Ethical Standards of the Declaration of Helsinki.

2.2 | VLPs and PPs production and purification

The methods for obtaining VLPs or PPs were adapted from previous studies.[45,47,48] Briefly, for the PP_S, 293T eukaryotic cells (ICAAC, Washington, DC) were cotransfected with plasmids encoding the Gag-Pol (core) proteins of Murine leukemia virus, the green fluorescent protein (GFP) or the chikungunya viral envelope glycoproteins, by the $CaCl_2$ method (Clontech Transfection Kit; Clontech, Fremont, CA) following the manufacturer's instructions. After transfection, the cells were incubated overnight at 37°C. The transfection was checked the next day by controlling the presence of GFP in the cells using a flow cytometer (FACS Calibur; Becton-Dickinson, Franklin Lakes, NJ). For VLPs, the same protocol was applied except that only one plasmid, containing the genes encoding the different structural proteins of the CHIKV, was used. After an additional 24 hours of incubation, the cell culture medium containing the unpurified VLPs or PPs (u-VLPs or u-PPs) was harvested and filtered using a 0.45 µm filtration unit (Merck Millipore, Burlington, MA).

The filtered cell culture medium was either frozen at −80°C or purified by ultracentrifugation. In this case, the medium was loaded on a 2 mL sucrose cushion (20% w/v in PBS1x) and was ultracentrifuged at 107 000*g*, for 2 hours at 4°C (SW 41 T rotor, Beckmann

Optima LE 80 K ultracentrifuge, Indianapolis, IN). The pellet containing the particles was resuspended in PBS1X and then frozen and stored at −30°C. About 60 µL of purified VLPs (p-VLPs) or purified PP_S (p-PPs) were recovered from a 10 cm Petri dish containing 7 mL of OPTIMEM medium (Invitrogen, Carlsbad, CA).

2.3 | Western blot analysis

Antigens were analyzed in nonreducing conditions. Briefly, 2.5 µL of antigen was mixed with 2.5 µL of 4X NuPAGE LDS Sample Buffer (Thermo Fisher Scientific, Waltham, MA). Then, 5 µL of deionized water was added (q.s. 10 µL). Samples were heated at 70°C for 10 minutes and transferred to a NuPAGE 4%-12% Tris-Bis 200 M gel (Invitrogen, Carlsbad, CA). The sample migration occurred in a 1X MES migration buffer (Thermo Fisher Scientific) over 52 minutes at 200 V, 400 mA, and 100 W. The transfer of migrated proteins on a PVDF membrane (Merck Millipore) was performed using an Invitrolon apparatus following the manufacturer's instructions (Thermo Fisher Scientific). Proteins were revealed with the 3E10A5 primary antibody and an AP-labeled antimouse secondary antibody (bioMérieux SA) using the Snap-iD 2.0 Protein Detection System (Merck Millipore), and the addition of NBT/BCIP Substrates (nitro-blue tetrazolium and 5-bromo-4-chloro-3′-indolyphosphate; Thermo Fisher Scientific). Protein bands on the blots were analyzed using a GS-800 scanner (BioRad, Hercules, Ca). The ImageJ software (https://imagej.nih.gov/ij/) was used to quantify the gray intensity level of each band. The height of each band was also evaluated using the ImageJ software by measuring the distance between the upper and lower zones of the bands.

2.4 | MAC-ELISA

IgM antibody capture ELISA proceeded according to standardized methodology.[43,49-51] Polystyrene 96-well plates were coated overnight at 4°C with 5 µg.mL^{-1} of goat anti-human IgM (Jackson ImmunoResearch, Baltimore Pike, PS) in PBS1x. Plates were washed with PBS1x containing 0.05% Tween 20 and blocked with a solution of PBS1x −0.5% BSA for 1 hour at 37°C. Fifty microliters of patient serum 1:200 diluted were added and incubated for 1 hour at 37°C. CHIKV antigens diluted in PBS1x −0.05% BSA −0.05% Tween 20 were then added and incubated for 2 hours at 37°C. The optimal antigen concentration was experimentally determined for each antigen: p-VLPs or p-PPs were diluted 1:20, u-VLPs or u-PPs were used undiluted, the E2 recombinant protein (Aalto Bio Reagent, Dublin, Ireland) was used at 2 µg.mL^{-1}, the viral lysate inactivated by β-propiolactone was diluted at 1:400. Finally, 0.5 µg.mL^{-1} of AP-conjugated anti-E2 monoclonal antibody (3E10A5; bioMérieux SA) was added into each well and incubated for 1 hour at 37°C. After intensive washing, the reaction was developed at room temperature for 15 minutes after adding a PNPP solution (P-NitroPhenyl Phosphate, Thermo Fisher Scientific), and was stopped by adding 2 N sodium hydroxide. The optical density (OD) was measured at 450 nm in a plate reader (Eon Biotek; Biotek Instruments, Winooski, VT).

2.5 | Paper devices manufacturing

Laser-cut PAD manufacturing was described in details in a previous publication.[34] Briefly, two ARcare7815 auto-adhesive plastic layers (Adhesive Research Inc, Limerick, Ireland) and a glass-fiber paper (MF1; GE Healthcare, Velizy, France) were cut using a 30 W CO_2 laser cutting machine (Speedy 100; Trotec, Niederhausbergen, France) following a pattern designed with Inkscape v.0.92. Parameters like speed displacement and laser power are optimized for each material (paper or adhesive) and the expected results. PADs are made of three layers. The bottom layer and the top layer are made of the adhesive film ARcare781, a 2 mil clear polyester film coated on one side with a medical grade acrylic pressure-sensitive adhesive. The intermediate layer is the MF1 glass-fiber based paper. Manufacturing and assembly steps are performed before any biological activation.

2.6 | PAD biological activation and CHIKV IgM testing

The Test area was coated with a capture antibody directed against the human IgM (0.5 µL at 4 mg.mL^{-1}, Jackson ImmunoResearch) in PBS1x. The Control area was spotted with an anti-alkaline phosphatase monoclonal antibody (14A10B7, bioMérieux SA; 0.5 µL at 0.5 mg.mL^{-1} in PBS1x). The Mock area was coated with 0.5 µl of PBS1x containing 0.5% BSA (PBS-BSA). One microliter of an anti-E2 AP-labeled monoclonal antibody (AP-3E10A5, bioMérieux SA), diluted to 0.05 mg.mL^{-1} in a buffer containing detergent and sucrose (VIKIA buffer, bioMérieux SA), was mixed with 1 µL of lyophilized unpurified PPs (u-PPs-lyo) for 5 minutes at room temperature, and the mix was loaded in the square-shaped sample hole (2 µL).

Alternatively, the Test area was directly coated with 0.5 µL of u-PPs-lyo. In that case, an AP-labeled anti-human IgM monoclonal antibody diluted in VIKIA buffer was loaded into the square-shaped sample hole (3 µL at 0.1 mg.mL^{-1}).

The functionalized PADs were dried for 1 minute 30 seconds at 60°C. Then, 0.5 µL of PBS-BSA was added to the Test area, to minimize background noise. Finally, the PADs were dried for 1 minute 30 seconds at 60°C again. Once functionalized, the PADs could be stored for several days at room temperature or at 4°C before use.

For IgM testing, the PAD was loaded with 30 µL of biological sample (serum). Once the sample was totally absorbed by the PAD, 30 µL of the precipitating, coloring substrate (5-bromo-4-chloro-3-indolyl-phosphate solution; BCIP; Promega, Charbonnières, France) was added. Finally, the PAD was incubated for a few minutes until BCIP absorption and the appearance of the signal – blue if the sample is positive. A picture was then taken using a smartphone, 8 to 10 minutes after the sample loading.

2.7 | Ethical approval

All procedures performed in studies involving human participants were in accordance with the ethical standards of the institutional and/or national research committee and with the 1964 Helsinki Declaration and its later amendments or comparable ethical standards.

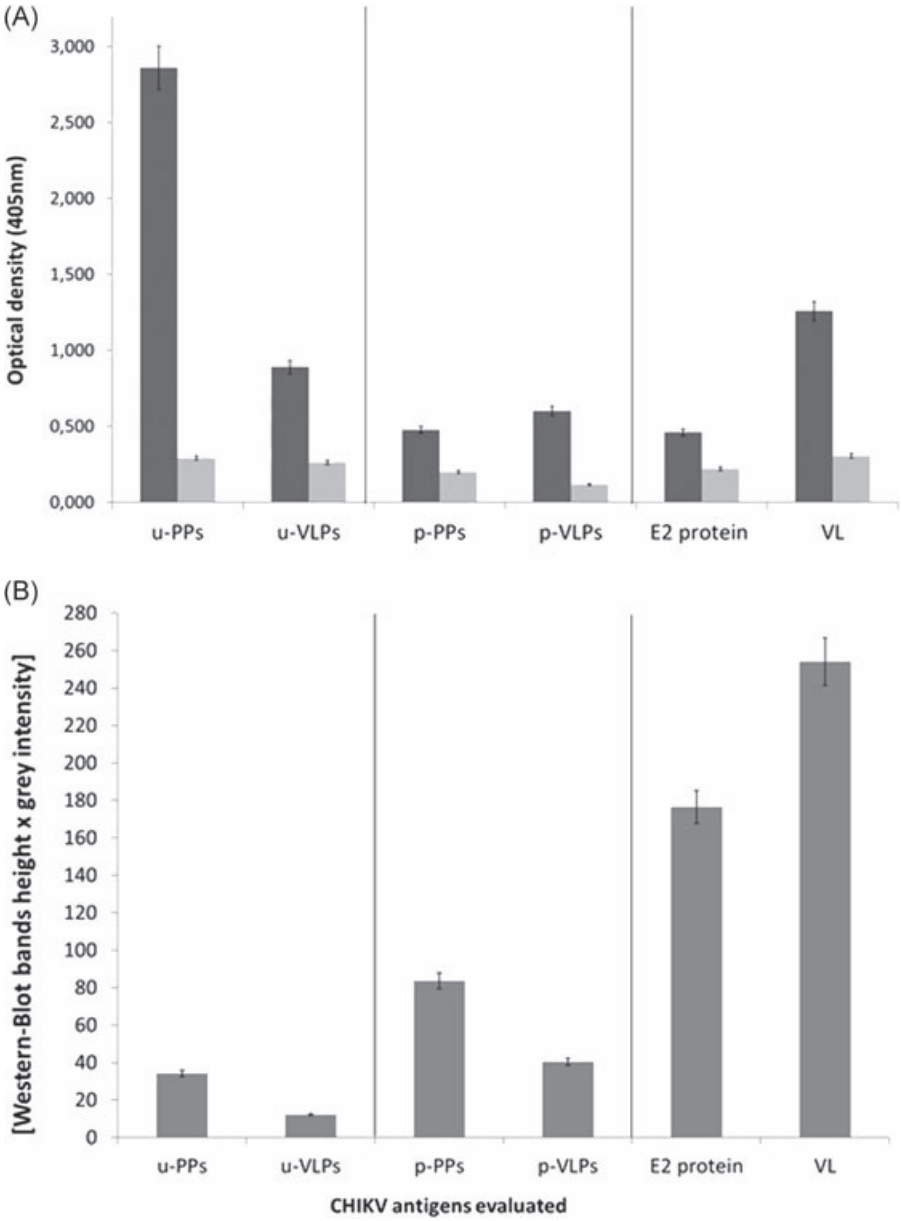

FIGURE 1 CHIKV IgM MAC-ELISA. (A) CHIKV IgM MAC-ELISA using different CHIKV antigens. Viral lysate (VL) corresponds to the reference antigen. Black bars: test; gray bars: negative control using a healthy patient serum (no CHIKV IgM). Each condition has been conducted at least 20-fold in duplicate; (B) relative quantity of CHIKV E2 protein estimated for each antigen by Western blot analysis and densitometry analysis. CHIKV, chikungunya virus; IgM, immunoglobulin M; MAC-ELISA, IgM capture enzyme-linked immunosorbent assay; p-PP/p-VLP, purified PP/VLP; u-PP/u-VLP: unpurified PP/VLP

3 | RESULTS

3.1 | Anti-CHIKV IgM detection on MAC-ELISA

It has previously been demonstrated that CHIK VL was the antigen of choice for sensitive IgM detection by MAC-ELISA.[43] Logically, CHIK VL seemed to be the ideal antigen for the PAD. However, producing CHIK VL and using it for serology requires a Level-3 laboratory and can be problematic in terms of safety. The CHIK VL is traditionally inactivated by treatment with a chemical reagent (eg β-propiolactone) that potentially has an impact on the viral protein structure. To find a safer and more convenient alternative solution to CHIK VL for CHIKV IgM serology, we compared a variety of other antigens, including CHIKV-PPs, CHIKV-VLPs, and CHIKV E2 recombinant protein.

These antigens were first evaluated by MAC-ELISA. As the VLPs/PPs purifications steps (ie centrifugation; see section 2) were time-consuming and could result in a significant loss of material, VLPs and PPs were tested either purified by ultracentrifugation (p-PPs and p-VLPs, around 0.1 $\mu g.\mu L^{-1}$ in PBS1x) or unpurified (u-PPs and u-VLPs). In this case, the cell culture supernatant that contained the VLPs/PPs was directly used. The E2 recombinant protein was used at 2 $\mu g.mL^{-1}$. Experiments were conducted on 20 CHIKV IgM-positive patient sera tested in duplicate. Twenty samples from healthy patients (without CHIKV IgM) were used as negative control.

As illustrated in Figure 1A, the highest signal was observed for a MAC-ELISA using the nonpurified PPs, u-PPs (OD = 2.860+/−0.140). The signal was approximatively 2.4 times higher than for CHIK VL (OD = 1.259+/−0.066), which is considered as the reference assay. The u-VLPs showed a signal 1.4 times lower than the signal observed for CHIK VL, and 3.2 times lower than for the u-PPs. Conditions using p-PPs or p-VLPs and E2 protein shared approximately the same signal level (OD between 0.461 and 0.602), ie approximately

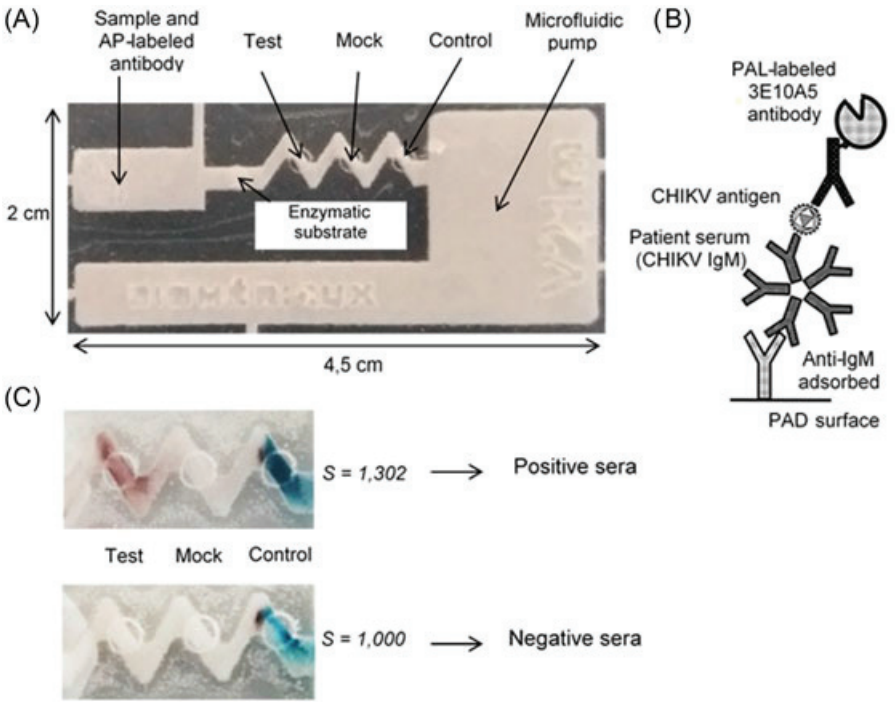

FIGURE 2 CHIKV IgM detection on PAD. (A) Picture of a ready-to-use PAD; (b) schematic depiction of the MAC-ELISA detection format (from Castellanos et al[51]); (C) examples of results obtained for IgM serology on PAD (for CHIKV IgM-positive sera and negative sera). S (specific detection signal) corresponds to the formula (gray level calculated for Mock area)/(gray level calculated for Test area). CHIKV, chikungunya virus; IgM, immunoglobulin M; MAC-ELISA, IgM capture enzyme-linked immunosorbent assay; PAD, paper-based analytical device

2.4 times lower than the signal of the reference assay, and 5.5 times lower than the u-PPs condition.

Antibody 3E10A5, used in the MAC-ELISA as a detection antibody, is directed against a conformational epitope of the E2 protein. To ensure that the signal observed in MAC-ELISA with u-PPs was not due to a difference in E2 protein concentration, the concentration for each antigen was estimated from the Western blot analysis using the 3E10A5 antibody and densitometry analysis. Figure 1B shows the values calculated from the Western blot picture. The value of each bar on the graph corresponds to the formula (band gray value intensity) × (band surface). The highest signal was observed for VL (gray intensity relative value, V = 254), which featured a value 1.4 times higher than for the recombinant protein E2 (V = 176.4). In comparison, the signal calculated for u-PPs (V = 34.2) was 7.4 times lower and 5.2 times lower than in the CHIK VL and the E2 recombinant protein, respectively. The same magnitude order was observed for p-VLPs. The p-PPs showed a signal 2.8 times higher than all others PPs/VLPs antigens tested.

The results showed that, among the various antigens tested by MAC-ELISA, the CHIKV-u-PPs have the highest signal intensity and can be used as an alternative antigen to VL.

3.2 | Anti-CHIKV IgM detection on PAD using different antigens

To confirm the results obtained with MAC-ELISA, the different CHIKV antigens were first evaluated on PAD (Figure 2A), functionalized as for CHIKV MAC-ELISA plates (ie with IgM-directed antibody as a capture tool; Figure 2B).[51] IgM detection was performed by loading 30 µL of serum onto the PAD. The addition of the sample resulted in the resuspension of the dried AP-3E10A5 antibody and the dried antigens that migrated along the PAD. After BCIP addition, the AP-3E10A5-antigen-IgM complex was revealed after capture by the anti-IgM antibody in the Test area. A blue signal in the Test area indicated that the sample was positive for CHIKV IgM. The test was validated by the presence of a blue signal on the Control area (functionalized with an AP-directed monoclonal antibody). No color should appear on the Mock area. The entire process, from the sample loading to the final picture, took less than 10 minutes.

A specific detection signal (S) was calculated for each experiment using the ImageJ software. The value of S corresponded to the formula (gray level calculated for Mock area)/(gray level calculated for Test area).[34] Thus, S takes into consideration the background observed in the Mock area. For negative sera, S had values between 0.95 and 1.032. For positive samples, a dark blue signal appeared on the Test area (Figure 2C) and S could reach values up to 1.95. The presence of blue color in the Control zone indicated that the test was successfully validated. The complete process, from the sample loading to the final picture, took around 8 minutes. Each antigen was tested in duplicate on three CHIKV IgM-positive sera and one healthy CHIKV IgM negative serum.

Despite the encouraging results obtained on MAC-ELISA, the first results obtained on the PAD with u-PPs and u-VLPs were negative. To assess whether the signal could be improved by increasing the concentration of the u-PPs or u-VLPs, 2 mL of culture media containing the u-PPs or u-VLPs were lyophilized at 13 µbar at −80°C (Usifroid lyophilisator; Société Nouvelle Usifroid, Elancourt, France). The lyophilisate was finally resuspended in 100 µL of ultrapure water to obtain a 20-fold concentrated antigen. For IgM serology, the lyophilized/concentrated antigens (u-PPs-lyo or u-VLPs-lyo) were loaded on the Test zone of the PAD.

The PAD functionalized with u-PPs-lyo gave a positive result for the detection of anti-CHIKV IgM (S = 1.302). All the other antigens such as VLPs, E2 recombinant protein, diluted or not diluted, showed negative results on PAD (S values between 1.013 and 1.037). For CHIK VL, the PAD was negative when used diluted at 1:400 as in MAC-ELISA (S = 1.000), but was positive when the VL was used undiluted (S = 1.117). In comparison, the S value for u-VLPs-lyo remained negative (S = 1.037), around 1.25 times lower than the S value for u-PPs-lyo (S = 1.302).

Thus, for CHIKV IgM serology on the PAD, u-PPs-lyo is to be used preferably as a capture antigen.

3.3 | CHIKV IgM PAD performances

To estimate the sensitivity of the PAD, a positivity threshold was first calculated. The Limit Of Detection (LOD) determines the threshold above which the test result can be considered positive. Twenty-four PADs were loaded with 30 µL of serum samples from healthy patients (without CHIKV IgM). For these PADs, the mean of S was 1.027 and the standard deviation (SD) was 0.02. Consequently, for CHIKV IgM detection on sera, a PAD was considered positive when the S value was higher than M + 2SD = 1.067.

PADs were evaluated by loading 30 µL of 14 CHIKV IgM sera. Twelve sera from patients without CHIKV IgM were also tested. Only five CHIKV sera of 14 (36.7%) were found to be positive on the PAD (S_{max} = 1.096 and S_{min} = 1.077; see Supporting Information Data 1).

Alternatively, the antigen (u-PPs-lyo) was directly spotted on the Test zone of the PAD, as capture tool (Figure 3A). The test was performed by loading 30 µL of the sample on the PAD. Detection was performed using an anti-human IgM AP-labeled monoclonal antibody.

For this new PAD format, a new positivity threshold was calculated as described above. Forty-four PADs were loaded with 30 µL of serum samples from healthy patients (without CHIKV IgM). For these PADs, the mean) of S was 1.002 and the SD was 0.018. Thus, for CHIKV IgM detection in sera, the PAD was considered positive when the S value was higher than M + 2SD = 1.039. Of the 44 negative sera tested, only one appeared positive, with a S value of 1.047.

Thirty-four sera samples (21 females/13 males; mean age, 37 years) were tested on PAD for CHIKV IgM serology. All samples had previously been tested by a CHIKV MAC-ELISA and were confirmed to be CHIKV IgM-positive by the providers.

The results illustrated by Figure 3B showed that among the 34 samples tested on PAD, 24 came up as positive, with an S mean of 1.110 and an SD of 0.059 (S_{min} = 1.042 and S_{max} = 1.527). The PADs that came up negative presented an S mean of 1.008, with an SD of 0.008 (S_{min} = 0.992 and S_{max} = 1.029). The Figure 3C depicted the results obtained with the 44 negative sera. Taken together, these data allowed to estimate the PAD sensitivity as 70.6% (95% CI: 52.52% to 84.89%). The specificity of the PAD was also calculated as 97.7% (95% CI: 87.98% to 99.94%; see Table 1).

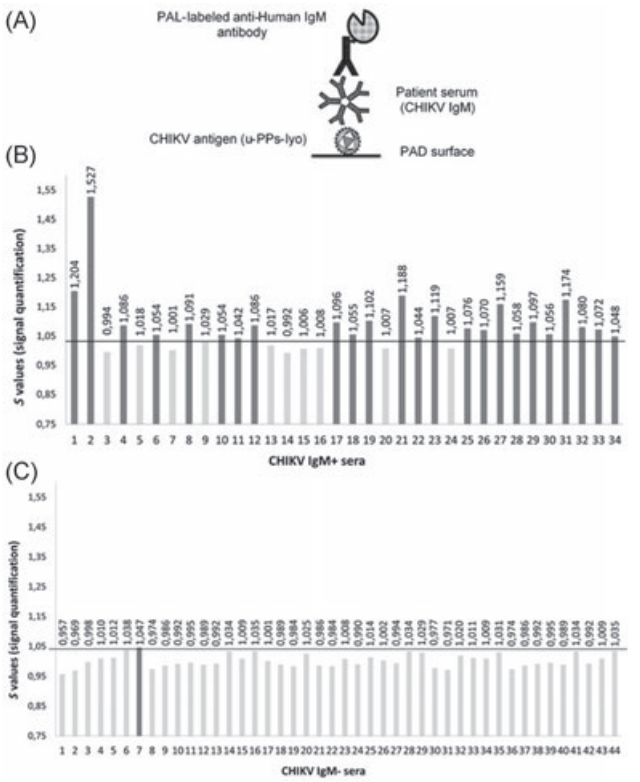

FIGURE 3 CHIKV IgM PAD performances. (A) Schematic depiction of the format using unpurified and lyophilized CHIKV pseudo-particules (u-PP-lyo) as capture antigen, directly coated on the PAD; (B) detection of CHIKV IgM on PAD using u-PP-lyo as capture antigen for 34 patient sera. Each test was conducted in duplicate or in triplicate. A PAD is considered positive when S is equal to or higher than 1.039 (positivity threshold); (C) CHIKV anti-IgM negative samples tested on the PAD using u-PP-lyo as capture antigen for 44 patient sera. Each test was conducted in duplicate or in triplicate. A PAD is considered positive when S is equal to or higher than 1.039 (positivity threshold). CHIKV, chikungunya virus; IgM, immunoglobulin M; PAD, paper-based analytical device

3.4 | IgM detection in plasma specimens from patients infected by other arboviruses

The PAD was evaluated for patient sera that were IgM-positive for other arboviruses such as dengue virus (DENV) and Zika virus (ZIKV; see Table 2). These sera were confirmed to be CHIKV IgM negative by sera providers. These viruses were chosen because of their recurrent cocirculation with CHIKV in tropical countries [52] and the capacity of the flavivirus genus to induce antibody cross-reactivity.[53] We also evaluated the sample from a patient infected with O'Nyong'Nyong viruses (ONNV), an alphavirus known to cross-react with CHIKV.[54,55] Thus, a total of 26 specimens, consisting of recently infected DENV (n = 11), ZIKV (n = 14), and ONNV (n = 1) patient samples, were evaluated in parallel using the CHIKV MAC-ELISA (ie the reference method), the CTK Biotech anti-CHIKV IgM LFA (CTK Biotech, San Diego, CA), and the PAD. In addition, 18 healthy samples were tested as negative controls.

TABLE 1 PAD performances for CHIKV IgM detection

	Reference test (MAC-ELISA)		
Test to evaluate (PAD)	Positive	Negative	Total
Positive	24	1	25
Negative	10	43	53
Total	34	44	78

Abbreviations: CHIKV, chikungunya virus; IgM, immunoglobulin M; MAC-ELISA, IgM capture enzyme-linked immunosorbent assay; PAD, paper-based analytical device.

All the DENV IgM-positive sera were found to be negative for CHIKV IgM with MAC-ELISA. When tested using the CTK Biotech rapid test, these samples were also found to be negative. Interestingly, by using the PAD, two sera were found lightly positive for CHIKV IgM ($S_1 = 1.093$; $S_2 = 1.056$).

As for the dengue samples, all the ZIKV IgM-positive sera were found negative by the CHIKV MAC-ELISA. However, one serum was observed to be positive on the CTK Biotech rapid test. On the PAD, three sera were found to be positive ($S_1 = 1.180$; $S_2 = 1.144$; $S_3 = 1.103$).

Concerning the ONNV IgM-positive serum, it was found to be negative with CHIKV MAC-ELISA.

The negative samples were always found to be negative.

4 | DISCUSSION

The development of immunological rapid point-of-care (POC) and home-based diagnostic tests, such as lateral flow assays, have greatly contributed to generating appropriate analytical results more rapidly, thereby accelerating patient management.[56] In this regard, it seems crucial to collect biological samples within a short period of time, close to the patient location, with the aim of administrating the most adequate treatment to the patient, or of adjusting it quickly.[57]

In previous publications, a new type of POC test, the paper-based analytical device, called PAD, was successfully developed for DENV NS1 proteins and specific IgM detection in various human biological samples. In both cases, the LOD was close to that obtained with a commercial rapid test.[33,34]

TABLE 2 Cross-reaction with other arboviruses

	PAD	LFA (anti-CHIKV IgM)	MAC-ELISA
DENV	2/11 (18%)	0/11 (0%)	0/11 (0%)
ZIKV	3/14 (21.4%)	1/14 (7.1%)	0/14 (0%)
ONNV	0/1 (0%)	0/1 (0%)	0/1 (0%)
Negative sera	0/18 (0%)	0/18 (0%)	0/18 (0%)

Healthy negative sera, DENV, ZIKV, ONNV IgM-positive sera were tested using the PAD functionalized for CHIKV IgM serology, a commercial lateral flow assay for the CHIKV IgM serology (CTK Biotech) and the CHIKV MAC-ELISA. The ratio and the percentage represent the number and the proportion of positive for each test. Each test has been conducted in triplicates.

Abbreviations: CHIKV, chikungunya virus; DENV, dengue virus; IgM, immunoglobulin M; LFA, lateral flow assays; MAC-ELISA, IgM capture enzyme-linked immunosorbent assay; ONNV, O'Nyong'Nyong viruse; PAD, paper-based analytical device; ZIKV, Zika virus.

In the present paper, the PAD was tested as a prototype for the detection of specific CHIKV IgM in sera. The reference method for specific CHIKV IgM detection is MAC-ELISA. In MAC-ELISA, CHIK VL is generally used as an antigen that binds specific IgM to be detected. However, obtaining viral lysate is time-consuming and requires that experiments be conducted in a Biosafety Level-3 laboratory.[58] Before any use, the virus must be inactivated using chemical treatment such as β-propiolactone (BPL).[59] It is generally recognized that BPL inactivates viruses through cross-linking of viral surface proteins. Consequently, BPL treatment could alter the overall structure of envelope viral proteins, which may modulate the affinity of antibodies for these proteins and thus decrease the sensitivity of the test.[60,61]

To overcome these drawbacks, alternative antigens to the viral lysate were produced and tested for specific CHIKV IgM detection.[43] Among these antigens, VLPs and PPs, two types of synthetic viruses, were chosen because of their innocuous nature due to the absence of viral genome. They can be produced in a simple Biosafety Level-2 laboratory. Moreover, they do not require chemical inactivation, as with viral lysate, reducing the risk of alterations of antigenic epitopes. Synthetic viruses are well characterized and have already been considered to be a powerful template to develop next-generation vaccines.[47,62-64] However, there are few references in the literature regarding the use of these antigens as diagnostic tools.[65,66]

Interestingly, using MAC-ELISA, a very strong detection signal for specific CHIKV IgM was observed for u-PPs in comparison with all other antigens, including CHIK VL. The difference of the signal was apparently not due to the relative quantity of E2 protein present in each antigen. The differences could be explained by the intrinsic nature of the antigens used. For example, E2 recombinant protein was produced in sf9 insect cells, not in mammalian cells. Between these two expression systems, the nature and linkage of monosaccharides to *N*-glycosylation sites are different and can lead to changes in the folding and three-dimensional structure of the E2 protein.[67] In this regard, two potential *N*-glycosylation sites have been identified on the E2 protein sequence (https://www.ncbi.nlm.nih.gov/Structure/cdd/cddsrv.cgi?uid = 279311). On the contrary, VLPs and PPs were produced in 293T eukaryotic cells, closer to the natural production cycle of the virus, and allowed to more effectively mimic the native CHIKV.

It has previously been shown that the PAD sensitivity is generally lower than that for ELISA.[33] Here, it has been necessary to concentrate the culture supernatant containing the PPs through a lyophilization step to obtain a specific signal from IgM-positive samples. Interestingly, a positive result for the detection of CHIKV IgM was also obtained with the CHIK VL. Preliminary experiments conducted on the wax-printed version of the PAD [33] showed negative results with CHIK VL for CHIKV IgM serology. The antigen u-PPs-lyo showed positive results with all PAD versions (wax-printed and laser-cut versions). In addition, the S value obtained for CHIK VL

was lower than the S value for u-PPs-lyo. Finally, as previously discussed, obtaining the u-PPs-lyo is easier and safer than the CHIK VL. Consequently, u-PPs-lyo could be used as capture antigen on the PAD instead of the CHIK VL.

In a previous study, Prat et al[24] evaluated two CHIKV IgM rapid tests: SD Bioline CHIKV IgM (Standard Diagnostics Inc., Yongin-si, South Korea), and OnSite Chikungunya IgM Combo Rapid Test (CTK Biotech Inc). The SD Bioline showed poor sensitivity (30%) and specificity (73%) for CHIK patients. Authors calculated that 39% and 57% of the results were false negatives and false positives, respectively. Concerning the CTK Biotech Kit, results showed 20% sensitivity and 93% specificity for CHIKV, with 36% of false negatives and 33% of false positives. These results led the authors to state the ineffectiveness of these kits. A similar study conducted by Kosasih et al[68] showed similar sensitivity results, but a higher specificity for CTK Biotech test, evaluated at 100%. However, for the SD Bioline Kit, the sensitivity reached 68.2% by increasing the time-to-result to 20 minutes instead of 10 minutes. Arya SC et al[69] evaluated the performances of the CTK Biotech kit as well,[69] and calculated sensitivity and a specificity of 71% and 100%, respectively. For the authors, these commercial kits are essential in healthcare centers for developing countries, to be used in the routine early diagnosis and to initiate control measures for CHIK.

The sensitivity of the solution presented here (70.6%) was comparable to these performances, with a time-to-result of 10 minutes. Clinical performances were calculated from a small cohort of patients (N = 78) and need to be confirmed on a larger cohort. Equivalent sensitivity was observed by Arya et al[69] for the same SD Bioline kit. By increasing the reading time to 20 minutes, as suggested by the manufacturer, the sensitivity of the SD Bioline test dropped to 68.2%.[68] However, this value remains lower than that obtained with the PAD. The performance of these kits is summarized in Supporting Information Data 2.

Rianthavorn et al[70] claimed that the sensitivity of these tests is correlated to the duration of symptoms. Consequently, rapid tests should not be used as a screening diagnostic tool during the first week of the disease, when IgM is present at low titers in infected patients. This could explain the poor performances of these tests.

In comparison, commercial ELISA designed for CHIKV IgM serology, have better performances than the LFA or the PAD. Drebot et al[18] evaluated commercial kits from Abcam, EuroImmun, and InBios, and found for each kit a sensitivity of 100%, and a specificity of 97% (Abcam, Cambridge UK ; EuroImmun, Lubeck Germany) and 100% (InBios, Seattle, WA). Despite their improved detection performance, these commercial ELISAs do not exactly match the ASSURED criteria defined by WHO: they require qualified staff, incubators, and readers, and they are expensive and time consuming. This could be an obstacle to their use in the poorest countries.

The PAD can overcome these hurdles by offering a faster time-to-result of 8 to 10 minutes, and a much cheaper diagnostic solution than ELISA tests, with clinical performances comparable to those of most commercialized rapid tests. Compared with a "traditional" LFA, the cost of goods of the PAD was found to be between 5- and 10-fold lower. In addition, the PAD has a reduced size (9 cm^2 surface area and 0.07 cm thickness) and is made of fewer materials, which is advantageous for storage and waste management.[34]

Some DENV and ZIKV IgM samples were found to be positive on the PAD for the detection of CHIKV IgM. In the literature, there is no report describing cross-reactions between these viruses regarding IgM serology. This could be due, in part, to the folding similarities observed between the alphaviruses and flaviviruses envelope proteins. Atomic resolution crystal structure of the alphavirus E1 protein showed a folding pattern related to the E protein of flaviviruses, suggesting homology of at least some genes between flaviviruses and alphaviruses.[71] In addition, flaviviruses were previously classified in the *Togaviridae* family, suggesting some similarities to the current members of this family. However, owing to viral cocirculation, improvements are required to lower the level of cross-reactivity observed with the PAD. It would be interesting to put flaviviruses specific antibodies upstream of the PAD Test area.

Cross-reactions between CHIKV and ONNV have already been reported.[72] The two viruses belong to the same Semliki Forest virus complex.[2,73,74] Interestingly, the PAD showed no cross-reaction with the ONNV sample. It will be necessary to test a larger panel of alphavirus patients other than CHIK patients, such as O'Nyong-Nyong or Ross River patients. However, this type of patients is quite rare and are difficult to find.

Clinical performances of the PAD suggest that it would be beneficial to improve sensitivity and reduce cross reactions. Many ways to enhance sensitivity detection of specific CHIKV IgM on PAD were investigated. Besides the nature of the antigens and their positions on the PAD, chemical pretreatments of the PAD were also studied. Thus, chitosan coating and glutaraldehyde cross-linking were used to modify the surface of the PAD to covalently immobilize antibodies on it. Moreover, these compounds simultaneously enhance the wet-strength of the PAD and the stability of immobilized antibodies, because chitosan is readily compatible with paper and imparts improved mechanical strength to the paper [75-79] However, no significant difference in sensitivity was observed in comparison with the PADs that were not functionalized with chitosan and glutaraldehyde.

Another way to enhance sensitivity performance was the addition of anti-Human IgG antibody or G protein on the PAD, upstream of the Test area. These proteins are expected to capture IgG from the sample tested, thereby decreasing IgG binding on the Test area, and in turn enhancing the specific IgM detection signal. Unfortunately, in our hands, no significant improvement was observed.

Alternatively, sensitivity could also be enhanced by testing various blocking agents such as Biolipidures (NOF America Corp, Irvine, CA), known to reduce nonspecific adsorption and to enhance specific signal.[80]

Currently, many approaches are being explored to improve the performance of arbovirus diagnosis on paper or on low-cost microchips. Thus, it is possible to use the aptamers as tools for CHIKV detection. Bruno et al[81] developed and screened a DNA

aptamers bank directed against CHIKV envelope proteins, for the use as diagnostic tools on paper. The selected aptamers were used for capturing and/or detecting CHIKV envelope proteins. Compared with the cost of production of monoclonal antibodies, aptamers can be considered as a low-cost raw material.

Electrochemical immunosensors also seem to be a promising approach for arbovirus detection. For instance, Kaushik et al[82] have developed an electrochemical immunosensor for the specific and sensitive detection of ZIKV, using a network of gold microelectrodes integrated to an immunodetection chip. The binding of the protein of interest to the microchip produces an electrical current that is measured by electrochemical impedance spectroscopy, allowing detection of the viral protein over a range of 10 pM to 1 nM. Another biosensor system uses an optical biosensor coupled to the CRISPR technology to detect the viral genome of ZIKV on paper.[83] Detection is highly selective due to the hybridization between the CRISPR-Cas9 sensor and ZIKV RNA. In a logical way, these methods using biosensors could be applied to the CHIKV diagnosis.

The cut-off values of a serodiagnostic test are calculated so as to minimize the total cost of misdiagnoses.[84] To determine the appropriate cut-off value above which a PAD will be regarded as positive, many variability factors must be weighed: the nature and quality of the tested sample (serum or blood), the signal quantification procedure (use of a specific software, impact of natural or artificial light, user experience, test repeatability). All these factors have to be considered to determine the best threshold value. For serology on the PAD, it was decided to set the threshold at M + 2SD, as described in the literature.[85] With this threshold, we obtained an acceptable specificity but average sensitivity (97.7% and 70.6%, respectively). By setting the threshold at M + 1.5SD, sensitivity remains unchanged, but specificity falls to 81.8%. At M + 1SD, sensitivity increases to 73.5%, but specificity decreases to 77.3%.

When using the gray-level analysis software (ImageJ), manual selection of the different PAD areas may impact the S value calculation which may slightly differ from one reading to another. Automating the S value calculation can be an alternative way of improving PAD sensitivity. Many previous studies have demonstrated the benefits of a smartphone for reading and obtaining a quantitative and objective result for an accurate diagnostic.[86-91] For the first version of the PAD,[33] an Android-based application was developed on a smartphone for reproducible and quantitative results from the raw signals. This application calculated, from a simple picture of the PAD, the S value and compared it with the cut-off value, to determine if the test was positive or negative. By limiting the variations in measurement that are inherent to the manual method, S values reproducibility was improved. A new version of this smartphone application is to be further developed for use with the improved version of the PAD presented in this publication, to enhance both the reproducibility and the sensitivity of detection. Recently, Quesada-González and Merkoçi[92] predicted that the development of smartphone biosensing will probably decentralize existing care systems and laboratories, in the near future. They also foresee the rapid spread of POC diagnostic tests and other monitoring devices to be used as close to the patient as possible. The use of a smartphone as a tool for diagnostic tests is compatible with the ASSURED criteria since the arrival of new phone manufacturers make smartphones accessible to the greatest number of people.[93]

In the present publication, a new solution using PPs on laser-cut PAD was evaluated in the context of a proof of concept for CHIKV IgM detection. The use of CHIK synthetic viruses, such as PPs, present an alternative way of developing new serological diagnostic tests for CHIK, and could be applied to the diagnosis of other viral diseases. By combining CHIKV and DENV diagnostics, PAD could be a very useful tool for multiplexed arboviruses diagnosis in endemic regions of the world, enabling to improve patient care at a very low price. However, it will be necessary to carry out a study on a larger cohort of samples to confirm the performance level obtained from the PAD. Moreover, the development of a smartphone-based PAD reader, combined with a dedicated application, would provide faster and more accurate diagnostic results, while also objectivizing the result obtained and making the reading easier for the operator and/or the patient.

ACKNOWLEDGMENTS

Authors thank Celine Roesch, Michèle Guillote (Immunoassays department of bioMérieux) for antibody productions; Florence Bettsworth, Blandine Le Levreur, and Marie-Claire Cavaud (Immunoassays department of bioMérieux) for antibody purification and labeling; Sandrine Ducrot and Xavier Lacoux (Raw Materials department of bioMérieux) for the lyophilization process; Frederic Foucault for PAD manufacturing. The final manuscript has been read and corrected by RWS life science, Lausanne, Switzerland, and Vincent Benoit (Innovation department of bioMérieux).

AUTHOR CONTRIBUTIONS

All of the authors contributed to the study conception. GT and FB performed research. FB and GT wrote the manuscript. All of the authors analyzed data, read, corrected, and approved the final manuscript. FB, PD, ILG, and CP performed the study coordination and funding. PPs/VLPs were produced by GT, CMP, ME, and MC. Samples screening was performed by GG and MG.

ORCID

Frederic Bedin http://orcid.org/0000-0003-1762-0508

REFERENCES

1. Furuya-Kanamori L, Liang S, Milinovich G, et al. Co-distribution and co-infection of chikungunya and dengue viruses. *BMC Infect Dis*. 2016;16(1):84.
2. Solignat M, Gay B, Higgs S, Briant L, Devaux C. Replication cycle of chikungunya: a re-emerging arbovirus. *Virology*. 2009;393(2):183-197.
3. Rathore MH, Runyon J, Haque TU. Emerging infectious diseases. *Adv Pediatr*. 2017;64(1):27-71.

4. Robinson MC. An epidemic of virus disease in Southern Province, Tanganyika Territory, in 1952-53. I. Clinical features. *Trans R Soc Trop Med Hyg*. 1955;49(1):28-32.
5. Lumsden WHR. An epidemic of virus disease in Southern Province, Tanganyika territory, in 1952–1953 II. General description and epidemiology . *Trans R Soc Trop Med Hyg*. 1955;49(1):33-57.
6. Hammon WM, Rudnick A, Sather GE. Viruses associated with epidemic hemorrhagic fevers of the Philippines and Thailand. *Science (New York, N.Y.)*. 1960;131:1102-1103.
7. Rougeron V, Sam IC, Caron M, Nkoghe D, Leroy E, Roques P. Chikungunya, a paradigm of neglected tropical disease that emerged to be a new health global risk. *J Clin Virol*. 2015;64:144-152.
8. Brouard C, Bernillon P, Quatresous I. Estimated risk of Chikungunya viremic blood donation during an epidemic on Reunion Island in the Indian Ocean, 2005 to 2007. *Transfusion*. 2008;48(7):1333-1341.
9. Schwartz O, Albert ML. Biology and pathogenesis of chikungunya virus. *Nat Rev Microbiol*. 2010;8(7):491-500.
10. Burt FJ, Chen W, Miner JJ, et al. Chikungunya virus: an update on the biology and pathogenesis of this emerging pathogen. *Lancet Infect Dis*. 2017;17:e107-e117.
11. Azami NAM, Moi ML, Takasaki T. Neutralization assay for chikungunya virus infection: plaque reduction neutralization test. *Methods Mol Biol*. 2016;1426:273-282.
12. Steinhagen K, Probst C, Radzimski C, et al. Serodiagnosis of Zika virus (ZIKV) infections by a novel NS1-based ELISA devoid of cross-reactivity with dengue virus antibodies: a multicohort study of assay performance, 2015 to 2016. *Euro Surveill*. 2016;21(50):30426.
13. Alcon S, Talarmin A, Debruyne M, Falconar A, Deubel V, Flamand M. Enzyme-linked immunosorbent assay specific to dengue virus type 1 nonstructural protein NS1 reveals circulation of the antigen in the blood during the acute phase of disease in patients experiencing primary or secondary infections. *J Clin Microbiol*. 2002;40(2):376-381.
14. Ho PS, Ng MML, Chu JJH. Establishment of one-step SYBR green-based real time-PCR assay for rapid detection and quantification of chikungunya virus infection. *Virol J*. 2010;7:13.
15. Mishra N, Caciula A, Price A, et al. Diagnosis of Zika virus infection by peptide array and enzyme-linked immunosorbent assay. *mBio*. 2018;9(2):e00095-e00118.
16. Hu J, Wang S, Wang L, et al. Advances in paper-based point-of-care diagnostics. *Biosens Bioelectron*. 2014;54:585-597.
17. Litzba N, Klade CS, Lederer S, Niedrig M. Evaluation of serological diagnostic test systems assessing the immune response to Japanese encephalitis vaccination. *PLOS Negl Trop Dis*. 2010;4(11):e883.
18. Drebot MA, Valadere AM, Goodman CH, Johnson BW, De salazar PM, Holloway K. Evaluation of commercially available chikungunya virus immunoglobulin M detection assays. *Am J Trop Med Hyg*. 2016;95(1):182-192.
19. Kafkova J. Rapid diagnostic point of care tests in resource limited settings. *Int J Infect Dis*. 2016;45:56-57.
20. Bissonnette L, Bergeron MG. Diagnosing infections–current and anticipated technologies for point-of-care diagnostics and home-based testing. *Clin Microbiol Infect*. 2010;16(8):1044-1053.
21. Huckle D. Point-of-care diagnostics: an advancing sector with nontechnical issues. *Expert Rev Mol Diagn*. 2008;8(6):679-688.
22. Jahn UR, Van Aken H. Near-patient testing – point-of-care or point of costs and convenience?. *Br J Anaesth*. 2003;90(4):425-427.
23. Fu E, Liang T, Houghtaling J, et al. Enhanced sensitivity of lateral flow tests using a two-dimensional paper network format. *Anal Chem*. 2011;83(20):7941-7946.
24. Prat CM, Flusin O, Panella A, Tenebray B, Lanciotti R, Leparc-Goffart I. Evaluation of commercially available serologic diagnostic tests for chikungunya virus. *Emerg Infect Dis*. 2014;20(12):2129-2132.
25. Rozand C. Paper-based analytical devices for point-of-care infectious disease testing. *Eur J Clin Microbiol Infect Dis*. 2014;33(2):147-156.
26. Liana DD, Raguse B, Gooding JJ, Chow E. Recent advances in paper-based sensors. *Sensors*. 2012;12(9):11505-11526.
27. Kettler H, White K, Hawkes SJ. *Mapping the Landscape of Diagnostics for Sexually Transmitted Infections: Key Findings and Recommendations*. World Health Organization; 2004.
28. Martinez AW, Phillips ST, Whitesides GM, Carrilho E. Diagnostics for the developing world: microfluidic paper-based analytical devices. *Anal Chem*. 2010;82(1):3-10.
29. Tay A, Pavesi A, Yazdi SR, Lim CT, Warkiani ME. Advances in microfluidics in combating infectious diseases. *Biotech Adv*. 2016;34(4):404-421.
30. Spicar-Mihalic P, Toley B, Houghtaling J, Liang T, Yager P, Fu E. CO2-laser cutting and ablative etching for the fabrication of paper-based devices. *J Micromech Microeng*. 2013;23(6):067003.
31. Jiang X, Fan ZH. Fabrication and operation of paper-based analytical devices. *Annu Rev Anal Chem*. 2016;9:203-222.
32. Xia Y, Si J, Li Z. Fabrication techniques for microfluidic paper-based analytical devices and their applications for biological testing: a review. *Biosens Bioelectron*. 2016;77:774-789.
33. Bedin F, Boulet L, Voilin E, Theillet G, Rubens A, Rozand C. Paper-based point-of-care testing for cost-effective diagnosis of acute flavivirus infections. *J Med Virol*. 2017;89:1520-1527.
34. Theillet G, Rubens A, Foucault F, et al. Laser-cut paper-based device for the detection of dengue non-structural NS1 protein and specific IgM in human samples. *Arch Virol*. 2018;163:1757-1767.
35. Songjaroen T, Dungchai W, Chailapakul O, Henry CS, Laiwattanapaisal W. Blood separation on microfluidic paper-based analytical devices. *Lab Chip*. 2012;12(18):3392-3398.
36. Lin Y, Gritsenko D, Feng S, Teh YC, Lu X, Xu J. Detection of heavy metal by paper-based microfluidics. *Biosens Bioelectron*. 2016;83:256-266.
37. Zhang M, Ge L, Ge S, et al. Three-dimensional paper-based electrochemiluminescence device for simultaneous detection of Pb2 + and Hg2+ based on potential-control technique. *Biosens Bioelectron*. 2013;41:544-550.
38. Liu S, Su W, Ding X. A review on microfluidic paper-based analytical devices for glucose detection. *Sensors (Basel)*. 2016;16(12):2086.
39. Wang X, Li F, Cai Z, et al. Sensitive colorimetric assay for uric acid and glucose detection based on multilayer-modified paper with smartphone as signal readout. *Anal Bioanal Chem*. 2018;410:2647-2655.
40. Tsai TT, Shen SW, Cheng CM, Chen CF. Paper-based tuberculosis diagnostic devices with colorimetric gold nanoparticles. *Sci Technol Adv Mater*. 2013;14(4):044404.
41. Bosch I, de Puig H, Hiley M, et al. Rapid antigen tests for dengue virus serotypes and Zika virus in patient serum. *Sci Transl Med*. 2017;9(409):eaan1589.
42. Meagher RJ, Negrete OA, Van Rompay KK. Engineering paper-based sensors for Zika virus. *Trends Mol Med*. 2016;22:529-530.
43. Martin DA, Muth DA, Brown T, Johnson AJ, Karabatsos N, Roehrig JT. Standardization of immunoglobulin M capture enzyme-linked immunosorbent assays for routine diagnosis of arboviral infections. *J Clin Microbiol*. 2000;38(5):1823-1826.
44. Yap G, Pok KY, Lai YL, et al. Evaluation of chikungunya diagnostic assays: differences in sensitivity of serology assays in two independent outbreaks. *PLOS Neglected Trop Dis*. 2010;4(7):e753.
45. Noranate N, Takeda N, Chetanachan P, Sittisaman P, A-Nuegoonpipat A, Anantapreecha S. Characterization of chikungunya virus-like particles. *PLOS One*. 2014;9(9):e108169.
46. Ang SK, Lam S, Chu JJH. Propagation of chikungunya virus using mosquito cells. *Methods Mol Biol*. 2016;1426:87-92.
47. Metz SW, Pijlman GP. Production of chikungunya virus-like particles and subunit vaccines in insect cells. *Methods Mol Biol*. 2016;1426:297-309.
48. Wu J, Zhao C, Liu Q, Huang W, Wang Y. Development and application of a bioluminescent imaging mouse model for chikungunya virus based on pseudovirus system. *Vaccine*. 2017;35(47):6387-6394.

49. Peyrefitte CN, Pastorino BAM, Bessaud M, et al. Dengue type 3 virus, Saint Martin, 2003–2004. *Emerging Infect Dis*. 2005;11(5):757-761.
50. Khan M, Dhanwani R, Kumar JS, Rao PVL, Parida M. Comparative evaluation of the diagnostic potential of recombinant envelope proteins and native cell culture purified viral antigens of Chikungunya virus. *J Med Virol*. 2014;86(7):1169-1175.
51. Castellanos JE, Parra-Álvarez S, Calvo DEP. Improving diagnosis of Zika virus infection: an urgent task for pregnant women. *Orion*. 2018
52. Rückert C, Weger-Lucarelli J, Garcia-Luna SM, et al. Impact of simultaneous exposure to arboviruses on infection and transmission by *Aedes aegypti* mosquitoes. *Nat Commun*. 2017;8:15412.
53. Mansfield KL, Horton DL, Johnson N, et al. Flavivirus-induced antibody cross-reactivity. *J Gen Virol*. 2011;92(Pt 12):2821-2829.
54. Smith JL, Pugh CL, Cisney ED, et al. Human antibody responses to emerging Mayaro Virus and cocirculating alphavirus Infections examined by using structural proteins from nine new and old world lineages. *mSphere*. 2018;3(2):00003-00018.
55. Caglioti C, Lalle E, Castilletti C, Carletti F, Capobianchi MR, Bordi L. Chikungunya virus infection: an overview. *New Microbiol*. 2013;36(3):211-227.
56. Ehrmeyer SS, Laessig RH. Point-of-care testing, medical error, and patient safety: a 2007 assessment. *Clin Chem Lab Med*. 2007;45(6):766-773.
57. Tolonen U, Kallio M, Ryhänen J, Raatikainen T, Honkala V, Lesonen V. A handheld nerve conduction measuring device in carpal tunnel syndrome. *Acta Neurol Scand*. 2007;115(6):390-397.
58. McFee RB. Selected mosquito-borne illnesses—Chikungunya. *Dis Mon*. 2018;64:222-234.
59. Perrin P, Morgeaux S. Inactivation of DNA by beta-propiolactone. *Biologicals*. 1995;23(3):207-211.
60. Fan C, Ye X, Ku Z, et al. Beta-propiolactone inactivation of coxsackievirus A16 induces structural alteration and surface modification of viral capsids. *J Virol*. 2017;91(8):-.
61. Bonnafous P, Nicolaï MC, Taveau JC, et al. Treatment of influenza virus with beta-propiolactone alters viral membrane fusion. *Biochim Biophys Acta*. 2014;1838(1 Pt B):355-363.
62. Urakami A, Sakurai A, Ishikawa M, et al. Development of a Novel Virus-Like Particle Vaccine Platform That Mimics the Immature Form of Alphavirus. *Clin Vaccine Immunol*. 2017;24(7):e00090-e00117.
63. Metz SW, Martina BE, van den Doel P, et al. Chikungunya virus-like particles are more immunogenic in a lethal AG129 mouse model compared to glycoprotein E1 or E2 subunits. *Vaccine*. 2013;31(51):6092-6096 .
64. Saraswat S, Athmaram TN, Parida, M, Agarwal A, Saha A, Dash PK. Expression and characterization of yeast derived chikungunya virus like particles (CHIK-VLPs) and its evaluation as a potential vaccine candidate. *PLOS Negl Trop Dis*. 2016;10(7):e0004782.
65. Zeltins A. Construction and characterization of virus-like particles: a review. *Mol Biotechnol*. 2013;53(1):92-107.
66. Park JS, Cho MK, Lee EJ, et al. A highly sensitive and selective diagnostic assay based on virus nanoparticles. *Nat Nanotechnol*. 2009;4(4):259-264.
67. Varki A, Cummings R, Esko J, Freeze H, Hart G, Marth J *Essentials of glycobiology*. Vol 1 1999.
68. Kosasih H, Widjaja S, Surya E, et al. Evaluation of two IgM rapid immunochromatographic tests during circulation of Asian lineage Chikungunya virus. *Southeast Asian J Trop Med Public Health*. 2012;43(1):55-61.
69. Arya S, Agarwal N. Rapid point–of–care diagnosis of chikungunya virus infection. *Asian Pac J Trop Dis*. 2011;1(3):230-231.
70. Rianthavorn P, Wuttirattanakowit N, Prianantathavorn K, Limpaphayom N, Theamboonlers A, Poovorawan Y. Evaluation of a rapid assay for detection of IgM antibodies to chikungunya. *Southeast Asian J Trop Med Public Health*. 2010;41(1):92-96.
71. Jose J, Snyder JE, Kuhn RJ. A structural and functional perspective of alphavirus replication and assembly. *Future Microbiol*. 2009;4(7):837-856.
72. Brault AC, Tesh RB, Powers AM, Weaver SC. Re-emergence of Chikungunya and O'nyong-nyong viruses: evidence for distinct geographical lineages and distant evolutionary relationships. *J Gen Virol*. 2000;81(2):471-479.
73. Schmaljohn AL, DM. Alphaviruses (*Togaviridae*) and Flaviviruses (*Flaviviridae*). In: Baron Se, ed. *Medical Microbiology*. 4th ed., 4. Galveston, TX: University of Texas Medical Branch at Galveston; 1996.
74. Bolling B, Weaver S, Tesh R, Vasilakis N. Insect-specific virus discovery: significance for the arbovirus community. *Viruses*. 2015;7(9):4911-4928.
75. Pang B, Zhao C, Li L, et al. Development of a low-cost paper-based ELISA method for rapid *Escherichia coli* O157:H7 detection. *Anal Biochem*. 2017;542:58-62.
76. Liu W, Guo Y, Zhao M, Li H, Zhang Z. Ring-oven washing technique integrated paper-based immunodevice for sensitive detection of cancer biomarker. *Anal Chem*. 2015;87(15):7951-7957.
77. Van Toan N, Hanh TT. Application of chitosan solutions for rice production in Vietnam. *Afr J Biotechnol*. 2013;12(4):382-384.
78. Gabriel EFM, Garcia PT, Cardoso TMG, Lopes FM, Martins FT, Coltro WKT. Highly sensitive colorimetric detection of glucose and uric acid in biological fluids using chitosan-modified paper microfluidic devices. *Analyst*. 2016;141(15):4749-4756.
79. Wang S, Ge L, Song X, et al. Paper-based chemiluminescence ELISA: lab-on-paper based on chitosan modified paper device and wax-screen-printing. *Biosens Bioelectron*. 2012;31(1):212-218.
80. Oyarzabal OA, Battie C. Immunological methods for the detection of campylobacter Spp.-current applications and potential use in biosensors. *Trends in Immunolabelled and Related Techniques*, 2012.
81. Bruno JG, Carrillo MP, Richarte AM, Phillips T, Andrews C, Lee JS. Development, screening, and analysis of DNA aptamer libraries potentially useful for diagnosis and passive immunity of arboviruses. *BMC Res Notes*. 2012;5(1):633.
82. Kaushik A, Yndart A, Kumar S, et al. A sensitive electrochemical immunosensor for label-free detection of zika-virus protein. *Sci Rep*. 2018;8(1):9700.
83. Kaushik A, Tiwari S, Jayant RD, et al. Electrochemical biosensors for early stage Zika diagnostics. *Trends Biotechnol*. 2017;35(4):308-317.
84. Vizard AL, Anderson GA, Gasser RB. Determination of the optimum cut-off value of a diagnostic test. *Prev Vet Med*. 1990;10(1-2):137-143.
85. Jacobson RH. Validation of serological assays for diagnosis of infectious diseases. *Rev Sci Tech*. 1998;17:469-486.
86. Lee S, Kim G, Moon J. Performance improvement of the one-dot lateral flow immunoassay for aflatoxin B1 by using a smartphone-based reading system. *Sensors (Basel)*. 2013;13(4):5109-5116.
87. You DJ, Park TS, Yoon JY. Cell-phone-based measurement of TSH using Mie scatter optimized lateral flow assays. *Biosens Bioelectron*. 2013;40(1):180-185.
88. Bates M, Zumla A. Rapid infectious diseases diagnostics using Smartphones. *Ann Transl Med*. 2015;3(15):215.
89. Ganguli A, Ornob A, Yu H, et al. Hands-free smartphone-based diagnostics for simultaneous detection of Zika, Chikungunya, and Dengue at point-of-care. *Biomed Microdevices*. 2017;19(4):73.
90. Erickson D, O'Dell D, Jiang L, et al. Smartphone technology can be transformative to the deployment of lab-on-chip diagnostics. *Lab Chip*. 2014;14:3159-3164.
91. Priye A, Bird SW, Light YK, Ball CS, Negrete OA, Meagher RJ. A smartphone-based diagnostic platform for rapid detection of Zika, chikungunya, and dengue viruses. *Sci Rep*. 2017;7:44778.
92. Quesada-González D, Merkoçi A. Mobile phone-based biosensing: An emerging "diagnostic and communication" technology. *Biosens Bioelectron*. 2017;92:549-562.

93. Mirani L. *$30 smartphones are here—and they're getting better every day*, 2014. https://qz.com/314285/30-smartphones-are-here-and-theyre-getting-better-every-day/

SUPPORTING INFORMATION

Additional supporting information may be found online in the Supporting Information section at the end of the article.

How to cite this article: Theillet G, Grard G, Galla M, et al. Detection of chikungunya virus-specific IgM on laser-cut paper-based device using pseudo-particles as capture antigen. *J Med Virol*. 2019;1–12. https://doi.org/10.1002/jmv.25420